THE BEHAVIOUR OF A STRUCTURALLY COMPLEX CLAY FROM AN ITALIAN LANDSLIDE.

by

RUTH FEARON

A thesis submitted for the Degree of
Doctor of Philosophy

City University
Civil Engineering Department

April 1998

TABLE OF CONTENTS

LIST OF TABLES

LIST OF FIGURES

ACKNOWLEDGEMENTS

During the three and a half years that I have spent at City University, I have gained a wealth of knowledge and have had the opportunity to work with some delightful people.

I must first thank my advisor, Dr. Matthew Coop for his time, his advice, constant encouragement and support throughout the course of my PhD project and for preventing me from despairing when it seemed like I was swimming upstream. His assistance in the laboratory was invaluable, where he shared his wealth of knowledge and experience in laboratory testing and helped to rescue a few potential disasters.

I also need to thank Professors John Atkinson and Neil Taylor for their thought provoking and insightful discussions, particularly when Dr. Matthew Coop was on sabbatical. I learnt during these conversations always to question what I was doing and why I was doing it.

Everybody at City University made my research here easier and more fun. It was a great place to do research. The technicians Mr Keith Osbourne, Mr. Lloyd Martika and Mr Reg Allen were always helpful and their technical assistance is greatly appreciated. I am also grateful to Dr. Sarah Stallebrass for her support, encouragement and chocolate when things were not going well, a relatively frequent occurrence when working in the laboratory. Mr Richard Grant was good company while writing up and I am grateful for the race to finish before him. I would also like to mention some of my colleagues at City University, Dr. Vojkan Jovicic, Mr Peter Ingram, Mr Bahardin Baharom, Dr. Emma Boyce, and Mr Ulrich Klotz, who have accompanied me along my journey.

The research for this project was funded as part of a European Community funded project entitled "Landslide Evolution controlled by Climatic Factors in a Seismic Area: Prediction Methods and Warning Criterion", which was carried out in conjunction with the Istituto di Geologia Applicata e Geotecnica of the Politecnico di Bari in Italy and Armines-CGI from the Ecole de Mines in Paris, France. I am grateful for the financial support of the European Community and the assistance of the other two partners. I would particularly like to acknowledge Dr. Janusz Wasowski with whom I spent many days at the landslide discussing landslide mechanisms and geology and Dr. Federica Cotecchia for the interesting discussions.

In conclusion I would like to dedicate this thesis to those friends that have helped and inspired me. I would never have started this PhD without their help. I would also like to thank my parents, my flat mates and my friends in particular Lara, Sarah, Tazmin, Barbara and Charlie for their help, patience and tolerance.

DECLARATION

I grant powers of discretion to the University Librarian to allow this thesis to be copied in whole or in part without further reference to me. This permission covers only single copies made for study purposes, subject to normal conditions of acknowledgement.

ABSTRACT

This thesis looks at the behaviour of a structurally complex clay formation from a landslide site in the Southern Italian Apennines. The argille scagliose or scaly clays which form the greater part of the argillaceous component of the geological sequence consist of small shear lenses (or scales) of clay, whose orientation may change within a few centimetres. These clays have a very complex structure in that they are both bonded and discontinuous. As a result of the tectonic history of these materials, they have a bonded micro-structure consisting of composite particles of clay minerals and a fissured macro-structure.

The behaviour of these soils was investigated using S.E.M., Atterberg limit, triaxial and ring shear tests in the laboratory. This research has considered soils with four different types of structure: natural samples from the underlying formation; soil from the landslide body which had been remoulded as a result of the landslide activity; and two different types of reconstituted samples (reconstituted and minced) prepared with different amounts of remoulding energy. The effect of different macro- and micro-structures could therefore be assessed by comparing the behaviours of these different materials with those of corresponding reconstituted samples, normalised where appropriate to account for their different stress states, specific volumes and natures. Several negative effects of structure on the strength and compressibility of these materials were observed. Samples which were vigorously disaggregated (minced) were able to exist at specific volumes not possible in the sample prepared using a less destructive method (reconstituted), whilst the scaly formation material sheared at its estimated in-situ stress level achieved strengths which were lower than those of the corresponding reconstituted samples at their critical states.

The effect of landsliding on the material behaviour was also assessed by comparing the behaviours of samples from inside and outside the landslide body, normalised with respect to that of a corresponding reconstituted sample. Remoulding as the result of the landslide activity showed a change in the appearance of these materials from a scaly clay to a clay matrix containing lithorelicts. This change in the macro-structure of the natural material, due to remoulding within the landslide body, resulted in a soil behaviour which was more similar to that of the reconstituted material than the underlying formation.

LIST OF SYMBOLS

A	constant in power law relationship between G_{max} and p' for a normally consolidated soil (Equation 2.6)
B	Skempton's pore pressure multiplier
c	p'_e/p' exponent in power law relationship between shear modulus and mean normal effective stress and p'_e/p' (Equation 4.13)
c_u	undrained shear strength
$c_{u\ intact}$	undrained shear strength of the intact clay
$(c_u)_{LL}$	undrained shear strength at the liquid limit
$(c_u)_{PL}$	undrained shear strength at the plastic limit
c_{ur}	undrained shear strength of the remoulded clay
C_c	coefficient of compressibility
C_c^*	intrinsic coefficient of compressibility
C_s	gradient of the swelling line
C_s^*	gradient of a swelling line for a reconstituted sample
CF	clay fraction
e	voids ratio
e_g	granular void ratio
e_L	voids ratio at the liquid limit
e^*_{1kPa}	voids ratio of a normally consolidated reconstituted sample at 1 kPa in one-dimensional compression
e^*_{100}	voids ratio of a normally consolidated reconstituted sample at 100 kPa in one-dimensional compression
e^*_{1000}	voids ratio of a normally consolidated reconstituted sample at 1000 kPa in one-dimensional compression
E_d	energy dissipated in breaking up and remoulding the moving material
E_f	frictional energy required to keep the soil mass moving

E_k kinetic energy used to accelerate the soil mass

E_p potential energy of a soil mass at failure

G shear modulus

G_{max} shear modulus at very small strains (or G_o)

G_o shear modulus at very small strains (or G_{max})

G_s specific gravity

G_u undrained shear modulus

I_p plasticity index

I_r remoulding index

I_v void index

J cross-anisotropic modulus (Equation 4.15)

K bulk modulus

K_{max} small strain bulk modulus

K_o in-situ earth pressure

m overconslidation ratio exponent in power law relationship between shear modulus and mean normal effective stress and overconsolidation ratio (Equation 2.6)

M stress ratio (q'/p') at the critical state

n mean normal effective stress ratio exponent in power law relationship between shear modulus and mean normal effective stress for a normally consolidated soil (Equation 2.6)

n* mean normal effective stress ratio exponent in power law relationship between shear modulus and mean normal effective stress and p'_e/p' (Equation 4.13)

N Intercept of the isotropic normal compression line at 1 kPa

OCR overconsolidation ratio

p' mean normal effective stress

p_r reference pressure (1kPa) in Equation 2.6

p'_{cs} equivalent pressure on the critical state line

p'_e equivalent pressure on the isotropic normal compression line

p'_o mean effective stress at the beginning of a loading stage

q' deviatoric stress

R_o overconsolidation ratio in terms of vertical effective stress

s' mean effective stress in plane strain

S^* constant in power law relationship between G_{max} and p' for a normally consolidated soil (Equation 4.13)

t maximum shear stress in plane strain

u pore pressure

v specific volume

v_s shear wave velocity

w_L liquid limit

Γ Intercept of the critical state line at 1 kPa

δ small increment of ...

Δ large increment of ...

ε normal strains

ε_a axial strain

ε_r radial strain

ε_s shear strain

ε_v volumetric strain

κ gradient of isotropic swelling line in v-lnp' space

κ^* gradient of reconstituted isotropic swelling line in v-lnp' space

$\kappa_{lnv\text{-}lnp'}$ gradient of isotropic swelling line in lnv-lnp' space

$\kappa^*_{lnv\text{-}lnp'}$ gradient of reconstituted isotropic swelling line in lnv-lnp' space

λ gradient of the isotropic normal compression line

ρ	mass density
σ'_a	axial effective stress
σ_c	cell pressure
σ'_n	normal effective stress
σ'_r	radial effective stress
σ'_v	vertical effective stress
σ'_{vy}	vertical stress at yield in one-dimensional compression
σ'_{ve}*	equivalent vertical pressure on the reconstituted one-dimensional compression line
τ	shear stress
τ_R	shear stress measured at the residual state
ϕ'	friction angle
ϕ'_p	peak friction angle
ϕ'_r	residual friction angle
ϕ'_{res}	residual friction angle

CHAPTER 1 INTRODUCTION

The principal aims of this research were to look at the mechanics of the clays from a landslide site in Southern Italy; to ascertain whether their behaviour could be assessed within a critical state framework; to assess the role that structure played in their behaviour; to determine how that structure changed as a result of landsliding; and to provide the numerical values of the parameters to be used in the stability analysis of the slope.

This research formed part of a European Community funded project entitled "Landslide Evolution controlled by Climatic Factors in a Seismic Area: Prediction Methods and Warning Criterion", which was carried out in conjunction with the Istituto di Geologia Applicata e Geotecnica of the Politecnico di Bari in Italy and Armines-CGI from the Ecole de Mines in Paris, France, as is described in greater detail in Section 1.1. The many landslides within the study area have been responsible for a large number of fatalities and partially for the region's poor economic status.

The particular landslide site on which this research was centred is the Acquara-Vadoncello landslide, which lies just outside the village of Senerchia in Southern Italy, which was activated in December 1993. This landslide is a subsidiary of the much larger Serra dell'Acquara landslide which was remobilised by the 1980 Irpinian earthquake. Figure 1.1 shows a photograph of the Serra dell'Acquara landslide and Figures 1.2 and 1.3 show photographs of the scarp and downslope regions of the Acquara-Vadoncello landslides respectively. The landslide is described in more detail in Section 1.1.1

The soils at the landslide site are a structurally complex clay formation. The materials have a very complex structure which results from their geological origin. The soils were originally deposited as turbidites, but have subsequently been moved by several hundred kilometres as a result of tectonic activity, as will be discussed in Section 2.3.1. The argille scagliose (scaly clays) which form much of the underlying formation consist typically of small shear lenses (or scales) of clay, whose orientation may change within a few centimetres.

One of the principal aims of this research was to assess the mechanical behaviour of these soils within a critical state framework, as has been done for other structured clays. The effects of the structure on the behaviour of these soils have been assessed by comparing the behaviour of the natural material with that of the reconstituted material, where structure is a combination of particle arrangements and interparticle attractions, as defined by Mitchell (1976). It was also possible to assess other aspects of the structure of these soils by comparing the behaviour of the reconstituted soil, prepared by swelling these soils by immersion in water, with that of a minced soil, prepared by passing the soil through an industrial food mincer to break down some of the silt-sized aggregates of clay particles.

The effects of the different structures of the natural and reconstituted materials and the reconstituted and minced materials have been assessed by comparing their Atterberg Limits, the locations of their normal compression lines, their shear strengths, residual strengths and shear stiffnesses, normalised where appropriate to account for different stress states, specific volumes and material characteristics.

In this chapter, a brief overview is given of the European Community project and the roles played by the different partners. Section 1.1.1 gives a description of the Acquara-Vadoncello landslide site and the site investigation carried out.

In Chapter 2, a literature review assesses the research that has been carried out on other structured clays. Within the context of the conclusions drawn from the research on structured clays in general, the literature on other structurally complex clays from Southern Italy is reviewed. The aim of this study is to assess the effects of the very evident structure of the structurally complex clays on the material behaviour. This has been carried out where possible by comparison of the natural soil behaviour with that of the corresponding reconstituted soils.

In Chapter 3, the equipment used for the laboratory study is described. Index tests were carried out to determine basic soil properties and for classification of materials across the site. Triaxial tests were carried out to determine the fundamental soil behaviour and in particular to determine strength and stiffness parameters for the numerical analyses. Ring shear tests were also carried out to determine the residual strength of the soils. This large displacement strength is appropriate for failures on pre-existing shear surfaces that occur in landslides. The main improvements to the triaxial apparatus

concerned the need to improve the resolution and accuracy of the data for the small strain stiffnesses to be calculated. The Bishop ring shear apparatus was instrumented to allow continuous data logging. This chapter also describes the preparation methods and test procedures that were used for these difficult soils.

Chapter 4 gives details of the results of the index tests, ring shear tests and the triaxial tests on the materials from the site. The work focuses on comparing the behaviour of corresponding undisturbed (natural), reconstituted and minced samples to assess the role that structure plays in controlling the behaviour of these soils. The properties compared include the Atterberg limits, the residual strengths, the positions of the normal compression lines of the minced and reconstituted samples, the critical state friction angles and the very small and small strain stiffnesses. The data were normalised where appropriate to account for their different specific volumes, stress states and material characteristics.

In Chapter 5 the different structures of the soils tested are assessed from the results of the Scanning Electron Microscope (S.E.M.) analyses and the data from the laboratory tests are interpreted within this context. The behaviour of soils from within and outside the sliding mass are then compared to assess the changes in the structure of the soil as a result of remoulding within the landslide body. Also given in Chapter 5 are the parameters interpreted from the laboratory tests used for the numerical modelling by Armines-CGI. Finally the conclusions of this thesis and recommendations for further work are presented.

1.1 Summary of the EC Project

As described in the previous section, the research for this thesis formed part of a European Community funded project entitled "Landslide Evolution controlled by Climatic Factors in a Seismic Region: Prediction Methods and Warning Criterion". The aim of the project as the title suggests was to "establish the effects of climatic events on the mechanical behaviour and the stability of soil slopes with special reference to those affected by neotectonic events" (Cotecchia et al. 1996).

This work was carried out in conjunction with Armines-CGI from the Ecole de Mines in Paris, who were responsible for the numerical modelling and the Istituto di Geologia Applicata e Geotecnica from the Politecnico di Bari, Italy, who were responsible for the geological, geomorphological, hydrological and seismical aspects. The Geotechnical Engineering Research Centre at City University were responsible for providing data to assist with classification of the soils in the landslide; to provide Armines-CGI with the input parameters for their numerical analyses and to assess any unusual features of these soils. This work forms the basis for this dissertation. The completed project is contained in a European Community report as part of the Environmental Research Programme (1991-1994) and is referenced in this thesis as Cotecchia at al. (1996). An outline of the parts of the project relevant to this thesis is presented in this section .

A study area was chosen which is located in the Southern Appenines between the provinces of Avellino, Salerno, Foggia and Potenza. Slope instability and earthquakes in this study area have had a drastic effect on the economy of the region and have resulted in the loss of thousands of human lives. The location of the study area is shown in Figure 1.4. Within the large study area, a specific landslide was chosen for a detailed investigation. The landslide site chosen was called the Acquara-Vadoncello landslide, a subsidiary of the Serra Dell'Acquara Landslide, located near the village of Senerchia.

The upper valleys of the Ofanto and Sele rivers have been hit in the past by some strong earthquakes, up to IX or X on the Mercalli scale. For example the 1980 earthquake whose epicentre was located in the upper Sele valley, measured X on the Mercalli scale. This earthquake was responsible for reactivating a number of ancient landslides which included those at Buoninventre, Senerchia, Calitri and Bisaccia. Reactivation usually occurred several days after the main shock. During the course of this two year project the seismic activity at the landslide site was monitored. Three low intensity earthquakes hit the study area. The strongest of these occurred on 3 April 1996 and had a magnitude of 4.3 on the Richter scale. It was felt at Senerchia, which was 20 to 30 km from the epicentre with an intensity of IV - V on the Mercalli scale.

1.2 The Acquara-Vadoncello Landslide

The Acquara-Vadoncello landslide is located on the south-eastern outskirts of the town of Senerchia. It is a subsidiary of the Serra Dell'Acquara slide which is a 2.5 km long mudslide, remobolised by the 1980 earthquake (Cotecchia and Del Prete, 1984). The Acquara-Vadoncello landslide was formed from a reactivation or enlargement of a subsidiary of the Serra Dell'Acquara slide after several days of intensive rainfall on 29 December 1993. It intersects the left flank of the middle to upper portion of the main slide, as shown in Figure 1.5. The slide caused the destruction of about 100 m of a secondary road and the relocation of one family whose house lay 20 m from the head of the scarp at the time the landslide was selected for study (August 1994). In January 1996, the house lay on the scarp and showed large structural cracks.

The Acquara-Vadoncello landslide lies in the upper valley of the Sele River in the Campanian-Lucanian Appenines, at the foot of the Picentini Mountains. The fractured and karstified limestones and dolomites of the Picentini Mountains overlie the clay-rich flyschoid sequences (Sicilide Units). At Senerchia several springs are located at the foot of the steep slopes of the Picentini Mountains, which discharge water into the slopes at rates of up to 200 l/s (Cotecchia et al, 1986).

The sequence exposed in the scarp of the landslide shows the substratum to be a carbonate rich turbidite or flysch with alternations of marlstones, marly clays, marly limestones, sandstones and clay shales. These materials are described in Section 2.3.1. At the head of the scarp there are lenses of what could be called a true 'varicolori' clay which are black, red and yellow-brown fissured clays or argillites. The geological and geotechnical properties of these structurally complex clays or turbidites are discussed in Chapter 2.

A plan and cross-section of the Acquara-Vadoncello landslide are shown in Figures 1.5 and 1.6 respectively. The total length of the landslide was determined to be over 550 m, with a maximum width of 140 m. The difference in elevation between the crown and the tip is 90 m. The average slope angle of the section between the headscarp of the 1993 slide and the side-scarp of the 1980 slide varies from 15° to 20°, reducing to 5° to 12° in the middle section. In the region of 'confluence' or interference between the 1980 and the 1993 slides the average slope of the ground surface slope is less than 5°.

The landslide evolution seems to be characterised by retrogression of the scarp. Monitoring of the scarp retrogression began in the summer of 1994, but the detailed monitoring was only commenced in the summer of 1995. The results of the scarp retrogression determined from this monitoring are shown in Figure 1.7. The retrogression of the scarp was fairly irregular both in space and in time. The major retrogression occurred in the summer of 1995, about 18 months after the initial mass movement. The rate then slowed down over the following winter period and by the end of September 1996 the process of retrogression appeared to be in a stationary state. Cotecchia et al. (1996) were not sure whether this was a result of the natural stabilisation of the slope and proposed further monitoring.

The retrogression of the scarp does not appear to be closely related to periods of rainfall. The major retrogression in the summer of 1994 occurred in a relatively dry period. It did, however, follow large movements in the downslope region in the wetter spring period. The processes were thought by Cotecchia et al. (1996) to be related, but there was a considerable time delay. The seismic events which affected the area did not correlate closely with the landslide movement either. The process of retrogression was therefore thought by Cotecchia et al. (1996) to be controlled by the lithological and structural heterogeneity of the scarp and the rate at which the material was moved from the base of the main scarp.

As part of the detailed analysis of this landslide, a site investigation was carried out. The first phase of the site investigation began in November 1994 and involved the rotary drilling of eight continuously cored boreholes (I1-I4 and P1-P4). The positions of these boreholes are indicated on Figure 1.5. High quality undisturbed samples for the laboratory testing were retrieved from these boreholes using the Osterberg and Mazier tube samplers. The number of good quality samples that could be obtained was limited by sampling problems in these heterogeneous materials. Disturbed samples were also obtained for index testing. In four of these boreholes inclinometer tubes were installed (I1 - I4), whilst in the other four boreholes (P1 to P4) Cassagrande and electrical piezometers were installed at a variety of depths. The large movements experienced by the landslide body in the spring-summer 1995 resulted in the loss of several of the inclinometers and piezometers. Therefore during the second phase of the site investigation, a further seven boreholes were drilled, also indicated on Figure 1.5 and two further inclinometers were installed.

This landslide is thought by this author to be of either a mudslide or a slump earthflow type as classified by Hutchinson (1988) and shown in Figure 1.8. The difference between these two types of slide is the nature of failure at the scarp. The location of the slip surface in the mudslide section was identified from the inclinometer readings. A typical example is shown in Figure 1.9, showing the depth of the landslide at this section to be approximately 17 m below ground level.

CHAPTER 2 LITERATURE REVIEW

2.0 Introduction

The aim of this chapter is to look at the role that structure plays in the behaviour of structurally complex clays. This effect has been considered within the context of the more advanced research on other structured soils.

In order to assess the role of structure, the concept of clay structure and factors influencing its formation have first been considered. Structure was defined by Mitchell (1976) as a combination of particle associations and arrangements (fabric), and interparticle forces. The difference between the behaviour of natural and reconstituted samples was attributed by Leroueil and Vaughan (1990) to the structure of the natural material as the reconstituted samples were considered to be 'destructured'. Cotecchia (1996) however showed that reconstituted samples were not 'unstructured' but instead had a different sedimentation structure to that of the natural soil, as is discussed in Section 2.2.1. The effect of the method of reconstitution on a soil's structure is therefore also examined.

When studying natural soils, Leroueil and Vaughan (1990) highlighted structure as being as important as stress history and porosity (or specific volume) in determining the behaviour of a soil. The effect of the structure on the mechanical behaviour of a natural clay was therefore assessed by comparing the behaviour of natural samples with that of the equivalent reconstituted samples for reference.

Structurally complex clay formations are found over much of Southern Italy. The complex geological origins of the Italian turbidites have resulted in sequences with a wide range of material properties and a great deal of tectonic distortion. These clays have complex structures which exist at a number of scales between the macro- and the micro-scale. The behaviour of these clays is considered within the light of existing research on structured clays.

Finally the effect of landsliding on the mechanical behaviour of clays has been considered by examining cases where comparisons are made between the behaviour of samples of clay from outside and inside the landslide body.

2.1 Soil Structure

2.1.0 Introduction

Structure was defined by Mitchell (1976) as a combination of particle associations and arrangements (fabric), and interparticle forces. This structure may exist at several levels as was illustrated in Figure 2.1 (Collins and McGown, 1974). Mitchell (1993) defined three levels: the micro-fabric which is the aggregations between particles and the very small pores between them; the mini-fabric which is the associations between the aggregates of micro-fabric and the pores between them; and the macro-fabric which considers the interassemblage of particle groups and the corresponding transassemblage pores such as cracks, fissures, laminations and root holes.

Due to the complexity of the soil structure of the structurally complex clay formations which are discussed in this thesis, two scales have been defined for these materials which are slightly different to those defined by Mitchell (1993). The structurally complex soils have a distinctive visible structure at the sample scale, which will be called in this thesis, the 'macro-structure'. The soils from the underlying formation have a scaly macro-structure, whilst the macro-structure of the material from inside the landslide body is characterised by lithorelicts (remnants of the unweathered parent material) in a clay matrix. The aggregations between the particles and the associations between the aggregates were also grouped together for simplicity and called the 'micro-structure'.

The nature of particle interactions in a natural clay has been shown by S.E.M. analyses to be very complex. This complexity is symptomatic of the many influences that affect a clay structure during its formation. Processes which can change the structure of the sedimented clay have been listed in Figure 2.2 (Mitchell, 1993) and include leaching, cementation, weathering, diagenesis, consolidation, wetting/drying, freezing/thawing, shearing and shrinking/swelling. Some of these factors are reviewed in this section.

2.1.1 Clay Mineralogy

Clay behaviour at the particulate level is greatly influenced by the mineralogy. The structures of the basic clay minerals are made up of combinations of sheets of two structural units the silicon tetrahedron and the aluminium or magnesium octahedron. The difference between the clay mineral groups is determined by the different stacking of these sheets and the manner in which successive sheets are held together. Differences between minerals within a group result from isomorphous substitution of the metal ions within the crystal structure (e.g. Fe^{2+} Mg^{2+}). For engineering purposes minerals in a group tend to have similar engineering properties (Mitchell, 1993). Typical clay mineral groupings are shown in Figure 2.3.

Bonding between the unit layers varies between mineral groups but may be sufficiently weak that the physical and chemical characteristics of these clays are controlled by the strength of these bonds. As a result of the substitution of metal ions within the crystal lattice, the unit layers often have a net surface electrical charge. In illites the charge deficiency between the octahedral sheets is balanced by a K^+ cation, which fits in the hole at the base of the silicon tetrahedron and provides a strong bond. A much weaker bond exists between the unit layers in the smectites, which is provided by hydrated cations. These cations can be easily substituted as the result of changes in the chemistry of the soil-water system. A change in the valency of these cations will change the basal spacing, the space between the unit layers. This weak bond is responsible for the swelling characteristics of these soils. Kaolinite has the most stable bonds as hydrogen bonding as well as Van der Waals forces exist between the unit layers. The hydrogen bonding is stable in the presence of water. The chlorites have an organised octahedral sheet between the unit layers which again provides a strong bond.

2.1.2 Particle Associations

The arrangement of particles created during sedimentation will depend on many factors including their mode of deposition; the electro-chemistry at the time of deposition; particle size, shape and gradation; clay mineralogy; exchangeable cations, particularly their valency; acidity; organic content; concentration of sediment and rate of deposition; depth and state of agitation of water; and seasonal drying out (Collins and McGown, 1974).

Particle associations in clay suspensions were described by van Olphen (1977) as being either dispersed (no face to face associations of clay particles), aggregated (face to face associations of several clay particles), flocculated (edge to edge or edge to face association of aggregates) and deflocculated (no association between aggregates) as shown in Figure 2.4. These diagrams are illustrative of the type of particle associations that are theoretically possible.

One factor that influences the tendency to disperse or flocculate is the clay-water electrolyte system. The thicker the diffuse ionic layer the less the tendency of particles to flocculate. When a clay is placed in water, any cations in excess of those required to achieve electrical neutrality of the clay particles go into solution. Because the absorbed cations cause a much higher charge concentration near the particle surface, the cations try to diffuse away from the surface to equalise the concentration in the surrounding fluid. The movement of these cations is, however, opposed by the negative charge on the surface of the clay particle. The charged surface and the adjacent distributed charge are together called the diffuse double layer.

The thickness of the double layer may be greatly affected by the concentration of hydrated cations. O'Brien (1971) looked at the micro-fabrics of kaolinite and illite flocculated in distilled water and in salt water. He showed that kaolinite, which essentially has no net electrical surface charge, had similar fabrics when flocculated in salt water and distilled water (stepped cardhouse). However illite, which flocculated in salt water, had a mixture of edge to face associations and stepped clusters of face to face oriented particles, whilst in distilled water it had an abundance of face to face oriented platelets.

Observations using the S.E.M. have shown that clay particles tend not to exist as single grained fabrics but aggregate together to form domains or groups of face to face oriented particles (Smart, 1971; Barden, 1972). Typical particle arrangements in natural soils are shown schematically in Figure 2.5 (Sfrondini, 1975). Identification of clay particle arrangements from S.E.M. has shown that a number of different types of micro-fabric can exist side-by-side in one soil, although one type of feature may be dominant and control the behaviour.

2.1.3 Changes in Structure Post-Deposition

Post-depositional changes in the structure of a clay can result from a number of physical and chemical processes as were summarised in Figure 2.2 (Mitchell, 1993). Processes which can change the structure of the sedimented clay include leaching, cementation, weathering, thixotropy, diagenesis, consolidation, wetting/drying, freezing/thawing, shearing and shrinking/swelling.

Thixotropy is defined as an isothermal reversible time-dependant process occurring under conditions of constant composition and volume whereby a material stiffens while at rest as a result of changes in the water-cation system surrounding the particles (Mitchell, 1993). Thixotropic hardening may account for the sensitivity of low to medium sensitivity clays (Skempton and Northey, 1952). It differs from diagenesis in that it is reversible.

Cementation may occur in soils that contain carbonates, iron oxides, alumina and organic matter any of which may precipitate at particle joints and act as a cementing agent. Breaking of these bonds can result in a loss of strength.

2.2 The Effect of 'Structure' on the Mechanical Properties of a Clay

2.2.0 Introduction

The critical state framework, developed for reconstituted soils, uses the stress state and specific volume to describe soil behaviour. However when studying natural soils, Leroueil and Vaughan (1990) highlighted structure as being as important as stress history and porosity (or specific volume) in determining the soil behaviour. Structure, which was described as being a combination of fabric and interparticle attractions, accounts for the difference between the behaviour of the reconstituted and the natural soils at the same specific volume and with a similar stress history.

2.2.1 Remoulding and Reconstitution

The difference between the behaviour of the natural and remoulded soils is frequently quantified by the sensitivity of the soil, i.e. the ratio of the undrained strengths of the natural and remoulded soils. Further work has also been carried out to assess the effects of structure on the behaviour of natural soils by comparing the properties of the natural soil with those of the reconstituted soil, normalising to take account of the different stress states and void ratios of the two soils (e.g. Leroueil and Vaughan, 1990; Cotecchia, 1996; Burland et al., 1996).

Burland (1990) suggested that a reconstituted sample should be made from a natural sample which is mixed with water to form a slurry, without air or oven drying the soil prior to mixing. The slurry should have a water content between the liquid limit (w_L) and 1.5 w_L. It is then consolidated, preferably under one-dimensional conditions. Ideally the water used for reconstitution should have a similar chemistry to the pore fluid. Burland called the parameters determined for a soil prepared in this manner as intrinsic, as these parameters were felt to be unique for a given soil type. Intrinsic parameters were denoted by an asterisk.

A remoulded sample should be prepared by vigorously mixing the natural sample at the original moisture content, although this term is sometimes inappropriately used. A remoulded sample is unlikely to have the same structure as the reconstituted sample at the same moisture content and the intrinsic sensitivity will therefore be defined as the ratio of the undrained compressive strength of the natural to the reconstituted soil at the same moisture content.

Mitchell (1993) postulated that the behaviour after remoulding will depend on the strength of the pre-existing fabric units and the mixing effort. The general effects of remoulding are to break down flocculated aggregates, destroy shear planes, eliminate large pores and produce a more homogeneous fabric at the macro-scale. It therefore follows that the behaviour of a reconstituted sample might depend on the effort used in the reconstitution process. Hence the reconstituted properties may not be truly 'intrinsic' as implied by Burland's definition. For example, Cotecchia (1996) noticed that when the Pappadai clay was reconstituted by swelling by immersion in water and mixing at this new water content, it was not sufficient to break down some of the aggregates. Simplistically, the water content at which the soil is mixed could be related

to the remoulding effort. This is because the energy that is required to remould the soil is related to the undrained strength of the soil, which in turn depends on the water content.

To ensure disaggregation of the particles Cotecchia (1996) reconstituted the Pappadai clay by drying the soil at a temperature of 60 degrees, mechanically grinding and then mixing to a slurry with distilled water. Drying can affect the properties of a soil, particularly if the soil contains organic matter or expansive materials (Head 1990). Dry grinding has also been shown to affect the grading of the clay, the features of the clay particles and the clay mineralogy (Picarelli, 1991). Dry grinding and mixing with distilled water is, however, a fairly common method of reconstitution. This method was used by Rampello and Silvestri (1993) to reconstitute samples of Vallerica and Pietrafitta clays; by Rampello et al. (1993) for Vallerica clay; and by Canestrari and Scarpelli (1993) for Ancona clay.

It is proposed here that a fabric that is resistant to disaggregation by unconfined swelling when immersed in distilled water and mixed as a slurry would be the most appropriate base fabric for comparison with the natural soil. It is thought that a base fabric reconstituted in this fashion is stable, homogenous, reproducible and as close to the natural as possible. The base micro-fabric which would be formed in the laboratory after disaggregating the clay particles by dry grinding is likely to be very different from that of the natural material, due to their different flocculation environments.

Burland (1990) and Leroueil and Vaughan (1990) referred to a reconstituted soil as 'destructured'. Cotecchia (1996) however showed that a reconstituted sample had a visible structure and was not in fact 'destructured'. Cotecchia proposed that the difference between the natural and the reconstituted soil was primarily due to the nature, stability and strength of their different structures. In reconstituted clays the bonding was of an electrostatic and electromagnetic nature and stable, whereas with natural sensitive clays the structure included some metastable components. Cotecchia proposed that the difference between the stabilities of their structures could be quantified by the sensitivity or the ratio of the undrained compressive strengths of the natural to the reconstituted material at the same water content.

2.2.2 Compression Behaviour of Reconstituted and Natural Clay

a) 'Intrinsic' Normal Compression Line

The normal compression lines for a number of reconstituted clays were analysed by Burland (1990). He normalised the data by plotting the void index against the vertical effective stress causing the curves to form a single line. The void index gives an indication of the 'intrinsic' compactness of a soil and is similar to the liquidity index. The void index was preferred as the void ratio is compared to measured mechanical properties rather than two essentially empirical tests. It is defined by Equation 2.1:

$$I_v = (e - e_{1000}^*) / (e_{100}^* - e_{1000}^*) \qquad \text{Equation 2.1}$$

where e^*_{100} and e^*_{1000} are the voids ratios of the reconstituted sample at vertical effective stresses of 100 and 1000 kPa respectively during one-dimensional compression. The difference between e^*_{100} and e^*_{1000} was defined the intrinsic compression index (C_c^*).

Cotecchia (1996) showed that the sensitivity of strength was approximately equal to the ratio of the yield stress of a natural sample in compression to the equivalent pressure for the natural water content taken on the intrinsic one-dimensional compression line, as is discussed in Section 2.2.2 (c). Hence the 'intrinsic' normal compression line provides a useful reference line to assess the sensitivity of natural soils. The 'intrinsic' normal compression line, defined by a test on a reconstituted sample, can then be considered as a contour in I_v-log σ_v' space with a sensitivity of one.

Burland (1990) correlated e^*_{100} and the intrinsic compression index C_c^* with the voids ratio at the liquid limit e_L, resulting in the following empirical equations:

$$e_{100}^* = 0.109 + 0.679e_L - 0.089e_L^2 + 0.016\, e_L^3 \qquad \text{Equation 2.2}$$

$$C_c^* = 0.256e_L - 0.04 \qquad \text{Equation 2.3}$$

Burland correlated the data with the voids ratio at the liquid limit rather than with the plasticity index as there was a better statistical fit. There is no theoretical basis for this correlation and it is this author's belief that it is only successful because all the soils

analysed by Burland plotted as a straight line on the Cassagrande A-line chart. These correlations should therefore only be used if the soil to which the correlation is to be applied plots within a similar band on the A-line chart as those analysed by Burland. The correlation derived by Muir Wood (1990), between the compression index of a soil and the plasticity index, may be a useful alternative as it has a theoretical basis.

b) Sedimentation Compression Line

The effect of sedimentation and gravitational compaction was assessed by Skempton (1970), who determined the variation of water content and hence liquidity index with depth for a number of natural soils. Excluded from the study were quick clays, diatomaceous clays, clays containing more than 5% organic matter and clays with a carbonate content of more than 25%. Burland (1990) replotted these data in terms of void index and compared them with the 'intrinsic' normal compression line determined from laboratory oedometer tests. Figure 2.6 shows that the data plot to the right of the reconstituted normal compression line, indicating the different structures of the natural and reconstituted soils, which can result from the changed depositional and consolidation environments. Sedimentation of a marine clay in the laboratory over a period of two and a half years by Bjerrum and Rosenqvist (1956) was shown by Burland (1990) (Figure 2.7) to give a sedimentation line which lay above the 'intrinsic' normal compression line. Leaching was also shown to further increase the sensitivity.

Mitchell (1993) plotted contours of sensitivity for several natural clays on a diagram of liquidity index versus vertical effective stress (Figure 2.8). Cotecchia (1996) proposed a schematic graph similar to Mitchell, showing contours of sensitivity on a graph of void index against vertical effective stress. These sensitivity loci represent different sedimentation curves which result from different sedimentation and post-sedimentation processes. Burland's sedimentation compression line, plotted in the middle of the sedimentation compression curves derived for soils which had sensitivities between 4 and 9 and was therefore considered by Cotecchia (1996) to be the sedimentation compression line for soils with a sensitivity of between 5 and 6.

c) The Effect of Structure on the Compression Behaviour of Clays

The behaviour of natural and reconstituted samples under K_0 and isotropic compression in laboratory tests was investigated by Leroueil and Vaughan (1990). They also found that the natural samples were able to exist at void ratios outside the state boundary surface of the reconstituted soil. Figure 2.9 shows a schematic diagram of the behaviour observed. The natural sample yields to the right of the normal compression line of the reconstituted soil and was followed by large compression strains tending toward the 'intrinsic' normal compression line at high stresses. The region in which natural soils were able to exist outside the state boundary at void ratios greater than those possible for the reconstituted material was termed 'structure permitted space'. The description 'structure permitted space' was based on the assumption that the reconstituted material could be defined as destructured. As shown by Cotecchia (1996), it is only a difference in structure that allows soils to exist at states outside the reconstituted state boundary surface and therefore the term 'natural structure permitted space' would be perhaps more appropriate.

Leroueil and Vaughan (1990) showed that the behaviour of the natural sample post-yield was related to the location of that yield. Yield was defined as a discontinuity in the stress-strain curve under a monotonic stress increase and did not refer to the limit of purely elastic behaviour of the soil. This yield point was related to the onset of fabric instability (Cotecchia, 1996) or destructuration (Leroueil and Vaughan, 1990). Leroueil and Vaughan noted that materials which yield in structure permitted space exhibited large compression strains as the state of the soil tended toward the 'intrinsic' state boundary surface. Large strains were, however, unlikely if yield occurred whilst the soil existed in space allowable for the reconstituted soil.

Leroueil and Vaughan postulated that a natural sample will only reach the 'intrinsic' normal compression line if isotropic compression induces sufficient 'destructuration'. Using a high pressure triaxial apparatus, Rampello and Silvestri (1993) showed that the compression behaviour of natural Vallerica clay, after yielding, did not converge with that of the reconstituted soil, tending instead towards a distinct and parallel normal compression line. Coop et al (1995) showed similar behaviour for Boom clay which they attributed to a different fabric in the natural sample (Figure 2.10). Coop and Cotecchia (1995) suggested that whereas bonding would be removed by increasing isotropic compression bringing the soil state back to the 'intrinsic' compression line,

fabric may have the effect of giving a compression line for the natural soil which was parallel to that of the reconstituted. This is, perhaps, a too simplistic view given the complex nature of clay structure.

The ratio of the yield stress to the equivalent pressure on the intrinsic one-dimensional compression line ($\sigma'_{vy}/ \sigma'_{ve}*$) was used by Burland et al. (1996) as a quantitative measure of the increased resistance under compression of the natural soil over the reconstituted soil. Cotecchia (1996) noted that this ratio was approximately equal to the sensitivity of the natural soil at a confining stress equal to the yield stress in compression.

d) Changes in Fabric with One-dimensional Compression

Tchalenko (1967) proposed that the effect of one-dimensional compression on the fabric of a reconstituted clay was to orientate uncemented clay particles perpendicularly to the consolidation stress. Griffith and Joshy (1990) studied the changes in the fabric of a reconstituted soil as a result of one-dimensional compression with the electron microscope. There was a tendency of particles to orientate, but orientation involved only part of the fabric and a random fabric was still observed in the particle assemblages. Yield occurred when some particle connectors were destroyed and the interassemblage porosity was lost. At higher stresses some reorientation was seen within the assemblages but areas of random fabric orientation still existed.

Quigley and Thompson (1966) looked at the degree of particle orientation in undisturbed and remoulded Leda clay, measuring the peak heights (amount) of illite lying perpendicular to the major principal plane using X-Ray diffraction. Figure 2.11 shows that the degree of orientation of the particles is greater for the remoulded soil. Orientation of the undisturbed sample increased at yield and tended towards that of the reconstituted. Yield occurred at a fairly high water content followed by rapid convergence towards the 'intrinsic' normal compression line. Once fabric instability had been initiated large volumetric strains occur.

Cotecchia (1996) carried out a detailed study of the effects of one-dimensional compression on the micro-fabrics of reconstituted and undisturbed Pappadai clay using S.E.M. analyses. Figure 2.12 shows one-dimensional compression lines for the natural

and reconstituted samples. Yield in oedometric compression was seen to break down the original features of fabric in the natural clay creating a chaotic and irregular fabric post-yield. Further compression reorganised the fabric creating a new regular fabric. Alternatively, oedometric compression of the reconstituted sample to higher pressures resulted in a non-uniform compaction, with chaotic particle arrangements. The micro-fabrics of the reconstituted and natural soils were different at all stress levels and tended to become increasingly so at larger stresses. The variation between the natural and reconstituted fabrics was perhaps accentuated by the aggressive reconstitution technique used by Cotecchia (1996) in which the natural material was dry ground to break down the clay aggregates.

e) Swelling Behaviour of Natural Clays

The effect of structure on swelling behaviour was studied by Schmertmann (1969), who noted that the gradients of the swelling lines of natural material can be much lower than those of reconstituted materials. He noted that the ratio of the swelling line gradients for the reconstituted and natural samples (C_s^*/C_s), which he termed the swelling sensitivity, could be used as an indicator of the influence of fabric and interparticle bonding in the natural soil.

The effect of structure on the swelling characteristics of Gault clay was discussed by Burland (1990), (after Samuels, 1975), who observed that two natural samples of Gault clay were much less expansive than the reconstituted soil (Figure 2.13). This was attributed to a carbonate bonding; the clay had a calcium carbonate content of 30 %. One-dimensional compression was shown to destroy some of the bonding as the natural sample, loaded to 7000 kPa, became twice as expansive as that which had only been unloaded from its in-situ stress. Leroueil and Vaughan (1990) noted that breakdown of a bonded structure may also result when a soil, which contains expansive minerals, is isotropically swelled in the laboratory.

2.2.3 Shear Behaviour of Natural and Reconstituted Clays

a) Peak Strength

Burland (1990) investigated the difference in the shear behaviour of natural and reconstituted samples, by normalising the peak strength values for samples of intact Todi clay with respect to the equivalent pressures taken on the 'intrinsic' compression line, to account for their different stress states and void ratios (Figure 2.14). The equivalent pressure σ'_{ve}, is the vertical effective stress on the 'intrinsic' compression line corresponding to the current void ratio of the soil e, defined by Equation 2.4:

$$\sigma'_{ve}{}^{*} = 10^{\left(\frac{e_{1kPa}{}^{*} - e}{Cc^{*}}\right)} \qquad \text{Equation 2.4}$$

where $e_{1kPa}{}^{*}$ is the intercept of the one-dimensional intrinsic compression line extrapolated to a vertical effective stress of 1 kPa. The peak strengths of the natural soil lay at states outside the 'intrinsic' state boundary surface and this greater strength was therefore attributed to the inherent structure in the natural sample.

Rampello et al. (1993) noted that the increase in strength observed for the natural samples could be the logical consequence of the normal compression line for the natural sample lying to the right of the 'intrinsic' normal compression line. Rampello et al. determined normalised strength envelopes from tests on natural and reconstituted samples of Vallerica clay. Figure 2.15 (a) shows the data for the natural soils normalised with respect to the isotropic normal compression line for the reconstituted material. The normalising parameter p'_e is defined by:

$$p'_e = e^{\left(\frac{N-v}{\lambda}\right)} \qquad \text{Equation 2.5}$$

where N and λ are the intercept of the normal compression line and v is the current specific volume of the sample. Figure 2.15 (b) shows the natural clay data normalised with respect to the isotropic normal compression line for the natural sample, while the data for the reconstituted samples are still normalised with respect to the intrinsic normal compression line. Even when normalised with respect to the relevant normal compression line, the strength data for the natural samples still reach stress states outside the 'intrinsic' state boundary surface. Normalising in this way with respect to

the appropriate normal compression line will account for differences in volume that result from the different particle arrangements of the natural and the reconstituted materials. The remaining increase in strength is then due to the additional shear resistance of the natural structure.

The structure in a stiff clay is thought to result from its geological history. Todi clay is a low to medium plasticity lacaustrine clay of Pleistocene age, which is overconsolidated and highly fissured. Vallerica clay is a medium plasticity, overconsolidated clay, which was deposited in a shallow marine environment. In contrast Coop et al. (1995) showed that the behaviour of natural and reconstituted samples of boulder clays from Chapelcross both gave similar peak strengths. This evidence that structure had little effect for this soil was attributed to the extensive remoulding of the natural soil by ice movements during deposition.

Leroueil and Vaughan (1990) also showed an increased strength for natural soils in comparison to their equivalent reconstituted soils for tests on an artificially bonded material, the Saint Vallier soft clay and an oolitic limestone. Because the peak strength in reconstituted soils is caused by dilation, when the peak strength in the natural materials occurs before the maximum rate of dilation, there must be some effect of the structure.

Quantification of this increased resistance has been assessed in several ways, as shown schematically in Figure 2.16. The simplest is the sensitivity, which is the ratio of the undrained strength of the natural soil to that of the remoulded soil (Skempton and Northey, 1952, Terzaghi 1944), or perhaps more fundamentally the ratio of the undrained strength of the natural soil to that of the reconstituted at the same void ratio (Cotecchia, 1996). Burland et al. (1996) suggested two parameters, the ratio of the cohesive intercepts of the Hvorslev surfaces (AB/AC) on Figure 2.16 and the ratio of normalised strengths at the intrinsic critical state (DE/DF). The former is not recommended by this author as the surface is often curved. Burland et al. (1996) thought that the ratio DE/DF was an indication of bonding. As this ratio takes no account of the different volumetric states occupied by the micro-structures of the natural and reconstituted soils and the curvature of this surface, this is unlikely to be correct.

b) Critical State and Post Rupture Strength

The stress-strain behaviour of a natural sample of Todi clay was analysed in detail by Burland (1990) and is shown in Figure 2.17. He observed a peak strength, which coincided with the formation of a slip surface, following which the stress fell after a few millimetres displacement to a well defined plateau, which he called the post-rupture strength. The post-rupture deformation consisted of a near rigid body sliding on a failure plane.

Atkinson and Richardson (1987) showed that for both drained and undrained tests on heavily overconsolidated reconstituted samples strain localisation often occurred as a result of local drainage. Once localisation had occurred volume changes within the shear zone caused the stress path to fall directly towards a critical state stress ratio instead of moving along the state boundary surface towards the true critical state, as is shown in Figure 2.18. The likelihood of strain localisation increased with the duration of the test, as this increased the possibility for local drainage to occur. As can be seen in Figure 2.18, the samples where strain localised occurred reached the correct critical state line in q':p' space, however they did not reach the correct critical state line in v:lnp' space.

This phenomenon was also evident for drained and undrained tests on natural samples. Viggiani et al. (1993) carried out a series of tests on three different overconsolidated clays to study localisation phenomena. As well as the softening effect of dilation, sensitive soils were found also to be subject to softening due to their fabric instability. Using local gauges to measure the axial displacement, strain localisation was demonstrated to start well before the peak stress ratio (q'/p') was reached, but then increased suddenly at the peak. A mid-height pore pressure transducer showed that the difference in pore pressure between the mid-height and the base for the undrained tests increased gradually until the peak was reached and then dropped suddenly as a result of the local drainage during strain localisation, as has been described by Atkinson and Richardson (1987). Post-peak, the pore pressures equalised throughout the sample.

The post-rupture strength for the Todi clay was found by Burland (1990) to be comparable with the 'intrinsic' critical state line in q':p' space over the range of normal effective stress (σ_v') 100 to 1000 kPa but dropped below the critical state line at larger

confining stresses (Figure 2.19). Similar behaviour was shown for samples of Pietrafitta clay, Vallerica clay and Corinth marl (Burland et al. 1996).

The post-rupture behaviour of the natural samples is comparable with that observed by Atkinson and Richardson (1985) for overconsolidated reconstituted samples. The natural samples reach the critical state line in q':p' space, but the correct critical state is not reached in terms of volume. Even if the post-rupture friction angles of the natural and reconstituted samples are the same, the peak strengths of the natural and reconstituted samples may still be different.

Burland (1990) showed that the operational undrained strength of fissured London clay en masse was close to the post-rupture failure envelope for a back-analysis of large diameter in-situ plate loading tests. This was also found to be the case for undrained tests on 38 mm and 98 mm diameter samples by Marsland (1974). In addition most tests on London clay from Ashford Common gave peak undrained strengths close to the post-rupture failure line. However, some of the strengths measured were somewhat lower. Burland et al. (1996) noted therefore, that for intensely fissured clays, the operational strength of the natural soil may be lower than that of the equivalent reconstituted soil. The behaviour of the intensely fissured structurally complex clays is discussed in the Section 2.3.

c) Normalised Shear Behaviour

Cotecchia investigated the shear behaviour of the Pappadai clay in the triaxial apparatus. Whereas the critical state line was similar in q'/p' space, Cotecchia found that for the Pappadai clay the natural material formed a unique critical state line in v:lnp' space which was different from that of the reconstituted, as shown in Figure 2.20. This is believed to result from the different volumetric states of the micro-fabrics. After yield as a result of shearing, the natural Pappadai clay forms a stable fabric which has a different specific volume to the reconstituted clay at the same stress.

Figure 2.21 shows the normalised shear behaviour of the Pappadai clay in q':p' space. The data was normalised by the equivalent pressure on the respective critical state line, which in this figure is labelled p'_e. She determined similar values of stress ratio at the critical state M = 0.91 for the reconstituted material whereas values of 0.78 to 0.93 were

determined for the natural material. Again the natural material was able to achieve states outside the state boundary surface of the reconstituted material, as was seen for the Todi clay by Burland (1990) and for the Vallerica clay by Rampello et al. (1993). The boundary between the zones of contractant (dry side) and dilatant (wet side) behaviour in normalised stress space was not the reconstituted critical state line, at a stress ratio of 0.85, as is the case for the reconstituted soil, but occurs at a stress ratio (q'/p') of 1.08, as indicated in Figure 2.21. Structural differences between the natural and reconstituted soils therefore exist even at the critical state. The stress-strain behaviour of the natural sample was considered to be mostly frictional, as there were linear flow rules for both the drained and undrained behaviour, i.e. the stress ratio q'/p' was proportional to the plastic strain increment ratio ($\delta\varepsilon_v^P/\delta\varepsilon_s^P$). Any non-frictional elements were attributed to structural degradation. The different flow rules for the drained and undrained behaviour are an unusual feature as it is difficult to understand how the soil knows whether it is subject to drained or undrained loading. The consequence of this would be that the soil would have an infinite number of flow rules depending on the nature of the loading. As there were a large number of assumptions made to determine the plastic strain increments, this unusual conclusion needs verification for other soils.

Cotecchia (1996) showed that yield in isotropic compression prior to shearing resulted in a reduction in the size of the normalised boundary surface, although the critical state stress ratio remained constant. As normalising with respect to the void ratio on the critical state line of the reconstituted sample did not produce a unique boundary surface during post-yield compression, she proposed normalising also with respect to yield stress.

2.2.4 Pre- Failure Deformations

Atkinson and Sallfors, (1991) showed that the stress-strain behaviour of soil is highly non-linear almost over the complete range of strains. Figure 2.22 shows their idealisation of the graph relating shear modulus with shear strain. There is a very small range of strains (typically less than 0.001 %) over which the shear modulus is approximately constant and has a value of G'_o or G'_{max}. This value is typically measured either statically using accurate local triaxial instrumentation or dynamically using a resonant column apparatus or piezo-ceramic bender elements. The small strain

region over which the stiffness is highly non-linear is typically between 0.001 and 1 % strain, and is therefore highly relevant to most engineering applications.

Viggiani (1992) investigated the effect of mean normal effective stress, p' and the effective overconsolidation ratio (R_o) on the shear modulus of the soil. The relationship was defined by a power law:

$$G/p_r = A(p'/p_r)^n(R_o)^m \qquad \text{Equation 2.6}$$

where p_r is used as a reference pressure of 1 kPa to keep the parameters A, n and m non-dimensional. The parameters A and n vary with strain magnitude as is shown in Figure 2.23. The parameter n varies from a value in the range 0.6 to 0.9 for G_{max}, depending on the plasticity of the soil, increasing to a value of 1 at a shear strain of about 1 %. This value of n = 1 indicates a direct relationship between the shear modulus and the mean normal effective stress, depicting a frictional material. The parameters A, n and m each vary with plasticity. The variation of these three parameters with plasticity index within the very small strain region is shown in Figure 2.25.

The parameter R_o is defined as the ratio of the maximum mean normal effective stress to which the soil has been subjected to the current mean normal effective stress ($p'_{max}/p'_{current}$). If the maximum mean normal effective stress is not known or if the soil has been subjected to some change in volume without moving along the state boundary surface, for example as a result of creep, p'_{max} is assumed to be the intersection of the current swelling line of the soil with the isotropic normal compression line.

a) Very Small Strain Behaviour - G_{max}

Bender element tests on reconstituted and natural samples of London clay (Figure 2.25), by Viggiani and Atkinson (1995a) showed a straight line in log:log space for the correlation between the shear stiffness (G_o) normalised with respect to the small strain shear modulus of a normally consolidated sample at the same mean normal effective stress at the same value of (G_{onc}) and the overconsolidation ratio (R_o). The authors concluded that for the London clay tested the stiffness is dependent on overconsolidation ratio and current stress, and is unaffected by structure.

Rampello and Silvestri (1993) determined values of G_0 for natural and reconstituted samples of Vallerica and Pietrafitta clays using resonant column-torsional shear (RC-TS) equipment. Figure 2.26 shows a plot of G_0/p'_e against p'/p'_e for the Vallerica clay in which the equivalent pressure p'_e is taken on the intrinsic normal compression line. The values for the natural samples lie above those for the reconstituted. The difference between these two sets of points was found to be equivalent to the difference in volumes between the reconstituted and natural normal compression lines and when the data were normalised with respect to the appropriate normal compression line, the two sets of data were found to be coincident (Figure 2.26(b)). There was no difference in the behaviour of the two different sets of natural samples of Vallerica clay, identified on these figures as natural (1990) and natural (1992). The first set of samples were swelled or compressed from the initial mean normal effective stress after sampling, whilst the latter were first compressed to $p' = 800$ kPa before being unloaded. The reconstituted samples were also consolidated to $p' = 800$ kPa before unloading.

Three sets of samples of Pietrafitta clay (Figure 2.27) were also tested: reconstituted, natural (1992) and natural (1990). The test procedures were the same as those used for the Vallerica clay. The authors observed higher values of G_0/p'_e even when the appropriate normal compression lines were used for normalisation. They concluded that this difference was accounted for by interparticle cemented bonds. The values of G_0/p'_e for the natural (1992) samples were consistent with those of the reconstituted. The authors suggested that for this soil, yielding in swelling erased the effects of this type of structure on soil stiffness. Unfortunately the normal compression line for the natural material was only assumed in their analysis as neither set of natural samples was compressed to sufficient stresses to be able to identify its position.

There is therefore no consistent effect of structure on the shear modulus of these stiff clays. The London clay samples showed no effect of structure on the stiffness properties measured. The Vallerica clay also showed no effect of structure on the stiffness parameters, when the data were normalised with respect to the relevant normal compression lines. However the Pietrafita clay showed an increased stiffness of the natural soil even when normalised with respect to the appropriate normal compression line. Whilst all these samples showed some effects of structure on their material behaviour at larger strains, only the structure of the Pietrafita clay affected the very small strain stiffness.

b) Small Strain Behaviour

Figure 2.28 shows undrained stiffness data for natural and reconstituted samples of Boom clay at strains of 0.01% and 0.1% (Coop et al., 1995). The values of G_u have been normalised with respect to $(p')^n$ and also with respect to M, as the stress ratio at the critical state changed with stress level. The mean effective stresses p' have been normalised with respect to the Hvorslev equivalent pressure p'_e, using the appropriate intrinsic or natural normal compression line, as the normal compression lines of the natural and reconstituted Boom clay were parallel. Although there was some scatter in the data, there was no clear distinction in the stiffnesses of the natural and reconstituted samples, which indicates there was no effect of structure other than on the volume.

Cotecchia and Chandler (1997) also found no differences between the small strain stiffnesses of natural and reconstituted samples of Pappadai clay. They did however find that the parameter m (Equation 2.6) did not appear to be constant at higher overconsolidation ratios. However at medium strains the differences became more noticeable.

Figure 2.29 shows a typical variation of shear modulus with strain for samples of Vallerica and Pietrafitta clays for both reconstituted and natural samples using the resonant column and torsional shear tests (Rampello and Silvestri, 1993). The difference between the cyclic and dynamic testing was more pronounced for the natural samples. This was thought to be due to the influence of cyclic loading and strain rate effects. When the shear moduli were normalised with respect to G_0, there was little variation of the normalised shear moduli with consolidation stress. Rampello and Silvestri also looked at the threshold shear strain, which was defined as the value of strain where stiffness is no longer constant. They showed that the reconstituted samples yield at higher strains than the natural, and that the yield of the latter is also more rate sensitive.

2.2.5 Residual Strength

a) Introduction

The residual strength is achieved when a soil is sheared along a discrete plane to large displacements. The soil particle mechanism of failure at the residual strength was shown by Lupini et al. (1981) to be either turbulent, transitional or sliding. The type of

mechanism was controlled by the particle shape, size and intergrain friction. Sands or soils with predominantly rotund particles failed with a turbulent motion, whereas clays with platy particles failed with a sliding mechanism. The transitional mechanism was a combination of both the sliding and turbulent mechanisms.

The turbulent mode of failure occurs in samples of predominantly rotund particles, where failure occurs by rolling and translation, as direct sliding is prevented by interlocking. Theoretically this occurs at the critical state, where shearing occurs at constant stress and volume. The residual friction angle for samples failing in a turbulent fashion was found typically to be greater than the value of interparticle friction and is also usually greater than 25°.

Platy particles were found to fail with a sliding mechanism. As the clay was sheared along a discontinuity, the displacement caused the particles to align relative to the shear surface, allowing the soil to strain soften. If sheared to large enough displacements, the particles will eventually become parallel to the slip surface, giving a limiting value or the residual strength. The residual strength is then controlled by the value of interparticle friction.

Lupini et al. (1981) hypothesised that the expected mechanism of failure should be a function of the granular void ratio e_g, which is the ratio of the volume of platy particles and water in the soil to the volume of the rotund particles, defined by Equation 2.7:

$$e_g = \frac{\text{volume of platy particles and water}}{\text{volume of rotund particles}} \qquad \text{Equation 2.7}$$

Their results are summarised in Figure 2.30. The granular void ratio is not however a simple parameter to measure for a natural soil as it requires the mineralogy of the soil to be known. The clay size fraction cannot be used alone to determine this parameter as it may contain both platy and rotund particles.

Kenney (1967) showed that the mineralogy of the grains was the most important factor determining the residual strength of soils. The mineralogy controls the particle size, shape and intergranular friction. He also found that changes in the pore water chemistry could effect the residual strength measured.

b) Variation of Residual Strength with Normal Stress

Lupini et al. (1981) and Kenney (1967) are among a number of authors who have noticed an increase in the residual friction angle at low stresses so that the failure envelope is curved, as can be seen in Figure 2.31. Skinner (1969) showed with tests on glass ballotini at a normal effective stress of only 6 kPa, that the apparatus effects were negligible and could not account for this observation.

The increase in the residual friction angle at low effective stresses was thought to occur because failure did not occur purely as a sliding mechanism. Mitchell (1993) suggested that less work may be required to shear the particles without complete reorientation than was required to orientate particles during shear, resulting in a transitional failure mechanism.

c) Variation of Residual Strength with Strain Rate

Lemos (1991) investigated the effect of strain rate on the residual strength of soils. The effect of increasing the strain rate was found to have either a positive, negative or neutral effect on the residual strength. The effect of the strain rate may be important for landslides subject to seismic activity.

A neutral rate effect was found in soils of rotund particles. Although a slight increase in the peak was detected for faster rates of shearing, this was followed by a reduction to the same value of residual strength angle as was measured for slow strain rates.

For soils composed predominantly but not entirely of clay particles, increasing the strain rate increased the residual strength. This was attributed to the disruption of the alignment of the platy particles in the shear zone by massive particles. The maximum disturbance and hence strain rate effect was noted for soils with a clay fraction of around 50 %.

For soils with clay fractions of between 5 and 40 % the result of increasing the strain rate was to reduce the residual strength. This behaviour was the most critical as it could have a dramatic effect on the stability of a landslide when sheared at fast rates. This behaviour was typically associated with materials which have a transitional mode of

failure when sheared with a slow strain rate. The decrease in strength was attributed to an increase in porosity in the shear zone. This increase in specific volume was demonstrated by Lemos (1991) using coloured water in the water bath of the ring shear apparatus which was found to migrate into the shear zone during shearing. The shear zone was determined to be in equilibrium without significant excess pore pressures during the phase of rapid shearing. When shearing was stopped the shear zone tried to contract and excess pore pressures were then generated.

d) Correlations of Residual Strength with Index Properties

Many authors have proposed correlations between residual strength and various index properties such as the liquid limit, plasticity index or clay fraction. Lupini et al. (1981) summarised the correlations that have been proposed between clay fraction or plasticity index and residual strength. These are shown in Figures 2.32 and 2.33. As can be seen, there is a large variation between the correlations.

Stark and Eid (1994) proposed a correlation based on liquid limit, clay fraction and normal effective stress, which recognised the non-linearity of the residual strength envelope and the fact that neither liquid limit nor clay size fraction alone adequately describes the particle size and shape.

As previously mentioned, the residual strength is controlled primarily by the particle size and shape and interparticle friction, all of which will influence the mechanism of failure. As stated by Kenney (1967), the mineralogy of the grains strongly effects the residual strength and will control the interparticle friction, particle shape and to some degree the particle size. Correlations will only work if they adequately describe these factors.

As the interparticle friction controls the residual strength when the failure mechanism is by sliding, the clay fraction should be a good indicator of the residual strength when the clay size fraction is kaolin, muscovite or chlorite as they all have similar angles of interparticle friction of 10 - 12 degrees. However if some of the clay size fraction was composed of rotund particles, the residual strength measured would be likely to be higher than the correlation. Figure 2.34 shows the residual friction angles determined for different clay and quartz mixtures. The illite and quartz mixtures have much higher

residual friction angles than the montmorillonite and quartz mixtures for the same clay fractions. The residual strength of the soil mixtures containing sodium montmorillonite and no salt also showed little change in the friction angle for clay contents larger than 20%. Additionally the plasticity index for kaolin is lower than that for illite but it has a lower residual friction angle. Therefore the curves for plasticity index against residual friction angle for these two common minerals will not be concurrent.

Another problem encountered when comparing index properties with residual strengths for clay shales, has been in the determination of the liquid limits for aggregated soils. Clay shales are highly overconsolidated clays with varying degrees of diagenesis. Mesri and Cepeda-Diaz (1986) found that the liquid limits determined for some shales could be increased by a more violent breaking up of the aggregates. Disaggregation, which is a breaking down of aggregates to their constituent particles, was found to increase the liquid limit and the clay fraction significantly. However, the effect on the residual friction angle was not determined as the residual strength was only measured for samples which had been disaggregated by air drying and ball grinding. Chandler (1966, 1969) found a higher clay fraction in the shear surface following triaxial tests and reversal shear box tests on Keuper Marl, indicating some disaggregation during shear. There has been much work published about the structurally complex clays that has shown this effect of aggregation on the liquid limits and this is discussed in detail in Section 2.3.2.

2.3 Structurally Complex Clays

2.3.0 Introduction

A literature review was carried out to assess the mechanical properties of clays of the structurally complex formations in Italy. The behaviour of these materials is of much concern, as the prevalence of landslides within these formations has resulted in a large number of fatalities and significant economic problems within the study area. The complex geological origins of the Italian turbidites has resulted in sequences with a wide range of material properties and a great deal of tectonic distortion. The review has therefore focused on the more clayey formations with a lapideous (stone) content of less than 20 %, which were thought to be more relevant to the stability of the landslide. The

effects of soil structure on the behaviour of these clays is assessed by comparing their properties with those of corresponding reconstituted samples.

2.3.1 Geological Origin and Classification

Structurally complex clay formations are found over much of Southern Italy. Their complex geological history has resulted in a wide variety of materials, with both geological complexity and geotechnical complexity. Geotechnical complexity refers to a heterogeneity in geotechnical parameters and geological complexity is caused by mineralogical and structural features. The geology of the study area was shown in Figure 1.4

The Italian turbidites are an example of a geotechnically complex formation (D'Elia, 1991). They were originally deposited on the continental shelf, and were subsequently transported as turbidity currents at high density and velocity and then deposited on the continental scarp, forming widespread submarine fans. The intense deformations due to subsequent tectonic activity have resulted in a highly structured material. Modern theories for the geology in this area suggest that the formations have been displaced horizontally by distances of more than 100 km from their sedimentation position to their current location (A.G.I. 1985).

As a result of their complex genesis, the turbidites are composed of a variety of materials with different mechanical properties. They usually consist of an argillaceous or pelitic component, which is often fissile and sheared, with a low mechanical strength, together with a lapideous or rock component, which may be arenaceous, calcareous or marly and has a higher strength. The Italian turbidites were subdivided by the A.G.I. (1979) into three main groups; calcareous-pelitic formations, pelitic formations and arenaceous-pelitic formations, whose characteristics are summarised in Figure 2.35.

Attempts have been made to classify the macro-structural features. Esu (1977) defined the types of structural complexity in the Italian turbidites in Figure 2.36. Group A was composed of homogeneous materials which were jointed (A1) or sheared (A2). The second group B had a lapideous component with ordered (B1), disarranged (B2) or chaotically arranged (B3) blocks. The fine grained component was sometimes jointed and frequently fissured. The soils in group C were the result of weathering or softening

of these materials, giving a soil of hard lithorelicts in a clay matrix. The lithorelicts are remnants of the unweathered material. A classification for the pelitic formations was proposed by D'Elia (1991) (Figure 2.37) who characterised the structural complexity using the percentage of the lapideous component and the amount of tectonic distortion, ranging from ordered to disarranged to chaotic.

Guerriero et al. (1995) categorised the structure of a variegated clay as one of four types. These consist of reconstituted (type α), bonded but not fissured (type β); intensely fissured clay shales (type γ) and softened shales (type δ). The latter consists of intact lithorelicts in a clay matrix. Sketches of types γ and δ are shown in Figure 2.38.

D'Elia (1991) summarised the features of macro-structure which affect the behaviour of structurally complex clays (Figure 2.39). The nature of the clay shale component was controlled by the mineral composition, diagenetic bonds, and fissuring and/or shearing. The nature of the lapideous component was controlled by the continuity of the rock layers and the size and shape of the rock fragments. The combined structure of the material was also controlled by the percentage of the rock fragments and their distribution.

The Sicilide Units, which form part of the pelitic formation, typically have weak diagenetic bonds and have structures of the types B2 and B3 as defined by Esu (1977) in Figure 2.36. The Acquara-Vadoncello landslide, which was studied in detail for this project, was comprised of these materials. In these variegated shales, the tectonic deformation has affected the bulk of the formations, leaving the soil generally chaotic and disarranged. The clay mass is formed of aggregates of plates whose sizes are of the order of 1 cm which are in turn comprised of smaller plates of the order of 1 mm or less, giving these soils their scaly appearance. The shear lenses have smooth polished sides and may show a weathered coating (Cotecchia et al., 1977). The lenses are iso-orientated (orientated in the same direction), but the predominant orientation may change within a few centimetres. Typical mineralogies for the variegated clay shales of Central Southern Italy are given in Figure 2.40. The scaly clay shales are unusual within the context of other structured clays, as they are both bonded, having elemental aggregations of bonded particles as a result of diagenesis, and discontinuous, being constituted of small fragments (Cicolella and Picarelli, 1990).

The Liguride Units, which form part of the calcareous-pelitic formations typically have stronger diagenetic bonds and lower plasticities than the Sicilide Units and may have structures of the types B1, B2 or B3, as defined by Esu (1977). The research presented in this thesis has focused on the behaviour of the Sicilide Units, which compose the geology of the site studied. Comparisons are made however with the behaviour of the Liguride Units.

2.3.2 Mechanical Behaviour

Structurally complex clays often consist of intact lithorelicts in a clay matrix. The two components may have very different mechanical properties. D'Elia (1991) investigated numerically the effect of increasing the lapideous component on the overall mechanical behaviour. The model consisted of cubic blocks of rock set regularly in a clay matrix. By assuming linear elastic parameters both for the soil and the rock, the overall shear and bulk moduli were determined. The overall shear modulus and bulk modulus used, which were referred to on Figure 2.41 as G_0 and K_0, were not the very small strain stiffnesses, but a linear approximation of the appropriate stress-strain curve. Figure 2.41 shows a graph of the overall shear modulus and bulk modulus, normalised with respect to those for the clay shale alone, plotted against the rock fraction. The influence of a rock fraction of less than 20% was considered to have a negligible influence on the overall behaviour. Given this assumption, the geotechnical characterisation of these soils can be based on laboratory samples of the matrix soil, which for these materials are the clay shales.

The lapideous fraction did, however, effect the measurements made of water content (Iaccarino et al., 1995 and Hutchinson, 1988). The water content of the matrix was significantly greater than the overall water content and could therefore lead to problems when normalising the stress-strain behaviour of the soil with respect to volumetric state (Figure 2.42).

a) Index Properties

Index properties for the Sicilide and Liguride clay shales of Southern Italy are plotted on a plasticity chart in Figure 2.43. The plasticity indices typically lie slightly above the

A-line, indicative of clays, with liquid limits of 20 to 130 %. This wide range of plasticities is typical of a geotechnically complex sequence, by definition. The wide range of materials results from their complex geological origin.

Index properties for the variegated shales of Southern Italy have been shown to be greatly affected by the sample treatment method (Rippa and Picarelli, 1977; Airo'Farulla and La Rosa, 1977; Bertuccioli and Lanzo, 1993). The index properties determined were found to depend on the degree of disaggregation and hence on the method of sample preparation. The effect of a more violent destructuration, by mechanical means on the index properties obtained, is demonstrated in Figure 2.44. The effect of this mechanical destructuration was to break down some of the aggregates of particles, increasing the clay fraction of the materials (Rippa and Picarelli, 1977; Bilotta and Umilta 1981; Bertuccioli and Lanzo 1993). The increase in the liquid limit is related to the increase in the clay fraction as can be seen in Figure 2.45, where the percentage change in the liquid limits is plotted against the percentage change in clay fraction using data from Rippa and Picarelli (1977).

b) Compression Behaviour

i) Intrinsic Compression Line

There has not been much work published in the literature which has determined the compression lines for reconstituted samples of structurally complex clays. Guerriero et al. (1995) determined the one-dimensional compression line for a single reconstituted sample of M. Marino clay in the oedometer and the isotopic normal compression line for a sample of reconstituted Bisaccia clay in the triaxial apparatus. Picarelli (1991) gives the reconstituted one-dimensional compression lines for Fiumarella clay shale and Laviano clay shale. The validity of the correlations between plasticity index and compressibility proposed by Mitchell (1976) is assessed for these materials in Figure 2.46. Although the correlation works well at lower plasticities, the data point for the Bisaccia clay appears to lie significantly below the correlation line. One of the problems with this correlation is that it ignores the curvature of the normal compression line. The stress range over which the gradient is determined using the correlation is approximately 2 to 200 kPa, which corresponds to the undrained strengths at the liquid and plastic limit. This range is lower than that over which the gradient of the corresponding compression line is usually determined.

To assess the validity of Burland's correlations (Equations 2.2 and 2.3), Figure 2.47 shows the void ratio at the liquid limit, plotted against the coefficient of compression (C_c*) and the void ratio at a vertical effective stress of 100 kPa (e_{100}*) for the published data on reconstituted structurally complex clays. A value of specific gravity of 2.74 was assumed in plotting these data, which was the value determined for soils from the landslide site at Senerchia. There are fewer data points plotted on these graphs than were plotted in Figure 2.46, as liquid limit data were not published for all the oedometric compression tests. The problem with the assessment of the validity of these empirical correlations is accentuated by the variation of the Atterberg limits with the method of preparation, particularly the liquid limit, as was discussed in the previous section. However, the Burland correlations provide a reasonable agreement with the data determined for the structurally complex clays.

In addition to the change in Atterberg limits with preparation method, from Figure 2.46 it can be deduced that the reconstitution method is also likely to greatly affect the behaviour of the reconstituted soil in compression, because of the change in C_c with plasticity index. The reconstitution method used by Guerierro et al. (1995) for the Bisaccia and M. Marino clays was to air dry the natural material and mix it to a slurry at a water content of 1.5 times the liquid limit. The natural and reconstituted samples of the Bisaccia clay tested by Guerriero et al. (1995) had plasticity indices of 127 and 104 % respectively. Similarly the natural, softened and reconstituted samples of M. Marino clay had plasticity indices of 27, 23 and 20 % respectively. The softened material was material that had been remoulded within the landslide body. The difference in the plasticity of the natural and reconstituted samples of the M. Marino clay could account for a difference in the coefficient of compressibility of 35 % based on the correlation proposed by Wood (1990) ($\lambda = 0.595\ I_p$).

ii) Compression Behaviour of Natural Samples

In order to assess the effect of structure on the behaviour of a natural sample it is useful to compare the behaviour of each natural sample with that of the corresponding reconstituted sample. Due to the lack of tests that have been carried out on reconstituted samples, Burland's empirical correlations discussed in the previous section have been used where required and when index data were available. The correlation proposed by

Wood (1990) was not used, as it only gives a correlation for the coefficient of compressibility and not e_{100}^* which is also required to locate the intrinsic normal compression line. Although the use of correlations instead of real test data is not ideal, the correlations do give a good approximation. Figure 2.48 shows the normalised compression data available from the literature for the natural samples, plotting the void index as defined by Equations 2.2 and 2.3 and discussed in Section 2.2.2 (a).

It is apparent that most samples do not reach the intrinsic compression line at the stresses used in the tests. Instead, most tend to form compression lines parallel to but below the intrinsic compression line. It cannot therefore be concluded from the available data whether the natural compression lines would eventually reach or cross those of the reconstituted soil. One possible hypothesis for the unusual compression behaviour observed in Figure 2.48 is that the effect of the aggregation of particles on the compression behaviour of a natural soil is to lower the position of the compression line. This hypothesis would be in agreement with the observed increase in Atterberg limits with disaggregation.

For these structurally complex clays, gross yield, defined by Leroueil and Vaughan (1990) as a discontinuity in the stress-strain behaviour under monotonic loading, was seen to occur for compression within the intrinsic state boundary surface. This yield can be attributed to the onset of structural degradation. The effect of yield on the swelling index of the Laviano clay shale was examined by Picarelli (1991) and is shown in Figure 2.49. There is a progressive structural breakdown with increasing maximum pressure, as can be concluded from the increase of the swelling index. The ratio of the swelling indices between natural and reconstituted samples of the same soil was shown by Schmertmann (1969) to be an indication of the degree of influence of structure, as was discussed in Section 2.2.2 (e). This breakdown of structure as a result of compression and swelling can eventually result in the natural soil reaching void ratios larger than the initial undisturbed value.

c) Shear Behaviour

The shear behaviour of undisturbed samples of structurally complex clays is generally contractant and ductile, sometimes with a small peak followed by a slight reduction in strength. (A.G.I., 1985). This is unusual given their high overconsolidation ratios.

Examples of materials, which exhibit this behaviour include the Bisaccia clay shale (D'Elia, 1991, Guerriero et al., 1995), the Santa Barbara clay shales (D'Elia, 1991), the M. Marino clay (Guerriero et al., 1995, Guerriero, 1995), the Roseto clay shale (Bertuccioli and Lanzo, 1993) and scaly clays from Bifarera and Piano Campo (Bilotta and Umilta, 1981).

In order to assess the effect of structure on the behaviour of these materials, it is useful to compare the results with the reconstituted behaviour. Again there has been very little work published that has looked at the behaviour of reconstituted structurally complex clays. Guerriero et al. (1995) have compared the behaviours of natural and reconstituted samples of M. Marino and Bisaccia clay shales, whilst Iaccarino at al. (1995) compared the large strain behaviour of natural, softened and reconstituted samples from a landslide in scaly clay. As before, the 'softened' clay shales described, comprised materials that had softened as a result of remoulding within the landslide body. Due to the variability of the materials locally within the structurally complex formations, it is also important to compare the behaviour of each natural sample with the corresponding reconstituted sample and not with a single reconstituted sample for the whole site as they have done.

As discussed previously in Section 2.2.3 (b), Burland (1990) noted that the post-rupture strength of fissured London clay was consistent with or slightly below the post-rupture failure line and the critical state line determined for the reconstituted soil. As these structurally complex clays are intensely fissured and the size and orientation of these fissures is small relative to the size of the sample and also randomly oriented, there is not usually a scale effect on the strength measured. As most samples tend to reach a plateau and peaks are only seen at higher confining stresses, not considered here, the peak and the post-rupture friction angles will therefore be considered to be coincident. The friction angle only drops towards that of the residual state at much larger displacements than are considered here. It is therefore proposed to compare here the peak friction angle of the fissured samples with the critical state friction angle defined by reconstituted samples.

As very little data were available for the strength of reconstituted materials, the peak friction angle for the natural samples and the reconstituted critical state friction angles have both been plotted against plasticity index in Figure 2.50. These peak friction angles have been obtained from the triaxial data assuming a zero intercept, to allow

correct comparison with the reconstituted critical state angles. The results in Figure 2.50 show that the intrinsic friction angle of the material typically lies slightly below the those predicted from the plasticity index using the correlation for clays in general proposed by Mitchell (1993). The peak friction angles for the natural samples have a larger scatter but are consistent with the intrinsic critical state friction angle. This result is similar to that observed by Burland, who noted that the post-rupture stress ratio of the natural soil is similar to that of the reconstituted critical state.

The apparent failure of the natural samples at a critical state stress ratio is similar to the strain localisation behaviour observed by Atkinson and Richardson (1987) for overconsolidated reconstituted clays, however the mechanism of localisation for the fissured soil is thought to be very different from that of a reconstituted soil. On reaching the state boundary surface, the stress paths of the overconsolidated reconstituted samples did not tend towards their true critical states, but instead the strains tended to localise so that the peak friction angle was less than might have been expected. Localisation however occurs in these fissured clays at a much lower stress ratios because the planes of localisation are pre-existing and are not formed during the test and so it is possible that the states of the samples head directly towards a critical state ratio with no peak at all. Although the post-rupture or critical state friction angles are the same for the reconstituted and natural samples, the peak strength of the reconstituted samples are however higher than those of the fissured samples.

The strengths of the natural samples can be seen to be lower than those of the reconstituted at a similar value of p'/p'_e, as is clearly demonstrated in Figure 2.51 (Guerriero et al. 1995) by normalised shearing path data for the natural and reconstituted M. Marino clay. The data are normalised with respect to an equivalent pressure, p'_e taken on the normal compression line for the reconstituted samples, thus accounting for differences in the void ratios and stress states of the various samples. Neither the natural nor the overconsolidated reconstituted samples reached critical states, as on reaching the appropriate state boundary surface, the samples did not dilate sufficiently to reach their critical states and strain localisation occurred. The reason the natural samples have lower strengths than the reconstituted samples is not because they have lower post-rupture or critical state friction angles, but as they do not dilate to give a peak, as the reconstituted samples did.

The difference between the peak strengths of the natural and reconstituted samples was more pronounced for the Bisaccia clay data which are plotted in Figure 2.52. At lower values of p'/p'_e, less than 0.4, the stress ratio of the soil at failure coincided with the critical state ratio. This reduction in peak strength was attributed by Guerriero et al. (1995) to slipping along discontinuities, upon which the strength tended towards a residual state. At higher values of p'/p'_e the friction angles of the natural material fall further below those of the reconstituted.

The reduction of the stress ratio at failure at higher values of p'/p'_e was believed to be the result of higher confining stresses. The friction angle could reduce as a result of the scales being sheared through at higher stresses to form a more planar shear surface. At lower stresses, shearing along the fissures is thought to be prevented by interlocking of the scales, as there is not sufficient energy to shear the aggregates. This process may occur either at the macro- or the micro-level. A similar behaviour has been observed in ring shear tests carried out by Picarelli (1991) on the natural and reconstituted clay as will be discussed in the following section.

d) Residual Behaviour

There have been a large number of ring shear tests published on the structurally complex clays due to the landslide-prone nature of this region. A number of results from the literature have been plotted on graphs of residual friction angle against clay fraction and plasticity index, shown in Figures 2.53 and 2.54 respectively. Also plotted are the correlations from the literature that were summarised by Lupini et al. (1981). The data generally plot within the limits given by the correlations. The scatter is not unexpected given the wide range of materials; small local variations between the properties of the soil used in the tests for the index properties and the tests for the residual strength; the changes in the Atterberg limits and clay fractions with preparation method; and the different testing methods used to determine the residual strength.

The influence of preparation method on the residual strength properties has also been investigated. Iaccarino et al. (1995) determined the residual strength of intact and reconstituted samples of a clay shale from the Basento Valley. The residual friction angles of the intact samples ranged from 8.1° to 10.0°. These were higher than those measured for the reconstituted samples which ranged from 5.5° to 7.3°. Similar results

were observed by Picarelli and Viggiani (1988) for a clay shale from a site near Melfi and Cotecchia et al. (1992) for clay from Senerchia and Buoninventre. Picarelli (1991) also observed a difference between the residual friction angles of intact and reconstituted samples of Laviano clay shale, measured using either direct or ring shear tests (Figure 2.55). The difference between the natural and reconstituted samples decreased with increasing normal stress. Aversa et al. (1993) attributed this behaviour to the different size, shape and angularity of the grains or particle aggregations for the natural and reconstituted samples. This hypothesis is consistent with the test data of Fenelli et al. (1982), who found similar residual friction angles for samples sheared perpendicular to and parallel to the scales for the Laviano clay shale. It is however different from the conclusions of Chandler (1966, 1969), for the Keuper Marl who found that the silt size aggregations of clay particles break down within the residual shear surface. As was discussed in Section 2.2.5 (b) Mitchell (1993) suggested that at lower stress levels, less work may be required to shear the particles without complete reorientation than was required to orientate particles during shear. Similarly it could also be suggested that at lower stress levels, less work is required to shear the aggregated particles without particle breakdown and reorientation at lower stress levels than is required to shear through the clay aggregates.

Lemos (1986) carried out direct and ring shear tests on two reconstituted samples from the Sierra Dell'Acquara slide at Senerchia. The results are shown in Figure 2.56. Residual friction angles of 7.8° and 5.7° were obtained by assuming a linear residual failure envelope. There is a noticeable increase in the residual strengths determined using the direct shear apparatus, compared with those from the ring shear apparatus. This is likely to be the result of incomplete orientation of particles along the slip surface due to changes in direction in the former apparatus. Tika (1989) investigated the effect of shear rate on the residual strength of a sample of clay from Senerchia. A residual friction angle of 4.6° to 5.0° was measured for slow shearing which increased to an angle of greater than 6.8° when the sample was sheared at 133 mm/min. A positive strain rate effect would increase the stability of a failing landslide during a seismic event.

2.4 Changes in Soil Properties as a Result of Landsliding

2.4.0 Introduction

The aim of this section is to assess the effect of landsliding on the geotechnical characteristics of these materials, focusing on the role that structure may play in the behaviour of a slope and how the structure of the soil may change as a result of landsliding. Due to the complex nature of these soils and their history, a preliminary method of assessing their behaviour is to compare the behaviour of material pre- and post-failure i.e. within and outside the landslide body. A review of landslides in structurally complex clays has not been attempted.

The geotechnical behaviour of landslides was divided into four stages by Leroueil et al. (1996), pre-failure, failure, post-failure and reactivation. At the pre-failure stage the soil is essentially intact. Large movements can still occur at this stage as a result of cycles of effective stresses. Failure is characterised by a continuous shear band through the slope. The friction angles mobilised at failure back-analysed from first-time slides in London clay correspond well to the critical state value (Skempton, 1977; Silvestri, 1980). This agrees well with the laboratory tests on natural samples which show that the post-rupture friction angles also lie close to the intrinsic critical state angle. For the intensely fissured clay shales found in this region the peak friction angle at lower overconsolidation ratios was shown in Section 2.3.2 (c) to be much lower than that at the corresponding critical states and so it might be expected that the same conclusion might not hold. Landsliding in the structurally complex clays is often a result of reactivation of existing slide and the strength along the shear surface is therefore likely to be controlled by the residual friction angle.

The post-failure stage includes movements just after failure until the landslide essentially stops. D'Elia et al. (1996) considered these post-failure movements simply from a consideration of the energy dissipated. The available potential energy (E_p) of a soil mass at failure is dissipated as the frictional energy (E_f) required to keep the soil mass moving along the shear surface and an energy release as a result of strain softening, as shown in Figure 2.57. This energy released was assumed to be dissipated in breaking up and remoulding the moving material (E_d) and accelerating it to a certain velocity (E_k). The differences between the rates of movement pre- and post-failure of two Italian slides at Allori and Bomba are shown in Figure 2.58. The brittle Bomba

clay had much faster post-failure movements than the ductile Allori clay. It is not clear whether the degree of remoulding would also vary in this way.

There has been very little work on the remoulding effect of landsliding, which will effect the behaviour of the material within the landslide body. Leroueil at al. (1996) noted that the ability of a clay to be remoulded depended on the height of the slope and the physical and mechanical characteristics of the clay. Very little work has been done on the energy required to remould a clay. Tavernas et al. (1983) showed that for a laboratory study of Eastern Canadian sensitive clays the energy required to remould the soil to a remoulding index of 75% increased with plasticity index (Figure 2.59). The remoulding index (I_r) was defined by Equation 2.8:

$$I_r = 100 \times \left(c_{u\,int\,act} - c_u\right) \Big/ \left(c_{u\,int\,act} - c_{ur}\right) \qquad \text{Equation 2.8}$$

where c_u is the undrained shear strength of the clay and $c_{u\,intact}$ and c_{ur} are the undrained shear strengths of the intact and remoulded clays respectively. Leroueil at al. (1996) stated that the structure of the formation is fully remoulded within the landslide body. Although there was found to be a remoulding of the large scale structure, it was concluded that there was still a macro-structure of the soil within the landslide body, as the landslide debris was observed to consist of lithorelicts in a clayey matrix. However, it is not clear to what degree the structure of the clay forming the matrix had been remoulded and this has been examined in Chapter 4, by comparing the behaviour of the material from inside and outside the Senerchia landslide.

2.4.1 Material Properties

(a) Fabric

The effect of remoulding on the landslide material can be seen visually by observing the materials inside and outside the slipped mass. The fissured clay shale described by Guerriero et al. (1995) as type γ is very different from the softened shales of the landslide debris again called type δ. As will be seen for the landslide examined here, the debris again consists of intact lithorelicts in a clay matrix. Sketches of types γ and δ are shown in Figure 2.38.

(b) Water Content

Changes in the water content of the soil within the landslide body have been observed by Iaccarino et al. (1995) for slides in the Bassento valley, Guerriero et al. (1995) for the M. Marino clay and Picarelli and Viggiani (1988) for a slope near Melfi, but were not seen by Baldassare et al. (1996) at Scalo di Trivigno. Changes in the water content in the vicinity of the shear surface were also observed by Iaccarino et al. (1995) and Guerriero et al. (1995). There are a number of difficulties with measuring the water content of a mudslide fabric as were highlighted by Hutchinson (1988) and demonstrated for the structurally complex clays by Iaccarino et al. (1995) (Figure 2.42). The water content of the matrix is higher than the overall water content, because of the lapideous component. Difficulties also arise when measuring the water content of the structurally complex clays due to the difficulty of sampling. The effect of the variability of the material properties could be reduced by comparing the liquidity indices. These data were not however available.

c) Index Properties

Baldassarre et al. (1996) compared index properties of materials inside and outside a landslide. Typically landslide deposits had a lower plasticity than the formation and lower activity but similar clay fractions and bulk densities. This was attributed to erosion of the more fine-grained materials near the surface and the remoulding of a greater variety of the formation materials into the clay matrix within the landslide body. The smaller range of index properties between samples tested from within the landslide deposits compared with those from the formation material may be due to the increased homogeneity of the landslide material, but could simply be related to the different number of samples tested; 6 samples from the landslide debris compared to 13 from outside the landslide. Picarelli and Viggiani (1988) noticed no difference between the activity and plasticity of samples from inside and outside a landslide near Melfi.

The changes in the material properties due to the variability of these materials and the difficulty of sampling do not allow any firm conclusions to be drawn. There is no evidence of a substantial increase in the plasticity of the materials due to a breaking down of the particle aggregates for the soils within the landslide body. It is therefore suggested that the remoulding due to landsliding is insufficient to break down the

aggregations (i.e. the micro-structure of the soil), as occurred during the Atterberg limit tests on vigorously remoulded samples, discussed in Section 2.3.2 (a).

d) Permeability

The degree of remoulding of the structure of these structurally complex clays in a landslide was demonstrated by Iaccarino et al. (1995) for clay shales from the Bassento valley by comparing the permeability of the intact material with that of the reconstituted. The permeabilities of both the landslide body and the formation were much higher than that of the reconstituted soil whereas the permeability of the shear zone was much closer to that of the reconstituted. The difference was thought to result from the presence of fissures in the formation increasing the overall permeability of the soil. These fissures were not visible in the shear zone and were thought to be erased by the remoulding of the soil within the shear zone.

e) Compression Behaviour

Guerriero (1995) and Guerriero et al. (1995) looked at the mechanical properties of soil from an active landslide in the Bassento valley, located about 18 km south-east of Potenza. The Masseria Marino clay is part of the Argille Varicolori formation. They compared the mechanical properties of soil samples from the landslide body, the shear surface and the unsoftened material from outside the slide with the behaviour of the reconstituted samples.

Figure 2.60 shows the behaviour in compression of four different samples of M. Marino clay subjected to cyclic oedometer tests. One was unsoftened (type γ) from outside the landslide, one was from the landslide body (type δ), one was from the shear surface (type δ) and one was reconstituted. The swelling index (C_s) increases with the degree of destructuration. The swelling indices of the softened materials (type δ) lie between the reconstituted and the type γ behaviour. The material in the shear zone was largely destructured and showed behaviour similar to that of the reconstituted. This sample of the softened clay crossed the intrinsic compression line and reached a compression line parallel to that of the reconstituted. The difference between the position of these two lines, which should represent the different structures of the natural and reconstituted

materials, may be affected by differences between the nature of the materials comprising these samples, as a result of the heterogeneity of soils within the landslide. Only one reconstituted sample was tested for the whole landslide. It may also be affected by the difficulty of assessing the void ratio of these inhomogeneous materials, as was demonstrated in Figure 2.42 (Iaccarino et al., 1995).

f) Shear Behaviour

Figure 2.61 shows the normalised shear behaviour of the M. Marino clay. The data were normalised with respect the equivalent pressures (p'_{eq}) taken on the normal compression line for the reconstituted samples. The shear strengths of the natural samples (type γ) were shown to be greatly affected by the natural discontinuities in the samples, which caused strain localisation in the samples before they reached the state boundary surface, so that they did not dilate along the boundary surface to the critical state. Samples retrieved from inside the landslide body (type δ) reached a higher stress ratio than the samples from the formation. The higher stress ratio achieved for the sample from inside the landslide body was attributed to an eradication of the scaly macro-structure of the formation material by landsliding, and hence a reduction in the number of discontinuities within the sample.

Remoulding due to landsliding was therefore thought to removes the macro- and not the micro-structure. The micro-structure was not broken down as a result of landsliding as aggregates still existed in the soils from the landslide body. The macro-structure could be seen to have changed visually from a macro-fabric (type γ) that was scaly outside the landslide to one that consisted of lithorelicts in a clay matrix (type δ) in the landslide body.

2.5 Summary

The effect of structure on the behaviour of a natural clays may be assessed by comparisons with the behaviour of corresponding reconstituted samples, as was shown for clays in general in Section 2.3 and for structurally complex clays in Section 2.4.

Cotecchia (1996) emphasised that reconstituted samples were not "destructured" as had been suggested by Leroueil and Vaughan (1990), but instead had a different fabric to that of the natural material. The aim of reconstitution is therefore not to produce a destructured soil but to create a homogeneous material with a stable base fabric. It was also suggested here that, ideally, the base micro-fabric, while fulfilling these conditions, should be as close as possible to the natural material in order to be an appropriate reference material.

By comparing the behaviour of natural samples of a structurally complex clay to that of corresponding reconstituted ones, it was shown that structure can have a negative effect on the soil behaviour, as well as the positive one usually seen. Figure 2.48 shows the normal compression lines for a number of structurally complex clays, normalised using the void index. The normal compression lines for the natural samples appear to plot to the left of those of corresponding reconstituted samples. This negative effect of structure was felt to result from the aggregations of soil particles in the natural material resulting in a less open micro-fabric than the reconstituted soil. A negative effect of structure was also seen for the shear behaviour of samples of M. Marino and Bisaccia clay shale, shown in Figures 2.51 and 2.52. The natural samples failed before reaching the intrinsic state boundary surface. This negative effect was felt to result from the fissured nature of these materials at the scale of the macro-fabric which promoted strain localisation in the samples before a critical state was reached.

The residual strength of these structurally complex clays was also shown to be affected by structure producing an increase in the residual strength of these materials particularly at low stresses. An effect of structure on the residual strength was thought to be related to the stability of the base micro-fabric.

CHAPTER 3 LABORATORY EQUIPMENT AND TEST PROCEDURES

3.0 Introduction

The experimental work looked at index tests, ring shear tests and triaxial tests carried out on samples retrieved during the site investigation. The soil testing focused on the more argillaceous materials as these are likely to control the stability of the landslide. They also form the greater part of the stratigraphy particularly in the scarp region. The testing programme set out to establish: the index properties to assist with the classification of the soils; the material parameters of a range of soils; and whether the soils exhibit any unusual behaviour. This chapter describes the equipment modifications and test procedures that were implemented for this research.

Triaxial tests were carried out on natural and reconstituted samples to determine strength and stiffness parameters for these soils. Due to the complex nature of the natural soil, preparation methods had to be developed to allow the triaxial samples to be trimmed. Another difficulty associated with the testing of these materials was their very low permeability, which greatly increased the duration of the tests. The test times of up to five months increased the possibility of transducer drift and the likelihood of a test loss. The number of tests that could be carried out was also restricted, even when ten different triaxial apparatus were used during the course of this project. The main modifications to these apparatus were to improve the quality of the data at the beginning of shearing to obtain small strain stiffness measurements of high accuracy.

Ring shear tests were carried out in the Bromhead and Bishop ring shear apparatus to determine the soil residual strength. The Bishop ring shear apparatus was instrumented and a data acquisition system was added to allow automatic logging of the data.

As was discussed in Section 2.3.2, Rippa and Picarelli (1977) highlighted the variability of Atterberg limits with preparation methods for these structurally complex soils. Therefore a series of Atterberg limit, ring shear and triaxial tests was carried out on corresponding minced and reconstituted samples to determine the effect of different degrees of destructuration on the material properties. The vigorously remoulded or minced samples were prepared by passing the soil through an industrial food mincer, whereas the reconstituted samples were prepared using a low energy method, swelling the natural soil by immersion in distilled water.

3.1 Index Testing

Basic soil tests were carried out on soil samples retrieved during the site investigation to determine fundamental soil properties and assist with the classification of materials across the site. Tests were carried out according to BS 1377 and Head (1990) to determine the Atterberg limits, particle size distributions, carbonate contents, organic contents, specific gravities and water contents of the samples. In order to increase the quantity of results that could be obtained, some of the Atterberg limits, the particle size distributions and the carbonate and organic contents were contracted out to Laing Technology Services (L.T.S., 1995).

The Atterberg limits of a structurally complex clay were shown by Rippa and Picarelli (1977) to be highly dependent on the preparation method, as was discussed in Section 2.3.2. Tests were carried out to determine this effect of preparation method and hence the degree of destructuration on the behaviour of these soils. The preparation methods used included a "standard" method, reconstitution, mincing and subjecting the soil to ultrasound, as described below.

Tests were carried out by Laing Technology Services and at City University, in accordance with BS 1377 Part 2. The soils were not dried, and particles larger than 425 μm were removed by hand. The liquid limit tests were conducted using the cone penetrometer four point method. Both liquid limit and plastic limit test procedures are described by Head (1990).

A *standard* preparation procedure was developed at City University for preparing the liquid limit samples. The soil was broken into small pieces and placed in a watertight bag with sufficient de-aired water to bring the sample to a water content slightly lower than the liquid limit. The soil was then allowed to swell overnight. Next, the sample was vigorously remoulded and the soil was again left to hydrate overnight, before the liquid limit test was carried out.

In order to assess the destructuring effects of reconstituting samples for the triaxial tests, comparative index tests were carried out on samples prepared using the standard and reconstituted preparation technique. The preparation method for the *reconstituted* sample was the same as that used for the reconstituted triaxial samples. The soil was cut

into pieces and placed in a bowl with sufficient water to bring the water content to around 1.1 to 1.5 times the liquid limit and the soil was allowed to swell overnight. The soil was then placed in a mechanical mixer for about two hours until a homogeneous slurry was formed. Any clumps of unmixed material, if formed at the bottom of the mixing bowl, were broken down by passing through a 1.18 mm sieve. The sample was then de-aired by placing it in a vacuum chamber. The water content of the slurry was reduced to a value at which the Atterberg limits could be measured by compressing in a consolidometer. The soil was thoroughly remoulded before testing to remove any induced structure from this one-dimensional loading.

The effect of a more vigorous preparation technique was investigated by mincing the soil with an industrial food mincer. The soil was remoulded as it passed along a screw conveyor 100 mm long with a diameter of 50 mm and passed out through grill holes of 8 mm diameter. The minced samples were fed through the mincer a specified number of times at a given moisture content, usually at approximately the plastic limit. Moisture content samples were taken throughout the mincing, to ascertain if moisture was lost due to the heat generated during the mincing. To counteract any possible moisture loss, the barrel of the mincer was periodically cooled by holding it under cold running water, taking care not to wet the sample. The soil was also sprayed with distilled water to counteract any possible drying. The minced material was then prepared for the liquid limit test using the same method as the standard preparation method.

It was suggested by one of the Italian co-workers on the E.C. project, that destructuration could be achieved by ultrasounding, without the need of significant mechanical energy. Therefore an ultrasounded sample was prepared by breaking the soil into small pieces and placing it in a sealable bag with sufficient distilled water to bring the sample to approximately 1.1 to 1.5 times the liquid limit. The soil was then allowed to swell overnight, before being remoulded and then placed in the ultrasonic bath for a period of approximately three hours. The water content of the slurry was finally reduced by compression to a value at which the Atterberg limits could be measured. The soil was again thoroughly remoulded before testing to remove any induced structure.

3.2 Triaxial Apparatus

3.2.0 Introduction

Triaxial tests were carried out on natural, reconstituted and minced samples to determine their strength and stiffness parameters. Different preparation methods were used to assess the role that structure plays. The natural samples were trimmed from 'undisturbed' samples taken during the site investigations, the reconstituted samples were made from the trimmings and the minced samples were prepared from trimmings passed through an industrial food mincer to vigorously remould the material. Tests were predominantly carried out on 38 mm diameter samples in hydraulic triaxial cells, similar to that described by Bishop and Wesley (1975).

Eight different Bishop and Wesley triaxial cells were utilised during this research project. A large number of apparatus were used because of the unusually long duration of each test. The time taken for one triaxial test on a reconstituted sample was five months. Each triaxial apparatus was slightly different: two different types of data logging/control system and two different types of air pressure controllers were used and also the local instrumentation varied between apparatus. A high pressure triaxial apparatus, of the type described by Taylor and Coop (1990), was also used to test at cell pressures of up to 5 MPa. The features of the different apparatus control systems and local instrumentation are summarised in Tables 3.1 and 3.2 respectively.

The main improvements to the triaxial systems, made for this project, focused on the internal instrumentation. Local axial gauges were added to most of the apparatus. A radial strain belt was designed and built for cell 9 and mid-height pore pressure transducers were added to cells 6 and 7. Due to the very long durations of the tests, particularly on the reconstituted samples, eight different triaxial apparatus were upgraded.

3.2.1 Standard Pressure Triaxial Apparatus

The standard tests were carried out using hydraulic stress path apparatus, similar to the type described by Bishop and Wesley (1975), with control systems similar to those described by Atkinson and Evans (1985). These computer controlled apparatus had the

ability to control the radial, axial and back pressure, whilst datalogging the stresses and axial and volumetric strains. Axial and radial pressures were applied through air-water interfaces, with a maximum air pressure of approximately 800 kPa. A 50 cc capacity volume gauge made by Imperial College acted as an interface for the back pressure.

Two different computer control systems were used to log and operate the triaxial cells. The 'BBC' system used a BBC microcomputer with a Spectra Micro - MS analogue to digital converter, whilst the 'PC' system used an IBM compatible computer with a plug in interface card which acted as an analogue to digital converter. The 'BBC' and 'PC' systems used electromanostats to control the pressure, whilst cells 2 and 10 used electro-pneumatic pressure regulators. Figure 3.1 shows a schematic diagram of the control system for the triaxial cells. This figure also shows a schematic for the bender element system which was used in cells 4 and 10 and the high pressure cell.

The 'BBC' system was used with cells 4, 7, 8 and 9. A Spectra Micro MS interface, manufactured by Intercole Systems Ltd, carried out an analogue to digital conversion on a 12 bit basis, automatically selecting the gain from eleven ranges to match the input from the transducer as closely as possible. This improves the resolution of the transducers provided they are used at positions close to their electrical zero. The resolution and accuracy of the transducers is discussed in Section 3.2.3. The Spectra had 32 analogue input channels available. The axial, cell and back pressures in the system were regulated by electromanostats which were driven by incremental stepper motors. The stepper motors were operated by relays, which were in turn controlled by the computer.

The 'PC' system was used with cells 2 and 6. The systems used an IBM compatible 286 or 386 computer with a Alpha Super Interface Card, manufactured by CIL. The CIL card acted as an analogue/digital and digital/analogue converter and had 8 analogue inputs, 4 analogue outputs and 4 relay outputs. As the CIL card only allowed a fixed gain to be selected via the software for each channel, the software was used to autorange, increasing the resolution of the transducer when used close to the electrical zero, as discussed in Section 3.2.3. A 'PC' system was also used with cell 10. However, this system used two data translation (DT) cards (Jovicic, 1997), which fulfilled a similar function as a CIL card.

In cell 6 the CIL card regulated the pressures using electromanostats controlled by relays in the interface card. As the CIL cards had only 4 relays and a total of 6 were required to control the cell, axial and back pressures, the back pressure was controlled manually because it was in any case often kept constant during tests. In cells 2 and 10 the pressures were regulated by electro-pneumatic regulators, controlled using the computer directly through the analogue output channels of the interface card.

Control of the pressures with the analogue-pneumatic converters was much more accurate than for the electromanostats, where the smallest stress change was limited to one step of the stepper motor; approximately ± 0.4 kPa. The minimum stress increment for the analogue-pneumatic pressure converter is theoretically limited to the resolution of the digital-analogue conversion. The electromanostats were however preferred for such long tests as pressure was not lost in the event of power failure, for example through loss of the battery power backup.

Axial loading could be carried out using stress or strain control. Stress controlled loading was applied using the pressure regulators acting through the air-water interface; strain controlled loading was applied using a motorised Bishop ram. This was placed between the air-water interface and the axial loading cylinder, with a valve to disconnect this closed volume system from the air-water interface. A stepper motor with a gear box on the Bishop ram was used to load or unload the sample at a constant strain rate controlled by the computer or a timed relay (clicker box).

3.2.2 High Pressure Apparatus

The high pressure tests were carried out in a high pressure apparatus with a cell pressure capacity of 5 MPa. The apparatus was similar to that described by Taylor and Coop (1990), but had been modified to include an internal load cell to measure the deviatoric force. An internal load cell was used as it was not subject to the friction between the axial loading ram and the o-ring in the top of the apparatus or the force of cell pressure acting on the ram.

A schematic of the high pressure system is shown in Figure 3.2. Water was used as a cell fluid due to its comparative ease of use. The axial load was applied using an axial hydraulic piston mounted on the top of a more conventional triaxial apparatus, as a

bellofram could not be used at the high pressures required to apply the axial stress. The axial, radial and back pressures were controlled hydraulically which allowed a complete range of stress paths to be applied. The stresses and strains were measured using conventional load cells, pressure transducers, displacement and volume gauges, each with appropriate ranges.

The cell pressure and axial pressure were applied though air-water and oil-water interfaces in the standard pressure range (0-800 kPa). The air pressures were regulated by electro-pneumatic regulators, controlled by an IBM compatible 286 computer, similar to the 'PC-system' used in the standard pressure apparatus. As was seen in cell '2' the regulators could be controlled directly through the analogue output channels of the interface card.

Pressure multipliers were used to achieve pressures above 800 kPa. The multipliers increased the air pressure that was applied by factors of approximately 8 and 12 for the axial and radial pressures respectively. Back pressures were always applied in the standard pressure range through a 50 cc volume gauge, which acted as an air-water interface.

Shearing was carried out under a constant rate of axial displacement using the motorised loading frame, with which the sample could be loaded at different rates, varying from 0.0001 to 5 mm/min.

3.2.3 Instrumentation

The standard instrumentation for the Bishop and Wesley cells consisted of an internal load cell to measure the axial load, two pressure transducers to measure the back pressure and the cell pressure, an LVDT to measure the external axial displacement and a volume gauge to measure the volumetric change. Details of the local instrumentation that was also used in each cell are given in Table 3.2. Most of the cells were fitted with internal axial strain gauges; cells 6 and 7 were fitted with mid-height pore pressure transducers; cells 7 and 9 were equipped with radial strain belts and cells 1, 4 and 10 and the high pressure cell were fitted with piezo-ceramic bender elements.

The reliability of the instrumentation was assessed for typical transducers in Table 3.3 by considering their accuracies and resolutions. Due to the large number of apparatus and hence transducers used, the resolutions and accuracies quoted are the typical values for each transducer type from Cuccovillo (1995). The accuracy of a transducer can be defined as the closeness with which the readings measured approach the true value and will be affected by noise, non-linearity, hysteresis and drift. The resolution is defined as the smallest change in mechanical input which produces a measurable change in output.

The noise is the electrical disturbance to the signal of the transducers arising for instance from the connections, small fluctuations in the power supply, temperature changes and interference of magnetic fields caused by the equipment. The electrical noise is related to the electrical system and is not a function of the output of the transducer and hence can be expressed in the units measured by the transducer. It was checked during calibration by holding the transducer under a given load, pressure or displacement and observing the fluctuation in the readings.

Hysteresis is the variation in the output of a transducer at the same stress, load or displacement after following a loading-unloading loop and is usually expressed as a percentage of full scale. The hysteresis was checked during calibration and was generally more problematic for load cells and pressure transducers. The non-linearity is the maximum variation of the output of the transducer from the best fit line through the data over the calibration range expressed as a percentage of full scale. This was again determined during calibration.

The drift of the electrical zero with time under conditions of constant load pressure or displacement can also cause errors in the transducer measurements. The drift of the load cells was simply checked by comparing the zero condition at the beginning and the end of each test. Due to the unusually long test durations, the drift of the load cells was found to be particularly problematic in some of the tests and errors greatly in excess of the typical values given in Table 3.3 were occasionally observed.

As previously stated the resolution is the smallest change in the mechanical input which produces a measurable change in output. The resolution depends on the gain selected by the data logger for the voltage input from the transducer, the number of bits over which the A/D conversion is operated and the calibration constant. In the PC system the output voltages from the transducers can be read over three scales, ±10V, ±1V or

±100 mV. The number of bits over which the analogue:digital conversion is operated is 16 bits. Hence the resolution when the data is read over the ±10 Volt scale would be 10 Volts / 2^{15} multiplied by the calibration factor, whereas the resolution read over the ±100 mV scale would be 100 times better or 100 mV / 2^{15} multiplied by the calibration factor. In the BBC system the transducers could be read over 11 ranges down to ±20 mV, however the number of bits over which the analogue:digital conversion was operated was only 12 bits.

Auto-ranging was used in all the systems to increase the resolution of the data close to the electrical zero. In the BBC system the micro spectra did this automatically. In the PC systems as a fixed gain had to be specified for the logging of each channel, this was achieved by rewriting the software. Auto-ranging was used to find the maximum gain (or minimum range) at which the input voltage could be read. This was achieved by reading the output voltage from each transducer with successively decreasing gains (or increasing scales) until the voltage could be read. Hence when the transducers were set to their electrical zero at the beginning of each shear stage, they could be read at the maximum gain and hence have the maximum resolution and accuracy. The speed of logging was also quicker when the transducers were close to their electrical zero, as the autoranging routine in the program started by reading the output voltage with the maximum gain, and proceeded by decreasing the gain until the transducer output could be read.

Design of the instrumentation initially focused on the need to increase the accuracy of the instrumentation at the beginning of shearing to allow the small strain stiffness to be calculated. Additional problems were also addressed which arose due to the very low permeability of the soil which greatly increased the lengths of the tests.

The axial load in the Bishop and Wesley type cells was generally measured with 5 kN internal load cells, manufactured by Maywood Instruments Ltd, based on the design by Surrey University. Internal load cells were used so the axial load measurements would not affected by friction on the shaft. The load cells were self compensating to account for changes in the cell pressure. In order to increase the resolution of the load cells, cells 2, 6, 8 and 10 and the high pressure cell were fitted with RDP S7-DC signal amplifiers. To maximise the resolution at the beginning of loading, the electrical zero was positioned so that it coincided with zero deviatoric load. A major problem was however caused in a few tests by faulty load cells whose electrical zero drifted with time

(up to 1.5 kPa per day). This problem was exaggerated by the very long duration of the tests, which increased the magnitude of the drift seen at the end of the test and reduced the possibility of repetition of the test, due to insufficient time. Faulty load cells were replaced when detected, but it was only possible to detect a drift in the load cell at the end of the test, when the suction cap was disconnected. In order to utilise data where it was not possible to repeat the test, if drift occurred, it was assumed that the drift varied linearly with time. In the latter stages of the testing programme, for some tests either a half ball connection was used between the sample and load cell during shearing (see Figure 3.11) or the suction cap was not connected until much later in the test, to reduce the significance of this effect. This was a compromise as it meant that no measurements of small strain stiffness could then be made. Measurements of cell and back pressure were carried out using two Druck pressure transducers with a range of 0 - 1000 kPa.

The external axial strain was measured in each apparatus with an LVDT displacement transducer, type 500A, manufactured by RDP Electronics Ltd. This gauge had a 25 mm linear range. Baldi et al. (1988) summarised the sources of error in external strain measurements as shown in Figure 3.3. External measurements can be corrected for the deformation of the apparatus and the seating error by carrying out a compliance test on an aluminium sample. A suction cap was used to force alignment of the sample, prior to the start of testing. Isotropic compression of the sample after connection of the suction cap and before the start of shearing should cause sufficient deformations in the sample to eradicate the bedding errors and the disturbance caused by connection. Whilst the use of a suction cap was found to be suitable for the reconstituted samples, it was not ideal for the natural samples. The natural sample would have needed to be saturated at an effective stress lower than that in-situ, in order that the sample could have been sheared at the estimated in-situ stress level, as sufficient compression is required after the suction cap has been connected and prior to the start of shearing to erase the disturbance caused by this connection. This cannot be done if the connection is made at the same confining stress (i.e. that in-situ) that is to be used during shearing. The alternative of saturating the sample at a lower confining stress would however have lead to swelling of the sample which can cause considerable destructuration, as was shown by Clayton et al. (1995).

The volumetric strain was measured using an Imperial College 50 cc capacity volume gauge. The volume gauge consisted of a freely moving piston in an accurately machined cylindrical steel vessel. The piston was sealed at both ends with rolling

belloframs. When compressed air was applied to the lower diaphragm, an equal pressure was transferred to the pore fluid in the upper bellofram. The volume gauge was therefore able to apply a back pressure, acting as an air-water interface. As water flowed into and out of the sample, the piston moved freely up or down. The change in the position of the piston was measured with an RDP LVDT, type 500A, as was used to measure the external axial strain. The displacement of the piston was calibrated to determine the volumetric strains. Leakage tests were carried out on dummy steel samples prior to testing to establish if there were any leaks in the volume gauges or drainage systems. Various combinations of the seals, belloframs and valves were replaced to eradicate any leaks found. One particularly troublesome volume gauge, even after considerable work to eradicate a leakage problem, continued to have a small leak of approximately 0.01 %/day. In order to utilise this apparatus, it was decided to correct the volumetric strain at the end of each test stage for this leakage. This procedure was believed to be acceptable as the volumetric strains were generally very large for these tests. The leakage of all the triaxial cells was again checked periodically during the testing programme.

The volume gauges were found also to be susceptible to fluctuations in temperature, even in a temperature controlled laboratory and daily fluctuations in the volumetric strain readings of up to 0.01% were recorded. Test stages, where the accuracy of the data was critical were therefore carried out at night or at the weekend, when temperature fluctuations were less severe. A radial strain belt was also built for one apparatus to check the reliability of the volume gauge data, by comparing the readings made by the volume gauge with the volumetric strains that could be calculated from the internal axial and radial strain measurements, as discussed later in this section.

At the beginning of a shearing stage, both the volume gauge and the external axial LVDTs were positioned at their electrical zero to increase the resolution and accuracy of the transducer along with the speed of logging. The time required to log each channel using the autoranging routine of the PC system or the automatic autoranging of the BBC system will be controlled by the number of scales over which the input voltage is read. The autoranging routine first read the output over the smallest scale and if the voltage was too large the voltage was then read over subsequent scales until the correct scale was found. Hence the speed of logging was fastest when the transducers were placed close to their electrical zero and the instrumentation was only read over one interval.

Local axial strain gauges were installed on most of the triaxial cells. They provided the most accurate measurement of axial strain as they are not subject to the compliance of the apparatus nor seating or bedding errors. The strains were measured over a gauge length, i.e. the distance between the two mounts of the transducers, of 50 mm. The mounts were glued to the samples, using Loctite super adhesive, instead of pinning, as it is difficult to push pins into the natural samples as they can contain intact lithorelicts (undecomposed remnants of the parent material) or stones. For the tests on the reconstituted samples which often took several months, the risk of leakage due to inadequate sealing of the holes was considered too high. Relative movement between the membrane and the sample was in any case unlikely at these pressures (Kim et al. 1994). The two types of local axial transducers which were used were the Hall effect transducers described by Clayton and Khatrush (1986) and the miniature LVDTs described by Cuccovillo and Coop (1997). A schematic diagram of the Hall effect local axial gauge is given in Figure 3.4.

The miniature LVDTs installed as part of this project were model D5/200, manufactured by RDP. The 10 mm linear range was considered small enough to give the accuracy required whilst allowing the entire stress-strain curve to be defined. A schematic diagram of the local gauge set-up is shown in Figure 3.5. The mounts were glued to the sample 50 mm apart and the LVDT was slid into the top mount and fixed in the desired position using the grub screw. In order to allow the armature to pass through the LVDT at large strains, the threads on the non-sensitive end of the armature were removed by machining. The armature rested on the bottom mount. The submersible cables to the LVDTs were coiled with copper wire to allow them to be bent into the desired position, when the transducer was positioned on the sample. The LVDTs were used with S7-AC amplifiers to increase their resolution. The resolution was further increased at the beginning of shearing by adjusting the zero potentiometer in the amplifier to the electrical zero.

Miniature pore pressure transducers were used to determine the pore pressure at the sample mid-height. As the external pore pressure transducer was connected hydraulically to the back pressure during drained loading, it could not give any indication of possible excess pore water pressures in the sample. Data from the first couple of tests on reconstituted samples showed large volumetric strains at the end of the isotropic loading stages, even though the loading rate of 1 kPa/hour was about the slowest rate that was practical with this apparatus. Mid-height pore pressure transducers

were therefore installed as part of this project to ascertain if these volumetric strains were the result of creep or equalisation of pore pressures in the sample. The pore pressure transducers were PDCR81s, manufactured by Druck, with a 700 kPa range. The PDCR81 mid-height probe was used with a specially constructed latex membrane, with a protruding nozzle, into which the transducer was installed with its face in contact with the surface of the sample. A diagram of a mid-height pore pressure probe is shown in Figure 3.6.

A diagram of the radial strain belt built for this work is shown in Figure 3.7. The radial strain belt was used to control the reliability on the volumetric strain data and glued on the sample at its mid-height. A weak beryllium copper spring held the belt against the sample. Changes in the diameter of the sample were determined using a miniature LVDT. The armature of the LVDT was cut and some of the non-sensitive section was replaced with a coaxial spring to allow flexibility as the gauge opened and shut. The LVDT used was similar to those used to measure the internal axial strain and an S7-AC amplifier was again used to increase the resolution of the transducer. The amplifier was again adjusted to the electrical zero at the start of shearing to increase the logging speed and the resolution of the transducer.

The tests with the radial strain belt showed limited success. Figure 3.8 shows the measured and calculated radial strain measurements. At larger strains there was a fairly close agreement between the calculated and measured radial strains. However at the very small strain levels (< 0.3 %) the agreement was not good, as is shown in Figure 3.8. The poor agreement at the start of shearing was thought to result from friction between the armature and the core of the LVDT causing a stick-slip behaviour.

Dynamic measurements of the very small strain stiffness were carried out using piezoceramic bender elements of the type developed at the Norwegian Geotechnical Institute and the University College of North Wales (Schulteiss, 1982). Bender elements were incorporated in the top and bottom platens. They transmitted and received shear wave pulses through a specimen, as shown in Figure 3.1. The system used was described in detail by Jovicic (1997).

The time taken for the shear wave to propagate through the length of the sample was measured using a digital oscilloscope. The shear wave velocity was then calculated from the arrival time and the distance between the bender element tips as was suggested

by Viggiani and Atkinson (1995b). The shear modulus was then calculated from the shear wave velocity using Equation 3.1, given below:

$$G_{max} = \rho v_s^2 \qquad \text{Equation 3.1}$$

The arrival time was determined using both sine and square waves to check for consistency, as was suggested by Jovicic et al. (1996).

3.2.4 Sample Retrieval and Preparation

a) Natural samples

The natural samples were retrieved from the landslide using driven and rotary sampling techniques. Two types of undisturbed samples were taken at the site, Osterberg and Mazier. Disturbed samples were also taken for classification purposes.

It was necessary to try and minimise the soil disturbance caused by sampling, as this can completely change the natural soil properties (Clayton et al., 1995). One major cause of disturbance can be the large volumetric and shear strains generated as a tube is pushed or hammered into the soil. The distortions were therefore minimised using a thin walled piston sampler.

The minimum disturbance that can occur is the loss of the deviatoric stress in the sample with the mean normal effective stress in the soil maintained only by suction. In order to allow these suctions to develop it is essential to maintain the in-situ water content of the soil, minimising the swelling of the soil as the stresses are relieved and making sure there is no free water in the sample before the ends are sealed. Swelling of the sample can destructure a soil.

An Osterberg piston sampler was used to recover stiff clay samples from the site. However in the stiffest materials at the landslide site, the Osterberg sampler did not give a good recovery. Typically only short sample lengths were obtained as the sampler was either prevented from being pushed further in to the ground by hard material or material was lost as the tube was pulled out of the ground. The Osterberg sampler is a thin walled, fixed piston tube sampler (Figure 3.9). The thin wall reduces the magnitude of the straining in the sampled material. Hydraulic jacking was used as it causes less

damage to the sample than would percussion, while a fixed piston was used to prevent the sample heaving inside the tube, by maintaining the vertical stress during sampling.

The Mazier sampler was used in the stiffer clays where recovery with the Osterberg was poor. The sampler had a good core recovery at the landslide site and was more robust than the Osterberg tube sampler when encountering harder material. The Mazier sampler has a triple-tube retractor barrel (Figure 3.10). It has a sprung extended inner barrel to reduce the swelling effect of the drilling fluid. There are two conflicting problems with this type of sampler. The inner barrel protrusion could cause disturbance due to the high area ratio of the cutting edge if it travels far ahead of the barrel. However travelling ahead of the outer barrel reduces the problems of the sample swelling due to absorption of the drilling fluid. Normally the inner barrel travels a small way ahead of the outer barrel as a compromise between these two conflicting requirements.

Preparation of the natural samples was carried out in a 95 % humidity controlled environment. The soil was extracted from the Osterberg sample tubes using a hydraulic ram, whilst the soil was extracted from the Mazier sample tubes by cutting through the plastic tubing with a high speed band saw. Using a standard procedure for trimming clay samples from the undisturbed soil, it was attempted to trim 38, 50 and 60 mm diameter samples in a manual soil lathe using a wire saw. However the saw was found to catch the discontinuities in the structured soil, removing large wedges from the sides of the specimen. This method was obviously unsuitable for this project and an alternative procedure was therefore developed for this soil type. It was found that the sample could be trimmed using a sharp knife to scrape the sides of the sample, but this procedure was very slow and the time taken to reduce the diameter sufficiently, particularly for the stiffer samples, allowed stress relief to open pre-existing discontinuities in the soil sample. Hence parts of the sample would detach whilst trimming or fractures would open whilst transferring the sample from the lathe to the apparatus.

The trimming procedure which was the most successful for a 38 mm sample was to use a high speed band saw to level the ends of the sample to a length of approximately 90 mm and to cut a rough outline of the sample to a diameter of approximately 50 mm. The sample was then scraped with a sharpened knife to reduce the diameter to 38 mm in the lathe. The band saw was then used again to cut the ends to the required length of

76 mm. Finally any small holes in the sides of the trimmed samples were filled with the remoulded cuttings. Six to eight water content measurements were made from the trimmings.

b) Reconstituted Samples

Reconstituted samples were prepared from the natural sample trimmings without air or oven drying. They were placed in a bowl with distilled water, covered and allowed to swell for several days. The softened soil was then placed in a mechanical mixer with any unmixed lumps broken down by sieving. The resulting slurry was de-aired in a vacuum chamber and placed in a consolidometer at a water content of approximately 20 - 50% greater than the liquid limit and consolidated to a vertical stress of approximately 50 kPa. The sample was finally extruded, trimmed to the correct length in a cradle with a wire saw and transferred to the triaxial cell. The trimmings were used for a water content determination.

c) Minced Samples

The effect of a more vigorous preparation method was investigated by testing a sample that had been remoulded in an industrial food mincer. Using the results obtained from the index testing the soil was fed through the mincer twelve times at approximately the plastic limit to maximise the remoulding effect. The minced material was then prepared in the same way as the reconstituted samples. Testing procedures for the minced samples were similar to those for the reconstituted samples.

3.2.5 Test Procedures

The general test procedures for the natural and reconstituted samples are summarised below. The general test procedures for the minced samples were the same as those used for the reconstituted samples.

Tests on the natural samples were carried out to assess the strength and stiffness parameters applicable to the soil in-situ. The natural samples were therefore sheared

from an isotropic effective stress which was a best estimate of the in-situ stress level determined from the depth of the sample in the ground and the piezometric level. Typically the natural samples (N6A, N7A, N8A, N8B, N9A, N9B and NCA) were saturated at an isotropic effective stress of 50 kPa less than the estimated in-situ stress level. The suction cap was then connected and they were isotropically compressed to the estimated in-situ stress level. The samples were then sheared to failure under drained conditions. Samples N2B and N4B were however saturated at approximately one quarter the estimated in-situ effective stress level. The suction cap was then connected and the samples were isotropically compressed to approximately one half of the estimated in-situ effective stress level, where a drained shearing probe was carried out. The sample was then isotropically compressed to the in-situ effective stress level where the sample was sheared undrained to failure.

Two natural samples were also tested in the high pressure apparatus. To install the samples in the triaxial cell, slots for the bender elements were excavated and then back-filled with remoulded soil to ensure a good contact with the bender element. The samples were saturated at the estimated in-situ stress level. The suction cap was then connected and the samples were isotropically compressed at a rate of 2 kPa/hour. The rate of loading was increased at higher stresses to reduce the time of the test, reaching up to 10 kPa/hour. Bender element readings were taken at regular intervals. A shear probe was also carried out on sample H2C. Sample HDA was lost during isotropic compression due to failure in the control of the axial loading system which caused the sample to extend rapidly.

For each natural sample tested, a corresponding reconstituted sample was also tested. The test procedure sought to determine the position of the normal compression line for the reconstituted material and its critical state friction angle. Stiffness data were also obtained by carrying out shear probes and bender element tests. During the test programme it was determined that a clear critical state could only be achieved if the sample was sheared undrained from a normally consolidated state. Strain localisation tended to occur before the critical state was reached in samples sheared either undrained from an overconsolidated state or drained from any state. When the critical state was not obtained due to strain localisation, an additional test was carried out on the reconstituted material, where possible. Samples R2B, R4B, R8A and RDA were sheared drained to failure, whilst Samples R2C, R6A, R7B, R7C, R8B, R9A, R9B, RCA, RDB, M7A, M7B and M9A were sheared undrained to failure.

Typically, after installation in the triaxial apparatus, the reconstituted samples were subjected to a one step consolidation to an effective stress of approximately 20 kPa. The suction cap was then connected. The reconstituted samples followed different stress paths consisting of isotropic compression and swelling stages which were often interspersed with drained shear probes. Towards the end of the test programme, time constraints dictated that there was a need for strength data rather than small strain stiffness data. Therefore the axial loading system was not connected until much later in the test to prevent any possible drift of the load cell causing the loss of results. A half ball connection was then used where possible instead of the suction cap. Very small strain stiffness data were still obtained from bender element readings for a number of these tests. Samples (R2C, RDA, R7C, M9A and R9B) were compressed using a series of one step consolidations rather than slow drained compression to reduce the duration of these tests.

a) Set Up Procedure

The samples were set up as shown in Figure 3.11. Top drainage was not used as it can greatly increase the likelihood of leakage in the drainage system. Radial filter paper drains were therefore used to reduce the drainage path length. Moisture content samples were taken as well as the sample's weight and initial dimensions to determine the specific volume.

b) Saturation (Natural Samples)

The natural samples initially gave very low B values ($\Delta u/\Delta\sigma_c$) (Skempton, 1954) when subjected undrained to an increase in cell pressure, even for soil samples retrieved from below the water table. It was consequently not possible to determine the in situ effective stress, p'_o from the soil suction. Therefore the samples were tested at the estimated in situ stress level determined from the depth below ground level of the sample and the piezometric level determined from the downhole piezometers. The natural samples were saturated under a constant back pressure until a B-value of greater than 0.95 was obtained. In order to obtain this value the drainage leads were flushed daily with de-aired water. If the required B-value was still not obtained the back

pressure and the cell pressure were increased concurrently keeping the effective stress constant.

A suction cap connection was used to connect the sample to the load cell, which can cause a certain amount of disturbance to the sample at the time of connection. The effective stress level at which saturation was undertaken was governed by the conflicting needs to reduce the influence of large swelling strains on the soil structure (Clayton et al. 1995) and the need to allow sufficient compression of the sample before shearing to eradicate this history of disturbance. It was attempted to use a halved ball connection (see Figure 3.12) to eliminate the need to swell the sample in this way as this connection could be made immediately before shearing. The halved ball connection, however, gave poor axial strain readings due to tilting at the start of shearing and was therefore considered inappropriate for tests in which measurements of the small strain stiffness were to be made.

c) One Step Consolidation (Reconstituted)

The reconstituted samples gave good B values (0.96 - 1.00) when the cell pressure was initially increased. Typically when the cell pressure was increased to 120 kPa the effective stress for the reconstituted samples was only about 10 kPa. The decrease in effective stress was a result of the disturbance caused when extruding the sample from the consolidometer. A one step consolidation to an effective stress of about 20 kPa was applied to the soil to assess the consolidation characteristics of the soil at this stress level and to increase the effective stress prior to the connection of the suction cap.

Later in the test programme, when the axial loading system was not connected until shortly before shearing, the normal compression line or swelling line was determined by a series of one step consolidation and swelling stages. Within the same time span more points on the normal compression line were obtained with a series of one step consolidations than slow isotropic compression. As during isotropic compression, the pore pressures were not equalised until the end of each test stage, the position of the normal compression line was in any case only known at these points.

d) Isotopic Compression and Swelling

The samples were all isotropically compressed, as the recent stress history of the soil was not known and is likely to be very complex. The samples were also known to be overconsolidated and so in the absence of better information, it was decided not to follow one dimensional compression and swelling paths but to use isotropic loading only. One dimensional consolidation was unlikely to be more appropriate as the intense deformations due initially to tectonic activity and later landslide movements were thought to have erased the previous one dimensional stress history and altered the sedimentation structure. Loading rates of 1 kPa/hour and 2 kPa/hour were used for the reconstituted and natural samples respectively. The volumetric strains were left to stabilise at the end of each test stage. It was not possible to conclude from the strain data whether the volumetric strains that were observed at the end of loading stages for the reconstituted samples were caused by creep or by pore pressure equalisation due to the very low permeability of the soil. However, mid-height pore pressure transducers on tests R6A and R8A, confirmed that they were the result of pore pressure equalisation. Loading rates of less than 1 kPa/hour were not feasible for these apparatus and therefore a compromise was made between ideal loading rates and feasible loading rates, with rest periods between the loading stages to allow equalisation of pore pressures. A plot of volumetric strain against the logarithm of time at the end of each loading stage was used to predict the final volumetric strain. As well as reducing the number of tests that could be carried out, the increase in the time taken for each test increases the risk of losing a test due to a compressor or battery back up failure.

e) Drained Shear Probes

This procedure involved shearing the sample drained to a small axial strain, typically 0.2 %, to assess its stiffness. The axial strain was less than that at which localisation of strain occurs and the difference between the value of p' for the final shearing and the probe was such that for the final shearing the sample had no memory of the previous probe, as sufficient strain had occurred to erase this memory. More loading probes were carried out on the reconstituted samples as there was no risk of destroying fabric due to loading cycles or swelling. Shearing was carried out with constant cell and back pressures.

At the end of the compression stage the samples were allowed to stabilise until the volumetric strains had become less than 0.01 %/hour and the axial strains were less than 0.005 %/hour so that they would be insignificant relative to the strains measured in the first hour of shearing. The strains were then rezeroed and the LVDTs which were used to measure the axial and volumetric strains were placed close to their electrical zero, to maximise their resolution.

Typically strain controlled loading was carried out as a more consistent loading rate was achieved. Data obtained from stress controlled loading often contained irregularities due to the slow loading rates required for these low permeability soils. At a loading rate of 1 kPa/hour the application of load was greatly influenced by the noise of the load cell, typically 1 kPa and the minimum size of the stress increment that could be applied, i.e. one step of the electromanostats or 0.4 kPa. The shape of the loading curves for the reconstituted samples were those most affected by noise, as the noise for the load cell readings was up to ± 0.5 kPa and the deviatoric stress at the end of the shear probe was sometimes only 10 kPa.

Strain controlled loading was applied using the Bishop ram, placed between the air-water interface and the loading ram, with a valve to disconnect this closed volume system from the air-water interface (see Figure 3.1). A stepper motor with a gear box on the Bishop ram was used to load the sample at a constant strain rate controlled by a timed relay (clicker box). The disadvantage of strain controlled loading was that the stress rate at the beginning of loading could be very large, even if a very high gear box ratio and slow clicker box rate were used. Although the mid-height pore pressure transducer showed an increase in pore pressure, typically 10% of the deviatoric stress, during what was nominally a drained loading, the rate of about 0.01 %/hour were found to be about the lowest practical limit of shearing rate.

Due to the difficulty of preparing the natural samples, shearing probes were carried out on the first two natural samples in order to maximise the data obtained for each test. These were undertaken at a stress level approximately one half of that used for the final shearing stage. The disadvantage of these probes was that the stress levels at which samples were saturated was approximately one quarter of those in-situ. This might cause destructuration as a result of swelling induced in the sample.

f) Final Shearing

All of the natural and some of the reconstituted samples were sheared drained to failure. Drained loading was carried out as this would resemble the drainage conditions in the landslide. The initial procedure for the final shearing was the same as that used for the shear probes. However instead of stopping the test at 0.2 % shear strain the sample was sheared to approximately 20 % axial strain or the limit of the stroke of the axial ram. After about 0.5 % axial strain, the strain rate was increased gradually from the initial rate of approximately 0.01 %/hour to a maximum of about 0.12 %/hour.

Undrained shearing was carried out on most of the reconstituted samples as with the drained loading strain localisation was found to occur prior to reaching a critical state. A similar procedure to the drained shearing stages was followed for the undrained shearing with the valve to the volume gauge closed. Typically undrained tests can be sheared much faster than drained tests as the time taken for the pore pressures to equalise is much less than that required for the sample to drain. However as the drained tests were sheared at a rate faster than was desirable, the same initial rate of loading was used for both the undrained tests and the drained tests. However although the initial rate of loading was the same, the rate was increased more rapidly for the undrained samples as the tests progressed.

g) End of Test Procedure

At the end of the each test, the sample was removed from the triaxial cell and the water content determined. The initial value of specific volume was determined as an average of four values calculated from: the moisture content of the trimmings; the initial mass of the sample and the final dry weight of the sample; the final moisture content of the sample; and the final dry weight and the initial sample dimensions. Out of the four values of initial specific volume, any extreme values were discounted, as these were thought to be due to poor initial saturation. An average value of specific gravity of 2.74 was used in these calculations. This was measured in specific gravity bottles for six of the triaxial samples N2B, N4B, N6A, N7A, N8A and N9A, using the procedure described by Head (1990). The results ranged from 2.73 to 2.75.

A zero reading was taken of the stress transducers after refilling the cell with water. Any drift that had occurred during the test was assumed to have taken place linearly with time over the course of the test. The stress data were then corrected for this drift. The load cells were very prone to drifting over these long duration tests and approximately ten load cells had to be replaced over the course of this project.

3.3 Ring Shear Apparatus

3.3.1 Introduction

Ring shear tests were carried out to determine the residual strength of soil samples retrieved during the site investigation. The residual strength is achieved when a sample is sheared to very large displacements, as occurs during landsliding. This limiting strength was measured in both the Bromhead (Bromhead 1980) and Bishop (Bishop et al. 1971, Garga 1970) ring shear apparatus. The ring shear apparatus was the preferred method of measuring the residual strength as it allows an annulus of soil with a constant cross sectional area to be sheared continually to large displacements.

Although the Bromhead ring shear apparatus is generally regarded as being inferior to the Bishop ring shear apparatus, it is widely used in industry as it is much cheaper and easier to use. The Bromhead ring shear apparatus was used here, to obtain preliminary data during the early stages of the project, while the Bishop ring shear apparatus was being modified. The data from the Bromhead apparatus was also used as a check on the data obtained from the Bishop apparatus. One of the main advantages of the Bishop ring shear apparatus is that the sample is sheared at its mid-height, whilst the sample in the Bromhead ring shear apparatus is sheared adjacent to a roughened platen. Other advantages of the Bishop apparatus are that the diameter is sufficient to minimise stress variations across the sample, friction in the apparatus is either minimised or measured, and undisturbed as well as remoulded samples can be tested.

Tests were carried out primarily on material that had been reconstituted. However a test was also carried out on a sample that had been prepared by mincing to assess the effect of the structure on the behaviour of the material. Tests were not carried out on 'natural' samples as there were no sufficiently large samples recovered and because saturation of the material in the apparatus could not be assured.

3.3.2 Equipment

a) Bishop Ring Shear Apparatus

The Bishop ring shear apparatus was described by Bishop et al. (1971) and by Garga (1970). A cross section of their apparatus is given in Figure 3.13. The main modification to this system has been the instrumentation of this apparatus to allow automatic datalogging. The original proving rings have been replaced by load cells and the dial gauges by displacement transducers.

The Bishop ring shear apparatus uses a 6 in. OD, 4 in. ID and 0.75 in. high annular soil sample, which is confined between sets of upper and lower confining rings. The sample is sheared by rotating the lower confining rings which are fixed to a rotating table, about a central axis, whilst the raised upper confining rings are restrained by the torque arm reacting against two load cells. The upper confining rings are raised during shearing to minimise the friction between the rings, whilst the friction between the confining rings and the specimen was measured in the modified apparatus with a load cell. The normal load is generated by applying dead weights to a load hanger at the end of a 10:1 lever arm. This load is transmitted through the main shaft to the loading yoke which rests on the loading platen.

The Bishop ring shear apparatus as described by Bishop et al. (1971) was a manual apparatus that required seven dial gauges to be read at standard intervals. As the length of each test stage was determined to be about five days for this project, due to the low permeability of the soils involved, the apparatus was instrumented and a data acquisition system added to allow efficient operation. Figure 3.14 shows a photo of the modified system.

The instrumentation was data-logged with an IBM compatible computer which contained an Alpha Super Interface Card, manufactured by CIL, to provide analogue to digital conversion. The system was the same as that used by some of the triaxial systems. The card provided 8 analogue input channels. Analogue to digital conversion was carried out on a 16 bit basis, which resulted in a resolution of approximately 1 to 32 000 of full scale. The interface card could only operate for one fixed gain which corresponded to full scale input voltages of 10 V, 1 V and 100 mV. Autoranging was therefore carried out using the software, which was written in Quickbasic, as described for the triaxial system in Section 3.2.3.

The proving rings used by Bishop et al. (1971) in the original apparatus were replaced with RDP precision low profile compression-extension load cells, Model 41E. Details of the instrumentation and their accuracies are given in Tables 3.4 and 3.5. As the resolution of the load cells was only 10 N for the 10 kN load cell and 5 N for the 5 kN load cell, even if read over the 100 mV range, RDP S7-DC amplifiers were used to increase the resolution that could be obtained.

The two 10 kN load cells were mounted on the opposing rigid columns to measure the torque generated. To allow the position of the load cells to be adjusted so that they were perpendicular to the torque arm, the bars through the rigid columns (Figure 3.14) were machined so that they could screw into the load cells. Their position could then be adjusted by the tightening and loosening the bolts, screwed onto either end of these bars, against the rigid column. The original vertically aligned wheels were machined to screw into a rigid plate bolted onto the load cell, as annotated on Figure 3.14. The wheels acted as an interface between the load cell and the torque arm and transmitted an axial load whilst allowing the torque arm to move vertically as the sample dilated or consolidated.

A 5 kN RDP load cell was used to measure the vertical friction between the upper confining rings and the sample. Again the original apparatus connections were machined so that they could be screwed into the load cell on one side and a thick steel plate bolted to the load cell on the other. The load cell was rezeroed before each test to take into account the weight of the yoke.

The changes in the height of the specimen and the gap opening were measured in the original apparatus with dial gauges. These were replaced with linear displacement transducers, as these could be datalogged and although they were less accurate than the LVDTs used in the triaxial apparatus they were considered to be sufficiently accurate. The accuracy of these measurements was not thought to be critical as they did not affect the residual strength calculated; the exact gap opening was not critical and the changes in the height of the specimen were only used to indicate when consolidation was complete. The change in specific volume of the sample could not be calculated from the change in height of the sample as soil was lost through the gap during shearing. Four displacement transducers measured the vertical displacement of the sample and the gap opening. They were held on the dial gauge bridge by grub screws in reamed holes.

b) Bromhead Ring Shear Apparatus

The Bromhead ring shear apparatus was designed by Bromhead (1976) and is manufactured by Wykeham Farrance Ltd. A cross section is shown in Figure 3.15.

The Bromhead ring shear apparatus tests an annular soil sample, confined radially between concentric rings. The sample is 5 mm thick and had an outer diameter of 100 mm and an internal diameter of 70 mm. The soil is loaded vertically through a porous bronze loading platen, by means of dead weights on a 10:1 ratio lever loading system.

The base platen is rotated using a variable speed motor and gear box driving a worm drive. As the base plate rotates the top platen is restrained by the torque arm, acting against a pair of sensitive proving rings, read by dial gauges. Shearing occurs adjacent to the top platen, as the artificially roughened platen prevents shearing along the soil-platen interface.

3.3.3 Sample Preparation

The procedure for preparing the reconstituted samples for the ring shear tests was identical to that used to prepare samples for the reconstituted index tests. The soil was similarly remoulded thoroughly prior to testing to remove any structure induced by the one-dimensional compression.

The effect of a more vigorous preparation method was investigated by testing a sample in the ring shear apparatus that had been vigorously remoulded in an industrial food mincer. Using the results obtained from the index testing the soil was fed through the mincer twelve times at approximately the plastic limit to maximise the remoulding effect. The minced material was then prepared in the same way as the reconstituted samples.

3.3.4 Testing Procedures

a) Bishop Ring Shear Apparatus

The testing procedure for the Bishop ring shear apparatus was documented by Bishop et al. (1971) and Garga (1970). The material to be tested was reconstituted, consolidated one-dimensionally and remoulded with a spatula before being moulded into the apparatus confining rings and levelled with the special tool. On top of the soil was placed the aligned upper platen with a new porous stone, the torque arm, the spherical seating and nut. The lever arm counterweight was then balanced, the nut tightened and the four guide pins inserted. After the load cell was zeroed to balance the weight of the linking yoke, the crosshead was mounted on the rigid columns and the eight fastening screws and two guide pins were inserted. The dial gauge bridge, holding the displacement transducers was then mounted and the zero readings taken.

Weights were then added to the lever arm, the water bath filled and the sample allowed to consolidate. When the vertical displacement readings had stabilised, the locking screws were removed and the upper confining rings were retracted. The sample was then sheared at a rate of approximately 0.02 mm/min until a peak was reached. At this stage the confining rings were closed to restrict the soil loss between the gap. The soil loss could be large, particularly at higher stress levels. The sample was sheared at a constant strain rate, with the rings retracted at regular intervals for periods of several hours, depending on soil loss, until a steady state was reached. The shearing was then stopped and the confining rings closed. More weights were added to the hanger and the consolidation and shearing was repeated at this higher stress level. Multi-stage tests were carried out to determine the frictional resistance at different normal stress levels.

b) Bromhead Ring Shear Apparatus

The testing method adopted for the Bromhead ring shear apparatus was based on the results of Stark and Vettel (1992). They emphasised that one of the problems with the Bromhead ring shear apparatus was that as soil is extruded during shearing, the top and base platen may come into contact creating frictional resistance. As it is not possible to measure this friction in the Bromhead apparatus it was necessary to minimise the vertical displacement and hence this error. Stark and Vettel recommended that the vertical displacement is limited to less than 0.75 mm. However in practice this was not found to

be possible for the soil tested as the quantity of soil extruded whilst shearing at the slowest possible rate resulted in settlements exceeding this figure.

The soil was reconstituted, one-dimensionally consolidated and remoulded prior to testing to break down the soil macro-structure and hence reduce the strain required to reach residual in the ring shear apparatus. The soil was then moulded into the base platen. Dead weights were added, zero readings were taken and the water bath was filled. After consolidation, if the vertical settlement was too large (greater than 0.6 mm) the top platen was removed and more soil was added to the mould before allowing a further period of consolidation. The samples were then tested without pre-shearing. BS1377 recommends that the top platen should be rotated through 1 to 5 complete revolutions before commencing the test, but several millimetres of vertical displacement would then occur in these soils, leaving the sample too thin to be tested. The samples were sheared at the slowest rate achievable in the Bromhead ring shear apparatus (0.018 mm/min or 0.024 deg/min). As well as reducing the amount of soil that was extruded between the platens, the slow rate also ensured that pore pressures in these low permeability soils could equalise. The permeability of these soils was in the range of 10^{-10} to 10^{-11} m/s. Multi-stage testing was carried out by removing the top platen and adding more soil before consolidation and shearing at a higher stress.

CHAPTER 4 LABORATORY TEST RESULTS

4.0 Introduction

The properties of the structurally complex clays from the landslide site were investigated using basic soil tests, triaxial tests and ring shear tests. This work focuses on the roles that micro- and macro-structure play in controlling the behaviour of these materials by comparing the behaviour of corresponding undisturbed (natural), reconstituted and minced samples.

The effect of the macro-structure could be assessed by comparing the behaviour of undisturbed material with that of the corresponding reconstituted soil, as the process of reconstitution erases the macro-structure of the natural soil. Reconstitution was shown, by eye and by using a scanning electron microscope (S.E.M.), to produce a more homogeneous fabric at the macro-scale consisting of small clastic particles in a clay matrix (Section 5.1). The standard reconstitution process, described in Section 3.4, did not, however, completely break down the aggregates of clay size particles. Hence the effect of micro-structure could be assessed by comparing the behaviour of a reconstituted sample with that of a corresponding minced sample. The minced samples were formed by passing the natural material through an industrial food mincer, as was discussed in Section 3.3.4, before reconstituting the material in the standard way.

The effect of the large distortions due to landsliding on the material properties was also assessed by comparing the liquidity indices and water contents of disturbed samples from both inside and outside the sliding mass and also by carrying out triaxial tests on undisturbed samples from the underlying formation and the landslide debris. These test data were normalised with respect to the behaviour of the corresponding reconstituted samples to account for the different characteristics of the various materials at this very heterogeneous landslide site.

4.1 Soil Description

The formation that comprises the landslide site is part of the Molise - Lucanian basin as was described in Chapters 1 and 2. The materials are comprised predominantly of marlstones, mudstones, claystones and clays, with isolated patches of sandstones and

carbonate breccia. The greater proportion of the soils may be described loosely as mudstones with varying degrees of carbonate content (varying from mudstones to marlstones) and diagenesis (varying from clays to shales) and with different types and frequencies of discontinuities, which ranged from intact to fissured to scaly materials. Figure 4.1 shows typical photographs of some of the different types of materials encountered.

The clays and mudstones were considered to be types B2 and B3 using the Esu (1977) classification illustrated in Figure 2.36, which is typical for a Sicilide unit. The material within the landslide was found to resemble type C using this classification. The changes to the formation material were thought to result from the remoulding due to landsliding and from weathering as a result of the proximity of the materials to the surface. At a scale equivalent to the sample sizes used in the laboratory, most of the soil could be simply classified as type δ and type γ, as described by Guerriero et al. (1995) and shown in Figure 2.38. The type δ materials form large parts of the landslide body, while the type γ materials form much of the argillaceous (clayey) component of the subsoil.

The influence of the more lapideous (rock-like) components on the behaviour of the landslide is difficult to assess. It is difficult to draw the line between argillaceous and lapideous material as there is a continuous gradation from stiff marly clays to marlstones. It is also practically impossible to determine the precise location of different materials in 3-dimensional space when the 'strata' have such chaotic arrangements.

The lapideous components were not considered in the site investigation as they were extremely difficult to sample undisturbed, and in any case, the stability of the slope was thought more likely to be controlled by the more argillaceous materials. This assumption was corroborated by the shallow angle of the failing slope, which would only be achieved if the shear surfaces lay predominately within the clayey soils. It was also reasoned, that the stiffness of the composite material could be assessed by considering the argillaceous component, as D'Elia (1991) showed that if the rock component was assessed to be less than 20 %, it would have a negligible effect on the overall stiffness, as discussed in Section 2.3.2. The rock component was roughly estimated from the borehole logs to be about 15 % at this site.

4.2 Basic Soil Tests

Basic soil tests were carried out on the more argillaceous components of the soil formation and the landslide body to determine their index properties, water contents and constituent minerals. Tests were used to determine the mineralogical composition, the carbonate content, the organic content and the particle size distribution of these materials. The locations of the boreholes from which the samples were retrieved are shown on Figure 4.2.

The effect of the landslide disturbance on their material properties was also investigated by comparing the soils from inside and outside the landslide body. Both these sets of soils, from the landslide body and the underlying formation, have a complex loading history as they have undergone large distortions as the result of the tectonic activity and may also have been subjected to deep-seated slope movements in the past. However in addition to these shear distortions, the samples from inside the landslide body were also likely to have been remoulded in the shallow mudslide, whereas samples from the underlying formation would not have been subjected to distortions of this type. The landslide debris was therefore visually very different to the underlying formation as was described in Section 4.1.

4.2.1 Index Properties

Atterberg limit tests for the purpose of classification were carried out using the standard preparation method as described in Section 3.1, as the results obtained were thought to be most representative of the natural material. The choice of preparation method, which was shown in Section 2.2.1 to be particularly important for the structurally complex clay formation, is discussed for these specific soils in Section 4.3.

The Atterberg limits have been plotted on a plasticity chart (Figure 4.3), where the A-line drawn is an empirical boundary between inorganic clays and silts. The test results lay predominantly just above the A-line, indicative of an inorganic clay. The samples had a large range of plasticities from low to very high; the liquid limit varies from 25 to 84 %. This large range is typical of a structurally complex clay (A.G.I., 1985). As discussed in Section 3.1, some of the index tests were carried out by Laing Technology

Services, while others were conducted by the author. The liquid limits measured by Laing generally tended to be slightly higher than the results from tests at City University on adjacent samples. The differences, between the liquid limits measured by City University and Laings on two adjacent samples, ranged between -7 and +24 %, as is shown on Figure 4.4. The Atterberg limit tests were carried out by both Laing Technology Services and City University without air or oven drying the samples and according to the BS 1377 Part 2. Ideally with hindsight, the tests carried out at Laings should have followed exactly the same method as carried out by the author. As there was no consistent change in the Atterberg limits with operator, the differences must in part be attributed to large variations in the material properties within a small distance along the core. Where there were small variations in the values of Atterberg limits obtained for different operators, this was not thought to be significant for the classification of the materials in this extremely complex landslide body. All Atterberg limit tests on the trimmings for all the triaxial samples were carried out by the author.

The Atterberg limits have been plotted, identifying samples from inside either the Serra dell'Acquara (1980) landslide or the Acquara-Vadoncello (1993) landslides and also samples from the underlying formation (Figure 4.3). The data show that the liquid limits for samples from outside a landslide body were generally slightly larger. The landslide that was analysed in detail for this research was the Acquara-Vadoncello landslide, which was initiated in 1993, as was discussed in Section 1.2. It is a subsidiary of the Serra dell'Acquara landslide which was reactivated by the 1980 earthquake. As there is a convergence of the Acquara-Vadoncello (1993) landslide with the larger Serra Dell'Acquara at its toe, samples retrieved at the toe of the Acquara-Vadoncello landslide from below the sliding mass may contain material from the 1980 landslide body. The liquid limits measured ranged from 25 to 84% and 56 to 82% for samples inside and outside a landslide body respectively. The low plasticity samples were retrieved from below the current Acquara-Vadoncello landslide in the old 1980 Serra dell'Acquara landslide. The slightly lower plasticities of the samples from the landslide body were thought to result from a mixing of some of the lapideous components with the higher plasticity materials within the landslide debris. As the plasticities of the lapideous component from soil outside the landslide would not have been tested for the soil, this resulted in the slightly lower average plasticity.

In order to assess whether the sample descriptions from the borehole logs could be used as an indication of sample type, the sample descriptions were detailed on a plasticity

chart in Figure 4.5. There is no clear distinction between the Atterberg limits of the materials described as marlstones, marly mudstones, marly clays, clays and claystones in the borehole logs. The material described as landslide debris does however typically have lower plasticities than the other materials.

4.2.2 Soil Composition

Particle size distribution analyses were carried out on ten samples from the site. These samples were believed to cover the range of argillaceous materials existing at the landslide site. The particle size distribution analyses were carried out at Laing Technology Services using wet sieving and pipette analyses. As with the index testing, the clay fraction was also shown in Chapter 2 to be highly dependent on the preparation method. In retrospect, it would have been ideal if the preparation method for the particle size distribution had been the same as that used for the index testing. However the tests were carried out commercially and a standard procedure was used which disaggreagated the soil with a chemical dispersant. The results are summarised in Figure 4.6. The soils tested were of predominantly clay sized particles with some silt. The clay fractions ranged from 53 - 75 %. Again there is little correlation between soil descriptions and the clay fraction. Samples described as 'clays' were expected to have a larger clay fraction. Although slightly higher clay fractions were observed, the differences were small.

The organic contents of ten samples from depths ranging from 7m bgl to 43 m bgl were determined by Laing Technology Services according to BS 1377. The organic contents varied from 0.4 to 1.3 % and averaged 1 %, which can be considered negligible. There was no discernible difference between the organic contents of samples from inside and outside the landslide body for the soils tested. The organic content could, however, increase closer to the surface and locally within the landslide body.

The carbonate contents of eleven samples were determined by gas emission. The carbonate content varied between 6 and 25.7 % and averaged 12.5 %. There was no correlation between the carbonate contents obtained by gas omission and the description "marly" or "marlstone" being applied to the soil. This could result, in part, from the difficulty of classifying these soils from visual observation. The greater part of this error is likely to arise from the existence of calcite as grains within these soils, as was

shown from the S.E.M. (Section 5.1). Hence the carbonate content does not directly relate to the material forming intergranular bonds which exist in a marlstone.

The approximate proportions of minerals present in the soil samples tested are shown in Figure 4.7. These were determined by x-ray diffraction of sample N8C (I4 16.0 - 16.4 m bgl), carried out by Geomaterials Research Services Ltd. This analysis was on the same sample as used for the S.E.M. work discussed in Section 5.1. X-ray diffraction is the most commonly used method of identifying clay minerals (Mitchell, 1993). The main constituents of the sample tested were chlorite, calcite and smectite, with smaller amounts of muscovite and quartz (Figure 4.7). The mineralogical components of the sample tested were comparable with those of other soils from the Molise-Lucania basin given in the literature, as was shown in Figure 2.40.

4.2.3 Water Content, Liquidity Index and Bulk Density

The water content of the triaxial samples of natural soils varied from 17.1 to 23.8 %, averaging 19.1 %. The water contents of the disturbed samples were not considered to be as accurate as those of the undisturbed samples since the drilling procedure used a water flush and the disturbed samples were only sealed in plastic bags and were not waxed. The average water content of the disturbed samples was 17.3 %, ranging from 14 to 21 %. The lower average water content could suggest that the material had dried but may also result from mineralogical differences in the disturbed material. Figure 4.8 shows the variation of water content with depth measured for the various boreholes. There was no recognisable distribution of water content measurement with depth or with location either inside or outside the landslide body.

In a homogeneous material, the water content will adequately reflect any softening of the soil along the borehole profile. However the materials encountered at this landslide were very variable. The liquidity index was therefore used, which relates the water content of a sample relative to its plastic and liquid limits and is an indication of the volumetric state. It can therefore give an idea of the degree of overconsolidation of the soil. The liquidity index of the triaxial samples varied from -0.39 to -0.12, averaging -0.25. The liquidity indices were negative as all the samples were drier than the plastic limit, indicating that the soils were all heavily overconsolidated. Again there was no

correlation found between the liquidity index and depth or location inside or outside the landslide body as is shown in Figure 4.9.

The macro-fabrics of the materials inside and outside the landslide were visually very different. Remoulding of the material within the landslide body changed the scaly fabric of the formation material (type γ) to that of the type δ material, lithorelicts in a clay matrix. However this remoulding did not noticeably affect the volumetric state of the soil, as the liquidity indices were similar for samples from both inside and outside the landslide body, contrary to the findings of previous work (e.g. Guerriero et al., 1995). The existence of soil remoulding within the shear zone at the base of the sliding mass would require a more detailed investigation of the water contents. Using a trial pit dug into their landslide, Iaccarino et al. (1995) could only identify a 10 cm thick shear zone, as was discussed in Chapter 2. The scatter of the data for the heterogeneous materials encountered at this site have obscured evidence of any volumetric changes as a result of remoulding. The differences in the water content measurements of the formation material along individual boreholes were greater than any changes between the water contents of samples from inside and outside the landslide body. Differences between the water contents of the clay matrix and the intact lithorelicts, as observed by Iaccarino et al. (1995) and Hutchinson (1988), could also disguise evidence of softening within the landslide body.

The bulk densities of the triaxial samples were determined from their weights and sample dimensions. The bulk densities varied from 20.2 to 21.7 kN/m^3. The degrees of saturation were calculated from the water content, bulk density and specific volume and varied from 92 to 100 %.

4.2.4 Activity

The activity of the clay is the ratio of the plasticity index to the clay fraction (I_p/CF) and is used to gives an indication of the influence of the clay fraction on the soil properties. The activity of the materials tested ranged from 0.6 to 1.0. This seemed fairly low considering the 21 % smectite content identified by x-ray diffraction. One reason for the low activity calculated was that some of the rotund particles were of clay size. As the activity is determined from a clay size fraction and not a clay mineral fraction, these rotund particles were included within the clay size fraction, but did not add to the

plasticity. Inconsistent destructuration of the soil samples, used for the index tests, could also be a possible explanation for the low activity as both the clay fraction and the Atterberg limits are highly dependent on the preparation methods, as was discussed in Section 2.3.2. The clay fraction measured was thought to be that of a disaggregated soil as the chemical disaggregation, used for the particle size distribution test to disaggregate the clay aggregates, was believed to be more successful than a mechanical destructuration technique. Therefore the increase in plasticity index due to destructuring by mincing, as was described in Section 3.3.4, resulted in an increase in activity. The activity of the samples inside the landslide tended to be slightly lower than those outside the landslide. There was found to be no correlation between the activity and the material descriptions from the borehole logs.

4.3 Reconstitution and Mincing

The effects of structure on the behaviour of natural soils can be assessed by comparing the behaviour of the natural soil with an appropriate reference material, usually the soil in its reconstituted state, as was shown by Burland (1990). In these variable materials, the behaviour of the reconstituted soil can also be used to normalise the behaviour of the natural soils to account for differences in the material type.

The aim of reconstitution is to remould the natural soil to achieve a homogeneous soil with a stable base fabric. In order to be a reference material for the natural soil, the material, from which the reconstituted soil is prepared, should be as similar to the natural material as is practically feasible. Hence the reconstituted sample is often made from the trimmings of the natural sample, as was done here.

In the literature review it was shown that the Atterberg limits of a structurally complex clay were highly dependent on preparation method. Aggregates of clay sized particles can be broken down with increased mechanical energy, resulting in an increase in the liquid limit. As a natural consequence of this, it might be expected that the mechanical behaviour of the reconstituted soil would also be dependent on the preparation method used to create it.

The reconstitution process defined by Burland (1990) was discussed in Chapters 2 and 3. Burland proposed that the reconstituted sample should be made from the natural sample, which is mixed with water to form a slurry, without air or oven drying the soil prior to mixing. As discussed in Section 2.3.2, the preparation method needs to be better defined for these soils. However the air drying and dry grinding approaches, used by Guerriero et al. (1995) and Olivares (1996) to reconstitute soil, would not fit into the definition proposed by Burland. The choice of an appropriate reference material is crucial to the assessment of structure in these soils. At an early stage in this project, it was decided that if a stable base fabric could be achieved without using large amounts of mechanical energy to break down the particle aggregates, that this might give a more appropriate base fabric for comparison with the natural material. The 'reconstituted' soil was therefore defined here to be a soil that had been swelled to a water content of approximately 1 to 1.5 times the liquid limit by immersion in water and then mixed to a slurry, as discussed in Chapter 3.

4.3.1 The Effect of Preparation Method on the Atterberg Limits

The Atterberg limits for structurally complex soils were shown by Rippa and Picarelli (1977) to be highly dependent on preparation method. The problem with determining the index properties was caused by the difficulty of destructuring the material. It was thought that bonding of the clay particles formed aggregations of particles which were difficult to break.

Tests were carried out to investigate the effect of preparation method and hence degree of destructuration on the Atterberg Limits. The preparation methods investigated included: the standard method of reconstituting the soil; using ultrasound to treat the soil; and mechanically mincing the soil. These methods are described in detail in Chapter 3. Ultrasounding and mincing were used to try and further disaggregate the soil particles using a more violent destructuration technique. The degree of destructuration was further investigated by varying the water content at which the samples were minced and the number of times that the soil was passed through the mincer. As the standard preparation methods for the Atterberg limit tests (standard) and the triaxial tests (reconstituted) were slightly different, the Atterberg limits of the soil, which had been prepared by reconstitution, were compared with those of a sample which had been prepared for the Atterberg limit tests in the standard way. For the standard preparation

method used for the Atterberg limit tests, the soil was mixed at a water content of approximately 5% less than the liquid limit, whereas when the soil was reconstituted, the soil was swelled to 1.2 to 1.5 times the liquid limit before mixing and one-dimensionally consolidating. A slight increase of 3 to 7 % in the water content at the liquid limit was measured for the sample prepared by reconstitution. This was attributed to a greater number of aggregates being broken down using the reconstitution technique than the standard preparation technique. It was also suggested by colleagues at Bari, who had tested similar materials, that ultrasounding could destructure the material without using a large amount of mechanical energy. However, this was not found to have a noticeable effect.

The liquid limit was shown to increase with the number of passes of the soil through a mincer, rising up to a maximum at about 12 passes (Figure 4.10). The increase in liquid limit due to mincing varied from 7 to 21%. The water content, at which the samples were minced, was also seen to have an effect on the way the mincer performed. If the soil was too dry, the soil would pass through the mincer like sugar, whereas if the material was too wet, the material would flow though the mixer like a slurry. Figure 4.11 shows the change in the liquid limit of samples minced ten to twelve times plotted against the water content in excess of the plastic limit. There is a tendency for the increase in the liquid limit to be greatest when the samples were minced at a water content just below the plastic limit. The scatter in the data was attributed to the difficulty of keeping the moisture content constant during mincing. The standard vigorously remoulded or "minced" soil was therefore defined as a material that had passed twelve times through the industrial food mincer at a moisture content of approximately the plastic limit.

Figure 4.12 shows a plasticity chart for undisturbed samples N7A and N9A which were from boreholes P2 (7.5 - 7.8 m bgl) and P4 (22.2-22.6 m bgl) respectively. N7A was retrieved from a position inside the landslide body, whereas N9A was retrieved from the undisturbed formation at the scarp. Both these samples show an increase in the values of the liquid limit obtained from the samples prepared using the reconstituted method and those prepared by mincing, by comparison with those prepared by the standard method. Therefore the liquid limit is highly dependent on the degree of destructuring of the particle aggregates. There was however no consistent change to the plastic limit when the sample was minced. This therefore shows that the more aggressive breakdown of particles affects the liquid limit but not the plastic limit. This does not

agree with the results of Rippa and Picarelli (1977) who noted a similar increase in liquid limit for destructured clays but also noted an increase in the plastic limit. Figure 4.12 shows that as a result of reconstitution or mincing, the samples increase in plasticity and move away from the A-line.

Samples N7A and N9A showed similar increases in the liquid limits with mincing of 17 % and 15 % respectively. As one was from inside and one was from outside the landslide body, it can therefore be concluded that the effect of remoulding due to landsliding was not sufficient to change the micro-structure of these materials, in contrast to the macro-structure which visual inspection showed to be changed significantly, as discussed in Section 5.2.1. Because the micro-structure of the material was not broken down as the result of remoulding within the landslide body, the base fabric of this 'remoulded' material was therefore concluded to be relatively stable. Hence the 'reconstituted' material, prepared by swelling the material by immersion in water to a water content of 1.2 to 1.5 times the liquid limit, before mixing to form a slurry, fulfilled the criterion defined here for an appropriate reference material. The reconstituted material has therefore been shown to have a relatively stable base fabric; to be homogeneous at a macro-scale; to have a base fabric as close to that of the natural as is possible; and to be reproducible. The 'reconstituted' and not the 'minced' soil will therefore be used as the reference material for normalisation of triaxial test data. The effect of the micro-structure was investigated further by comparing the behaviour of the 'minced' and 'reconstituted' materials in the triaxial and ring shear apparatus.

4.4 Compression Behaviour

The behaviour of the natural, reconstituted and minced samples was investigated in the triaxial apparatus under isotropic compression. The equipment and test procedures were described in Chapter 3. One of the aims of the testing programme was to compare the normal compression lines for corresponding natural, minced and reconstituted samples in order to assess the effect of the macro- and micro-structures on the compressive behaviour. It was thought that the effect of the macro-fabric on the compression behaviour could be assessed by a comparison of the reconstituted and natural materials as these materials have similar micro-fabrics, whilst the effect of the micro-fabric could be assessed by comparing the behaviours of the reconstituted and minced soils. The

reconstituted and minced samples had similar macro-fabrics but very different micro-fabrics. Unfortunately, it was not possible to determine the normal compression line for any natural samples due to equipment failures in the high pressure apparatus.

The normal compression lines for all the different reconstituted samples were determined for use as the reference behaviour, to allow normalisation of the test data for the natural samples. The decision to use the reconstituted material as a reference material as opposed to the minced was discussed in the previous section. The reconstituted soil was shown to be homogeneous, to have a stable base fabric, to be reproducible and to have a base fabric as close to that of the natural as was possible. The gradients of the normal compression lines for the reconstituted and minced samples were also compared with data from the literature both for other 'standard' clays and for structurally complex clays, in order to assess whether they exhibit any unusual behaviour.

The triaxial samples have been labelled by grouping together the soil extracted from the same tube sample and by identifying the type of preparation method and whether it is a high pressure test or not. Therefore sample H2C refers to specimen C, from tube 2, which is a high pressure test on the natural soil; sample M7A refers to specimen A, from tube 7, which is a test on the minced soil in the standard pressure apparatus; sample R7A refers to specimen A, from tube 7, which is a test on the reconstituted soil in the standard pressure apparatus; and sample N7A refers to specimen A, from tube 7, which is a test on the natural soil in the standard pressure apparatus. A summary of the triaxial test results is given in Table 4.1, which also identifies the boreholes and depths from which the samples were retrieved. The position of the samples is also identified on the cross-section in Figure 4.2.

4.4.1 Reconstituted Samples

The compression data for a reconstituted sample, R8A, are shown in Figure 4.13. The specific volumes are plotted against the mean effective stresses using the standard v-lnp' plot. The mean effective stresses have been calculated using both the pore pressures at the base of the sample and the pore pressures at mid-height. The pore pressures were measured at the sample mid-height as it was not possible to tell whether the large and prolonged volumetric strains at the end of loading in earlier tests, which often continued

for periods in excess of 2 weeks, had been a result of creep or pore pressure equalisation. The loading rate of 1 kPa/hour was about the slowest rate that was practical with this apparatus. Therefore the continuous loading was stopped at the end of each loading stage to allow stabilisation of the volumetric strains.

Figure 4.14 shows the pore pressures at the base and the mid-height of the sample and the volumetric strains at the end of a one step consolidation for sample R8A from a mean effective stress of 10 kPa to a mean effective stress of 20 kPa. This graph shows that the pore pressures at the mid-height of the sample were much larger than those at the base of the sample, the latter simply being equal to the back pressure used. Volumetric strains therefore occurred as the result of pore pressure equalisation. There was occasionally some additional volumetric strain after the base and mid-height pore pressures had equalised. This was attributed to an excess pore pressure in the middle of the sample that was not picked up by the mid-height probe mounted on the sample perimeter. The volumetric strains at the end of each loading stage can therefore be attributed to the equalisation of excess pore pressures and were not primarily the result of creep. The pore pressures measured at mid-height appear therefore to be a better approximation of the average excess pore pressures in the sample, rather than the maximum value.

In order to determine the correct position of the normal compression line, where no mid-height pore pressure measurements were available, the volumetric strains at the end of consolidation stage were assessed from a graph of volumetric strain against the logarithm of time. Where slow compression was used, i.e. the cell pressure was increased at a rate of 1 kPa/hour whilst holding the back pressure constant, the volumetric strains after the end of loading were plotted against the elapsed time since the end of loading.

The time required to allow equalisation of pore pressures was found to increase with stress level. This was attributed to the decrease in permeability with the specific volume and the reduction in the efficiency of the filter paper drains with the duration of the test. Table 4.1 shows values of N and λ, the gradients and the intercepts of the normal compression lines, determined for each of the reconstituted samples on a v-lnp' graph. Butterfield (1979) recommended plotting compression data in lnv-lnp' space as this gives a straight line over a greater range of stresses. The data have however been plotted here in v-lnp' space for simplicity, as it can be seen that reasonable straight lines

are obtained over the stress range considered. The normal compression lines do however need to be extrapolated to allow normalisation of the data for the natural samples. This is where discrepancies will arise between straight lines on v-lnp' and lnv-lnp' plots. As there is no compression data for the reconstituted samples at these higher stresses, any extrapolation will produce some uncertainty and hence v-lnp' is used consistently in the absence of any better information.

The isotropic normal compression lines for the reconstituted samples are summarised in Figure 4.15. There is a wide range of gradients (λ) and intercepts (N) for the normal compression lines. The gradients vary from 0.146 to 0.333 and the specific volumes of the samples at 100 kPa on the isotropic normal compression line range from approximately 1.9 to 2.6. The wide scatter is indicative of the variability of the soils at the site and stresses the need, when normalising data, to compare the soil behaviour to that of an appropriate reference material and not just use one reconstituted soil for the whole site as, for example, Guerriero et al. (1995) had done.

Figure 4.16 shows a graph of the gradients of the normal compression lines for the reconstituted samples plotted against the plasticity index, I_p. By determining the equivalent strengths of samples at the liquid and plastic limits, a correlation was determined between compressibility and plasticity by Muir-Wood (1990). Muir-Wood noted that the undrained shear strengths at the liquid limit $(C_u)_{LL}$ and the plastic limit $(C_u)_{PL}$ were approximately 2 and 200 kPa respectively. It therefore followed that the plasticity index could be related to the compressibility index using the following equation:

$$\lambda = \left(\frac{I_p * G_s}{\ln\left(\frac{(C_u)_{PL}}{(C_u)_{LL}} \right)} \right) \qquad \text{Equation 4.1}$$

The scatter in the data partly arises from the assumption that the undrained strengths at the liquid and plastic limits are the same for all soils. As the Atterberg limit tests are essentially empirical, they do not relate directly to fundamental soil parameters due to the complexity of the failure mechanisms involved. Mitchell showed the scatter of undrained strengths at the liquid limit to be approximately 2 kPa and the scatter at the plastic limit was estimated to be 200 kPa i.e. ± 100 kPa about a mean of 200 kPa. The

data points plotted lie predominantly above the correlation line predicted by Muir-Wood. They do not however lie outside the scatter he reported for this correlation. Only the two samples both from the landslide debris of the Acquara-Vadoncello slide, fall below this line.

Burland (1990) correlated the coefficients of one-dimensional compression for reconstituted samples (C_c^*) with the void ratio at the liquid limit (e_L) using Equation 4.2:

$$C_c^* = 0.256e_L - 0.04 \qquad \text{Equation 4.2}$$

The isotropic and one-dimensional compression lines are generally parallel with a ratio λ/C_c^* equal to 2.303. Although the soil lay within the specifications recommended by Burland, i.e. the Atterberg limits plotted above the A-line, had a liquid limit of between 25 and 160 % and a carbonate content of less than 25 %, the data points for the compression indices for the Senerchia samples generally plot above Burland's empirically derived line (Figure 4.17). This is perhaps a result of differences in the mineralogy of these soils to those considered by Burland. As discussed in Section 2.2.2, Burland's correlation is thought only to apply if the index data plot within the narrow band on Cassagrande's A-line chart determined for the soils from which the empirical correlations were derived.

The data from the literature for other similar soils from the area studied did however agree better with the Burland correlation. There could be several explanations for this disagreement, for example differences between the natures of the soil from the literature and the soil from this study and perhaps the use of different methods of reconstitution. The data from the literature were typically for samples created by air-drying and mechanical grinding (not mincing) and tended to have lower plasticities.

4.4.2 Minced Samples

In a similar fashion to the behaviour of the reconstituted samples, isotropic compression of the minced samples also resulted in large and prolonged volumetric strains at the end of each isotropic compression stage. This was again attributed to pore pressure equalisation at the end of the loading stage. The time, for pore pressure to equalise at

the same stress level with a similar stress history, was found to be greater for the minced samples, which suggested that the minced samples were less permeable than the reconstituted. This reduction in permeability was attributed to the different micro-structures as the mincing process was thought to break down the soil micro-structure. The silt sized aggregates of clay particles in the reconstituted samples were thought to give rise to a more permeable fabric than the disaggregated clay particles in the minced sample. Iaccarino et al. (1995) showed also that the permeability of the natural materials was much higher than those of reconstituted samples, which was attributed to their different macro-structures. The macro-structure of the reconstituted materials consisted of a clay matrix surrounding small discrete particles, whereas the macro-structure of the natural soil was dominated by their scaly nature. The increased permeability of the natural soil was attributed to its many fissures. These results imply that both the macro- and micro-structure affect the permeability of these materials.

Figures 4.18 and 4.19 show the normal compression lines for both the minced and reconstituted samples from sample tubes 7 and 9. The normal compression lines for the minced samples lie outside those for the corresponding reconstituted samples throughout the stress ranges considered. The minced samples existed at much higher specific volumes at lower end of these stress ranges and their behaviour under isotropic compression converged as the stresses increased, towards that of the reconstituted samples. It is not clear from the tests carried out whether the compression lines of the minced samples would eventually join with those of the reconstituted samples. The ability of the minced material to exist at states outside the normal compression line of the reconstituted soil is in agreement with the increase in Atterberg limits, discussed in Section 4.3.1.

The gradients and intercepts of the normal compression lines of the minced samples are shown in Table 4.1 and are larger than those for the corresponding reconstituted samples. Figure 4.16 shows the gradients of the normal compression lines plotted against the plasticity indices for corresponding reconstituted and minced samples. The increases in the parameters defining the normal compression line (λ and N) did not, however, correspond exactly to the increases in the plasticity indices, although the new data points for the minced samples still lie within the scatter observed by Muir-Wood.

One of the features that is usually attributed to structure is that it can allow soil to exist at states outside the intrinsic state boundary surface. Here instead, the effect of breaking

down the aggregated micro-structure of the reconstituted sample causes the location of the state boundary surface of the minced material to move to higher volumes. A similar negative effect of structure on the compression behaviour was observed in Section 2.3.2, where the breaking down of the structure of natural samples was also shown to increase the apparent size of the state boundary surface.

4.4.3 Natural Samples

The compression behaviour of natural and reconstituted samples of structurally complex clays was discussed in Chapter 2. Figure 2.48 showed that for the data obtained from the literature on structurally complex clays, natural samples when compressed did not always reach the intrinsic compression line within the stress ranges applied and instead, formed compression lines parallel to, but below, the intrinsic compression line. It was initially thought that the lowering of the position of the normal compression line for the natural soil was the result of their different macro-fabrics. However the S.E.M. analyses showed that some of the clay aggregates were broken down as a result of the reconstitution process and hence this negative effect of structure might also be a result of the micro-fabric. The reconstituted material described in the literature by Guerriero et al. (1995) was reconstituted by dry grinding, before mixing to a slurry. As the plasticity index of their typical reconstituted material was less than that of their typical natural sample, the material they called reconstituted was thought to be more similar to the material described as reconstituted in this thesis than the material labelled minced. The apparent reduction in the plasticity index from the natural to the reconstituted soils was attributed to differences in the natures of the materials tested.

The behaviours of two natural samples, H2C and HDA, were investigated in isotropic compression in the high pressure triaxial apparatus. Sample H2C was loaded to a mean effective stress of about 3.5 MPa (Figure 4.20). Unfortunately, the test on sample HDA had to be aborted at a mean effective stress of 0.9 MPa, as the sample was destroyed, due to the failure of the control system. As no yield point was observed in either case, it was clear that the normal compression lines for these natural samples was not reached for either soil. The lack of any further suitable samples prevented any more high pressure tests from being carried out. Further work is required to determine the positions of the natural normal compression lines for these materials.

4.5 Swelling and Recompression Behaviour

Schmertmann (1969) showed that the ratio of the slopes of the one-dimensional swelling lines for reconstituted and natural samples, Cs*/Cs can be a sensitive indicator of the influence of fabric and interparticle bonding in the natural soils. It should therefore follow that the ratio of the gradients of the swelling lines (κ^*/κ) for two corresponding materials with different structures (natural:reconstituted or reconstituted:minced) would also give a comparison of the influence of the fabric and interparticle bonding in these materials. This comparison is qualitative rather than quantitative.

As the swelling lines are noticeably curved, Schmertmann suggested considering the gradients at similar overconsolidation ratios. An alternative could be to consider the swelling lines in lnv-lnp' space when they become approximately straight, as can be seen in Figures 4.19 and 4.20. This method was used due to the limited amount of data available. Figure 4.19 shows the gradients of the swelling lines for the reconstituted and minced samples R9A and M9A. Values of $\kappa_{lnv\text{-}lnp'}$ (lnv-lnp' axes) of 0.037 and 0.040 were obtained for the reconstituted and minced samples respectively. The ratio of $\kappa^*_{lnv\text{-}lnp'}$ / $\kappa_{lnv\text{-}lnp'}$ was close to unity for samples R9B and M9B which therefore indicates that the swelling behaviour of these samples was not affected by the micro-structure.

Figure 4.20 shows the swelling and recompression data for samples H2C and R2C. As there were no swelling data for the natural samples, the gradients of the recompression lines for the natural and reconstituted samples were compared. Using a lnv-lnp' scale, values of $\kappa_{lnv\text{-}lnp'}$ of 0.021 and 0.031 were obtained for the natural and reconstituted samples respectively. The gradient of the recompression line for the reconstituted sample was however subject to some uncertainty due to the limited data available. The difference between the recompression line gradients was small for samples H2C and R2C and suggested that the recompression behaviour and so probably also the swelling behaviour of these samples was not greatly affected by the macro-structure.

4.6 Shear Behaviour

The shear behaviours of the natural, reconstituted and minced samples were investigated in the triaxial apparatus, using the preparation methods and testing procedures described in Chapter 3. An explanation of the nomenclature of the sample labels was given in Section 4.3. The details of the different tests are also summarised in Table 4.1.

The reconstituted samples were used as a reference material to normalise the corresponding behaviour of the natural and minced samples to account both for their volumetric and stress states and also for their different material properties. The behaviour of the reconstituted samples was also assessed independently to determine whether it exhibited any unusual features.

The effect of the micro-structure of the samples was assessed by comparing pairs of minced and reconstituted samples, whilst the effect of the macro-structure on the soil behaviour was investigated by comparing the behaviour of natural samples with that of their corresponding reconstituted samples.

Two sets of corresponding minced and reconstituted samples were tested. One set of samples was from sample tube 7 (M7A, M7B, R7B and R7C), which was soil from the landslide body, whilst the other set, which was from sample tube 9 (R9A, R9B and M9C), was from material located outside the landslide body.

The natural samples were sheared drained from an isotropic stress state estimated to be equivalent to the in-situ stress level as this was thought most likely to give stiffness and strength data which would be representative of the landslide behaviour. Normalisation of the data was essential to allow comparison of samples with different material properties and at different stress states and specific volumes.

4.6.1 Reconstituted Samples

The reconstituted samples were made from the trimmings of the corresponding natural samples. Each of the samples was compressed or swelled to an isotropic state prior to the start of loading. As samples, which were sheared either drained or undrained from

overconsolidated states, were not thought to reach their true critical states due to strain localisation (Atkinson and Richardson, 1987), it was decided that one sample from each group should be sheared undrained from a normally consolidated state to accurately determine the position of the critical state line. Complete details of all the tests are given in a separate data report (Fearon, 1998) and are summarised in Table 4.1. This section reviews the results from typical drained and undrained tests.

The results of the final shearing for the drained tests are presented as graphs of the deviatoric stress (q') and volumetric strain (ε_v) each plotted against the shear strain (ε_s). In order to calculate the deviatoric stress from the load measured, the cross sectional area of the sample was assumed to remain as a right cylinder. The changes in the dimensions of this cylinder were calculated from the volumetric and axial strain measurements. Whilst the cross-sectional area at the mid-height was noticeably larger than the average as a result of barrelling, the most appropriate cross-section for calculation of the deviatoric stress is the projection of the slip surface onto a horizontal plane. This projected cross-section is much closer to the average calculated using the right cylinder correction.

Corrections have not generally been made to the data for either the restraint of the membrane or for the changing sample area as a result of the slip plane formation. This was because the geometry of the slip planes in the natural samples was generally too complex to allow a meaningful correction to be made. The typical corrections that would be applied to the shear data as a result of membrane restraint and the change in sample area were thought to be around 2-3% of the maximum stress ratio for the reconstituted and minced samples and as much as 10% for some of the natural samples when very well defined slip surfaces were seen. The constraining effect of the membrane was less for the reconstituted samples as thinner membranes (0.3 mm) were used. Thicker membranes (0.6 mm) were used for the natural samples to reduce the likelihood of a lithorelict puncturing the membrane. The constraining effect of the membrane on the shear data of the natural sample (N9A) is discussed in Section 4.6.3. These corrections only affect the large strain behaviour.

The strains calculated were linear strains (displacements/initial dimensions) rather than the more theoretically correct natural strains (displacements/current dimensions). The difference between these two values of strain is negligible at smaller strains and only becomes noticeable at larger displacements. However, at these larger displacements, the

magnitudes of the strains calculated were less critical, particularly where strain localisation had occurred, because the calculations of strain assume the sample to be a continuous, uniformly displacing element. The accuracy of the strain data at the large axial strains is also not so important since the stresses and volumetric strains are typically constant, a critical state having been reached.

The shear strain (ε_s) was calculated from the axial and radial strains using Equation 4.3:

$$\varepsilon_s = \frac{2}{3}(\varepsilon_a - \varepsilon_r) \qquad \text{Equation 4.3}$$

where ε_r was calculated from the axial and volumetric strains assuming the sample remained a right cylinder, using Equation 4.4:

$$\varepsilon_r = \left[1 - \sqrt{\frac{(1-\varepsilon_v)}{(1-\varepsilon_a)}}\right] \qquad \text{Equation 4.4}$$

The reconstituted sample R2B was normally consolidated and sheared under drained conditions from an initial p' of 300 kPa (Figure 4.21), giving a value of M, or q'/p' at the critical state, of 0.48. The sample was ductile and compressive as would be expected for a normally consolidated clay. Strain localisation occurred during shearing and slickensides were seen on the failed surface after the end of the test. As it was felt that the strain localisation may have caused the sample to fail before critical state was achieved, a plot of the stress ratio q'/p' against the rate of dilation $(\delta\varepsilon_v/\delta\varepsilon_s)_{total}$ (Figure 4.22) was extrapolated to give a corrected M value of 0.54. The ratio of the total strain increments $\delta\varepsilon_v/\delta\varepsilon_s$ was determined by a least squares linear regression of the relevant volumetric and shear strain data. Typically a total of 41 pairs of data points (out of a total of 1000 lines of data) were used for each regression point plotted on Figure 4.22. This large number of points was used for the regression as the data were fairly scattered as a result of the slow strain rates used.

It is not straightforward to separate the elastic and plastic components of the total strain increments, but the contribution of the elastic strains during drained loading should be negligible close to the critical state. The discrepancy caused by using total rather than plastic shear strains was assessed by comparing the total and estimated plastic strain increments for Sample R2B (Figure 4.22). The elastic shear strains were calculated

from the very small strain stiffness G_{max} determined using Equation 4.5 from the bender element tests on sample R2C, which was another test on the same reconstituted soil.

$$(\varepsilon_s)_{elastic} = \frac{q'}{3G_{max}} \qquad \text{Equation 4.5}$$

The elastic volumetric strain increments were approximated by fitting a power law to the isotropic swelling data for sample R2C. The elastic volumetric strains were then calculated using Equation 4.6:

$$(\varepsilon_v)_{elastic} = \left[1 - \left(\frac{p_o'}{p'}\right)^{\kappa_{lnv-lnp'}}\right] \qquad \text{Equation 4.6}$$

where p_o' is the mean effective stress at the beginning of the shear stage and $\kappa_{lnv\text{-}lnp'}$ is the gradient of the isotropic swelling line using a lnv-lnp' plot. Ideally a κ_{max} value should have been used to ascertain the elastic component of the volumetric strains but this was not obtainable from the triaxial test data as the unloading path could not be accurately defined due to the very low permeability of these materials. The extremely slow rate of unloading that would be required to allow complete pore pressure equalisation for such low permeability soils was not possible in this apparatus. The elastic volumetric strains calculated are likely to be slightly too large.

The ratio of the strain increments $(\delta\varepsilon_v/\delta\varepsilon_s)_{plastic}$ was hence determined by a least squares regression of the plastic volumetric and shear strain data, and is also plotted on Figure 4.22. This figure shows that although the use of the plastic components of the strain increments would be desirable when considering stress-dilatancy, the ratio of either the plastic or total strain increments can be used adequately to extrapolate to determine the correct stress ratio at the critical state, M.

Figure 4.23 shows a plot of the deviatoric stress and change in pore pressure during the final shearing for the reconstituted sample R2C. The sample was sheared undrained from a normally consolidated state, after being isotropically compressed to 500 kPa. The sample, when sheared undrained, was contractant and ductile as would be expected. Figure 4.24 shows a plot for Sample R2C of the stress-ratio plotted against the rate of change in the plastic component of the pore pressure with plastic shear strain

$(\delta u/\delta\varepsilon_s)$plastic. The plastic component of the change in pore pressure δu_p was calculated using Equation 4.7:

$$\delta u_p = \delta u_T - \frac{\delta q'}{3} \qquad \text{Equation 4.7}$$

where δu_T is the total change in pore pressure from the start of the test. As was the case for the drained test R2B, the sample appears to have failed prior to reaching its correct M. Extrapolating the line $(\delta u/\delta\varepsilon_s)_{plastic}$ gives a corrected M value of 0.53, which is similar to that obtained for the drained sample.

Samples R2C and R2B reach similar stress ratios, but a plot of the mean normal effective stress versus specific volume (Figure 4.25) shows that the drained test R2B did not compress sufficiently to reach the critical state line. This is believed to result from incomplete dissipation of pore pressures due to the very low permeability of these soils, so that volumetric strains prior to strain localisation were smaller than they should have been. As a result of the very low permeability of these materials, the average length of the final shearing stage was in the order of 10-12 days, which was thought to be about the slowest rate that was practical. In spite of the slow shearing rate used, it appears that the samples were still sheared too quickly. Strain localisation prevents samples reaching the critical state, as when localisation occurs, further pore pressure changes or volumetric strains are curtailed. This effect was worse for the drained sample than for the undrained sample, as strain localisation is thought to occur at smaller strains in the drained sample. Strain localisation occurs as the result of local drainage, which occurs more readily in the drained sample as it is sheared slower and there is a greater movement of water within the sample.

Figure 4.26 shows a comparison of the stress-dilatancy relationships for the undrained and drained tests R2C and R2B. The plastic shear and volumetric strains were calculated for both the drained and undrained tests using Equations 4.5 and 4.6 respectively. For the undrained test, as the total volumetric strains are equal to zero, the plastic and elastic components of the volumetric strains must be equal and opposite. The elastic volumetric strains and hence the plastic volumetric strains are therefore calculated from the change in mean normal effective stress using Equation 4.6. Different stress-dilatancy relationships for undrained and drained tests were reported by Cotecchia (1996) for Pappadai clay. The difference may result either from the fact that

there was incomplete dissipation of pore pressures during the drained test or from the assumptions made when calculating the plastic strain increments.

a) Correlations with Soil Plasticity

The critical state friction angles for undrained tests on normally consolidated reconstituted samples have been plotted against plasticity index in Figure 4.27. These data have been corrected for any strain localisation that may have occurred using the stress dilatancy plots discussed in the previous section. Their values are given in Table 4.1. An empirical correlation for the friction angle (ϕ') for normally consolidated soils with I_p was proposed by Mitchell (1993) which is:

$$\sin \phi_p' = 0.35 - 0.1 \ln(I_p) \qquad \text{Equation 4.8}$$

The data all lie below the correlation line given by Mitchell (1993), but are within the scatter of his data. Similar values of friction angle were observed for other samples of reconstituted structurally complex clays in the review of literature in Section 2.3.2. The difference between the observed values and the empirical correlation was seen to increase with plasticity index.

The validity of the correlation is limited by the ability of the plasticity index to describe adequately the size, shape and mineralogy of the particle grains. For example, illitic and montmorillonitic soils were shown by Mitchell to lie below this correlation.

b) Normalised Behaviour

In order to allow comparison of the triaxial tests, the shearing data were normalised to account for the different stress states and specific volumes of the samples. Initially, the shearing data were normalised with respect to an equivalent pressure taken on the normal compression line. This was because the location of a critical state line requires at least three tests to be carried out on identical samples at different mean normal effective stresses. As the duration of each test on a reconstituted sample was three to

five months and as a critical state line had to be defined for each of the natural samples tested, this was impracticable.

One of the problems, when normalising was carried out with respect to the normal compression line, was that the critical state occurred at different values of p'/p'_e. The test data were therefore normalised with respect to the critical state lines for the reconstituted samples assuming that the gradient of the critical state line λ was the same as the gradient of the normal compression line. The intercept of the critical state line, Γ, was calculated using λ and the values of mean effective stress p' and specific volume v at the critical state for a single test for each soil, using the equation:

$$v = \Gamma - \lambda \ln p' \qquad \text{Equation 4.9}$$

For each sample group, at least one test was carried out on a reconstituted sample, which had been sheared undrained to failure from a normally consolidated state, to determine the position of the critical state line. When strain localisation was seen for these samples, it was thought to occur very close to the critical state and hence did not cause a serious error in the value of p' at the critical state used for the calculation of Γ. The value of Γ determined from this test was thought to be sufficiently accurate. As was discussed in Section 4.6.1, strain localisation was more critical when determining the critical state from drained tests on normally consolidated samples of these materials. Atkinson and Richardson (1987) also noted that strain localisation can cause difficulties in obtaining the critical state for any test on an overconsolidated sample.

The shearing data were therefore normalised with respect to the equivalent pressure p'_{cs}, which was the value of the mean normal effective stress on the critical state line at the same specific volume, given by the equation:

$$p'_{cs} = e^{\left(\frac{\Gamma - v}{\lambda}\right)} \qquad \text{Equation 4.10}$$

The plot of q'/p'_{cs} against p'/p'_{cs} showed a lot of scatter in the data, which was partially caused by the difference in the critical state friction angles for the different materials. The data were therefore further normalised by dividing the deviatoric stress by the stress ratio q'/p' at the critical state, M. The value of M was determined from an extrapolation

of the stress-dilatancy data, as was discussed earlier. Figure 4.28 shows the final plot of q'/Mp'_{cs} against p'/p'_{cs}. The critical state lies at the point (1,1).

The stress ratios at the critical state and the position of the critical state lines were defined using the undrained tests on the normally consolidated clay and therefore, these samples all converge on the point (1,1) by definition. Some of the samples reached a value of q'/Mp'_{cs} slightly higher than that at the critical state before falling to the critical state line. This was thought to be as a result of pore pressures not having dissipated sufficiently as tests were carried out, even though the shearing typically took 10 - 12 days.

The drained test on the normally consolidated reconstituted sample R2B reached a plateau at a stress state apparently outside the state boundary surface, defined by the other tests. This was thought to result from the sample not compressing sufficiently during shearing to reach the true critical state line because of too rapid shearing and localisation as was discussed earlier.

The undrained test on the overconsolidated reconstituted sample R7C reached a stress ratio slightly above the critical state stress ratio, before moving towards the critical state line. The sample did not quite reach the critical state line as the strains appeared to localise, the stress ratio then dropping towards that of the critical state. This behaviour is typical of undrained tests on overconsolidated soils as was observed by Atkinson and Richardson (1987).

The overconsolidated reconstituted samples (R8A, RDA and R9B) were sheared drained from states on the dry side of critical. Sample RDA reached the critical state stress ratio but was unable to dilate sufficiently to reach the critical state as strain localisation occurred. Sample R8A reached a plateau of constant stresses and strains at a stress ratio above the critical state, whilst sample R9B only reached a stress ratio below that at the critical state. The low stress ratio achieved by R9B was again attributed to strain localisation as a clear shear surface was seen on the failed sample. The results from the test on sample R8A must be subject to some doubt as the load cell drifted substantially during this test. The data were corrected assuming a linear drift of the deviatoric stress with time and hence the data points plotted start at a high deviatoric stress. The marked tendency towards strain localisation was thought to result from the slow strain rates used for these tests because of the low permeabilities of these soils. The different behaviours

observed could also have resulted from differences in the natures of the materials in the different sample groups.

As a result of the heterogeneity of these soils, a single boundary surface is not obtained for the reconstituted soils, even when normalised with respect to their respective critical state lines. This is partly because the normal compression lines plot at different values of p'/p'_{cs}. Hence only a typical reconstituted state boundary surface can be drawn on Figure 4.28 and this represents an average for all the materials.

4.6.2 Minced Samples

Three minced samples were sheared to failure, M7A, M7B and M9C. Samples M7B and M9C were sheared undrained from normally consolidated states, whilst M7A was sheared undrained from an overconsolidated state.

Figure 4.29 shows a graph of q'/p' for corresponding minced (M7B) and reconstituted (R7C) samples both sheared undrained from normally consolidated states to failure. The samples were both ductile and contractant as would be expected for normally consolidated samples. Both samples follow very similar stress-strain curves, reaching similar stress ratios at the critical state.

Figure 4.30 shows a graph of the stress ratio (q'/p') against the shear strain for the normally consolidated undrained tests for the reconstituted and minced samples from sample group 9. The stress-strain curves for the reconstituted and minced samples are very different, in contrast to sample group 7. The stress-strain curve for the minced sample has a slight peak which is unusual as it was sheared from a normally consolidated state. It is thought that the reason for this strain-softening is a result of particles reorienting as the strains localised. Ring shear tests on minced and reconstituted samples (Section 4.7) showed that the minced samples reached the residual strength with a smaller displacement. Figure 4.31 shows the stress-dilatancy relationships for the two samples. The two lines have very similar gradients, but the minced and reconstituted samples have stress ratios at failure of 0.56 and 0.82 respectively. These stress-dilatancy curves were extrapolated to give values of M of 0.65 and 0.84 for the reconstituted and minced samples respectively and therefore strain localisation is not responsible for this discrepancy.

Figure 4.27 showed Mitchell's correlation between plasticity index and the critical state friction angle. The effect of mincing for sample group 7 was to increase the plasticity index as was shown in Section 4.3.1. However there was no corresponding decrease in the critical state friction angle. The critical state friction angle therefore does not appear in this case to be affected by the micro-structure of the soil. In contrast the effect of mincing for sample group 9 was again to increase the plasticity limit of the soil, but in this case a decrease in ϕ' was seen, which was comparable with that which would be expected from Mitchell's correlation.

Figures 4.32 and 4.33 show the normalised shearing data for sample groups 7 and 9. The data were again normalised with respect to the estimated critical state line for the reconstituted material as discussed in the previous section. Hence the start of the shearing data for the normally consolidated minced samples lies outside the intrinsic state boundary surface. This is a consequence of the normal compression line for the minced sample lying to the right of that of the intrinsic normal compression line. Although samples M9C and M7A seem to reach similar critical states to the reconstituted soil, Sample M7B clearly does not. The position of the critical states for the minced and reconstituted samples is also plotted in Figures 4.18 and 4.19. The position of the critical state lines in v-lnp' space is different for the reconstituted and minced samples and this is why the data for the minced samples when normalised with respect to reconstituted critical state do not reach a single state boundary surface.

4.6.3 Natural samples

The natural samples were mostly sheared under drained conditions from isotropic initial stresses estimated to be equivalent to those at the in-situ. The stress level was estimated from the depth of the sample below ground level, the bulk unit weight of the soil and the piezometric data. The locations of the piezometers which were installed as part of the site investigation, are given in Figure 1.5, whilst full details of the piezometric data are given in the final report for the European Community project, of which this work formed a part (Cotecchia et al., 1996). Drained shearing was used as it was most likely to reflect the conditions in the landslide. Sample H2C was however sheared undrained in the high pressure apparatus from an initial mean normal effective stress of 3.5 MPa. The values of the stress ratios achieved at failure are summarised in Table 4.1.

The samples typically failed along multiple shear surfaces. Figure 4.34 shows sketches of typical failed samples. Development of the failure surfaces was thought to occur in the natural samples as a result of the inherent discontinuities in the sample, localisation occurring along the pre-existing discontinuities of the scaly macro-structure. Visual inspection of the failed samples showed no noticeable orientation of the particles along the failure surface and it is thought that the strains were not sufficient to cause reorientation. This lack of orientation at these strain levels was thought to be an effect of the scaly macro-structure of the natural samples not breaking down within the shear surfaces.

Figure 4.35 is an example of the behaviour typically seen for the natural samples and shows plots of q'/p' against ε_s and ε_v against ε_s for sample N2B. The behaviour of the natural samples when sheared drained was ductile, with no peak strength and a slightly contractant volumetric behaviour. This behaviour was unusual considering the high overconsolidation ratio (OCR). Sample N2B had an initial value of p'/p'_{cs} of 0.18, where p'_{cs} is the value of the normal effective stress on the critical state line of the reconstituted soil at the same specific volume, which was given by Equation 4.10. This was very approximately equivalent to an OCR of about 7. By examining the state path in v-lnp' space the small volumetric contraction was thought to be due to the increase in p' for drained shearing. This ductile and contractant behaviour has been observed frequently for the structurally complex clays. Examples of materials, which exhibit this behaviour include the Bisaccia clay shale (D'Elia, 1991, Guerriero et al., 1995), the Santa Barbara clay shales (D'Elia 1991), the M. Marino clay (Guerriero et al., 1995, Guerriero, 1995), the Roseto clay shale (Bertuccioli and Lanzo, 1993) and scaly clays from Bifarera and Piano Campo (Bilotta and Umilta, 1981).

A plateau of constant deviatoric stress was usually reached at about 4 - 5 % axial strain (e.g. N9B, Figure 4.36), although in some cases the deviatoric stress continued to increase gradually (e.g. N9A, Figure 4.36). These increasing values of q'/p' with continued shear strain while the volume remained constant were slightly unusual, as the value of q'/p' would be expected to remain constant, representing a critical state, whilst if a residual surface formed it would be expected to fall due to reorientation of the particles along the slip surface. However, when studying the failure mechanisms of the samples, where q'/p' continued to rise (N6A and N9A), it was noted that these samples had more heavily defined slip surfaces. The increase in the value of q'/p' was thought

then to be a result of the constraining effect of the membrane (La Rochelle et al., 1988). Corrections have not generally been made to the data for this, nor for the changing sample area on the slip plane, as the geometry of the slip plane was usually too complex to allow a meaningful correction to be made.

In order to investigate the effect of sample size on the mechanical properties of this structurally complex clay, a 38 mm (N9A) and a 60 mm (N9B) diameter sample, taken from the same sample tube, were tested (Figure 4.36). The smaller sample was found to be slightly stiffer at smaller strains than the larger sample and achieved a slightly larger stress ratio at failure. The values of q'/p' for the 60 mm and 38 mm diameter samples were 0.57 and 0.64 respectively. The critical state for both cases also occurred at comparable specific volumes. The major difference between the two tests was that the stress-strain curve for the larger sample tended towards a well defined plateau whilst the deviatoric stress for the smaller sample continued to rise gradually. Comparing the shapes of the failed samples, the smaller sample had formed a well defined shear surface whilst the larger sample had barrelled. The restraining effect of the membrane could therefore account for the greater strength of the smaller sample. It was concluded that the smaller sample had a greater tendency to form a well defined slip surface, as the random orientation of discontinuities are more likely to connect together and form a continuous failure surface.

An attempt to correct the data for the 38 mm sample (N9A) for the confining effect of the membrane and for the reduction in the sample area as a result of the slip plane has been based on the corrections proposed by La Rochelle et al. (1988). The area correction applied assumed that the diameter of the sample in the direction of the strike of the shear plane was that calculated from the right cylinder correction. The diameter in the direction of the dip of the shear plane used the diameter calculated assuming a right cylinder reduced by the horizontal displacement caused by the shear plane.

The corrected data for sample N9A are shown in Figure 4.36. The corrections were not thought to have been very successful as a plateau was still not reached. This was attributed to the complex geometry of the slip plane and the difficulty of establishing the strain at which localisation began in this heterogeneous sample. The corrections due to the restraining effect of the membrane and the reduction in area due to movement along the slip surface were most important for the two natural samples with defined slip surfaces (N6A and N9A). The correction calculated for these two samples was

estimated to be about 10 % for the stress ratio. For the samples with the less well defined slip surfaces, the correction was estimated to be in the order of 5 %.

As the correction for the reduction in sample area for a sample with a slip surface and the correction for membrane constraint cannot be meaningfully determined, strong conclusions cannot be drawn about the effect of sample size on the shear strengths calculated. However if the samples could be corrected properly, it is thought that the two samples would give similar strengths, although strain localisation was thought to be more easily developed for the smaller sample. The effect of sample size did not have a significant effect on the stiffness properties for which these corrections are unimportant.

Sample H2C was sheared undrained in the high pressure triaxial apparatus from an initial mean normal effective stress of 3.5 MPa. Undrained loading was used due to time constraints. Figure 4.37 shows a graph of deviatoric stress and changes in pore pressure plotted against shear strain. The sample was ductile and contractant as would be expected from a sample sheared on the wet side of critical (as defined by the reconstituted sample). The sample reached a plateau at a critical state stress ratio of only about 0.34, very much less than the ratios obtained either for the corresponding reconstituted sample (0.49) or for a similar natural sample (0.84) sheared at lower stresses. Possible explanations for this reduction in strength are discussed in the following section.

a) Normalised Data

In order to allow comparison of the various triaxial tests, the data were normalised to account for the different stress states and specific volumes of the samples. As for the reconstituted samples, the stresses were normalised with respect to an equivalent pressure on the corresponding critical state line derived from a reconstituted sample of the same soil. The locations of the normal compression lines and the critical state lines for the natural samples were not known. The normal compression lines for the natural soils could only be determined from high pressure tests on similar natural samples for each group. This was not possible due to the shortage of similar undisturbed soil. The critical state lines for the natural samples could not be determined, due to the tendency of the natural samples to strain localise, making it impossible for the natural soil to get anywhere near its true critical state. The data have again been further normalised to

account for the different critical state friction angles of the various soils by dividing the normalised deviatoric stress (q'/p'_{cs}) by the value of M for the corresponding reconstituted sample. Figure 4.38 shows the resulting plot of q'/Mp'_{cs} against p'/p'_{cs} for the natural samples compared with the intrinsic state boundary surface derived for the reconstituted.

The initial states of most of the natural samples had low values of p'/p'_{cs}, indicating that the samples were highly overconsolidated in-situ. There was little variation in the values of p'/p'_{cs} between samples inside and outside of the landslide body, indicating that there was little influence of the landslide movements on the volumetric state of the soil. This finding agreed with the results of the liquidity index data.

The natural samples, which were tested at their estimated in-situ stress levels, each headed towards the boundary surface defined for the tests on the reconstituted samples with little change in the ratio p'/p'_{cs}. At the boundary surface, it was expected that the samples would then dilate and move along the boundary surface to the critical state. However, the samples were found not to dilate sufficiently to reach a true critical state and strain localisation occurred, almost certainly promoted by the natural discontinuities in the sample. This pattern of the natural samples, failing upon reaching the boundary surface instead of dilating to the critical state, was also observed by Guerriero et al. (1995).

Sample H2C reaches a normalised stress state outside the intrinsic state boundary surface. The sample is likely to have undergone localisation of strains due to the inherent discontinuities in this scaly clay. The stress ratio at failure for Sample H2C was significantly less than those of the corresponding reconstituted sample and natural sample tested at in-situ stress levels. The difference between the maximum stress ratios of samples H2C and the adjacent sample N2B was thought to result from their different discontinuity patterns. Sample H2C was described as scaly, which contrasts with the adjacent sample used for the standard pressure test, which was described as intact clay with isolated fissures running through the sample. There could also be a reduction in the strength along the slip surface at this higher stress level. The friction measured along a rough failure plane is a function both of the friction of the material and the roughness of the failure plane. At higher stresses, the roughness of the shear surface created by the scales in these structurally complex clays could reduce as the scales are sheared through.

Samples N2B, NCA and N7A, which were taken from within the landslide body, each had a maximum stress ratio equal to or above M of the equivalent reconstituted samples, whilst samples N6A, N7A, N8A and N9A which were retrieved from outside the landslide had maximum stress ratios which were only approximately 70 % of M for the reconstituted soil. Sample H2C reached a stress ratio of only 0.6 M. This reduction of the stress ratio at failure of the natural samples compared with the reconstituted samples was also observed by Olivares (1996) for the Bisaccia clay shale. Burland (1990) also noted that although the initial stress path of a fissured sample of London clay was similar to that of the intact samples, premature failure occurred on a pre-existing fissure truncating the stress path and eliminating most or all of the dilatant portion. The shear strength of samples of London clay containing fissures plotted close to or slightly below the post-rupture failure line determined for intact samples and the reconstituted critical state line (Section 2.2.3 (b)). The post-rupture strength of the Bisaccia clay shale always lay below the critical state line.

The effect of the scaly macro-structure on the behaviour of the intact formation was therefore to reduce the stress ratio of the soil at failure when sheared at the estimated in-situ stress level. The ratio of the friction angles of the natural to the reconstituted material is thought to decrease with the confining stress, although more tests would be required to test this hypothesis. The reduction in stress ratio at failure for the natural samples at higher stresses was thought to result from scales being sheared through at the greater confining stresses, allowing particle alignment along the shear surface.

Both reconstituted and natural samples from the landslide body, when sheared drained from an overconsolidated state, reached stress ratios equivalent to or above the value of M determined from undrained tests on equivalent normally-consolidated reconstituted samples. Hence, the effect of the macro-structure on the drained strengths of the landslide material and the reconstituted material were fairly similar. The effect of the macro-structure on the drained strength of the formation material was more noticeable, as the maximum stress ratios reached were less than those of the equivalent reconstituted samples or M. The macro-structures of soils from the underlying formation and the landslide body are very different. The samples from the formation were typically scaly, having structures similar to the γ type material, proposed by Guerriero et al. (1995), whilst samples with the landslide body consisted of lithorelicts of the original formation within a clay matrix; type δ materials (Figure 2.38). The

remoulding effect of landsliding was thought to change the macro- and not the micro-structure of the soil. This is discussed in more detail in Section 5.2.

4.7 Shear Stiffness

4.7.0 Introduction

The stress-strain response of soils is highly non-linear and is dependent on strain level, as was shown schematically in Figure 2.22 (Atkinson and Salfors, 1991). The stiffness of the soil has been examined at three scales, the very small strain stiffness or G_{max}, the small strain stiffness between 0.01 to 0.1 % strain and the large strain behaviour. The very small strain stiffness was measured dynamically using piezo-ceramic bender elements. The larger strain behaviour was assessed using local axial strain gauges in the triaxial cell. Stiffness is also dependent on the stress path followed and therefore the drained behaviour has been analysed as this is most likely to affect the behaviour of the landslide. The results of the stiffness data have been normalised to account both for the mean effective stress and the overconsolidation ratio.

The errors which affect the large strain behaviour of the samples arising from the strain localisation, the restraint of the filter paper and membrane and the changes in cross-sectional area are negligible at smaller strains and hence do not affect the measurements of stiffness.

4.7.1 Very Small Strain Stiffness - G_{max}

The shear modulus G_{max} is the stiffness in the very small strain region (typically < 0.001 %) over which the soil behaves elastically. It can be measured under monotonic loading in the triaxial apparatus with local instrumentation if the instrumentation is sufficiently accurate, or more simply, dynamically using resonant column apparatus or piezo-ceramic bender elements. G_{max} was measured here using the piezo-ceramic bender elements (Schulteiss, 1982), described in Section 3.3.3.

Six different samples were tested using the bender element technique which included two natural samples, one minced sample and their corresponding reconstituted samples.

Bender element measurements of G_{max} were taken for the two natural samples (HDA and H2C) tested in the high pressure apparatus at increasing mean effective stresses during isotropic compression. Sample HDA was lost during testing due to an equipment failure at a mean normal effective stress of 1000 kPa. Bender element readings were taken for the minced and reconstituted samples only in the standard pressure triaxial cells.

The testing and interpretation procedures used were discussed in detail in Chapter 3. Figure 4.39 shows examples of the oscilloscope traces taken using a sinusoidal and a square wave. There was good agreement between the two readings of the arrival time which gives added credibility to the values calculated.

Figure 4.40 shows the results of the bender element tests for the minced and reconstituted samples from tube 9, whilst Figures 4.41 and 4.42 show the results of the bender element readings for the natural and reconstituted samples of groups 2 and D. The bender element readings were taken at the mean effective stresses and specific volumes indicated by a data point in the v-lnp' plot of each figure. The shear stiffnesses were calculated, using the procedures described in Chapter 3, from the shear wave arrival time and the sample density and height.

Viggiani (1992) showed that the shear modulus of a fine grained soil was related to the mean normal effective stress, p' and the effective overconsolidation ratio (R_o), using the power law relationship described in Section 2.4 and given below:

$$\frac{G_{max}}{p_r} = A\left(\frac{p'}{p_r}\right)^n (R_o)^m \qquad \text{Equation 4.11}$$

The values of the pressure exponent n, determined from the bender element tests on the reconstituted soil at normally consolidated stress states, ranged from 0.9 to 0.96. The value of the n was shown by Viggiani and Atkinson (1995a) to vary with plasticity index as is shown in Figure 4.43. The values of the pressure exponent for the very small strain stiffnesses of these soils, although slightly higher than those measured by Viggiani and Atkinson, are not inconsistent with their results.

Figure 4.40 (a) shows the compression behaviour of the minced and reconstituted samples from group 9. These samples were loaded using one-step consolidation loading stages. The duration of these stages was a minimum of seven days. Due to the low permeability of these materials, this allowed between 80 and 100 % of the total volumetric strains to occur and was a compromise between the available testing time and the need for complete pore pressure equalisation. Hence when the samples were unloaded, there is still a slight increase in the volumetric strains of these samples. The slight increase in the shear stiffness with unloading (Figure 4.40 (b)) corresponds with this volumetric strain.

Figure 4.40 (b) shows the shear moduli for the normally consolidated reconstituted and minced samples of each group plotted against the mean normal effective stress p'. There is a power law relationship between the shear moduli and the mean normal effective stress for the normally consolidated samples of both the reconstituted and minced samples prior to isotropic swelling. However, after the isotopic swelling and recompression stages, the shear moduli for the minced samples did not return to the same line. The most likely explanation for the discrepancy measured was thought to result from the undissipated pore pressures. However, it could also result in part from the extreme deformations to which the sample had been subjected. The minced sample had been subjected to 50 % volumetric strains prior to the start of the final shearing, resulting in the length of the sample being only 44 mm at this stage. The short arrival time therefore resulted in a more severe near field effect for the same frequency (Jovicic et al., 1996). The value of the pressure exponent n of the minced sample was consistent with that of the corresponding reconstituted one.

In order to assess the effect of the overconsolidation ratio on the shear moduli, the values of G_{max} were normalised with respect to the mean normal effective stress p' raised to the power of the pressure exponent n, whilst the mean normal effective stresses p' were divided by the equivalent pressure p'_e. The equivalent pressure p'_e used was the value of the mean effective stress on the normal compression line for the equivalent reconstituted sample at the same specific volume, given by the Equation 4.12.

$$p'_e = e^{\left(\frac{N-v}{\lambda}\right)}$$ Equation 4.12

Since the maximum previous applied normal effective stress was not known for the natural samples, p'/p'_e was used as a measurement of the overconsolidation ratio as p'/p'_e is related to $1/R_o$. This approach was used by Rampello et al. (1997) and Coop et al. (1995). Rampello et al. defined the 'overconsolidation ratio' exponent c using Equation 4.13:

$$\frac{G_{max}}{p_r} = S^* \left(\frac{p'}{p_r}\right)^{n^*} \left(\frac{p'_e}{p'}\right)^c \qquad \text{Equation 4.13}$$

where S*, n* and c are the constant, p' exponent and p'_e/p' exponent respectively in this power law relationship. The parameter c can be related approximately to m using Equation 4.14:

$$c = \frac{m}{\left(\frac{\lambda - \kappa}{\lambda}\right)} \qquad \text{Equation 4.14}$$

The values of c and hence m determined for the reconstituted samples are larger than those quoted in the literature for similar plasticity indices (Figure 4.44). This indicates that the overconsolidation ratio has a greater effect for this soil than would normally be anticipated.

Figure 4.40 (c) shows the normalised G_{max} data for the minced and reconstituted samples R9B and M9C respectively. The values of p' are normalised with respect to the equivalent pressures for the reconstituted sample in both cases. As a consequence of the data being normalised with respect to the normal compression line of the reconstituted soil, the data for the normally consolidated minced samples do not plot as a single point. It can be clearly seen that the shear moduli of the normally consolidated minced samples are lower than those of the normally consolidated reconstituted samples. Otherwise, both the reconstituted and minced samples define a unique relationship between normalised shear modulus and p'/p'_e. The effect of the normal compression line being different for the minced and reconstituted samples appears to be cancelled by the minced material being softer. It is not clear whether this result is coincidental. Apart from the influence of the different volumetric states of the reconstituted and minced samples, the stiffness therefore does not appear to be affected by the micro-structure.

Figures 4.41 (a) and 4.42 (a) shows the compression data for the natural and reconstituted samples from sample groups D and 2. Again the decreasing specific volumes, when the reconstituted samples were unloaded, were attributed to the lack of pore pressure equalisation at the end of the previous loading stages. A longer period of pore pressure dissipation was impractical as the durations of these tests were already three and five months respectively. The lack of pore pressure dissipation was not thought to be particularly significant, although its effect is noticeable with changes of loading direction. As a result of these undissipated pore pressures, Figures 4.41 (b) and 4.42 (b) both show an initial increase in the stiffnesses of the samples with unloading.

Figure 4.41 (c) shows the G_{max} data for the natural and reconstituted samples HDA and RDA respectively. Again these data were normalised with respect to the equivalent pressures (p'_e) defined by the reconstituted sample, to account for their different stress states and specific volumes. There is no noticeable difference between the normalised stiffness data of the samples RDA and HDA. For these samples there therefore does not appear to be an effect of the macro-structure on the stiffness behaviour.

Figure 4.42 c) shows the G_{max} data for the natural and reconstituted samples H2C and R2C respectively. The normalised stiffness data for sample H2C plot above those of the reconstituted sample R2C. For these samples there is an effect of the macro-structure on the stiffness behaviour, in contrast to the tests on samples RDA and HDA where there was not. The reason for the difference between the behaviours of these two groups of samples is not clear as the appearances of the two natural samples are fairly similar.

4.7.2 Small Strain Stiffness (0.01 - 0.1 %)

The small strain stiffness of both natural and reconstituted samples was investigated in the triaxial cells instrumented with local axial gauges. Stiffness data in addition to those for the final shearing were obtained by carrying out stress probes both on the natural and reconstituted samples at intervals during isotropic compression or swelling.

The shear stiffness of the samples was investigated by plotting $\delta q'/3\delta\varepsilon_s$ against the shear strain and plots for each test are given in the data report (Fearon, 1998). For convenience the shear modulus, G', was taken to be equivalent to the term $\delta q'/3\delta\varepsilon_s$.

This is a simplification and ignores the effect of cross-coupling between the volumetric and shear strains, defined by Equation 4.15 (Graham and Houlsby, 1983).

$$\begin{bmatrix} \delta p' \\ \delta q' \end{bmatrix} = \begin{bmatrix} K' J' \\ J' 3G' \end{bmatrix} \begin{bmatrix} \delta \varepsilon_v \\ \delta \varepsilon_s \end{bmatrix} \qquad \text{Equation 4.15}$$

The effect of cross-coupling could potentially be quite large. However comparisons were possible between the data for various tests as the term $\delta q'/3\delta\varepsilon_s$ was used consistently throughout.

The values of $\delta q'/3\delta\varepsilon_s$ were calculated by least squares regression of the triaxial data. Figures 4.45, 4.46 and 4.47 show only typical examples of the stiffness data obtained for a natural, a reconstituted and a minced sample (N7A, R7B and M7C). Scatter in the stiffness data was attributed to noise of the load cell and temperature fluctuations of the volume gauge which, even though the laboratory was controlled to ± 1 °C, proved to be a problem because of the extreme length of the tests, particularly because shearing was drained in the cases where stiffness was examined. This problem was most noticeable for the softer reconstituted and minced samples tested at low confining stresses. The stiffnesses were typically calculated over a 41 point regression which was generally equivalent to a range of shear strain of approximately 0.007 % at a shear strain of 0.01%. However where the scatter in the data was particularly bad, a curve has been drawn by hand through the stress-strain data and the stiffness was calculated by taking a tangent to this smoothed line, as is shown in Figure 4.48. The point calculated from the tangent drawn to the stress-strain curve was plotted along with the scatter of points determined using the normal linear regression. This procedure was carried out for approximately 10 % of the test stages.

Values of $\delta q'/3\delta\varepsilon_s$ at 0.01% and 0.1% shear strain have been plotted against the mean normal effective stress for the shearing probes from normally consolidated states for reconstituted sample R2B in Figure 4.49. As the samples were normally consolidated, $R_o = 1$, and therefore values of n could be determined for each of the strain levels from Equation 4.11. There appears to be a decrease in the value of n with increasing strain level for Sample R2B, in contrast to the results of Viggiani and Atkinson (1995a), who showed the value of n to increase with strain level to 1 at the critical state. Re-analysing the data here, the change in the value of n with stress level was smaller than the scatter

of the data and at each strain level, a value of n of 1 equally well fits the data. As the values of n for the very small strain shear moduli G_{max} were greater that 0.9 and n should increase with strain level, this assumption was not considered unreasonable.

Figure 4.50 shows the shear moduli for probes conducted from normally consolidated states for the reconstituted and minced samples of sample tube 7. There is no identifiable difference between the shear stiffnesses of minced and reconstituted samples at strain levels from 0.01 to 0.1 %, again suggesting that micro-structure has little effect on stiffness. Although, unlike the bender element data for sample tube 9, there was found to be no need to account for the differences in the volumes of the reconstituted and minced soils. When volume is accounted for, there is still no visible difference between the stiffnesses of minced and reconstituted samples.

In order to look at the effect of overconsolidation ratio on the shear stiffness, the data were then normalised with respect to $(p')^n$, assuming a value of n of 1 for strain levels above 0.01 %. Graphs of $(\delta q'/3\delta\varepsilon_s)/(p')^n$ were plotted against p'/p'_e for corresponding reconstituted, minced and natural samples at strain levels of 0.01%, 0.05% and 0.1%. The values of G_{max} from the bender element tests were also plotted on these graphs. The mean normal effective stress p' was again normalised by the equivalent pressure p'_e, defined on the reconstituted normal compression line. Using this normalisation which accounts for the volumetric states of the samples, the stiffnesses of the reconstituted and minced samples could be compared to those of the natural samples. Figures 4.51 and 4.52 show the normalised stiffnesses for sample groups 2 and 9 respectively.

Figure 4.51 shows the normalised stiffness for sample group 2. The relationship between the normalised stiffness and the overconsolidation ratio is clearly non-linear, unlike the linear relationship proposed by Rampello et al. (1997). There does not appear to be a difference between the stiffnesses of the natural and reconstituted samples at larger strains. A difference only exists between the stiffness behaviour of the natural and reconstituted samples at the very small strain stiffness (G_{max}). Soils from this sample tube were retrieved from a position beneath the current Acquara-Vadoncello landslide in the old Serra Dell'Acquara landslide. The macro-structures of the two natural samples H2C and N2B were quite different. The high pressure sample H2C had a scaly macro structure, whilst the sample N2B was more homogeneous, having only a couple of planar discontinuities. It appears that the macro-structure of this soil only has

an effect on the stiffness behaviour of this soil at the very small strain stiffness G_{max} and has no effect at larger strains considered. This was slightly surprising as it was thought the scaly macro-structure of Sample H2C could have caused a reduction in the stiffness as a result of strain localisation. Clearly this may still occur at larger strains, but unfortunately there are not the data to validate or refute this statement as shear probes could not be carried out to the required strain magnitudes.

The increase in G_{max} for the natural sample is relatively small, with a ratio of G_{max} for the natural to the reconstituted of about 2. Only the elastic stiffness and not the stiffness in the region of plastic behaviour is greater for the natural sample. This could result from a weak bonding in the natural material, which is broken down by very small shear strains but not isotropic compression. This seems unlikely. It could also result from connected stiffer particles in the natural material carrying the load at the very small strain levels, however outside this small elastic region the load is carried by the matrix. In the reconstituted material, the load is always carried by the matrix as the discrete particles are not connected. No increase in the value of G_{max} was observed between the natural and reconstituted samples from sample group D.

Figure 4.52 shows the normalised stiffness data for sample group 9. The normalised very small strain stiffnesses are plotted for the reconstituted and minced samples, R9B and M9C and the small strain stiffnesses are plotted for the reconstituted and natural samples, N9A, N9B, R9A and R9B. Again no noticeable difference between the normalised shear moduli of the reconstituted and minced samples can be seen. Similar behaviour was also seen for sample groups 6 and 8. The effect of the micro-structure was therefore deduced to have little effect on the stiffness behaviour within the small strain region.

In summary the micro-structure has little or no effect on stiffness, particularly if the data are normalised to account for their different volumetric states. The macro-structure has no effect on the stiffness within the small strain region but may have a relatively small effect on G_{max}.

4.8 Residual Strength

4.8.0 Introduction

The residual strength was determined using both the Bishop and Bromhead ring shear apparatus, following the procedures described in Chapter 3. Samples were tested in reconstituted and minced forms only as undisturbed samples of sufficient size were not available to carry out tests on the natural samples. The residual strengths determined were compared with the correlations summarised by Lupini et al. (1981).

Using the procedures described in Chapter 3, ring shear tests were carried out on six different reconstituted samples and one corresponding minced sample. The detailed results of the ring shear tests, including the graphs of shear against normal stress are given in the data report (Fearon, 1998) and are summarised in Table 4.2. The locations from which the samples were retrieved for these tests are illustrated on the cross-section in Figure 4.2. Examples are given here to illustrate specific points.

4.8.1 Reconstituted Samples

Figure 4.53 shows an example of a stress-strain curve, for sample RSC (Borehole P2, 10.2 - 10.5 m bgl) and the residual failure envelope defined for the test. Multi-stage tests were carried out to determine the frictional resistance at different stress levels. The results at different stress levels are plotted against cumulative displacements. Several stages were carried out, the sample being consolidated to successively higher stresses at each of which shearing was continued.

The sample was sheared in the Bishop ring shear apparatus, using the test procedures described in Section 3.2.5. To minimise the soil loss through the gap, some of the shearing is carried out with the confining rings closed, which is standard for this apparatus (Bishop et al. 1971). The gaps in the loading curve correspond to periods when the confining rings were closed and the stress data were therefore not available. There was some fluctuation in the value of frictional resistance with axial strain for each test stage. The scatter in the results is shown in Figure 4.53 (b). This variation in the shear resistance was approximately 3-4 kPa and was equivalent to the noise of the load cells.

Figure 4.53 (b) shows the residual strength envelope obtained. The residual friction angle was slightly higher at the low vertical effective stresses, becoming constant at higher stresses. This is consistent with the results of other research (e.g. Lupini et al. 1981). Mitchell (1993) suggested that a transitional failure mechanism would occur if less work was required to shear the particles without complete reorientation than was required for particle reorientation. For these soils, it could follow that the work required to shear the aggregated particles without degradation, may be less at low normal stresses than that required to break them down. For ease of comparison, the residual strength friction angles quoted ignore this slight increase in the residual strength at low normal stresses and assume a linear failure envelope as is shown in Figure 4.53 (b).

The residual friction angle for sample A was measured using both the Bishop ring shear apparatus and the Bromhead ring shear apparatus, giving 5.2° and 6.1° respectively. This reasonably close agreement for two completely different testing procedures gave added confidence in the data obtained.

In general, the residual friction angles appear to be very low (5.0° - 6.9°) but were reasonably consistent with the low angle of repose of the slope, discussed in Section 1.2. The Bishop ring shear tests carried out on samples of clay from the 1980 Serra Dell'Acquara slide by Lemos (1986) gave residual friction angles of 7.8° and 5.7°.

Lupini et al. (1981) showed that for soils which contained a large proportion of platy particles, the failure mechanism was by sliding. In the case where the residual strength was the result of a sliding mechanism, the residual friction angle was related to the angle of interparticle friction of the clay particles. Therefore the low values of residual strength obtained here were likely to be a result of the montmorillonitic component of the soils. Mitchell (1993) gives typical values of residual friction angle for basic minerals of 4° to 10° for montmorillonite; 35° degrees for calcite and quartz; and 10.2° for illite (muscovite).

The results of the ring shear tests were compared with the correlations summarised by Lupini et al. (1981). Correlations based on either clay fraction or plasticity index tend to over-estimate the value of ϕ'_r for these soils as can be seen in Figures 4.54 and 4.55. An average value of clay fraction was used in plotting the data on Figure 4.55 as particle size distributions were not carried out on the ring shear samples. As was discussed in Chapter 2, the limitations of these correlations have been well documented. They do

not always adequately describe the mineralogy and shape of the clay particles. The soils here were thought to be failing by means of a sliding mechanism dominated by the montmorillonitic component of the mineralogy.

Incomplete destructuration when determining the liquid limits was also identified as a problem by Mesri and Cepeda-Diaz (1986) when trying to correlate residual friction angles with the plasticity index. The increase in liquid limit with rigorous remoulding has already been identified as a feature of these soils and may in part be responsible for the poor correlations in Figure 4.54. The effect of the incomplete destructuration is assessed by comparing minced and reconstituted samples of the same soil in the following section.

The residual strength data from this landslide site plot significantly below the data from the literature for similar structurally complex clays. This could result from differences between the mineralogies of the two groups of materials; different preparation methods, which have been shown to have an effect in these soils (Section 2.3.2); or the residual strength not being reached in the direct shear apparatus or Bromhead ring shear apparatus used. Figure 2.56 showed the difference between the residual strengths determined in the direct shear box and the Bishop ring shear apparatus for these soils.

4.8.2 Minced Samples

Figures 4.56 and 4.57 show the stress-strain curves for the reconstituted (RSD) and minced (RSD(M)) samples (Borehole I4, 7.5 - 7.8 m bgl) and the residual failure envelopes defined for the tests over the stress ranges used. At higher normal effective stresses, the residual friction angle measured was the same for the minced and reconstituted samples.

Whereas the reconstituted sample showed a slight curvature in the residual strength failure envelope, the residual strength failure envelope of the minced sample was not curved over the stress range investigated of 100 - 400 kPa. The difference between the minced and reconstituted behaviour was most evident for the first shearing at a normal effective stress of 100 kPa. The peak strength measured for first shearing was much higher for the reconstituted sample than for the minced sample. The peak values of $\tan(\phi')$ were 0.42 and 0.15 respectively. The residual stress ratio $\tan(\phi'_r)$ was also

higher for the first loading interval for the reconstituted sample than the minced, being 0.098 and 0.081 respectively. Ideally the reconstituted sample should have been sheared to greater displacements at a normal effective stress of 100 kPa, to confirm that the residual strength of the reconstituted sample had been reached.
Lupini (1981) found a similar friction angle from ring shear tests on a mudstone retrieved from a site near Abervan. One sample was prepared by dry grinding, whilst the other was prepared by a gentle remoulding. There was a greater increase in the residual strength at low normal effective stresses for the gently remoulded sample than for the dry ground sample.

Figure 4.54 shows the result for the minced sample plotted on the correlations with plasticity index summarised by Lupini et al. (1981). The result of mincing sample RSD is an increase in the plasticity index from 26 to 45 %, while the residual friction angle remained unchanged. Hence the effect of mincing the sample was to move the data point to the right. The data point for the minced sample still lies below most of the plasticity index:residual friction angle correlations.

There was therefore no effect of the micro-structure on the value of the residual strength of these materials at normal stresses greater than 100 kPa. At lower normal stresses, there may be a slight increase in the value of the residual strength for the reconstituted sample by comparison with the minced. This could imply that the work required to shear disaggregated particles with a sliding mechanism at a normal effective stress of 100 kPa was less than that required to shear aggregated particles.

4.9 Summary of Results

The testing of the soils from this landslide site was not easy. The difficulties arose primarily from: the difficulty of sampling soils from the landslide site; the heterogeneity of the materials at the landslide; and their low permeabilities. As a result of the heterogeneity of materials at the site, for every natural sample tested a corresponding reconstituted sample had to be tested. The very low permeability of the reconstituted samples resulted in the duration of these tests averaging about five months. Also as a consequence of their low permeabilities, problems were encountered as a result of lack

of pore pressure dissipation and strain localisation during shearing, which occurred frequently at these very slow shear rates.

The effect of structure on the behaviour of soils from this landslide was assessed by comparing the soil with four different structures, the natural soil from the underlying formation, a soil remoulded by the mudslide and their equivalent reconstituted and minced samples.

The natural soils from the underlying formation have been greatly affected by the tectonic deformations and its clay mass is characterised by aggregates of plates of the order of 1 mm or less, giving these soils their scaly appearances. These shear lenses have smooth polished sides and may show a weathered coating (Cotecchia et al., 1977). The orientation of these lenses may vary within a few centimetres and hence these soils can be considered fairly homogeneous at the sample scale (38 mm diameter). These soils were considered to be of type γ as shown schematically in Figure 2.38.

The soils from the landslide body were thought to have been remoulded as a result of slope movements. The landslide debris considered of lithorelicts of the parent material in a remoulded clay matrix. These soils were considered to be of type δ as shown schematically in Figure 2.38.

The reconstituted samples were prepared by taking the trimmings from the natural soils and swelling them to a water content of between 1.2 and 1.5 times the liquid limit, by immersion in water. The soil was then mixed to a slurry before consolidating one-dimensionally.

It was shown, by an increase in the liquid limit with preparation method, that the samples reconstituted in the manner described above could be broken down further with an aggressive remoulding technique. Therefore the effect of the micro-structure of these materials could be assessed by comparing the reconstituted and minced samples. The minced samples were prepared by passing the soil 12 times through an industrial food mincer before reconstituting the soil in the usual way.

As a result of the heterogeneous nature of this landslide, it was necessary to normalise the behaviour of these soils not only for their different stress states and specific volumes but also for their different natures. The material prepared by the reconstitution method

described above and not the minced material was chosen as the most appropriate reference material. The reconstituted material was shown to be homogeneous at the macro-scale; to have a relatively stable base fabric as the aggregations of particles were not broken down as a result of remoulding within the landslide body; to be as similar as possible to the natural material; and to be repeatable. The reconstitution process was said to be repeatable as the normal compression lines of two samples of the same soil reconstituted separately in this manner were very similar.

The effect of the macro-structure on these soils can be investigated by comparing the behaviour of either of the two types of natural samples with that of the corresponding reconstituted samples. Alternatively the effect of the micro-structure can be assessed by comparing the behaviour of the reconstituted samples with that of the minced samples of the same soils.

The effect of structure on the behaviour of structured clays in general was shown in Section 2.2 to increase the size of the state boundary surface in both compression and shear. In contrast it was however shown in Section 2.3 that the effect of structure on the behaviour of structurally complex clays could have a negative effect on the position of the state boundary surfaces, which was also shown for these soils.

The effect of the micro-structure on the compressive behaviour of the soil was assessed by comparing the reconstituted and minced samples of the same soil, as discussed above. The effect of breaking down the micro-structure as a result of mincing was to move the normal compression line for the minced sample to the right of that for the reconstituted soil. The increased plasticity of the minced samples relative to the reconstituted samples resulted in an increase in the gradients and intercepts of the normal compression lines. The compressive behaviour of the reconstituted soil is thought to be controlled by a clay matrix containing aggregated particles, whereas the behaviour of the minced sample is thought to be controlled by a clay matrix where the particles are separated and free to swell and compress. The effect of the macro-structure on the compression characteristics of these clays could not be assessed as the normal compression line of the natural sample was not reached at the maximum mean normal effective stress applied (3.5 MPa).

There were some effects of the micro-structure on the stress:strain characteristics of these soils during shearing. The most noticeable was that the minced and reconstituted

samples had different critical state lines, an unsurprising result, considering the different positions of their normal compression lines. One set of samples (group 7) showed similar critical state stress ratios for the minced and reconstituted samples. The other set showed a decrease in the critical state stress ratio for the minced sample relative to the reconstituted sample. This decrease was not inconsistent with the increase in the plasticity of the sample determined from the Atterberg limits.

The effect of the macro-structure on the post-rupture friction angles of the natural samples from the underlying formation was clearly negative. The samples at lower confining stresses only achieved about 70 % of M for the reconstituted soils. This effect of the macro-structure was attributed to its scaly nature and localisation was thought to occur along the polished faces of these scales. This ratio was also thought to decrease with increasing mean normal effective stress, as the high pressure test H2C achieved a stress ratio at failure of only 60 % of M. This sample did however achieve a stress state outside the instrinsic state boundary surface. The lower failure envelope is because the behaviour is determined by the post-rupture behaviour on pre-existing fissures and not shearing to a true critical state.

The negative effect of the macro-structure on the shear behaviour of the natural samples from the landslide debris was less severe than that observed for the formation material. These samples achieved stress ratios at or above that of the reconstituted critical states determined from undrained tests on normally consolidated samples.

The micro-structure had little or no effect on stiffness, particularly if the data is normalised to account for their different volumetric states. The macro-structure had no effect on the stiffness within the small strain region and had a relatively small effect on one of the two samples tested at G_{max}.

The effect of the micro-structure on the residual strength was again assessed by comparing the behaviour of the reconstituted and minced soils. The slight increase in the residual friction angle at low effective stresses seen for the reconstituted soils was not seen for the minced samples. This was thought to result from the aggregated particles of the reconstituted soil not being sheared through at low effective stresses, slightly increasing the strength obtained.

CHAPTER 5 DISCUSSION

5.0 Introduction

The aims of this chapter are to summarise the results of the laboratory tests described in Chapter 4 and to discuss the implications of these results for the behaviour of other structurally complex clays and structured clays in general. The parameters that were selected for the numerical analysis of the landslide are also presented.

5.1 The Effect of Structure on the Behaviour of a Structurally Complex Clay

5.1.0 Introduction

The effect of structure on the behaviour of fine grained soils has often been assessed by comparing the results of tests on the undisturbed soil with those from a corresponding reconstituted sample, as was described in Section 2.2. The macro-structure of the natural samples retrieved from outside the sliding mass was characterised by its scaly macro-fabric as was shown in the photographs in Figure 4.1 (b) and schematically as a type γ material in Figure 2.38, whilst the macro-structures of the reconstituted samples consisted of small discrete particles in a clay matrix, which was shown in the photographs in Figure 4.1 (c) and schematically as a type δ material in Figure 2.38. The difference between the behaviours of the natural and reconstituted soils was thought to result mainly from their different macro-structures.

As the preparation method for the reconstituted samples of structurally complex clays can result in very different behaviour, the effect of the micro-structure was also assessed by comparing samples prepared by two different methods, standard reconstitution and mincing. The difference between these two methods of preparation is characterised by an increase in liquid limit of up to 30%. The reconstituted samples were made by swelling the trimmings from a natural sample and mixing the soil to form a slurry at about 1.2 to 1.5 times the liquid limit, as suggested by Burland (1990). The minced samples were made by passing the trimmings through an industrial food mincer twelve times at about the plastic limit, before being prepared as a slurry in the same manner as the reconstituted samples. The difference between the reconstituted and minced samples was thought to result from silt sized aggregates of clay minerals being broken

down by the mincing process. The micro-structures of the natural, minced and reconstituted samples were investigated using the electron microscope, as discussed in the following section.

The structurally complex clays are very difficult to test and therefore there has been very little study of these materials. The materials are both difficult to sample due to their complexity and troublesome to trim as a result of their fissured nature. Testing programmes for these soils have to be fairly time-consuming and extensive due to the heterogeneous nature of these materials and their very low permeabilities. As a result of the large variation in material properties across the landslide site, for every natural sample a corresponding reconstituted sample had to be tested. The reconstituted samples had very low permeabilities, which resulted in test times of several months. The long test durations limited the number of tests that could be carried out within the time frame of this research.

5.1.1 Assessing the Structure using S.E.M.

In order to assess the different structures of the natural, reconstituted and minced samples, Geomaterial Research Services Ltd. were contracted to carry out a scanning electron microscope study of these materials. This section summarises the results of this work, emphasising the elements that are relevant to this thesis.

Figures 5.1 to 5.3 show digitised images from the Scanning Electron Microscope for the natural sample (N8B), reconstituted sample (R8B) and minced sample (M9B) of sections which are approximately 100 μm. Sample N8B was also used for the x-ray diffraction analysis described in Section 4.2.2. The sample contained 21% smectite, 8% quartz, 21% calcite, 3% siderite, 13% muscovite, 34% chlorite and less than 1% each of dolomite and pyrite. A bulk analysis, carried out in the electron microscope over the areas shown in Figures 5.1 to 5.3, showed very similar quantities of each of the elements for the minced, reconstituted and natural samples. This bulk analysis cannot be used to determine the precise mineralogies of the samples as it only shows the percentages of different elements, but can be used as an indication that the mineralogies of the minced, reconstituted and natural samples are similar.

Figure 5.1 shows the micro-fabric of a section of the natural material which is approximately 100 μm across. The structure of the natural sample was very chaotic. The sample used for the S.E.M. study was soil which was sampled using the Mazier core sampler and had not been tested in the laboratory. Clastic fragments of calcite, gypsum, iron oxide, pyrites, feldspar and quartz were observed in a clay matrix formed of the clay minerals, illite, smectite and chlorite. Aggregates of the clay particles can also be identified from the digitised image. These are characterised by grey areas, which a point analysis showed are composed of layer silicates, surrounded by darker areas indicating voids. The size of the clastic fragments was surprising as quartz fragments as small as 3 μm were seen. Such small quartz fragments are likely to have been formed in a high stress environment. Another unusual feature was the composite particles, i.e. particles of more than one mineralogy, which may again be symptomatic of a high stress environment. These features are likely to result from their tectonic history.

Figure 5.2 shows the micro-fabric of a section of the reconstituted sample which is approximately 100 μm across. The reconstituted sample had been one-dimensionally compressed to about 50 kPa, before it was placed in the triaxial cell. This sample was then isotropically compressed to 150 kPa, before it was sheared undrained to a shear strain of about 20 %. The reconstituted sample was found to be more homogeneous across the sample than the natural soil, consisting of clastic fragments in a clay matrix. There was some ordering of the layer silicates (clay particles) around the clastic fragments. The bulk chemical analysis of the clay matrix showed that the mineralogy of the clay matrix for the section that was 100 μm across was similar to that determined locally. This would indicate that the mineralogy of the clay matrix is homogeneous at the microscopic scale. Some larger aggregates of clay particles were also observed on the digitised image.

Figure 5.3 shows the micro-fabric of a section of the minced sample which is approximately 100 μm across. The minced sample had been also one-dimensionally compressed to about 50 kPa, before placing in the triaxial cell. However this sample was isotropically compressed to 500 kPa, the sample was then sheared undrained to a shear strain of about 20 %. Ideally the reconstituted and minced samples should have had identical testing histories to allow a direct comparison of the micro-fabrics. However as the aim of these S.E.M. analyses was to assess the nature of the micro-fabric and not how it changed as a result of this loading history, these two samples with

slightly different loading histories could be compared. The minced sample was similar to the reconstituted sample in that at this scale as there were clastic fragments in a clay matrix. However no aggregates of clay particles were observed and there was also a noticeable orientation of the voids. This could either result from the initial one-dimensional compression of the sample not being erased by the subsequent isotropic loading or from the undrained shearing on the sample imposing a preferred orientation on the structure of the sample.

Figures 5.4 and 5.5 show S.E.M. photographs of the natural soil at different scales, which are indicated on the photographs. Figure 5.4 shows a flake of mica in a fine grained clay matrix. The clay is structured with numerous thin impersistent lenticular cavities, one of which is identified on the photograph. Figure 5.5 shows the detailed structure of the clay matrix. The clay matrix contains a number of composite particles. These may consist of a mica or chlorite flake with clay mineral particles attached. The size of these composite clay mineral particles can be larger than clay size (> 2 μm). There is a chaotic arrangement i.e. no consistent orientation of the particles in the clay matrix.

Figures 5.6 and 5.7 show S.E.M. photographs of reconstituted soil at different scales. Figure 5.6 shows a detail of a 30 μm calcite fragment in a fine grained clay matrix. There is no evidence, in the reconstituted material, of the lenticular cavities between aggregates observed for the natural material, although zones of weakness are observed along the surfaces of the shell fragments. The fine grained clay-matrix of the reconstituted material (Figure 5.7) appears more homogeneous than that of the natural material (Figure 5.5). Some composite particles are still seen at the greater magnification in the reconstituted sample, but they tend to be smaller than those of the natural material. There are some differences between the micro-fabrics of the natural and reconstituted materials, which suggest that there has been some particle breakdown as a result of the reconstitution process. Hence the differences between the structures of the natural and reconstituted soils are not purely a result of macro-fabric as originally thought.

Figures 5.8 and 5.9 show S.E.M. photographs of minced soil at different scales. Figure 5.9 shows a large 40 μm calcite fragment along with a number of smaller clastic particles in a fine grained clay matrix. A discontinuity has developed along the side of the larger calcite fragment. The fine grained matrix of the minced sample has a very

different structure to those of the natural and reconstituted materials, although its bulk constituents are very similar. No composite particles are seen and the sheet silicates show a clear orientation. The orientation of the particles, as stated previously, could either result from the initial one-dimensional compression of the sample not being erased by the subsequent one-dimensional compression or from the undrained shearing of this sample. The latter is thought to be the most likely.

In summary, it is thought that the result of reconstitution was to produce a more homogeneous macro-fabric removing the fissures seen at the sample scale. The fabric of the reconstituted material viewed at the lower magnitudes in the S.E.M. was fairly homogeneous, consisting of clastic particles in a clay matrix. Aggregates of clay minerals and the composite particles observed in the natural material were still seen in the reconstituted material, but tended to be smaller. After mincing, no aggregates or composite particles were seen in the sample viewed in the electron microscope.

5.1.2. Reconstitution (and Mincing)

One of the points highlighted throughout this thesis is the need to compare the natural soil with an appropriate reference material. An appropriate material should have a homogeneous stable base fabric as similar as possible to the natural and be reproducible by other researchers. The simple preparation method of swelling the soil to a slurry before mixing it at a water content of 1.2 to 1.5 times the liquid limit was felt best to fit these criteria. Reconstitution after drying and grinding the material was not thought appropriate as it can significantly change the behaviour of the soil (Wiewiora et al. 1993).

Scanning electron microscope work on the natural, reconstituted and minced soils showed that the reconstituted samples, whilst being much more homogeneous than the natural sample, had a more similar base micro-fabric to the natural soil than the minced sample. The aggregations of clay particles seen in the S.E.M. photographs of the natural and reconstituted samples were not found in those of the minced sample.

5.1.3 Compression Behaviour

It was intended as part of this research to determine the normal compression line for two natural samples. This was unfortunately not possible as the samples were lost as a result of failure of the control system on the high pressure triaxial apparatus and there were insufficient high quality samples to repeat these tests. Hence the only data available which compares the behaviour of natural and reconstituted samples of structurally complex clays in one-dimensional or isotropic compression were those published in the literature.

Initially it was thought that by comparing the behaviour of natural and reconstituted samples, the effect of the macro-structure on the compression behaviour of these clays could be assessed. However as a result of the S.E.M. analyses of these materials, it was shown that although the differences between the structure between these materials is primarily at the macro-scale, there are some differences also at the micro-scale.

A comparison of oedometer test data from the literature for natural and reconstituted samples was shown in Figure 2.48. Although the samples were reconstituted by dry grinding, there was very little difference between the Atterberg Limits of the natural and the reconstituted materials and the samples were therefore considered to be more comparable with the reconstituted tests presented in this thesis than with the minced. The compression data for the natural samples plotted slightly to the left of those for the reconstituted indicating a negative effect of structure on the volume of the natural sample during compression. This is highly unusual.

Burland (1990) plotted a single sedimentation line for natural soils which lay to the right of the intrinsic compression line defined by reconstituted soils. Cotecchia (1996) noted that this line could be thought of as a sedimentation compression line for samples with a sensitivity of 4 to 9 and that there existed a family of parallel sedimentation compression lines of different sensitivities. It is thought likely that the original s d' en 'on compression line for the structurally complex clays as deposited would to the right of the intrinsic compression line. However as a result of the post-sitional processes the normal compression lines for the natural soils now lie to the left of the intrinsic compression line. Given the geological history, a possible sequence of post-depositional changes in the structure could be as follows. The soil is deposited and one-dimensionally consolidated. At some point in geological time, there is some

strengthening of the soil as a result of diagenesis. The soil is then sheared as a result of the tectonic activity, resulting in particles which are aggregates of the diagenesised parent material.

Cotecchia (1996) emphasised the point that all samples have a structure and not just natural samples. The negative effect of structure seen here again highlights this point. The existence of the disaggregated soil outside the state boundary surface of the reconstituted material also shows that the term 'structure-permitted space', used by Leroueil and Vaughan (1990) to indicate a region outside the intrinsic state boundary surface at which only a structured soil can exist, is only legitimate if all soils are considered as structured.

The different structures of the natural and reconstituted samples were investigated by electron microscopy and were discussed in Section 5.1.1. The structure of the natural sample is typified by a chaotic arrangement of fragments of calcite, gypsum, iron oxide, pyrites, feldspar and quartz, together with the clay minerals of illite, smectite and chlorite. The fabric of the reconstituted soil is typified by fragments of clastic materials in a clay matrix. The clay matrices of the natural and reconstituted soils were fairly similar. They both contain composite particles, although these tend to be larger in the natural material. The difference between the positions of the normal compression lines for the natural and reconstituted samples was thought to have resulted from a breakdown of some of the larger aggregates and composite particles. This would indicate as S.E.M. photos suggest that although the difference between the reconstituted and minced samples is all micro-fabric, the difference between the natural and reconstituted is primarily macro-fabric but there is some micro-fabric. The difference in the compression behaviours of the natural and reconstituted soils is thought to result primarily from their different micro-fabrics. It was attributed to the micro-structure as this was seen when comparing the reconstituted and minced to greatly affect the compression behaviour. The small differences in the micro-structure would correspond with the slight changes observed between the compression behaviours.

t of micro-structure of thes soils was also assessed by comparing the isotropic pressive behaviour of reconstituted and minced samples of the same soil. The minced sample was made by passing the soil through an industrial food mincer to further disaggregate the soil, as was discussed in Section 3.2.4. The minced samples were able to exist at stress states outside the reconstituted state boundary surface, as was

shown in Figures 4.18 and 4.1.9. Again a negative effect of structure was observed. The more the structure was broken down the further the normal compression line moved to the right, instead of the left as is usually observed. The S.E.M. work showed that the arrangement of the layer silicates (the clay minerals) in the minced sample were very different to those in the reconstituted sample. The composite particles, seen in the reconstituted sample, appear to have been broken down as the result of mincing as they were not visible in the minced sample. The layer silicates in the minced sample were much more orientated than those of the reconstituted soil. The result of increasing the energy used to reconstitute the soil is to break down more of the composite particles. The composite particles once separated can swell more easily. The more open structure of the minced sample allows it to exist at states outside the reconstituted state boundary surface. The different "intrinsic" normal compression lines of the reconstituted and minced materials agree with the view expressed by Cotecchia (1996) that there is no such thing as a soil without structure as stated by Leroueil and Vaughan (1990).

It would be interesting to see whether the normal compression lines of the natural, reconstituted and minced samples converged at higher stresses. The S.E.M. work shows very different distributions of voids within the samples, indicating that the samples are likely to have different compression curves as a result of their "depositional histories".

The compression behaviours of the different structured materials are illustrated in a schematic diagram in Figure 5.10. The normal compression line for the minced material lies to the right of that of the corresponding reconstituted sample in v:lnp' space, as was seen in Section 4.4.2. This is because the minced soil is able to exist at states outside the state boundary surface of the reconstituted material as a result of its more open micro-fabric. This is in contrast to the compression behaviour of the natural material, which has a more aggregated micro-fabric. The normal compression line of the fissured natural soil can therefore lie to the left of that of the reconstituted material and hence the natural samples may not reach the intrinsic state boundary surface in v:lnp' space, as was seen in Section 2.3.2 (c). The normal compression line of the landslide debris was h ev r found to be fairly consistent with that of a corresponding reconstituted sample

on the M.Massero clay by Guerriero et al. (1995) and discussed in ion 2.4.1 (e).

5.1.4 Shear Behaviour

The effect of structure on the shear behaviour was again assessed by comparing corresponding natural, reconstituted and minced samples. The shear behaviour of the reconstituted and minced samples was not particularly unusual when considered within a critical state framework. The samples did however have a tendency to strain localise when sheared under drained conditions, even from a normally consolidated state. This was thought to result from local drainage occurring at the very slow shear rates used. Such slow rates were required because of the very low permeability of these soils. Hence to obtain a true critical state, samples were sheared undrained from a normally consolidated state.

The shear behaviour of the natural samples did however appear comparatively unusual. The natural samples, when sheared drained from an estimated in-situ stress state, were ductile with no peak and the volumetric strains were compressive. This was unusual considering the high overconsolidation ratio, but has frequently been observed in the literature for these soils, as was discussed in Chapter 2. This small amount of volumetric compression was attributed to the increase in the mean normal effective stress during shearing. Strain localisation was thought to occur in these samples before a peak was reached. This strain localisation was thought to be initiated by the macro-structure of the natural material, along one or a combination of the very small existing fissures or scales. The formation and propagation of any strain localisation in the minced or reconstituted samples is very different to that in natural material. The S.E.M. photographs show a discontinuity along the sides of a large calcite grain in the reconstituted and minced material. It is thought that strain localisation in the reconstituted and minced soils may be initiated along these zones of weakness.

In order to compare the behaviour of their natural, reconstituted and minced samples the data were normalised with respect to the equivalent pressures on the critical state lines for the corresponding reconstituted samples. The shearing data were also normalised with respect to the critical state stress ratios for the reconstituted samples.

The effect of the scaly structure of the natural samples on their shearing behaviour was assessed by comparing the normalised behaviour of the natural samples having scaly macro-structures and those without, as was shown in Figure 4.38. The scaly samples not only did not reach the peak strengths of the reconstituted but also failed to reach the

reconstituted critical state stress ratio. However the samples which had been remoulded inside the landslide body and were not scaly in appearance reached peak friction angles ratios comparable with those measured for the reconstituted samples. Hence it was thought that the effect of the scaly macro-structure was to promote strain localisation along the fissures, reducing the post-rupture strength of the natural samples. Hence there was a negative effect of the scaly structure on the strength. A similar reduction in the friction angle post-rupture was also seen by Burland (1990) for some samples of fissured London clay.

The effect of the micro-structure on the strength of these soils was assessed by comparing the reconstituted and minced samples, as was shown in Figures 4.32 and 4.33. Whilst the effect of mincing was to reduce the critical state friction angle for one sample group, it had no effect on the other. The main difference between the normalised behaviour of the reconstituted and minced samples is that the minced samples were able to exist at states outside the state boundary surface of the reconstituted material as a result of their different micro-structures. Both the normal compression lines and the critical states lines of the minced soils lie to the right of those of the reconstituted samples.

The effect of the different structures of the samples on the shear behaviour is summarised in a schematic diagram in Figure 5.11. The diagram shows the predicted behaviour, normalised with respect to a corresponding reconstituted sample, to account for the different friction angles, specific volumes and stress states. The state boundary surface for the reconstituted sample is similar to those observed for other clays. The state boundary surface for the minced sample is different to that of the reconstituted sample as the minced sample may have a different critical state friction angle as a result of a different frictional resistance of its base fabric and the normal compression and critical state lines of the minced sample tend to lie to the right of those of the reconstituted sample. The constant a is the ratio M for the minced sample to M for the reconstituted soil.

The post-rupture failure surface for the formation material (scaly clay) has been less well defined by the tests carried out, due to the problems encountered with the high pressure triaxial apparatus. Data from the literature suggest that scaly clays may have a normal compression line slightly to the left of that of the reconstituted material. Drained triaxial tests carried out on the fissured material show that this material tends to

strain localise at a lower stress ratio than the reconstituted material as indicated on Figure 5.11. The ratio of the stress ratio post-rupture of the fissured material tested at its in-situ stress levels to the stress ratio at the critical state for the reconstituted soil is defined on this diagram as b. Failure may however occur outside the reconstituted state boundary surface at higher stress levels. This is because the compression characteristics of the natural material are different to that of the reconstituted in shear. It was shown that samples sheared at higher confining stresses had lower post-rupture friction angles than those of the samples tested at their in-situ stress levels. This was thought to occur as a more planar failure surface will develop, shearing through aggregates as well as along their sides. A lower friction angle at higher confining pressures was observed for Sample H2C and also by Guerriero et al. (1995) for the Bisaccia clay shale.

5.1.5 Shear Stiffness

Previous research has shown that the shear stiffness of natural and reconstituted soils is non-linear over almost the complete range of strains, as was highlighted in Section 2.2.4. The effect of structure on the stiffness of natural and reconstituted soils has been investigated using a normalisation to account for different mean normal effective stresses and overconsolidation ratios and specific volumes.

The shear stiffness at the very small strains (G_{max}) was measured in the laboratory using piezo-ceramic bender elements for two pairs of natural and reconstituted samples and also for one pair of a reconstituted and a minced sample. The results showed that the shear stiffness of the natural sample was slightly larger than that of the reconstituted sample, when normalised with respect to the normal compression line of the reconstituted sample (Figures 4.41 and 4.42). This decrease in shear stiffness for the reconstituted samples may result from the fact that the reconstituted sample consisted of clastic particles in a clay matrix, whereas in the natural sample there was some connectivity of the aggregated clay particles.

The very small strain stiffness of the reconstituted soil was very similar to the minced soil (Figure 4.40). Any difference was reduced further when the data were normalised with respect to the normal compression line of the reconstituted material to account for their different specific volumes.

At larger strains, the reconstituted and minced samples continued to have similar shear stiffnesses when correctly normalised (Figure 4.50). At these strains, the natural samples now also had similar normalised stiffnesses to the reconstituted samples (Figures 4.51 and 4.52).

It is slightly surprising that the effect of such different micro-structures and different macro-structures had so little an effect on the drained shear stiffnesses of these materials, particularly as the results of Section 5.1.3 would suggest that the natural, reconstituted and minced samples all had distinctly different normal compression lines, so that at any stress they would all have different volumes.

5.1.6 Residual Strength

The mechanisms governing the residual strengths of fine grained soils were discussed in Section 2.2.5. The mechanism of failure at residual state was shown by Lupini et al. (1981) to be either turbulent, transitional or sliding. The type of failure mechanism and hence the magnitude of the residual strength, was found to be controlled by the particle size, shape and intergranular friction angle. A turbulent failure mechanism was common in soils which were predominantly formed of rotund particles whereas a sliding mechanism was common in soils formed of platy particles. The curvature of the residual failure envelope at low normal stresses was attributed to a transitional failure mechanism, where less work was required to shear the particles without re-orientation than was required to shear the particles in sliding shear (Mitchell, 1993).

Very few tests have looked at the residual strength of natural soils. This is both due to the difficulty of obtaining good quality undisturbed samples of sufficient size and because early tests on London Clay did not show any effect (Bishop et al., 1971). Mesri and Cepeda-Diaz (1986) highlighted the importance of chemical induration (hardening) as a result of diagenesis on the behaviour of clay shales. They noted that the liquid limit of the Curacha shale could change from 49 to 156%. Unfortunately the residual strength tests they carried out were on material that they had prepared by air drying and ball grinding to destructure the materials which probably removed this effect of the diagenesis of the clay shales.

Picarelli (1991) made a comparison of the results of direct shear tests on undisturbed samples of a structurally complex clay with direct shear and ring shear tests on remoulded samples of the same material, as was shown in Figure 2.55. It is unfortunate that the tests on the natural material were only carried out in the direct shear apparatus. He showed that the natural samples typically had larger residual strengths, particularly at low normal stresses. As discussed in Section 2.3.2 (a), the increase in strength for the natural material was attributed to its structure. The macro-structure of the natural sample consisted of scales or small iso-orientated shear lenses. An increase in the strength measured along the shear surface could have resulted from these scales not being broken down at low normal stresses. This increase at low normal stresses could have a large effect on the stability of a shallow landslide in these materials. The increase in the tangent of the residual friction angle as a result of the natural structure is estimated to be approximately 50% at 100 kPa.

The effect of the micro-structure on the residual strength was assessed by comparing the results of ring shear tests on the reconstituted and minced samples. The reconstituted samples showed a small increase in the residual friction angle at low normal stresses (Figure 4.53), whereas the residual strength envelope for the minced sample was straight, down to a normal stress of 100 kPa (Figure 4.57). Where only a slight curvature was observed for the reconstituted sample, this was thought to result from there being sufficient disaggregated clay particles to reach the disaggregated residual strength and a further breakdown in clay aggregates would have little effect on the residual strength. This is similar to the behaviour of clay-sand mixtures, where above a certain clay fraction the large particles are thought to float in the clay matrix and not influence the residual strength measured. This is shown in Figure 2.32, which gives correlations between the residual strength friction angle and the clay fraction. As can be seen, at high clay fractions an increase in clay fraction has no effect on the residual strength. The samples tested here all had fairly high plasticities. It is thought that the effect of the micro-structure may, however, be larger for samples with a lower plasticity and clay fraction.

The effect of the structure of the natural material on the residual strength of a structurally complex clay needs to be studied in more detail. As a result of the work on structurally complex clay, some doubt has also been cast over the original assumption that the residual strength is not affected by structure. Therefore it would follow that if other types of clay shales have similar composite particles resulting from their

diagenesis, their residual strength could be affected in the same way. This increase in the residual friction angles due to indurated particles will be most noticeable at low normal stresses as would occur in shallow landslides.

5.2 Landsliding

5.2.0 Introduction

This thesis has focused on the material properties of the soils from a landslide body and from the surrounding formation. One of the aims of the research was to compare the behaviour of the soils from inside and outside the sliding mass, soils from the surrounding formation not having been subjected to intense remoulding as a result of the landslide activity.

This section also presents the material properties that were used for the numerical analysis by Armines-CGI. The choice of parameters was therefore controlled by the type of numerical model that Armines-CGI used.

5.2.1 Changes in the structure of structurally complex clays as a result of landsliding.

The previous section stressed the importance of the macro- and micro- structure in determining the material properties. The effect of landsliding on the structure of these materials was assessed by comparing the materials from inside and outside the landslide body, as was discussed in Chapter 4. The behaviour of the soils inside the landslide body was found to vary significantly from that of the intact formations. This section reviews the changes that were observed to result from landsliding, examining data from both the literature and from Chapter 4 and assessing the relevance of these findings.

a) Visual Observations

The difference between soil extracted from inside and outside the sliding mass can be observed visually. The landslide debris consisted of lithorelicts in a clay matrix and was

illustrated schematically by Guerriero et al. (1995) (Figure 2.38). The lithorelicts were either remnants of the more argillaceous parent material which had not been remoulded or fragments of the more lapideous material which did not breakdown as a result of remoulding. The more argillaceous component of the formation material typically has a scaly appearance and is represented by the type γ material in Figure 2.38. Landsliding appears to remould the argillaceous component, removing the scaly structure and often incorporating within the clay matrix fragments of the more lapideous component of the parent material.

b) Changes in water content

One effect of landsliding that is frequently noted in overconsolidated soils is a softening or an increase in the specific volumes of soil both in the shear zone and in the landslide body. By comparing the water contents and, more fundamentally, the liquidity indices in Section 4.2.3, no apparent change in the volumetric state of the landslide material was found. In Section 4.6.3 it was also found that at the estimated in-situ stress level there was little variation in the values of p'/p'_{cs} between samples taken from inside and outside the landslide, again indicating that there was little influence of the landslide movements on the volumetric state of the soil.

The identification of any distinct change in the volumetric states of these materials is restricted by the scatter of data observed. This scatter results from the large variety of materials that are present at the site (Figure 4.1) and the heterogeneity of these soils, particularly in the landslide body (Figure 2.42). Attempts to normalise the data to account for the different soil properties of the materials by using the liquidity index or the ratio p'/p'_{cs} were not sufficient to reduce this scatter.

Iaccarino et al. (1995) looked at the variation of water contents within a landslide body formed of structurally complex clays. When large numbers of samples were taken from a trial pit, Iaccarino et al. did note an increase in the water content in the shear zone and to a lesser degree in the landslide body. They did however investigate a more homogeneous material. In such heterogeneous soils as were encountered at Senerchia, to assess any change of volumetric state in the shear zone or landslide body, water content measurements should have been taken at a much closer spacing, perhaps every 10 cm, which was the thickness of the shear zone encountered by Iaccarino et al..

The reason that a change in the volumetric state of a soil can be encountered in landslides in overconsolidated clays is that soils are expected to dilate as they are sheared within the landslide body or on the shear surface. Although the type of loading applied in the triaxial apparatus, is significantly different to those that the soil is likely to experience in the landslide, drained shearing of these soils showed that these samples tend to strain localise with small compressive strains rather than to dilate significantly. It is perhaps therefore not that surprising that there is little change between the volumetric states of samples inside and outside the slide. Softening of the samples within the shear zone could still occur however as a result of the breakdown of the soil aggregates.

c) Compression Behaviour

The difference between the compressive behaviour of the material from the surrounding formation (type γ) and from the landslide (type δ) was shown schematically in Figure 5.10. This diagram was based on the test data by Guerriero et al. (1995) discussed in Section 2.4.1 (e). The behaviour of the type δ material had a normal compression line similar to that of the reconstituted material, whereas the type γ material had a normal compression line within the state boundary surface of the reconstituted soil. Again the difference between the compression behaviour of the formation material and the reconstituted material was thought to result from a slight breakdown of the micro-structure as a result of remoulding within the landslide. The view that only the macro-structure and not the micro-structure of the material from the landslide body was changed as a result of slope movements now appears to be too simplistic.

d) Shear Behaviour

i) Peak Strength

The effect of landsliding on the shear behaviour of the natural samples was assessed by considering the normalised behaviour shown in Figure 4.38. The effect of the different material properties and different volumetric states was accounted for by normalising both with respect to the stress ratio at critical state of the reconstituted sample and an equivalent pressure p'_{cs} defined on the critical state line of the reconstituted soil. As stated in the previous section, there was no noticeable difference between the volumetric

states of the material from inside and outside the sliding mass due to the heterogeneity of these soils. The difference in the peak strengths of the soil from inside and outside the landslide body was however fairly pronounced. Samples of the formation material sheared drained from their estimated in-situ states tended to reach peak stress ratios approximately 70% of those defined at the critical state of the corresponding reconstituted sample. This reduction in strength was attributed to strain localisation due to the fissured nature of the parent material. In contrast samples from the landslide body sheared, also at their estimated in-situ stress state, reached peak friction angles similar to those expected for the corresponding reconstituted samples. Sample H2C, which was from inside the old Serra dell'Acquara landslide body, had a scaly appearance and behaved in a similar manner to the samples from the parent formation. Significant remoulding of this sample of soil was not therefore thought to have occurred. The lack of remoulding in Sample H2C was a thought to be a local phenomenon, as the adjacent sample N2B did not have a scaly appearance and appeared remoulded. It is thought that there are larger lithorelicts in the larger landslide and H2C is formed of one of them.

Similar differences between the landslide debris and the formation material were observed for the M. Marino clays reported by Guerriero (1995). The difference between the behaviour of samples from inside and outside the landslide body was again attributed to their different macro-structures. Remoulding within the landslide body was thought to remove the fissured nature of the soil (the macro-structure) as seems to be the case here.

ii) Residual Strength

Residual strength tests were not carried out on the natural soils, as sufficiently large undisturbed samples of the soils at Senerchia were not available for tests in the Bishop ring shear apparatus and it is not possible to test natural samples in the Bromhead ring shear apparatus. As no examples were found in the literature of tests which looked at the effects of remoulding due to landsliding on the residual strength of a structurally complex clay, the likely response is predicted from the tests on the natural and reconstituted Laviano clay shale by Picarelli (1991).

Picarelli (1991) carried out direct shear box tests on samples of a structurally complex clay. He showed that the residual strength of the natural soil was larger than that of the

corresponding reconstituted samples, particularly at low normal stresses (Figure 2.55). The residual strengths determined in the direct shear box are likely to be a little large, as was shown for the soil from Senerchia in Figure 2.56. The influence of structure was however shown to be very important at low normal stresses (< 100 kPa). At stresses above 200 kPa the residual strength of the natural soil was approximately the same as that of the reconstituted.

As shown in the previous sections, it is thought that the effect of remoulding as a result of landsliding on the natural material is to remove the scaly macro-fabric. The behaviour of the landslide debris more closely approximates that of the reconstituted material than that of the natural formation. Hence it is believed that as a result of remoulding due to landsliding, the residual strength of the soil from the landslide mass would not show the large increase in strength as a result of the structure seen for the formation material.

e) Summary

The large shear distortions undergone by the sliding mass are believed to remould the soil, with little change in the volumetric state, removing the macro- but not the micro-structure. The change in the macro-structure was seen by direct comparison of the visual appearances of samples inside and outside the landslide body, as the fissured structure of the parent material was not evident within the soil of the sliding mass. The micro-structure is not thought to have been changed by the landslide movements as the Atterberg limits increased to a similar degree with mincing for samples both inside and outside the sliding mass. The behaviour of the soil within the landslide body is fairly similar to that observed for the reconstituted soils.

There was no identifiable change in the water contents or liquidity index for samples tested within this research project, although a slight increase was identified in the shear zone by Iacarrino et al. (1995). The reduction in the peak strength due to the fissured macro-fabric observed for the parent material was not observed for the soil remoulded by sliding. It is thought that the increase in the residual strength at low normal stresses due to the scaly structure of the formation material, observed by Picarelli (1991) by comparing results from direct shear tests on natural and reconstituted Laviano clay shale, would not be observed for the landslide debris. The normal compression line for

the soil remoulded by landsliding lies outside that of the formation material and is similar to that of the reconstituted soil.

5.2.2 Material Parameters for the Geotechnical Model of the Landslide

This section presents the material parameters that were used by the French partners (Armines-CGI) in the numerical analysis of this landslide. The material properties chosen were appropriate to the analysis technique used for this modelling. Both the initial mobilisation and a subsequent reactivation were modelled in the numerical analysis.

a) Location of Materials

As stated previously, the materials at this site are comprised predominantly of marlstones, mudstones, claystones, clays, with isolated patches of sandstones and carbonate breccia. Modelling the distribution of materials in these chaotic soils requires some simplification, as the materials have little recognisable distribution vertically and horizontally and it is difficult to tell their spatial distribution from the limited number of boreholes drilled.

In Chapter 4, it was shown that the predominant materials were marly clays and clayey marls. The numerical analysis of the landslide was carried out using the parameters determined for these materials. These materials were thought to control the stability of the landslide, as the shallow angle of the failing slope would only be achieved if the shear surfaces lay predominantly in the more clayey soils. D'Elia (1991) also showed that the overall stiffness of a composite material of rock fragments in a clay matrix was controlled by the clay matrix if the rock component is less than 20%, as was discussed in Section 2.3.2. The rock component of this landslide was estimated to be 15 % from the borehole logs.

The soils in the slope were roughly divided into regions with similar plasticity indices for the analysis, as is shown in Figure 5.12. This division of the landslide was carried out at the initial stages of the project, prior to the findings of this thesis, to allow the French partners to begin the numerical analyses. In light of the results of the work

comparing the soil inside and outside the sliding mass, the soil within a reactivated landslide body should have been assigned different friction angles to those of the surrounding formation material. They should have been similar to those of the reconstituted material.

Probably the only way to provide a more accurate assessment of the spatial distribution of the different materials would be to carry out a probability study. Unfortunately it is felt that there are too many variables and too few data for this to be realistic at present.

b) Material properties

The soil model used for the numerical modelling carried out by Armines-CGI is shown in Figure 5.13. The soil was assumed to behave linear-elastically up to failure, with zero plastic volumetric strains post-yield. Yield was defined using a Mohr-Coulomb failure criterion. After yield, the soil was modelled as perfectly plastic and reducing linearly to a residual strength value. The soil parameters therefore required were a large strain shear stiffness G and the parameters for the Mohr-Coulomb failure criterion at the critical state and at the residual state. The peak and critical failure envelopes for the scaly clays were coincident, as these natural materials when sheared drained were ductile with no peak. The material properties were assigned to the regions defined in Figure 5.13 using correlations with plasticity index.

Initially the 'critical state' friction angles for the natural samples were determined by assuming a linear correlation between the critical state friction angle and the plasticity indices as can be seen in Figure 5.14. It is more usual to assume a linear correlation between $\sin(\phi'_{cs})$ and the plasticity index, as shown in Figure 5.15. However over the friction angles plotted, there is very little difference between the two linear correlations. The correlations were determined for all reconstituted and natural samples that were available at the time of plotting. In retrospect, it would have been more appropriate to assume two different correlations for soils inside and outside the landslide body. The friction angles for the soil within the landslide body should be determined from the reconstituted samples. The friction angles for the formation material should be determined from the drained triaxial tests on the scaly clays.

The model used by Armines-CGI in the finite difference program FLAC assumed that the material behaved linear elastically when sheared. This is unrealistic as the stress-strain behaviour of soils is highly non-linear, as was shown for the soils from this site in Section 4.7. The secant stiffness was calculated for these soils between 0 and 75% of the deviatoric stress at the critical state, using Equation 5.1,

$$G = \frac{0.75q_{cs}}{(3\varepsilon_s)_{0.75q_{cs}}} \qquad \text{Equation 5.1}$$

where q_{cs} is the deviatoric stress at the critical state and $(\varepsilon_s)_{0.75q_{cs}}$ is the shear strain at a deviatoric stress equal to 75% of that at the critical state.

The secant stiffness was normalised with respect to the mean normal effective stress p' and correlated with the plasticity index. These values were plotted against plasticity index in Figure 5.16. Additionally the secant stiffness between 0 and 50% of the deviatoric stress was also plotted on this graph, defined as a ratio of $0.5q_{cs}/\ 3(\varepsilon_s)_{0.5q_{cs}}$. The consequence of using an average shear stiffness will be that the modelled material will deform much more than the actual soil under smaller deviatoric stresses and much less closer to peak. It is thought that as a result of the initial shear deformations being inaccurately modelled, the shear surface could be formed at the wrong location.

A numerical average value of the residual friction angles measured, equal to 5.5°, was used for all soils within the slope. A numerical average was used rather than a correlation with plasticity index, because for the soils tested there was no noticeable increase in residual friction angle with plasticity index (Figure 4.54). This value of the friction angle was thought to be appropriate in the downslope region, as the effect of the macro-structure was thought to be negligible at vertical effective stresses above 200 kPa. However in the scarp region where the normal effective stress are much less, the residual friction angle is likely to be larger as a result of the macro-structure of these materials. As no tests were carried out on the natural material and the likely increase is not known, this was not considered in the analyses.

The bulk unit weight was assumed by Armines-CGI to increase with depth, according to the relationship shown in Figure 5.17. On this graph are also plotted the bulk unit weight data obtained for the undisturbed natural samples tested and the change in the

bulk unit weight defined by isotropic compression during high pressure test H2C. The increase in bulk density, assumed by Armines-CGI was comparable with the compression data.

c) Seismicity

The effects of earthquake loading on a landslide are very complex and therefore their influences were considered using a pseudo-static approach in the numerical analyses. The two effects that were considered important were the horizontal component of force on the landslide which results from the seismic accelerations and the pore pressure changes that result from the cyclic nature of this loading.

A pseudo-static horizontal acceleration of 0.1g was used as an input for the calculations. Earthquakes having an acceleration of 0.1-0.2g have been found to occur about 10 times in 500 years in the Senerchia area (Cotecchia et al. 1996). The 1980 earthquake had a higher acceleration of about 0.3-0.4g, whereas accelerometers installed at the landslide site for this project recorded a maximum horizontal acceleration over the two year monitoring period (1994-1996) of 0.04g in April 1996. As the pore pressures measured in the laboratory cyclic tests were in each case relatively small for the large seismic event (0.1g), smaller seismic events were not modelled in the laboratory tests, as the pore pressure changes would have been too small to resolve. The reason that 0.1g was chosen as the magnitude for a large seismic event and not the 0.4g recorded during 1980 earthquake was that this information was not available at the time of the testing and the value of 0.1g from a neighbouring site was used.

To simulate the effect of cyclic loading on the landslide, cyclic triaxial tests were carried out on two of the natural samples to determine the pore pressure response. These cyclic tests were carried out only at rates of cycling at which the pore pressure responses could be measured by the apparatus. In order to determine the relevance of these data to the faster loading of a seismic event, the effect of the rate of loading was investigated by carrying out tests on Samples N8B and NCA with periods of both one day and 30 minutes. As the rate of pore pressure increase reduced with the number of cycles (Figure 5.18), a direct comparison of the data for the two rates of loading was not possible. The difference in the pore pressure response of the last slow cycle and the first

fast cycle was however negligible, so that for the rates considered, it appears that rate does not have a large influence on pore pressures generated.

In order to try and simulate the behaviour in the field, the sample was first sheared drained to an initial deviatoric stress prior to the start of cyclic loading. This initial stress was calculated using an equivalent slope angle α of 11 degrees, an average slope angle for the whole slide, using Equation 5.2:

$$\alpha = \tan^{-1}\left(\frac{\tau}{\sigma_n}\right) \qquad \text{Equation 5.2}$$

The effect of earthquake loading was then simulated by cycling the deviatoric stress with the sample undrained, and measuring the pore pressure response. The amplitude ($\Delta\tau$) of the cycles was determined from the equivalent acceleration of 0.1g for a large seismic event, using the equation:

$$\left(\frac{\Delta\tau}{(\sigma_n')_{initial}}\right) = 0.1 \qquad \text{Equation 5.3}$$

The stress ratio ($\Delta q'/p'$) used in the triaxial apparatus was assumed to be twice the stress ratio ($\Delta\tau/\sigma'_n$). Two tests were also carried out in the simple shear apparatus at the Politecnico di Bari to complement the cyclic tests conducted in the triaxial apparatus. The simple shear apparatus loads the sample under plane strain conditions which more accurately models the mode of shearing in the landslide than the axi-symmetric loading of the triaxial apparatus. The results of these tests are discussed in detail by Cotecchia et al. (1996).

The data obtained for cyclic tests are summarised in Table 5.1. Samples N8B, I6/1 and I5/2 were retrieved from outside the landslide whilst NCA was from within the landslide body. Several cyclic loading stages at different normal stress levels or different modelled slope angles were carried out using each sample in order to maximise the data obtained. The pore pressure changes under cyclic loading varied from -12 to +50 kPa and so were relatively small compared with the confining stresses of 100 to 300 kPa. The pore pressure responses for the samples tested at their estimated in-situ stress level

from both inside and outside the landslide were similar and would indicate that the pore pressure response of the soil to a seismic event was not affected by the shear distortions due to landsliding. The negative pore pressure responses occurred for samples which were sheared from lower confining stresses and hence higher overconsolidation ratios than would be typical in-situ.

Instability could occur due to seismic activity as a result of a decrease in effective stresses, caused by generation of positive pore pressures. Even for cyclic testing equivalent to a very large earthquake, the pore pressure changes generated by cycling were relatively small and became negative at low confining stresses equivalent to shallow depths. Seismic events could therefore generate positive pore pressures at depth and failure in areas of limiting stability may occur later as pore pressures dissipated upward.

CHAPTER 6 CONCLUSIONS

Leroueil and Vaughan (1990) highlighted the importance of structure when considering the behaviour of natural soils. In order to assess the behaviour of a soil, it is necessary to have an understanding of its structure and the stability of the different elements. As the structure of the materials from this landslide site is very complex as a result of their geological history, it has allowed a detailed investigation to be carried out of how different types of structure affect the behaviour of the soils. The natural, reconstituted and minced soils considered had a variety of different macro- and micro-structures.

The behaviour of the soils was considered within a critical state framework, normalising to account for their different stress states, specific volumes and natures. The behaviours of the natural soils were compared with those of corresponding reference materials, which in this case were reconstituted samples prepared from the trimmings of the natural samples. This research has considered soils with four different types of structure: natural samples from the underlying formation; natural samples from the landslide body; reconstituted samples; and minced samples.

The natural soils from the underlying formation were fairly typical of an argille scagliose or scaly clay. The macro-structure of these materials consists of small shear lenses of material, the orientation of which may change within a few centimetres. These materials are fairly homogeneous at the sample-scale. The micro-structure of these samples observed using S.E.M. is very chaotic, as a result of their complex geological history. Aggregates of clay sized particles were present in the natural material, which could only be broken down by an aggressive remoulding technique, for example mincing.

The natural soils from inside the sliding mass are fairly typical of landslide debris. The macro-structure of these samples consists of stiffer fragments within a clay matrix. The structure is formed from remoulding all the materials within the landslide body and hence these fragments consist of lithorelicts of the unweathered argillaceous materials and also fragments of a more lapideous nature. The micro-structure of these materials was not thought to be broken down by the remoulding effect of the landslide, as an increase in Atterberg limits with mincing was still observed.

The reconstituted soils were prepared by swelling the sample to between 1.2 and 1.5 times the liquid limit, by immersion in water (Section 3.2.4 (b)). The soil was then minced to form a slurry and was one-dimensionally consolidated. The macro-structure of the reconstituted soil was homogeneous, consisting of small particles (e.g. quartz or calcite) within a clay matrix. The clay matrix did not consist solely of individual particles but contained aggregated particles, which reduced the plasticity by comparison with that of the disaggregated material created by mincing.

The minced material was formed by passing the natural soil at approximately the plastic limit 10 to 12 times through an industrial food mincer, before reconstituting as above (Section 3.2.4 (c)). The result of mincing the soil was to produce a much more open fabric at the micro-scale, the macro-fabric being very similar to that of the reconstituted soil. A result of mincing the material was to increase the plasticity of the soil, as determined by the Atterberg limits.

As stated in Section 5.1.2, the reconstituted soil and not the minced material was thought to be the most appropriate reference materials for comparing with the natural soil. The reconstituted material was homogeneous, had a stable base fabric which was not removed as a result of landsliding, was reproducible and was as close to the natural material as possible.

After normalising the data to account for their different stress states, specific volumes and material characteristics, the effects of the different macro-structures of the natural soils were assessed by comparing their behaviours with those of the corresponding reconstituted samples and the effects of different micro-structures could be determined by comparing the behaviours of the reconstituted samples with those of corresponding minced samples.

The compression behaviour of these soils is greatly affected by the micro-fabric, as was shown in Section 5.1.3 by comparison of the two soils with different micro-fabrics; the reconstituted and minced samples. The effect of disaggregating the micro-fabric was to allow the normal compression line for the minced sample to lie to the right of that of the reconstituted sample. The samples both consist of clay matrices containing discrete particles. The difference between the two samples is the structure of the clay matrix. The individual layer silicates of the minced sample act singularly as small thin

individual particles in contrast to the layer silicates in the reconstituted sample which act together as larger composite particles.

It was determined in Section 2.2.2 from the data presented in the literature, that the normal compression lines for natural structurally complex clays generally lie to the left of those of corresponding reconstituted samples. This difference between the compression behaviours of samples of the underlying formation and the reconstituted materials was attributed to the slightly different micro-structures of the two materials. No difference was observed between the compression behaviours of the reconstituted samples and of samples of the landslide debris (Section 2.4.1 (e)). The reason for the different compression behaviours of the formation material and the reconstituted material is not so obvious. It is thought to result from the slightly different micro-structures of the two materials.

The effect of the different micro-structures of the minced and reconstituted samples on the shear behaviour was also investigated (Sections 4.6.2 and 5.1.5). The micro-structure of one pair of samples was shown not to influence the stress ratio at critical state, whilst it did have an effect on the value of M for the other pair. Whereas the shear behaviour is thought to be controlled by the matrix material, the compressive behaviour is controlled by the bulk properties.

Corresponding to the different positions of the minced and reconstituted normal compression lines, the critical state lines for these two materials were also shown in Section 4.6.2 to be different. As a result of the data being normalised with respect to the critical state line of the reconstituted material, the normalised state boundary surfaces of the minced and reconstituted materials do not coincide.

The shear behaviour of the natural soils from the underlying formation was found to be controlled by the scaly nature of the macro-structure (Sections 5.1.4 and 4.6.3). Samples which were sheared drained from an estimated isotropic in situ stress level were observed to strain localise at a stress ratio of approximately 70 % of the value of M for the corresponding reconstituted samples. This ratio was found to decrease with increasing stress level. The normalised stress paths of the natural soils from the landslide debris reached stress ratios at or slightly above those of the corresponding reconstituted samples at critical state. These natural samples were still found to strain localise, preventing them from reaching their true critical state, a form of behaviour also

observed for the drained tests on the reconstituted samples. Hence it was concluded that it was the inherent discontinuities in the scaly clays that caused the reduction in the post-rupture strength of these samples.

The micro-structure of these soil was found to have no effect on the stiffness properties of these materials at either the very small strain level or the small strain level (Sections 4.7.1, 4.7.2 and 5.1.5). For one pair of natural and reconstituted samples, the macro-structure was shown to have an influence on the very small strain stiffnesses, increasing the stiffness of the natural sample, for another pair of samples it had no effect. The macro-structure had no effect on the stiffness in the small strain range. This would suggest that only the elastic component of stiffness is affected by the macro-structure.

The residual strength did not appear to be affected by the micro-structure at higher normal effective stresses (Section 4.8.2). In the low stress region there was a slight increase in the value of residual strength obtained for the reconstituted sample. This was thought to result from aggregated particles being broken down in the shear surface only at the higher stress levels. Unfortunately no samples of sufficient size were available to carry out ring shear tests on the natural material. Direct shear tests by others have shown an increase in the residual strength for natural soils (Section 2.2.5). However tests in the direct shear apparatus are not ideal for the measurement of residual strength.

The effect of landsliding on the material behaviour was assessed by comparing the behaviours of samples from inside and outside the landslide body (Section 5.2.1). Remoulding as the result of the landslide activity showed a change in the appearance of these materials from a scaly clay to a clay matrix, containing lithorelicts, as was described earlier. The most obvious difference in the macro-structures of these materials is the absence of inherent discontinuities in the landslide debris. This change in the macro-structure resulted in a behaviour, which was more similar to that of the reconstituted material. There was not thought to be a change in micro-structure as a result of remoulding due to landsliding as similar increases in liquid limit with mincing were observed for samples from inside and outside the landslide body.

6.1 Limitations of this Research and Proposals for Further Work

The main limitation of this research project was the restriction in the number of tests that could be carried out, arising from the difficulties of testing these materials. The soils were firstly difficult to sample, due to the chaotic distribution of materials within this landslide. The heterogeneity of the soils also meant that for every natural sample tested a corresponding reconstituted sample had to be tested to allow correct normalisation of the data. The low permeability of the soils, particularly when minced or reconstituted was perhaps the main restriction on the testing programme. A test on a reconstituted sample to determine its intrinsic normal compression line, typically took several months. The durations of all of the triaxial tests added up to eight equipment-years.

The natural samples that were tested also focused on the more argillaceous materials, as these were thought to control the stability of the landslide. This assumption was corroborated by the shallow angle of the slope. The lapideous component of 15 % estimated for this landslide from the borehole records should not, based on the analyses by D'Elia (1991), have an effect on the shear and bulk properties.

The test programme was mainly carried out in the triaxial apparatus under axi-symmetric conditions. However the stress paths of soil samples in the landslide would be better approximated by plane-strain conditions and the effect of the rotation of the principal stresses cannot be modelled in the triaxial apparatus. The reason that tests were carried out in the triaxial apparatus was that as very little work has been carried out on these complex materials and it was important to determine their behaviour under simple loading conditions before investigating the effects of principal stress rotation. The effect of principal stress rotation on the behaviour of these materials needs to be studied in more detail.

The research presented here provides some insight into the behaviour of the structurally complex clay formations that cover much of the Southern Italian Apennines. There is unfortunately insufficient test data, to be able to define a complete framework of behaviour for this scaly soil. From the data available there is no reason to suggest that a critical state framework could not be used. More work needs to be done to determine the state boundary surface for both the natural and reconstituted materials in v:lnp'

space. It is not thought that a state boundary surface can be determined in q':p' space for the natural material as strain localisation has been shown to cause failure at a post-rupture failure surface. This would require a number of tests to be carried out on the natural material in the high pressure apparatus. Ring shear tests also need to be carried out on natural samples of the formation material and landslide debris to assess the effect of the macro-structure on the residual strength envelope.

The different types of micro- and macro-structures observed in the structurally complex clays are likely to be encountered in other clay shales. More research needs to be carried out to investigate whether there is an influence of a micro-structure of composite particles on the behaviour of other materials. The stability of the composite particles will no doubt be the controlling factor.

REFERENCES

A.G.I. 1979. Some Italian experiences on the mechanical characterization of Structurally complex formations. Proc. 4th ICRM, Montreaux, Vol. 1, pp. 827-846.

A.G.I. 1985. Geotechnical properties and slope stability in structurally complex clay soils. ISSMFE Golden Jubilee Volume, Ed. A.G.I., pp. 198-225.

Airo' Farulla, C. and La Rosa, G. 1977. An analysis of some factors influencing Atterberg limits determination of stiff fissured clay. Proc. Int. Symp. on the Geotechnics of Structurally Complex Formations, Capri, Vol. II, pp. 23-29.

Andronopoulous, B. 1977. The complex geological structure and the relation to landslides (Panagopoula - Greece). Proc. Int. Symp. on the Geotechnics of Structurally Complex Formations, Capri, Vol. I, pp. 1-9.

Atkinson, J.H. and Evans, J.S. 1985. Discussion on: The measurement of soil stiffness in the triaxial apparatus by Jardine, R.J., Symes, N.J. and Burland, J.B. Géotechnique, Vol. 35, No. 3. pp. 378-382.

Atkinson, J.H. and Richardson D. 1987. The effect of local drainage in shear zones on the undrained strength of overconsolidated clay. Géotechnique, Vol. 37, No. 3. pp. 393-403.

Atkinson, J.H. and Sallfors, G. 1991. Experimental determination of stress-strain-time characteristics in laboratory and in-situ tests. Proc. X ECSMFE, Firenze, Vol. 3, pp. 915-956.

Aversa, S., Evangelista, A., Leroueil, S. and Picarelli, L. 1993. Some aspects of the mechanical behaviour of "structured" soils and soft rock. Proc. Int. Symp. on the Geotechnical Engineering of Hard Soils-Soft Rocks, Athens, Vol 1, pp. 359-366.

Baldi, G., Hight, D.W. and Thomas, G.E. 1988. A re-evaluation of conventional triaxial test methods. Advanced Triaxial Testing of Soil and Rock, ASTM, pp. 219-263.

Baldassarre, G., Radina, B., Robotti, F. and Cortelazzi, M. 1996. A contribution to a geotechnical knowledge of the Varicoloured Clays of Italy's Basilicata Region, with specific reference to a test slope. Proc. 7th Int. Symp. on Landslides, Trondheim, Vol. 2, pp. 617-622.

Barden, L. 1972. The relation of soil structure to the engineering geology of a clay soil. Q.J.E.G. Vol. 5, pp. 85-102.

Belviso, R., Cherubini, C., Cotecchia, V., Del Prete, M. and Federico, A. 1977. Effects of tectonization on the geomechanical behaviour of the multicoloured clays. Proc. Int. Symp. on the Geotechnics of Structurally Complex Formations, Capri, Vol. II, pp. 323-326.

Beomonte, M. and Cavallo, R. 1977. Measuring the landslide pressures on a pier foundation. Proc. Int. Symp. on the Geotechnics of Structurally Complex Formations, Capri, Vol. I, pp. 67-76.

Berry, P., Brizzolari, E., Pantaleoni, G., Ribacchi, R. and Sciotti, M. 1977. Static behaviour of a tunnel excavated in a complex mudrock formation. Proc. Int. Symp. on the Geotechnics of Structurally Complex Formations, Capri, Vol. I, pp. 77-94.

Bertuccioli, P. and Lanzo, G. 1993. Mechanical properties of two Italian structurally complex clay soils. Proc. Int. Symp. on the Geotechnical Engineering of Hard Soils-Soft Rocks, Athens, Vol 1, pp. 383-389.

Bilotta, E. 1987. Contributo allo studio della resistenza al taglio di argille a scaglie con prove di laboratorio. R.I.G. pp. 133-143.

Bilotta, E. and Umilta, G. 1981. Indagini sperimentali sulla resistenza a rottura di argille a scaglie. Riv. It. di Geotecnica, Vol. XVIII, pp. 52-56.

Binnie, M.A., Clark, J.F.F. and Skempton, A.W. 1967. The effect of discontinuities in clay bedrock on the design of dams in the Mangla project. Trans. 9th Int. Congr. Large Dams, Istanbul, Vol. 1, pp. 165-183.

Bishop, A.W., Green, G.E., Garga, V.K., Andersen, A., and Brown, D.J. 1971. A new ring shear apparatus and its application to the measurement of residual strength. Géotechnique. Vol. 21, No. 4, pp. 273-328.

Bishop, A.W. and Wesley, L.D. 1975. A hydraulic triaxial apparatus for controlled stress-path testing. Géotechnique, Vol. 25, No. 4. pp. 657-670.

Bjerrum, L. 1954. Geotechnical properties of Norwegian marine clays. Géotechnique, Vol. 4,. pp. 49-69.

Bjerrum, L. and Rosenqvist, I. 1956. Some experiments with artificially sedimented clays. Géotechnique, Vol. 6, pp. 124-136.

Blondeau, F. and Josseaume, H. 1976. Mesure de la résistance au cissaillement résiduelle en laboratoire. Bulletin de Liaison des Laboratoires des Ponts et Chaussées. Stabilité de talus, Vol. 1, numéro spécial II, pp. 90-106.

Borowicka, H. 1965. The influence of the colloidal content on the shear strength of clay. Proc. 6th Int. Conf. Soil Mech., Montreal, Vol. 1, pp. 175-178.

Bromhead, E.N. 1979. A simple ring shear apparatus. Ground Engng., Vol. 12, No. 5, pp. 40-44.

Bucher, F. 1975. Die Restscherfestigkeit natürlicher Böden , ihre Einflussgrossen und Beziehungen als Ergebnis experimenteller Untersuchungen. Report No. 103. Zürich: Institutes für Grundbau und Bodenmechanik Eidgenössiche Technische Hochschule.

Burland, J.B. 1990. On the compressibility and shear strength of natural clays. Géotechnique, Vol. 40, No. 3, pp. 329-378.

Burland, J.B., Rampello, S. Georgiannou, V.N. and Calabresi, G. 1996. A laboratory study of four stiff clays. Géotechnique, Vol. 46, No. 3. pp. 491-514.

Butterfield, R. 1979. A natural compression law for soils. Géotechnique, Vol. 36, No. 4, pp. 593-597.

Canestari, F. and Scarpelli, G. 1993. Stress-dilatancy and strength of Ancona Clay. Proc. Int. Symp. on the Geotechnical Engineering of Hard Soils-Soft Rocks, Athens, Vol 1, pp. 417-424.

Chandler, R.J. 1966. The measurement of residual strength in triaxial compression. Géotechnique, Vol. 16, No. 3, pp. 181-186.

Chandler, R.J. 1969. The effect of weathering on the shear strength properties of Keuper Marl. Géotechnique, Vol. 19, No. 3, pp. 321-334.

Chandler, R.J. 1984. Recent European experience of landslides in over-consolidated clays and soft rocks. State of the Art Report. 4th Int. Symp. on Landslides, Toronto, Vol. 1, pp. 61-81.

Cherubini, C., Coppola, L. Cotecchia, V., Cucchiararo, L., Giasi, C.I., Tagnani, C. and Zechini, P. 1990. Analisi statistica applicata alla caratterizzazione geotecnica delle argille varicolori affioranti nell'Appennino Lucano. Geologia Applicata e Idrogeologia. Vol. 25. pp. 1-27.

Cicolella, A. and Picarelli, L. 1990. Decadimento meccanico di una tipica argilla a scaglie di elevata plastica. Rivista Italiana di Geotecnica. Vol. 24. pp. 5-23.

Clayton, C.R.I. and Khatrush, S.A. 1986. A new device for measuring local axial strains on triaxial specimens. Géotechnique, Vol. 36, No. 4, pp. 593-597.

Clayton, C.R., Simon, N.E. and Matthews, M.C. 1982. Site Investigation. 1st edition, Granada Technical Books. London. 424 pp.

Clayton, C.R., Simon, N.E. and Matthews, M.C. 1995. Site Investigation. 2nd edition, Granada Technical Books. London. 424 pp.

Collins, K. and McGown, A. 1974. The form and function of microfabric features in a variety of natural soils. Géotechnique, Vol. 24, No. 2, pp. 223-254.

Coop, 1997. Personal Communication.

Coop, M.R., Atkinson, J.H. and Taylor, R.N. 1995. Strength, yielding and stiffness of structured and unstructured soils. Proc. XI ECSMFE, Copenhagen, Vol. 1, pp. 55-62.

Coop, M.R. and Cotecchia, F. 1995. The compression of sediments at the archaeological site of Sibari. Proc. XI ECSMFE, Copenhagen, Vol. 8, pp. 19-26.

Cotecchia, F. 1989. Studio di un movimento franoso nelle Unita Irpine dell'alta valle dell Ofanto. R.I.G. pp. 57-84.

Cotecchia, F. 1996. The effects of structure on the properties of an Italian Pleistocene clay. PhD thesis, University of London.

Cotecchia, F. and Chandler, R.J. 1997. The influence of pre-failure behaviour of a natural clay. Géotechnique, Vol. 47, No. 3, pp. 523-544.

Cotecchia, V, Calcagnile, G., Calvaruso, A., Cotecchia, F., Daurù, M., Del Gaudio, V., Di Gioia, R., Donnaloia, M., Dragone, M., Mascia, U., Parise, M., Pierri, P., Polemio, M., Trizzino, R., Wasowski, J., Cojean, R., Atkinson, J.H., Coop, M.R., Fearon, R.E. 1996. Landslide evolution controlled by climatic factors in a seismic area: Prediction methods and warning criteria. Final report submitted to the Commission of European Communities. Contract EV5V-CT94-0451.

Cotecchia, V. and Del Prete, M. 1977. Structurally complex formations in Basilicata and their behaviour in relation to landslide phenomena. Proc. Int. Symp. on the Geotechnics of Structurally Complex Formations, Capri, Vol. II, pp. 63-70.

Cotecchia, V. and Del Prete, M. 1984. The reactivation of large flows in the parts of Southern Italy affected by the earthquake of November 1980, with reference to the evolutive mechanism. Proc. 4th Int. Symp. on Landslides, Vol. II, pp. 33-38, Toronto.

Cotecchia, V., Lenti, V., Salvemini, A. and Spilotro, G. 1986. Reactivation of the large "Buoninventre" slide by the Irpinia earthquake of 23 November 1980. Geol. Appl. Idrogeol. Vol. 21. pp. 217-253.

Cotecchia, V., Monterisi, L., Salvemini, A., Spilotro, G. and Trisorio-Liuzzi, G. 1977. Geolithological, structural and geotechnical aspects of some arenaceous-marly formations cropping out in central southern Appenines. Proc. Int. Symp. on the Geotechnics of Structurally Complex Formations, Capri, Vol. II, pp. 71-78.

Cotecchia, V., Salvemini, A., Simeone, V. and Tafuni, N. 1992. Comportamento geotecnico delle unita Sicilidi ed Irpine affioranti nelle alte valli dei fiumi Sele ed Ofanto a forte evoluzione sismotettonica. Geol. Appl. e Idrog. Vol. 27, pp. 1-47.

Cuccovillo, T. 1995. Shear behaviour and stiffness of naturally cemented sands. PhD thesis, City University.

Cuccovillo, T. and Coop, M.R. 1997. The measurement of local axial strain in triaxial tests using LVDT's. Géotechnique, Vol. 47, No. 1, pp. 167-171.

D'Elia, B. 1977. Geotechnical complexity of some Italian variegated clay shales. Proc. Int. Symp. on the Geotechnics of Structurally Complex Formations, Capri, Vol. 2, pp. 215-221.

D'Elia, B. 1991. Deformation problems in the Italian structurally complex clays. Proc. X ECSMFE, Firenze, Vol. 4.

D'Elia, B., Federico, G., Grisola, M., Rossi Doria, M. and Tancredi, G. 1977. Mechanical behaviour of a highly tectonized miocenic "mudstone". Proc. Int. Symp. on the Geotechnics of Structurally Complex Formations, Capri, Vol. 1, pp. 183-198.

D'Elia, B., Picarelli, L., Leroueil, S. and Vaunat, J. 1996. Geotechnical characterisation of slope movements in structurally complex clay soils and stiff jointed clays. Submitted for publication to Géotechnique 1996.

Del Prete, M. and Trisorio Liuzzi, G., 1992. Reactivation of mudslides after a long quiescent period: the case of Buoniniventre in the Southern Apennines. Proc. French-Italian Conf. Slope Stability in Seismic Areas. Bordighera, Italy. pp. 33-45.

Esu, F. 1977. Behaviour of slopes in structurally complex formations. Proc. Int. Symp. on the Geotechnics of Structurally Complex Formations, Capri, Vol. II, pp. 292-304.

Evangelista, A., Paparo Filomarino, M. and Pellegrino, A. 1977. On the mechanical behaviour of variegated clay shales of Irpinia. Proc. Int. Symp. on the Geotechnics of Structurally Complex Formations, Capri, Vol. I, pp. 229-237.

Fearon, R.E. 1998. Laboratory test results for a structurally complex clay: a data report. City University Internal Report.

Fenelli, G.B., Paparo Filomarino, M., Picarelli, L. and Rippa, F. 1982. Proprieta fisiche e maccaniche di argille varicolori dell'Irpinia. R.I.G. pp. 110-124.

Fiorillo, F. and Parise, M. 1995. Prime considerazioni di carattere geologico, geomorfologico e di instabilità dei versanti nell'alta valle del Fiume Sele. CNR-CE.RI.S.T., Bari, Rapporto Interno No. 31, 22pp.

Fleischer, S. 1972. Scherbruch- und Schergleitfestigkeit von Bindigen Erdstoff. Neue Bergbautechnik. Vol. 2, No. 2, pp. 98-99. Freiburg: Mining Academy.

Garga, V.K. 1970. Residual shear strength under large strains and the effect of sample size on the consolidation of fissured clay. PhD thesis, University of London.

Graham, J. and Houlsby, G.T. 1983. Anisotropic elasticity of a natural clay. Géotechnique, Vol. 33, No. 2, pp. 165-180.

Griffith, F.J. and Joshy, R.C. 1990. Clay fabric response to consolidation. Applied Clay Science, 5 pp. 37-66.

Guerriero, G. 1995. Modellazione sperimentale del comportamento meccanico di terreni in colata. PhD. Thesis, Università di Napoli "Federico II".

Guerriero, G., Olivares, L. and Picarelli, L. 1995. Modelling the mechanical behaviour of clay shales: some experimental remarks. Colloquium on Chalk and Shales, Brussels.

Head, K.N. 1990. Manual of Soil Laboratory Testing, Vol. 1. Soil Classification and Compaction Tests. 2nd edition. Pentech Press, London.

Horseman, S.T., Winter, M.G. and Entwistle, D.C. 1987.Geotechnical characteristics of Boom clay in relation to the disposal of radioactive waste. CEC Report EUR 10987.

Houston, W.N. 1967. Formation mechanisms and property interrelationships in sensitive clays. PhD thesis, University of California, Berkeley.

Hutchinson, J.N. 1988. Morphological and geotechnical parameters of landslides in relation to geology and hydrogeology. Proc. V Int. Symp. on Landslides, Lausanne, Vol 1, pp. 3-35.

Hutchinson, J.N. and Del Prete, M. 1985. Landslides at Calitri, Southern Appenines, reactivated by the earthquake of 23 November 1980. Geol. Appl. Idrogeol. Vol. 20. pp. 9-38.

Iaccarino, G., Peduto, F., Pellegrino, A. and Picarelli, L. 1995. Main features of earthflow in part of the Southern Apennines. Proc. XI ECSMFE, Copenhagen, Vol. 4, pp. 69-76.

Jovicic, V. 1997. The measurement and interpretation of small strain stiffness of soils. PhD thesis, City University.

Jovicic, V., Coop, M.R. and Simic, M. 1996 Objective criteria for determining G_{max} from bender element tests. Géotechnique, Vol. 46, No. 2, pp. 357-362.

Kanji, M.A. 1974. The relationship between drained friction angles and Atterberg limits of natural soils. Géotechnique, Vol. 24, No. 4. pp. 671-674.

Kenney, T.C. 1967. The influence of mineralogical composition on the residual strength of natural soils. Proceedings of the Oslo Geotechnical Conference, on the Shear Strength Properties of Natural Soils and Rocks, Vol I, pp. 123-129.

Kim, Y.-S., Tatsuoka, F. and Ochi, K. 1994. Deformation characteristics at small strains of sedimentary rocks by triaxial compression. Géotechnique, Vol. 44, No. 3, pp. 461-478.

La Rochelle, P., Leroueil, S., Trak, B., Blais-Leroux, L. and Tavenas, F. 1988. An observational approach to membrane and area corrections in triaxial tests. Advanced Triaxial Testing of Soil and Rock, ASTM, pp. 715-731.

Lemos, L.J.L. 1986. The effect of rate on residual strength of soil. PhD thesis. University of London.

Lemos, L.J.L. 1991. Shear strength of shear surfaces under fast loading. Proc. X ECSMFE, Firenze, Vol. 1, pp. 137-141.

Leroueil, S. Locat, J., Vaunat, J., Picarelli, L., Lee, H. and Faure, R. 1996. Geotechnical characterisation of slope movements. Proc. 7th Int. Symp. on Landslides, Trondheim, Vol. 1, pp. 53-74.

Leroueil, S. and Vaughan, P.R. 1990. The general and congruent effects of structure in natural soils and weak rocks. Géotechnique, Vol. 40, No. 3, pp. 467-488.

L.T.S. 1995. Results of basic soil tests on soil from the Senerchia landslide. Data Report.

Lupini, J.F., Skinner, A.E., and Vaughan, P.R. 1981. The drained residual strength of cohesive soils. Géotechnique, Vol. 31, No. 2, pp. 181-213.

Marsland, A. 1974. Comparison of the results from static penetration tests and large in-situ plate tests in London Clay. Proc. European Symp. Penetration Testing, Stockholm.

Mesri, G. and Cepeda-Diaz, A.F. 1986. Residual shear strength of clays and shales. Géotechnique, Vol. 36, No. 2, pp. 269-274.

Mitchell, J.K. 1976. Fundamentals of Soil Behaviour. 1st edition, John Wiley and Sons, Inc. New York/Chichester/Brisbane/Toronto/Singapore.

Mitchell, J.K. 1993. Fundamentals of Soil Behaviour. 2nd edition, John Wiley and Sons, Inc. New York/Chichester/Brisbane/Toronto/Singapore.

Moum, J. and Rosenqvist, I. Th. 1961. On the weathering of a young marine clay. Proc. Int Conf. Soil Mech. and Found. Eng., London, Vol. 1, pp. 77-79.

O'Brien, N.R. 1971. Fabric of kaolinite and illite floccules. Clays and Clay Minerals. Vol. 19. pp. 353-359.

Olivares, L. 1996. Catterizzazione dell'Argilla di Bisaccia in condizioni monotone, cicliche e dinamiche e riflesi sul comportamento del "Colle" a seguito del terremoto del 1980. PhD. Thesis, Università di Napoli "Federico II".

Osterberg, J.O. 1973. An improved hydraulic piston sampler. Eng. News Record, Vol. 148, No. 17, pp. 77-78.

Pane, V. and Burghignoli, A. 1988. Determizione in laboratorio delle cratteristiche dimanche dell'argilla del Fucino. In Atti del I Convegno del Grup. Naz. di Ing. Geotec. Monselice, Italy, pp. 115-140.

Picarelli, L., 1991. Discussion of the paper: The general and congruent effects of structure in natural soils and weak rocks by S. Leroueil and P.R. Vaughan. Géotechnique, Vol. 41, pp. 281-284.

Picarelli, L. and Viggiani, C. 1988. A landslide in a structurally complex clay. Proc. 5th Int. Symp. on Landslides, Lausanne, Vol. 1, pp. 289-294.

Quigley, Q.M. and Thompson, C.D. 1966. The fabric of anisotropically consolidated sensitive marine clay. Canadian Geotechnical Journal. Vol. 3, No. 2, pp. 61-73.

Rampello, S. and Silvestri, F. 1993. The stress-strain behaviour of natural and reconstituted samples of two overconsolidated clays. Proc. Int. Symp. on the Geotechnical Engineering of Hard Soils-Soft Rocks, Athens, Vol 1, pp. 769-778.

Rampello, S., Silvestri, F. and Viggiani, G. 1994. The dependence of small strain stiffness on stress state and history for fine grained soils: the example of Vallerica clay. Proc. Int. Symp. on Prefailure Deformations of Geomaterials. IS-Hokkaido. Vol. 1: pp. 273-279. Balkema.

Rampello, S., Viggiani, G. and Georgiannou, V.N. 1993. Strength and dilatancy of natural and reconstituted Vallerica clay. Proc. Int. Symp. on the Geotechnical Engineering of Hard Soils-Soft Rocks, Athens, Vol 1, pp. 761-768.

Rampello, S., Viggiani, G.M.B., and Amaruso, A. 1997. Small-strain stiffness of reconstituted clay compressed along constant triaxial effective stress paths. Géotechnique, Vol. 47, No. 3, pp. 475-508.

Rippa, F. and Picarelli, L. 1977. Some Considerations on index properties of Southern Italy shales. Proc. Int. Symp. on The Geotechnics of Structurally Complex Formations, Capri, Vol 1 pp. 401-406.

Santaloia, F. 1994. La stabilita'dei versanti in formazioni strutturalmente complesse: movimenti gravitativi nell'area di Cervarezza. PhD thesis. Università degli Studi di Milano.

Samuels, S.G. 1975. Some properties of the Gault Clay from the Ely-Ouse Essex water tunnel. Géotechnique 25, Vol. 25, No. 2, pp. 239-264.

Schofield, A.N. and Wroth, C.P. 1968. Critical State Soil Mechanics. McGraw-Hill, London

Schmertmann, J.H. 1969. Swelling sensitivity. Géotechnique, Vol. 19, No. 4, pp. 530-533.

Schulteiss, P.J. 1982. Influence of packing structure on the seismic velocities in sediments. Ph.D. Thesis. University College of North Wales.

Seycek, 1978. Residual shear strength of soils. Bull. Int. Ass. Engng Geol. Vol. 17. pp. 73-75.

Sfrondini G. 1975. Catteristiche microtessiturali e microstrutturali di alcuni sedimenti argillosi connesse con la natura ed il tipo delle sollecitazioni subite. Geol. Appl. Idrogeol. Vol. 10. pp. 300-320.

Silvestri, V. 1980. The long term stability of a cutting slope in an overconsolidated sensitive clay. Canadian Geotechnical Journal, Vol. 17, pp. 337-351.

Skempton, A.W. 1954. The pore pressure coefficients A and B. Géotechnique, Vol. 4, No. 4, pp. 143-147.

Skempton, A.W. 1964. Long term stability of clay slopes. Géotechnique, Vol. 14, No. 2, pp. 77-102.

Skempton, A.W. 1970. The consolidation of clays by gravitational compaction. Q.J. Geol. Soc., No. 125, pp. 373-411.

Skempton, A.W. 1977. Slope stability in cuttings in brown London clay. Proc. 9th Int. Conf. Soil Mech. and Found. Eng., Tokyo, Vol. 3, pp. 261-270.

Skempton, A.W. and Northey, R.D. 1952. The sensitivity of clays. Géotechnique, Vol. 3, pp.30-53.

Skinner, A.E. 1969. A note on the influence of interparticle friction on the shearing strength of a random assembly of spherical particles. Géotechnique, Vol. 19, No. 1, pp. 150-157.

Smart, P. 1971. Contribution to stress-strain behaviour of soils. Proc. Roscoe Memorial Symposium, Cambridge University, pp. 253-255.

Stallebrass, S.E. 1990. Modelling the effect of recent stress history on the deformation of overconsolidated soils. PhD Thesis, City University.

Stark, T.D. and Eid, H.T. 1994. Drained residual strength of cohesive soils. ASTM Geotech. J., Vol. 120, No. 5, pp. 856-871.

Stark, T.D. and Vettel, J.J. 1992. Bromhead ring shear test procedure. ASTM Geotechnical Testing Journal, Vol. 15, No. 1, pp. 24-32.

Tavernas, F. Flon, P. Leroueil, S. and Lebuis, J. 1983. Remoulding energy and risk of slide retrogression in sensitive clays. Proc. Symp. on Slopes on Soft Clays, Linkoping, SGI Report No. 17, pp. 423-454.

Taylor, R.N. and Coop, M.R. 1990. Stress path testing for Boom clay from Mol, Belgium. Proc. 25th Annual Conf. Eng. Group Geol. Soc.

Tchalenko, J.S. 1967. The influence of shear and consolidation on the microscopic structure of some clays. PhD thesis, University of London.

Terzaghi, K. 1944. Ends and means in soil mechanics, Engineering Journal of Canada, Vol. 27, pp. 608.

Tika, T.M. 1989. The effect of fast shearing on the residual strength of soils. PhD thesis, University of London.

Van Olphen, H. 1977. An introduction to Clay Colloid Chemistry, 2nd ed., Wiley Interscience, New York, 318 pp.

Vaughan, P.R., Hight, D.W., Sodha, V.G., and Walbancke, H.J. 1978. Factors affecting the stability of clay fills in Britain. Clay Fills, pp. 203-217. London: Institution of Civil Engineers.

Viggiani, G. 1992. Small strain stiffness of fine grained soils. PhD thesis, City University.

Viggiani, G. and Atkinson, J.H. 1995a. Stiffness of Fine Grained Soils at Very Small Strains. Géotechnique. Vol 45, No. 2, pp. 249-265.

Viggiani, G. and Atkinson, J.H. 1995b. The interpretation of the bender element test. Géotechnique. Vol 45, No. 1, pp. 149-155.

Viggiani, G., Rampello, S. and Georgiannou, V.N. 1993. Experimental analysis of localisation phenomena in triaxial tests on stiff clays. Proc. Int. Symp. on the Geotechnical Engineering of Hard Soils-Soft Rocks, Athens, Vol 1, pp. 849-856.

Voight, 1973. Correlation between Atterberg plasticity limits and residual shear strength of natural soils. Géotechnique. Vol 23, No. 2, pp. 265-267.

Wasowski, J. and Falco, P., 1996. Misure della retrogression della frana Acquara-Vadoncello nei pressi di Senerchia (AV). CNR-CE.RI.S.T., Bari, Rapp. Tecn. Int. n. 45, 18 pp.

Wasowski, J. and Lasorsa, M. 1995. Primi risultati delle indagni geognostiche sulla frana di Acquara-Vadoncello del 1993. CNR-CE.RI.S.T., Bari, Rapp. Tecn. Int. n. 39, 20 pp.

Weiler, W.A. 1988. Small strain shear modulus of clay. Proc. Geot. Eng. Div. Speciality Conf. on Earthquake Eng. and Soil Dynamics. II ASCE. Park City. Utah. pp. 331-345.

Wiewiora, A., Sanchez-Soto, P.J., Aviles, M.A., Justo, A. and Perez-Rodriguez, J.L. 1993. Effect of grinding and leaching on the polytypic structure of pyrophyllite, Applied Clay Science, 8, pp. 261-282.

Wood, D.M. 1990. Soil behaviour and critical state soil mechanics. Cambridge University Press.

Zeniou, E. 1993. The behaviour of Boom clay under K_o compression and shearing. Part III Project Report; Dept of Civil Engineering, City University.

Cell No.	Pressure Range	Sample Size (mm)	Computer System	Analogue/ Digital Interface	Pressure Regulators Electromanostat
1	Standard	38	BBC	Spectra	Electromanostat
2	Standard	38	PC	CIL alpha card	Analogue-pneumatic
4	Standard	38	BBC	Spectra	Electromanostat
6	Standard	38	PC	CIL alpha card	Electromanostat
7	Standard	38	BBC	Spectra	Electromanostat
8	Standard	60	BBC	Spectra	Electromanostat
9	Standard	38	BBC	Spectra	Electromanostat
10	Standard	38	PC	DT card	Analogue-pneumatic
High Pressure	High	50	PC	CIL alpha card	Electromanostat

Table 3.1 Summary of different control systems used with the triaxial apparatus

Cell No.	Local Axial Gauges	Bender Elements	Radial Strain Belt	Mid-height PPT
1	None	Yes	No	No
2	LVDT	No	No	No
4	None	Yes	No	No
6	Hall Effect	No	No	Yes
7	None	No	Yes	Yes
8	LVDT	No	No	No
9	LVDT	No	Yes	No
10	LVDT	Yes	No	No
High Pressure	Hall Effect	Yes	No	No

Table 3.2 Summary of local instrumentation used with the triaxial apparatus

Function	Instrument	Working Range	Output Voltage	Resolution	Noise	Typical error due to non-linearity, hysteresis and drift
Axial Stress	Surrey University Wykeham Farrance Load Cell	± 5 kN	20 mV (unamplified)	0.05 N	±1.0 N	± 1 % F.S.
Pore Pressure Cell Pressure	Druck pressure transducer WF 17060	0 - 1000 kPa	100 mV	0.03 kPa	±0.2 kPa	± 0.2 % F.S.
Axial Strain	LVDT displacement transducer 500A RDP Electronics Ltd	25 mm	± 2 V	0.0015 mm	± 0.0015 mm	± 0.5 % F.S.
Volumetric Strain	50 cc Imperial College volume gauge + LVDT 500A RDP	35 cc	± 2 V	0.0035 %	± 0.001 cm^3	± 0.5 % F.S.
Local Axial Strain	Surrey University Hall Effect Transducer	5 mm	± 1 V	0.00012 mm	± 0.001 mm	± 1 % F.S.
Local Axial Strain	LVDT D5/200 RDP	10 mm	± 2 V	0.00003 - 0.002 mm	0.00001 mm	± 0.14 % F.S.
Mid-height Pore Pressure	Druck Miniature pore pressure transducer PDCR 81	0 - 700 kPa	100 mV	0.015 kPa	±0.2 kPa	± 0.2 % F.S.

Table 3.3 Characteristics of typical transducers used in the standard pressure range triaxial apparatus (modified after Cuccovillo, 1995) (drift, hysteresis and non-linearity are expressed as a percentage of the full scale working range)

Function	Instrument	Working Range	Typical Output at Full Range
Shear Stress	RDP precision low profile load cell Model 41E	± 10 kN	30 mV (unamplified)
Vertical Friction	RDP precision low profile load cell Model 41E	± 5 kN	30 mV (unamplified)
Gap Opening	Displacement Transducer	10 mm	70 mV
Sample Height	Displacement Transducer	10 mm	70 mV

Table 3.4 Characteristics of transducers used in the Bishop ring shear apparatus

Transducer	Resolution	Noise	Hysteresis	Non-Linearity
RDP 10 kN load cell	0.003 N[1] (10 N)[2]	± 1 kPa	± 0.08 % F.S.	± 0.1 % F.S.
RDP 5 kN load cell	0.001 N[1] (5 N)[2]	± 0.5 kPa	± 0.08 % F.S.	± 0.1 % F.S.
displacement transducer[4]	0.002 mm	± 0.01 mm	± 0.02 % F.S.	± 0.2 % F.S.

[1] Resolution at maximum gain with amplification used
[2] Resolution at maximum gain without amplification
[3] Drift, hysteresis and non-linearity are expressed as a percentage of the full scale working, quoted from the manufacturers literature.
[4] Values from Stallebrass (1990)

Table 3.5 Resolution and accuracy of transducers used in the Bishop ring shear apparatus

Triaxial Test	Borehole Depth (m bgl)	Inside/ Outside Landslide	Natural/ Reconst/ Minced	Duration of Test (days)	PI (%)	N	λ	Final Shearing nc/oc[1] p'_o (kPa)	q'/p'^2 const. vol.	Γ^3	M^2	$\phi'_{critical}$ (deg)	Other Information
N2B	I1 21.0-21.4	Inside old slide	Natural	26	41.4	-	-	oc - drained $p'_o = 250$	0.84	-	-	-	probe[4](kPa) $p'_o = 125$
H2C	I1 21.0-21.4	Inside old slide	Natural	90	41.4	-	-	oc - undrained $p'_o = 3600$	0.34	-	-	-	probes[2] (kPa) $p'_o = 700,1250$ BE[5]
R2B	I1 21.0-21.4	Inside old slide	Reconst	67	41.4	4.12	0.333	nc - drained $p'_o = 300$	0.49	-	-	-	probes[2](kPa) $p'_o = 100,200$
R2C	I1 21.0-21.4	Inside old slide	Reconst	150	41.4	4.12	0.333	nc - undrained $p'_o = 500$	0.49	3.95	0.54	14.1	BE[3]
N4B	P4 40.5-40.8	Outside	Natural	35	36.6	-	-	oc - drained $p'_o = 550$	0.65	-	-	-	probes[2] (kPa) $p'_o = 300$
R4B	P4 40.5-40.8	Outside	Reconst	120	36.6	3.79	0.299	oc - drained $p'_o = 50$	0.92	-	-	-	probes[2] (kPa) $p'_o = 100,200,400$

[1] normally consolidated/overconsolidated
[2] not corrected for strain localisation using stress-dilatancy plots
[3] corrected for strain localisation using stress-dilatancy plots
[4] drained probes carried out as described in Section 3.3.5
[5] bender element tests carried out

Table 4.1 Summary of Triaxial Tests and Results

Triaxial Test	Borehole Depth (m bgl)	Inside/ Outside Landslide	Natural/ Reconst/ Minced	Duration of Test (days)	PI (%)	N	λ	Final Shearing nc/oc[1] p'_o (kPa)	q'/p'^2 const. vol.	Γ^3	M^2	$\phi'_{critical}$ (deg)	Other Information
N6A	P3 12.1-12.7	Outside	Natural	34	37.7	-	-	oc - drained $p'_o = 200$	0.43* 0.35		-	-	-
R6A	P3 12.1-12.7	Outside	Reconst	135	37.7	3.96	0.320	oc - undrained $p'_o = 400$	0.68	3.85	0.68	17.8	probes[2] (kPa) p'_o =100,200,50
N7A	P2 7.5-7.8	Inside	Natural	44	25.9	-	-	oc - drained $p'_o = 170$	0.99	-	-	-	-
R7A	P2 7.5-7.8	Inside	Reconst	160	25.9	2.62	0.146	sample lost	-	-	-	-	probes[2] (kPa) $p'_o = 300$
R7B	P2 7.5-7.8	Inside	Reconst	145	25.9	2.62	0.146	nc - undrained $p'_o = 300$	1.01	2.53	1.01	25.6	probes[2] (kPa) p'_o =100,200
R7C	P2 7.5-7.8	Inside	Reconst	60	25.9	2.62	0.146	oc - undrained $p'_o = 100$	0.99	-	-	-	-
M7A	P2 7.5-7.8	Inside	Reconst	270	44.0	2.94	0.193	oc - undrained $p'_o = 100$	0.89	-	-	-	probes[2] (kPa) p'_o =100,200,300
M7B	P2 7.5-7.8	Inside	Reconst	26	44.0	2.94	0.193	nc - undrained $p'_o = 100$	1.01	2.83	1.01	25.6	-

Table 4.1 Summary of Triaxial Tests and Results

Triaxial Test	Borehole Depth (m bgl)	Inside/ Outside Landslide	Natural/ Reconst/ Minced	Duration of Test (days)	PI (%)	N	λ	Final Shearing nc/oc[1] p'_o (kPa)	q'/p'^2 const. vol.	Γ^3	M^2	$\phi'_{critical}$ (deg)	Other Information
N8A	I4 16.0-16.4	Outside	Natural	34	31.0	-	-	oc - drained $p'_o = 235$	0.75	-	-	-	-
N8B	I4 16.0-16.4	Outside	Natural	85	31.0	-	-	oc - drained $p'_o = 235$	0.81	-	-	-	cyclic loading
R8A	I4 16.0-16.4	Outside	Reconst	168	31.0	3.27	0.220	oc - drained $p'_o = 50$	1.18	-	-	-	probes[2] (kPa) p'_o=100,200,400
R8B	I4 16.0-16.4	Outside	Reconst	30	31.0	3.27	0.220	nc - undrained $p'_o = 150$	0.96	3.18	0.97	24.6	-
N9A	P4 22.2-22.6	Outside	Natural	37	34.9	-	-	oc - drained $p'_o = 285$	0.64	-	-	-	
N9B	P4 22.2-22.6	Outside	Natural	48	34.9	-	-	oc - drained $p'_o = 285$	0.57	-	-	-	
R9A	P4 22.2-22.6	Outside	Reconst	66	34.9	3.71	0.288	nc - undrained $p'_o = 200$	0.82	3.47	0.84	21.6	probe[2] (kPa) $p'_o = 100$
R9B	P4 22.2-22.6	Outside	Reconst	135	34.9	3.71	0.288	oc - drained $p'_o = 100$	0.70	-	-	-	BE[3]

Table 4.1 Summary of Triaxial Tests and Results

Triaxial Test	Borehole Depth (m bgl)	Inside/ Outside Landslide	Natural/ Reconst/ Minced	Duration of Test (days)	PI (%)	N	λ	Final Shearing nc/oc[1] p'_o (kPa)	q'/p'^2 const. vol.	Γ^3	M^2	$\phi'_{critical}$ (deg)	Other Information
M9C	P4 22.2-22.6	Outside	Minced	120	57.0	6.50	0.720	nc - undrained $p'_o = 500$	0.56	4.46	0.65	17.1	BE[3]
NBA	I6 34.0-34.5	Outside	Natural	52	-	-	-	oc-undrained $p'_o = 435$	0.47	-	-	-	-
NCA	P3 4.5-4.65	Inside	Natural	45	27.0	-	-	oc - drained $p'_o = 90$	1.24	-	-	-	cyclic loading
RCA	P3 4.5-4.65	Inside	Reconst	80	27.0	2.79	0.154	nc - undrained $p'_o = 200$	0.94	2.70	0.99	25.1	
HDA	I5 20.2-20.5	Outside	Natural	30	34.4	-	-	sample lost	-	-	-	-	BE[3]
RDA	I5 20.2-20.5	Outside	Reconst	100	34.4	3.11	0.212	oc - drained $p'_o = 100$	0.85	-	-	-	BE[3]
RDB	I5 20.2-20.5	Outside	Reconst	30	34.4	3.11	0.212	nc - undrained $p'_o = 100$	0.85	3.00	0.87	22.3	-

Table 4.1 Summary of Triaxial Tests and Results

Sample	Borehole Depth (m bgl)	Inside/ Outside Landslide	Sample Type	LL (%)	PL (%)	Bromhead Bishop	Residual Friction angle (°)[1]
I	I2 9.4 - 9.6	Inside	Osterberg	55	27	Bromhead	6.9
II	I1 21.0 - 21.4	Inside Old slide	Osterberg	72	30	Bromhead	5.2
A	I2 11.2 - 11.5	Inside	Disturbed	55	33	Bromhead Bishop	6.1 5.2
B	P4 15.8 - 16.0	Outside	Disturbed	79	40	Bishop	6.6
C	P2 10.2 - 10.5	Inside	Disturbed	58	26	Bishop	5.2
D	I4 7.5 - 7.8	Outside	Osterberg	58	33	Bishop	5.0
D(M)[2]	I4 7.5 - 7.8	Outside	Osterberg	71	26	Bishop	5.0

Table 4.2 Summary of Ring Shear Test Results

[1] Residual friction angles quoted assume linear failure envelopes and ignore any slight increase in the residual strength ..at low normal stresses

[2] Minced sample prepared as detailed in Section 3.2.3

Sample	Apparatus	Test Stage	Initial q' (kPa)	Initial p' (kPa)	Initial q'/p'	Initial τ/σ'_n	Equivalent Slope Angle (degrees)	$\pm\Delta q'$ (kPa)	Equivalent Acceleration (g)	Maximum Mean Pore Pressure Rise (kPa)	No of cycles Required to reach max. pore preesure
N8B I4 16-16.4	Triaxial[1]	1	40	248	0.161	0.081	4.6	20	0.04	32	5
		2	50	252	0.199	0.099	5.7	30	0.06	50	6
		3	72	259	0.278	0.139	7.9	52	0.10	45	6
		4	115	273	0.421	0.210	11.9	55	0.10	35	6
NCA P3 4.5-5.1	Traixial[1]	1	40	103	0.387	0.19	11.0	20	0.10	17	7
			τ (kPa)	σ'_n (kPa)				$\pm\Delta\tau$ (kPa)			
I6/1	Simple Shear[2]	1	20	100		0.2	11.3	10	0.10	-10	7
		2	57	300		0.19	11.0	27	0.09	28	7
I5/2	Simple Shear[2]	1	20	100		0.2	11.3	10	0.10	-12	5
		2	57	300		0.19	11.0	27	0.09	12	3

[1] Triaxial tests carried out at City University

[2] Simple shear tests carried out at Politecnico di Bari

Table 5.1 Results of Cyclic Tests

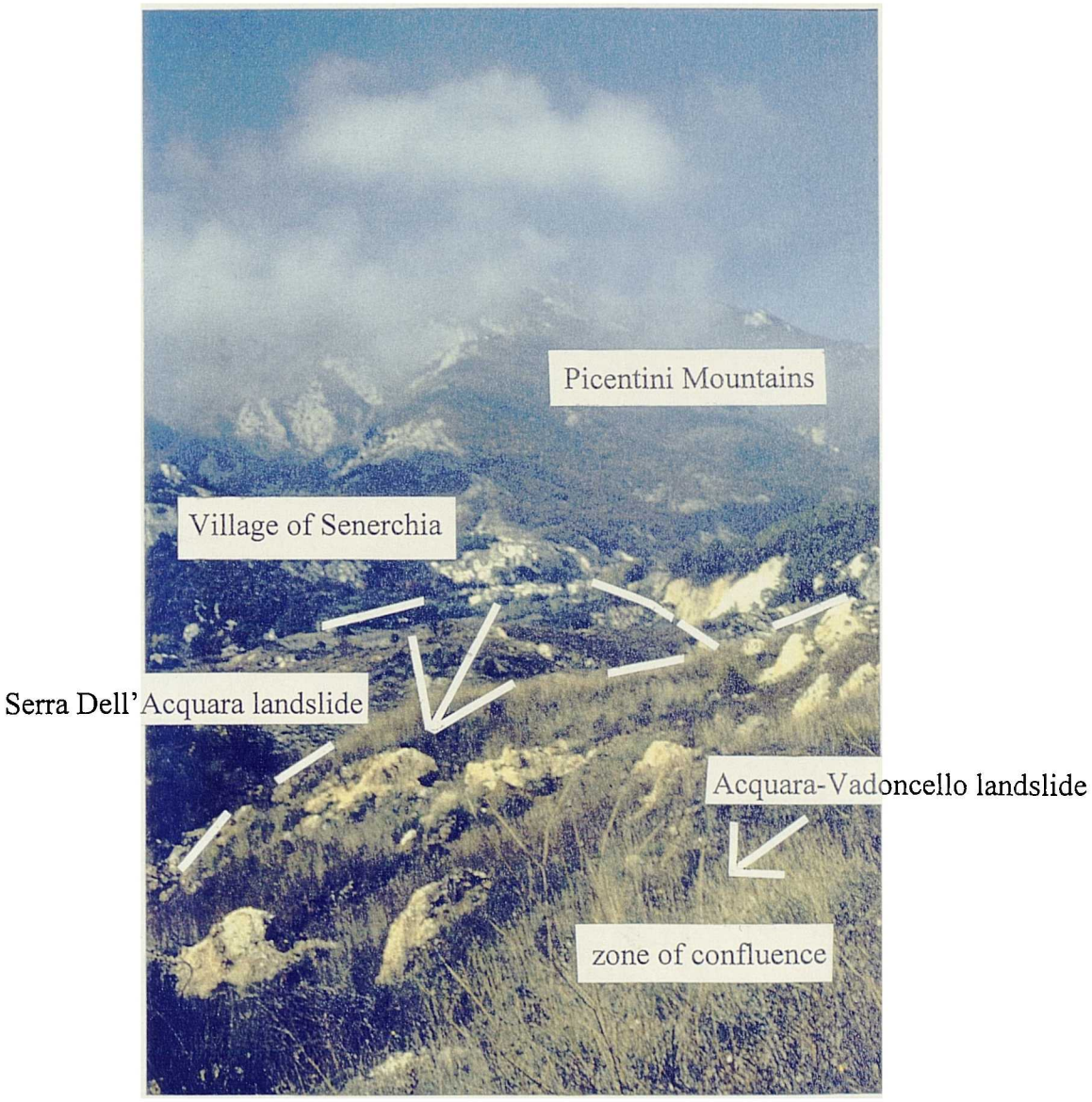

Figure 1.1 Photograph of the Serra Dell'Acquara Landslide taken from the region of confluence between the Serra Dell'Acquara and Acquara-Vadoncello landslides.

Figure 1.2 Photograph of the scarp of the Acquara-Vadoncello landslide.

Figure 1.3 Photograph of the downslope region of the Acquara-Vadoncello landslide.

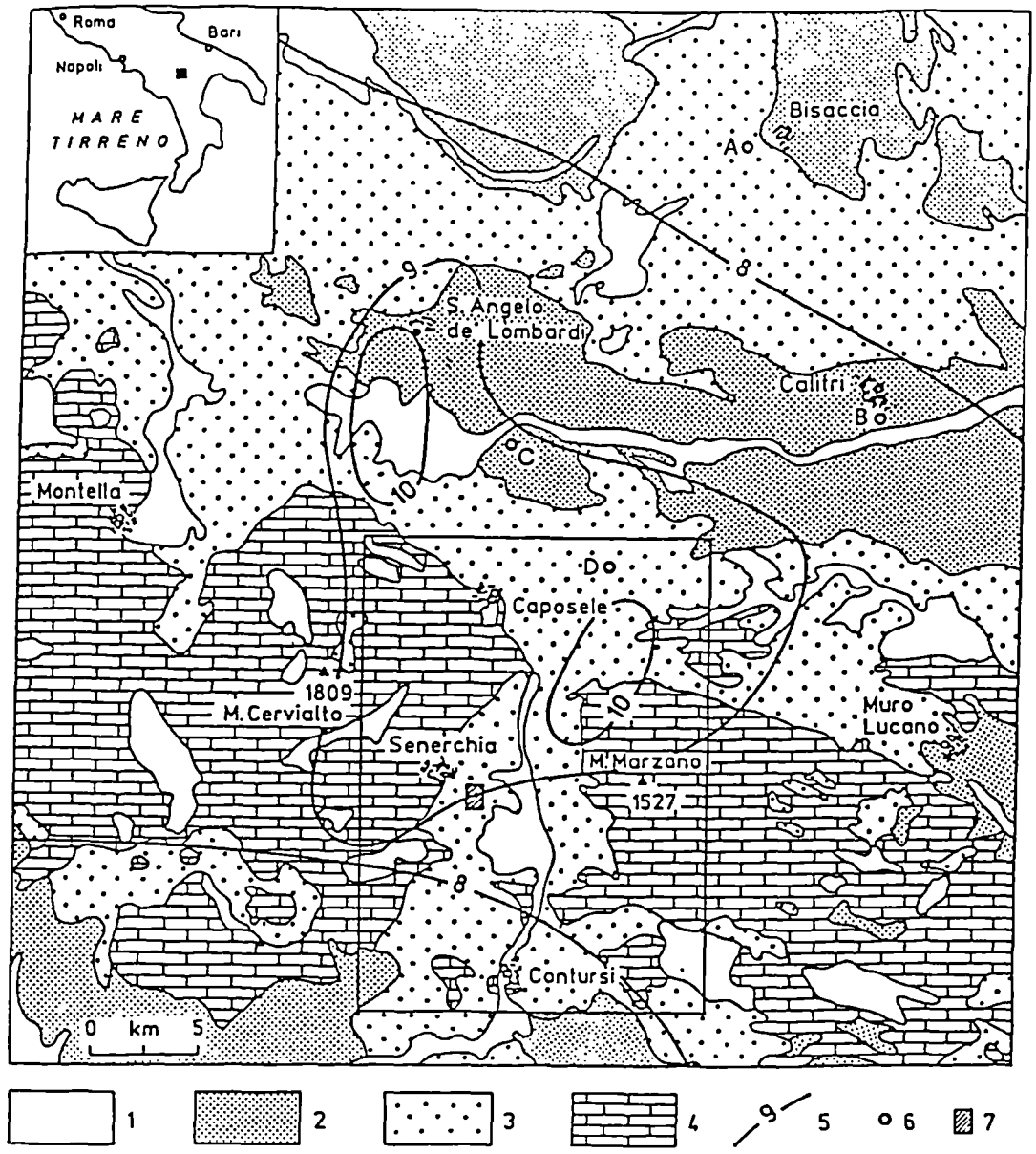

1) Recent deposits: lacaustrine fluvio-lacustrine, littoral, deltaic and alluvial deposits. PLEISTOCENE - HOLOCENE
2) Intermontane basins: marine conglomerates, sands and clays. LOWER-MIDDLE PLIOCENE
3) Molise-Lucanian basin: argillites, siliceous marls, limestones with chert, varicolori clays. MIDDLE TRIASSIC - MESSINIAN
4) Campania-Lucanian shelf: limestones, dolomitic limestones and dolomites. UPPER TRIAS - LANGHIAN
5) Isoseismal lines of 1980 earthquake.
6) **A** Bisaccia landslide; **B** Calitri Landslide; **C** Lioni landslide; **D** Buoninventre landslide
7) Detailed study area containing the Acquara-Vadoncello landslide.

Figure 1.4 Schematic geological map of the large study area, showing the location of the landslide site at Senerchia chosen for the detailed study (after Fiorillo and Parise, 1995).

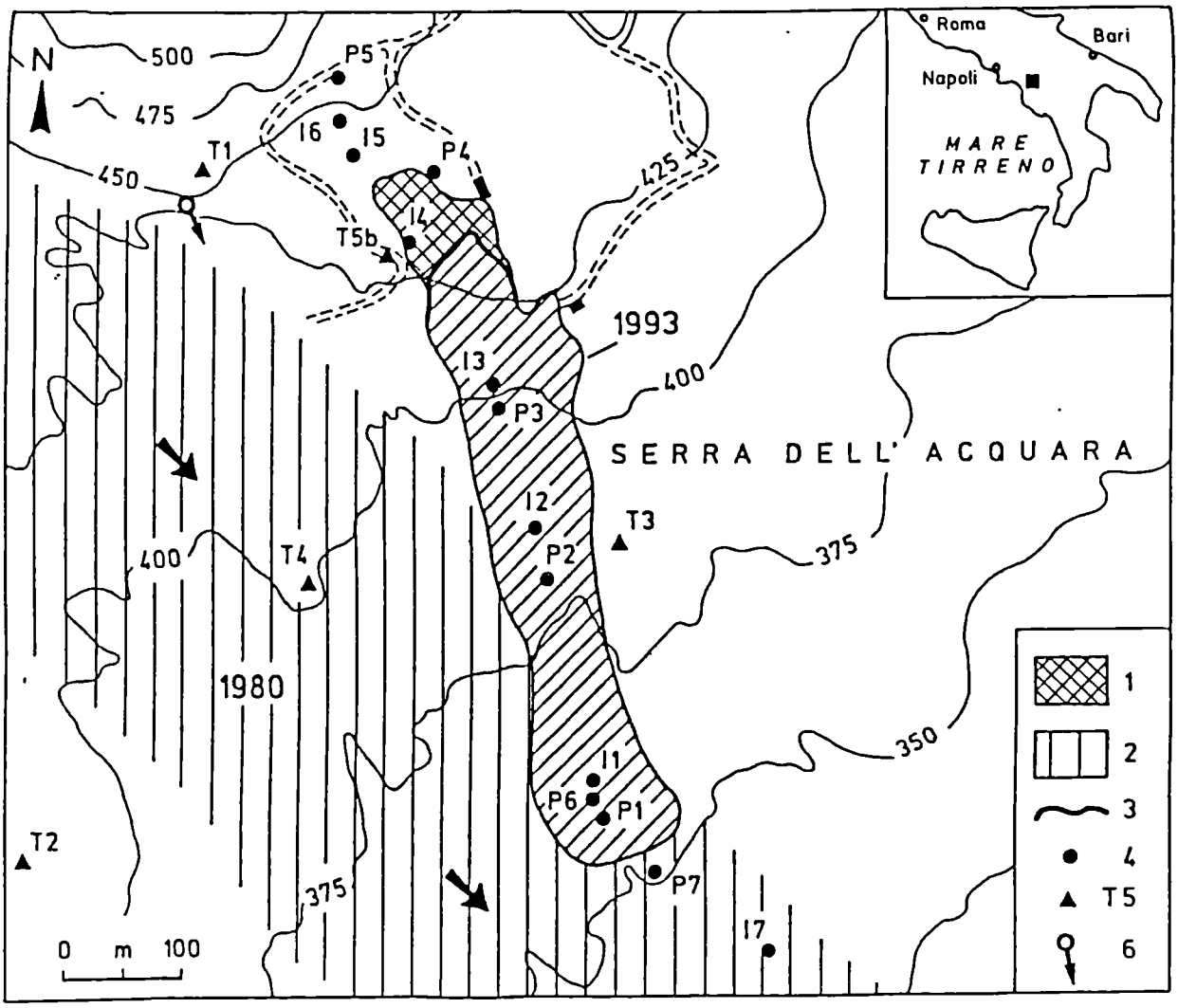

1) Amount of retrogression from June 1995 to May 1996.
2) Central portion of the Serra dell'Acquara mudslide.
3) Mainscarp of the 1993 Acquara-Vadoncello landslide in June 1995.
4) Locations of inclinometer (I) and piezometer (P) boreholes
5) Local control point for topographic monitoring
6) Spring

Figure 1.5 Schematic map showing the locations of the 1993 Acquara-Vadoncello landslide (diagonal lines) and the 1980 Serra dell'Acquara mudslide (vertical lines) (after Cotecchia et al. 1996).

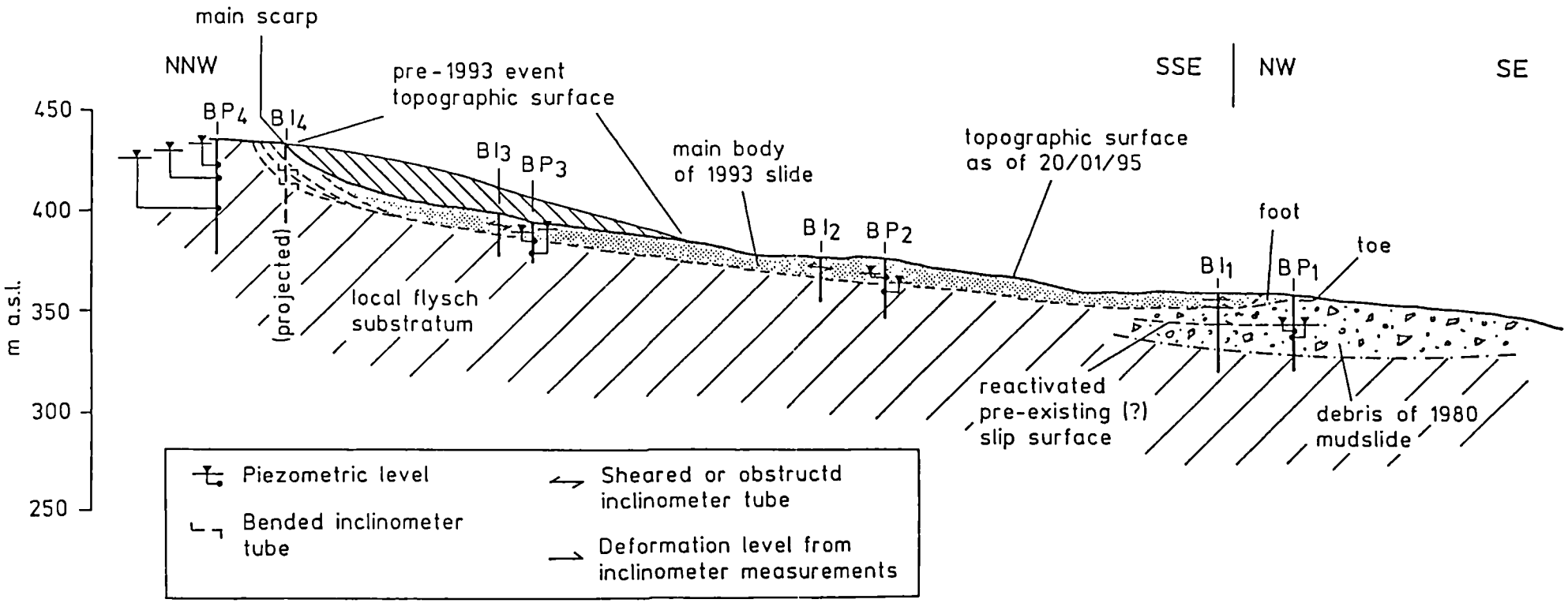

Figure 1.6 Schematic geologic profile of the 1993 Acquara-Vadoncello landslide. The inferred subsurface limits of the 1993 earthflow body are based on information from the detailed borehole logs and the results of the inclinometer monitoring. The ground water levels refer to Cassagrande piezometer data from February 1995 (after Wasowski and Lasorsa, 1995).

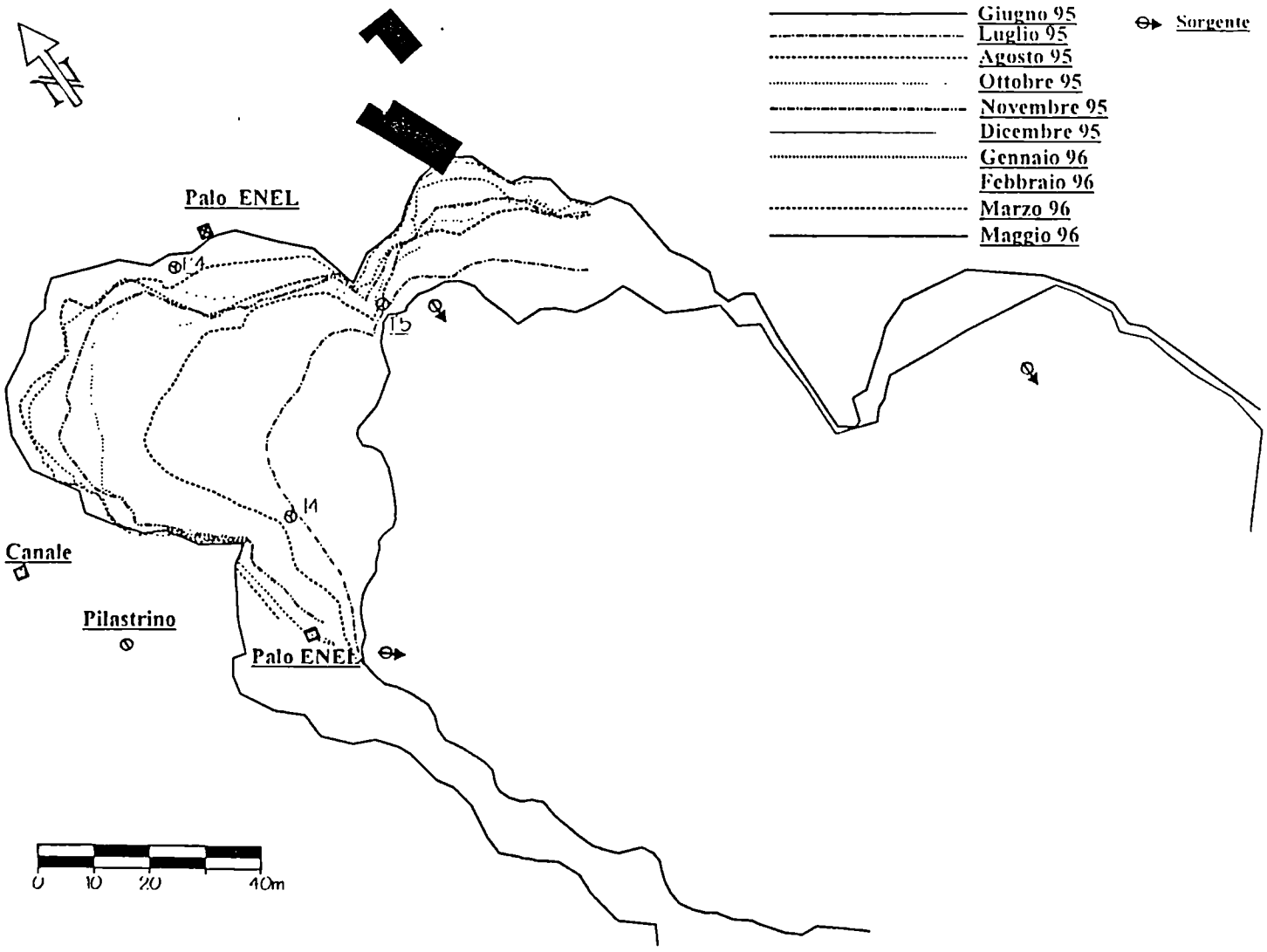

Figure 1.7 Successive positions of the 1993 Acquara-Vadoncello slide headscarp from June 1995 to May 1996 (after Wasowski and Falco, 1996).

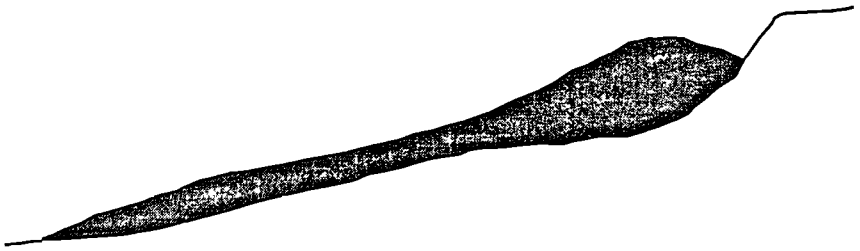

a) slump earthflow

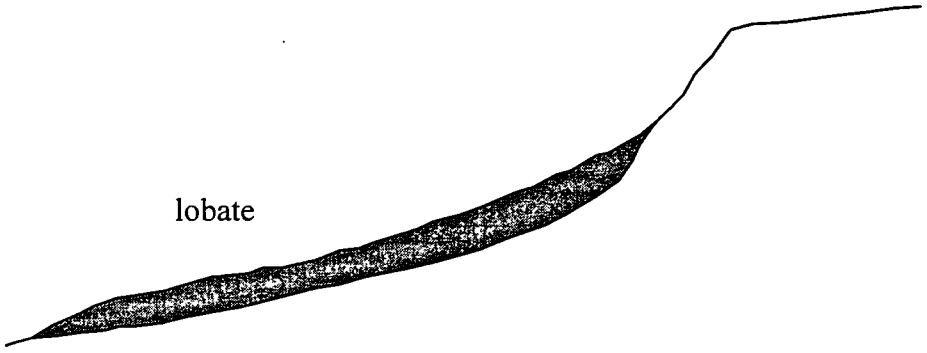

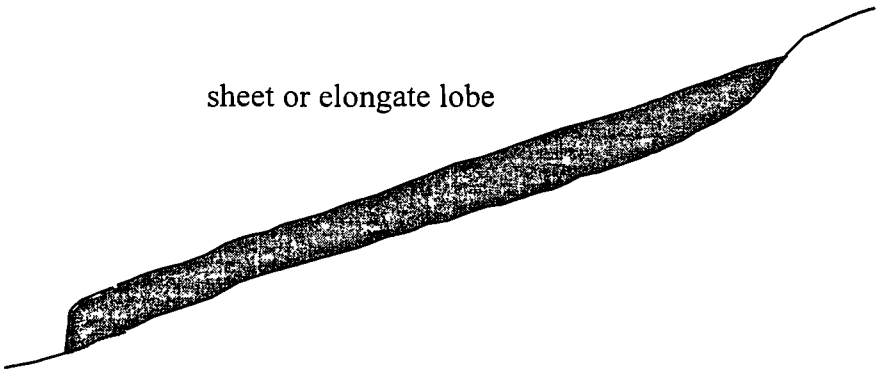

b) mudslides

Figure 1.8 Examples of landslide types (after Hutchinson, 1988)

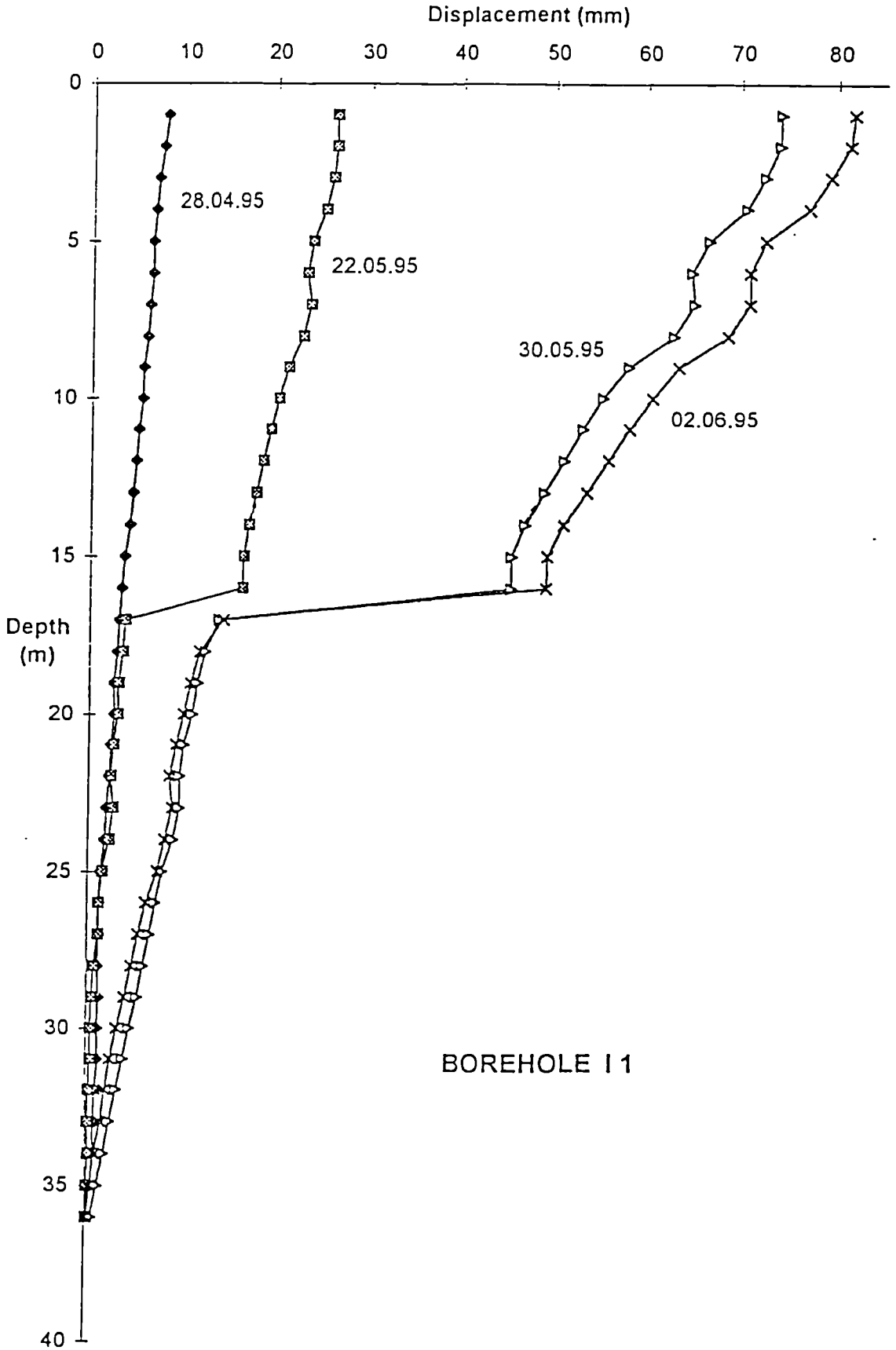

Figure 1.9 Results of the inclinometer measurements in borehole I1 (after Wasowski and Lasorsa, 1995)

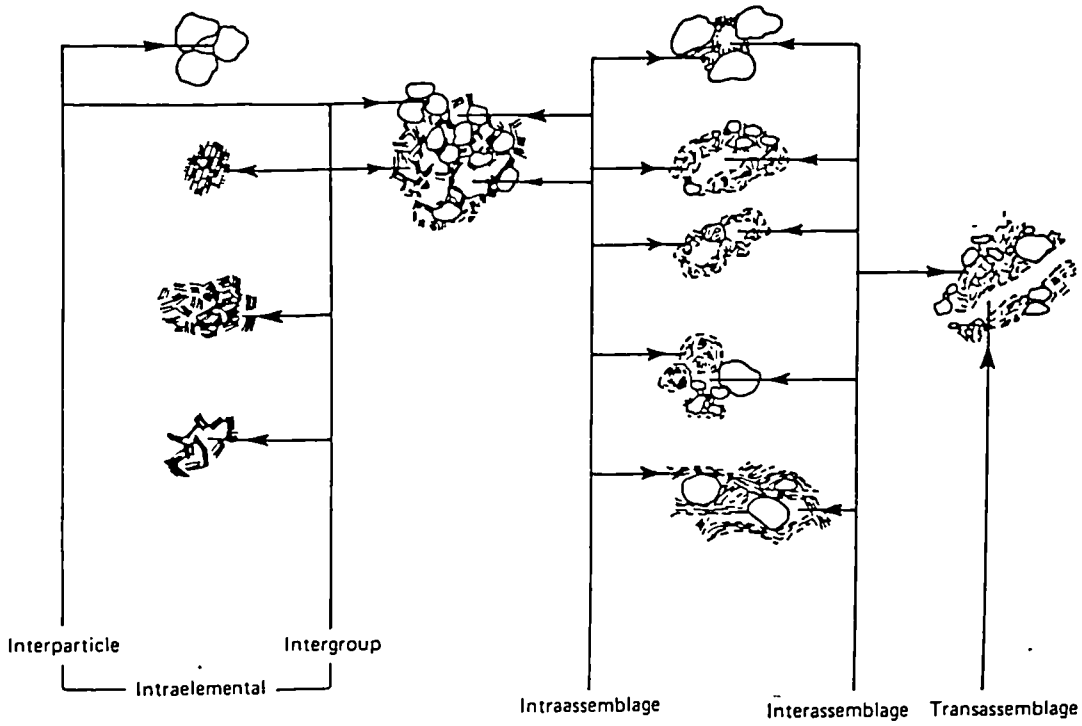

Figure 2.1 Schematic representation of pore space types (after Collins and McGown, 1974)

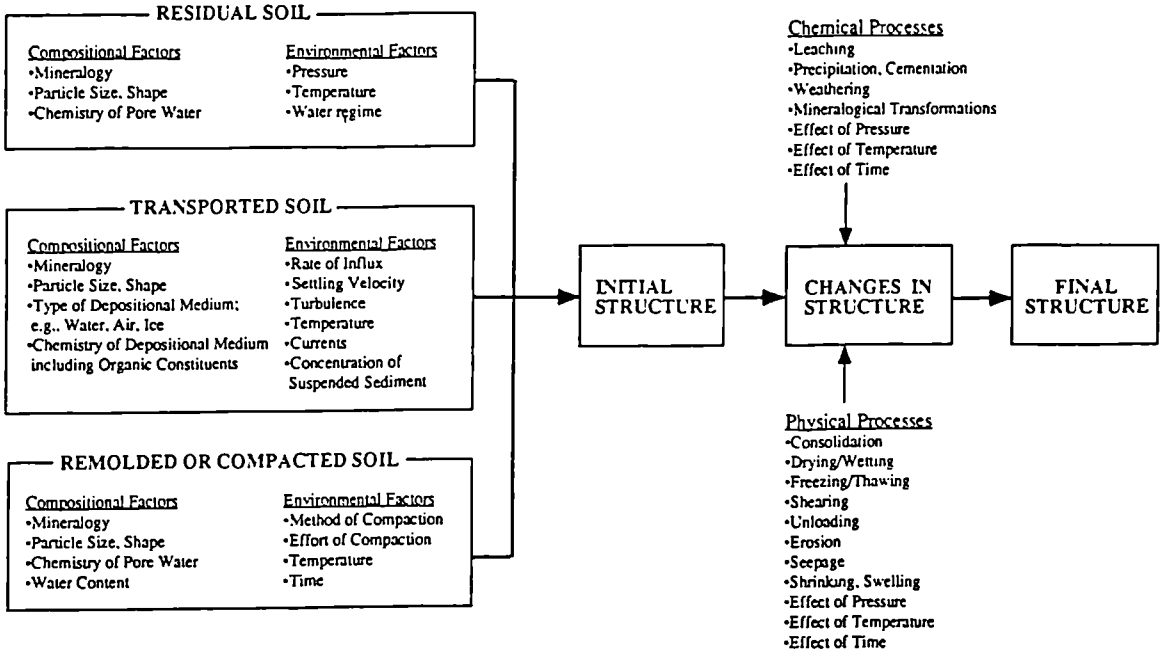

Figure 2.2 Structure determining factors and processes (after Mitchell, 1993)

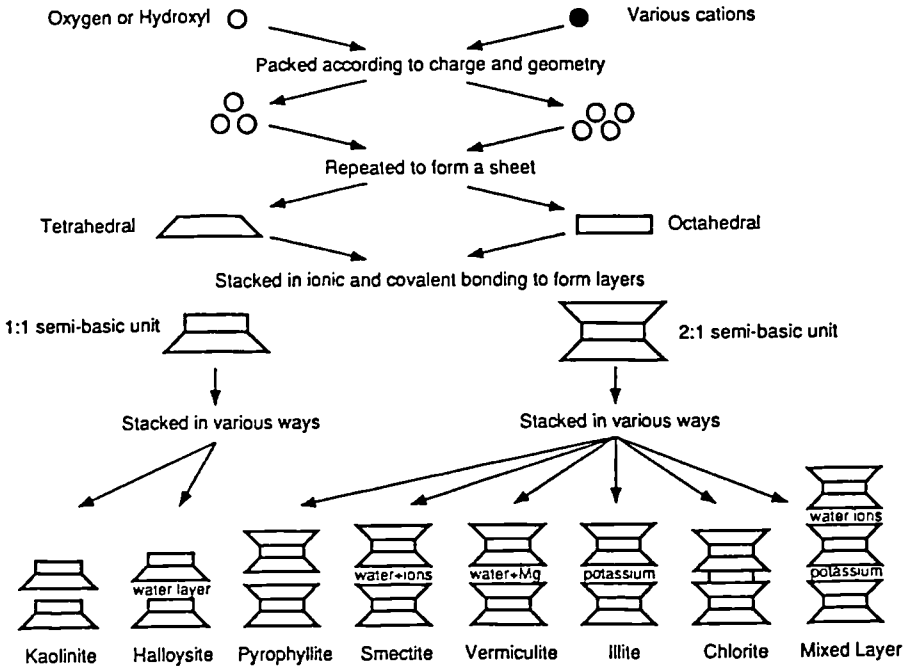

Figure 2.3 Synthesis pattern for the clay minerals (after Mitchell, 1993)

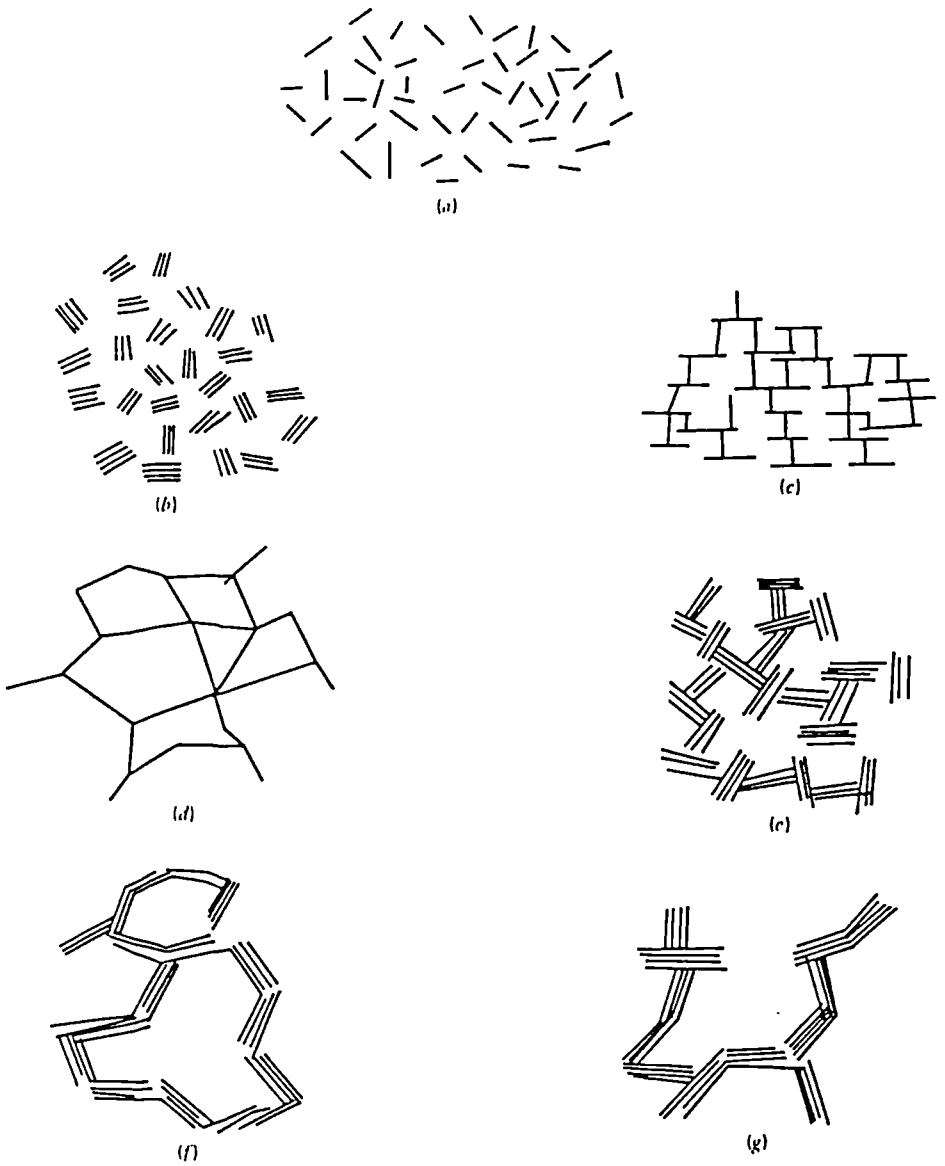

Figure 2.4 Modes of particle associations in clay suspensions: a) dispersed and deflocculated; b) Aggregated and dispersed; c) Edge-to-face flocculated but dispersed; d) Edge-to-edge flocculated but dispersed; e) Edge-to-edge flocculated and aggregated; f) Edge-to-edge flocculated and aggregated; g) Edge-to-face and edge-to-edge flocculated and aggregated. (after van Olphen, 1977).

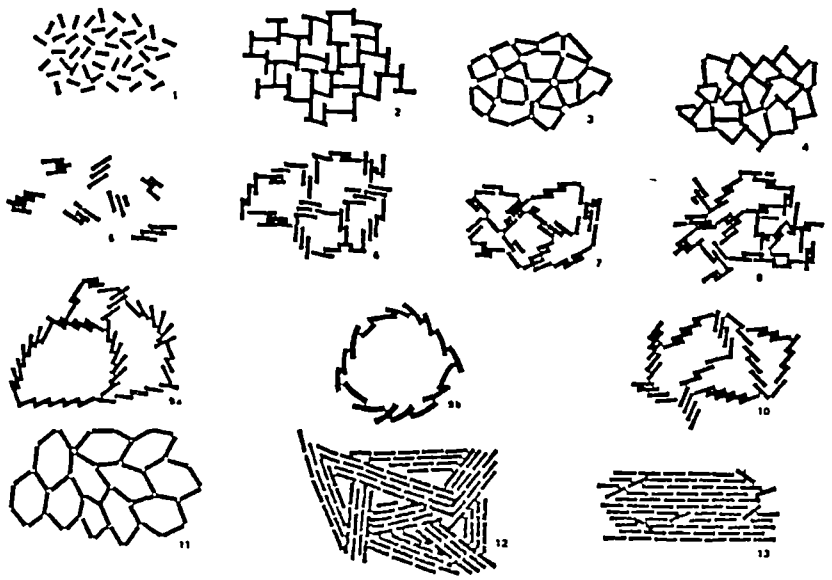

Figure 2.5 Summary of the principal elementary structures of sedimented clays: 1) dispersed and deflocculated; 2) Edge-to-face flocculated and dispersed; 3) Edge-to-edge flocculated and dispersed; 4) Edge-to-face and edge-to-edge flocculated and dispersed; 5) Aggregated and deflocculated. 6) Edge-to-face flocculated and aggreggated; 7) Edge-to-edge flocculated and aggreggated; 8) Edge-to-face and edge-to-edge flocculated and aggregated; 9a) Cardhouse fabric (kaolinite), 9b) Cardhouse fabric (illite), 10) Bookhouse fabric, 11) Honeycomb fabric, 12) Turbostatic fabric, 13) Stack fabric. (after Sfrondini, 1975)

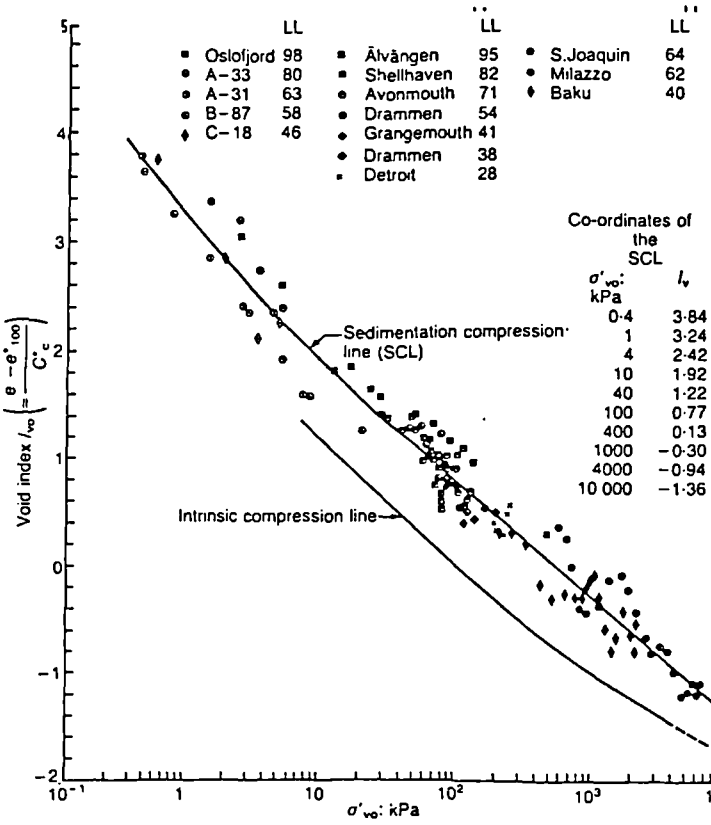

Figure 2.6 The sedimentation compression line (SCL) for normally consolidated clays (after Burland, 1990).

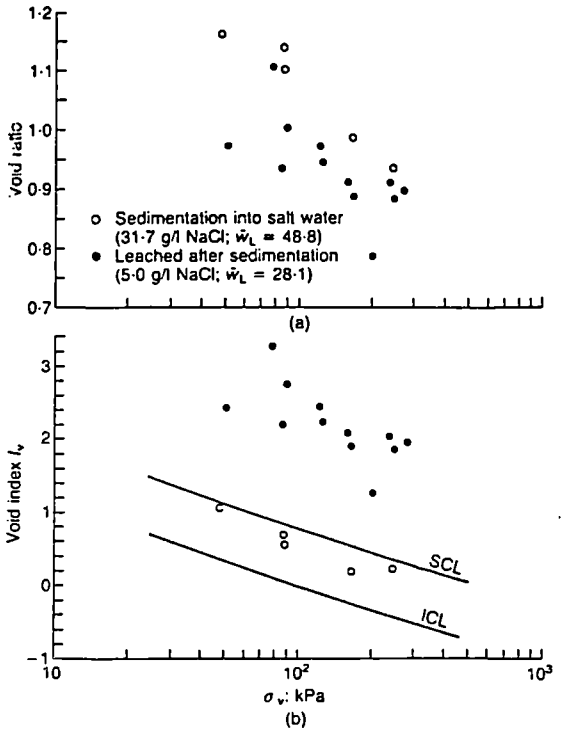

Figure 2.7 The sedimentation compression behaviour of a laboratory sedimented marine clay (after Burland, 1990; data from Bjerrum and Rosenqvist, 1956).

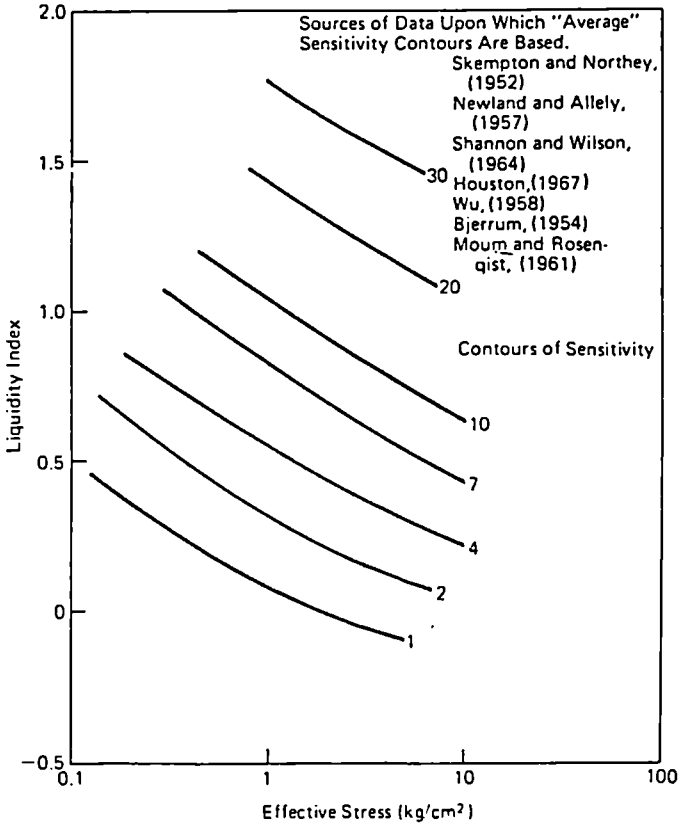

Figure 2.8 General relationships between sensitivity, liquidity index and effective stress (after Mitchell, 1993).

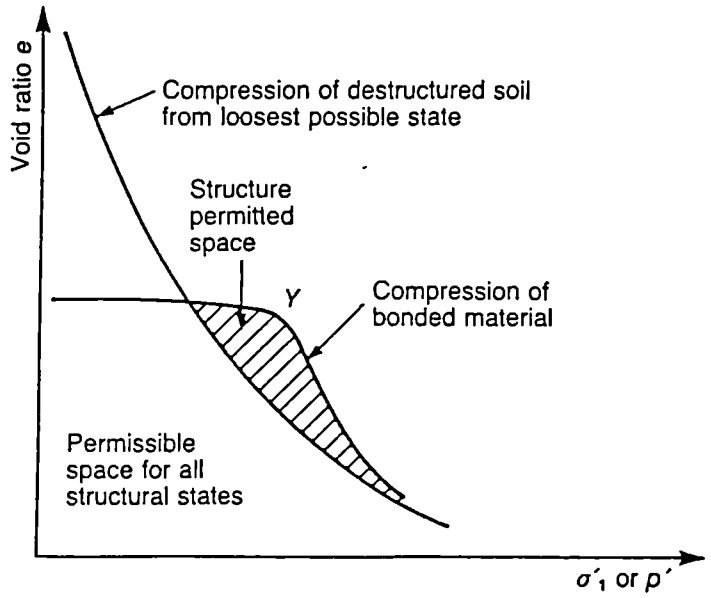

Figure 2.9 A schematic diagram of the compression of 'structured' and 'destructured' soils in the oedometer test (after Leroueil and Vaughan, 1990).

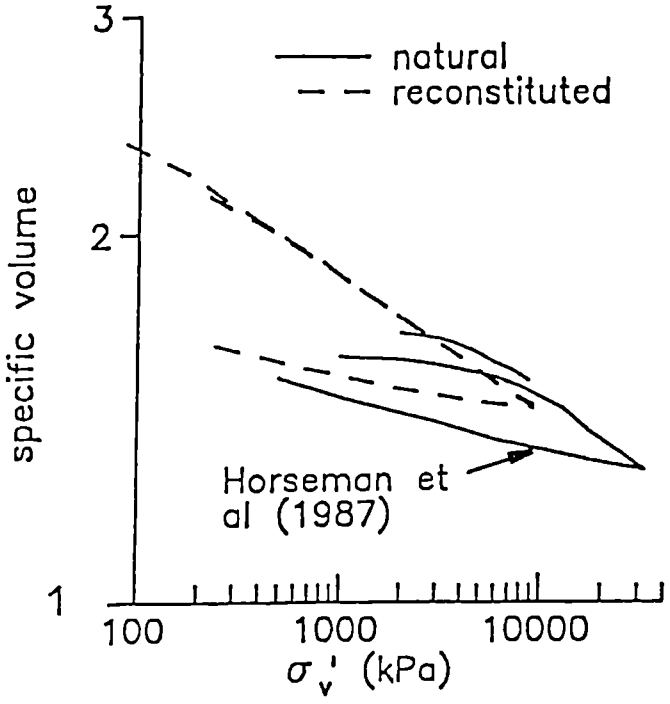

Figure 2.10 One-dimensional compression of Boom Clay (after Coop et al. 1995 and Zeniou, 1993).

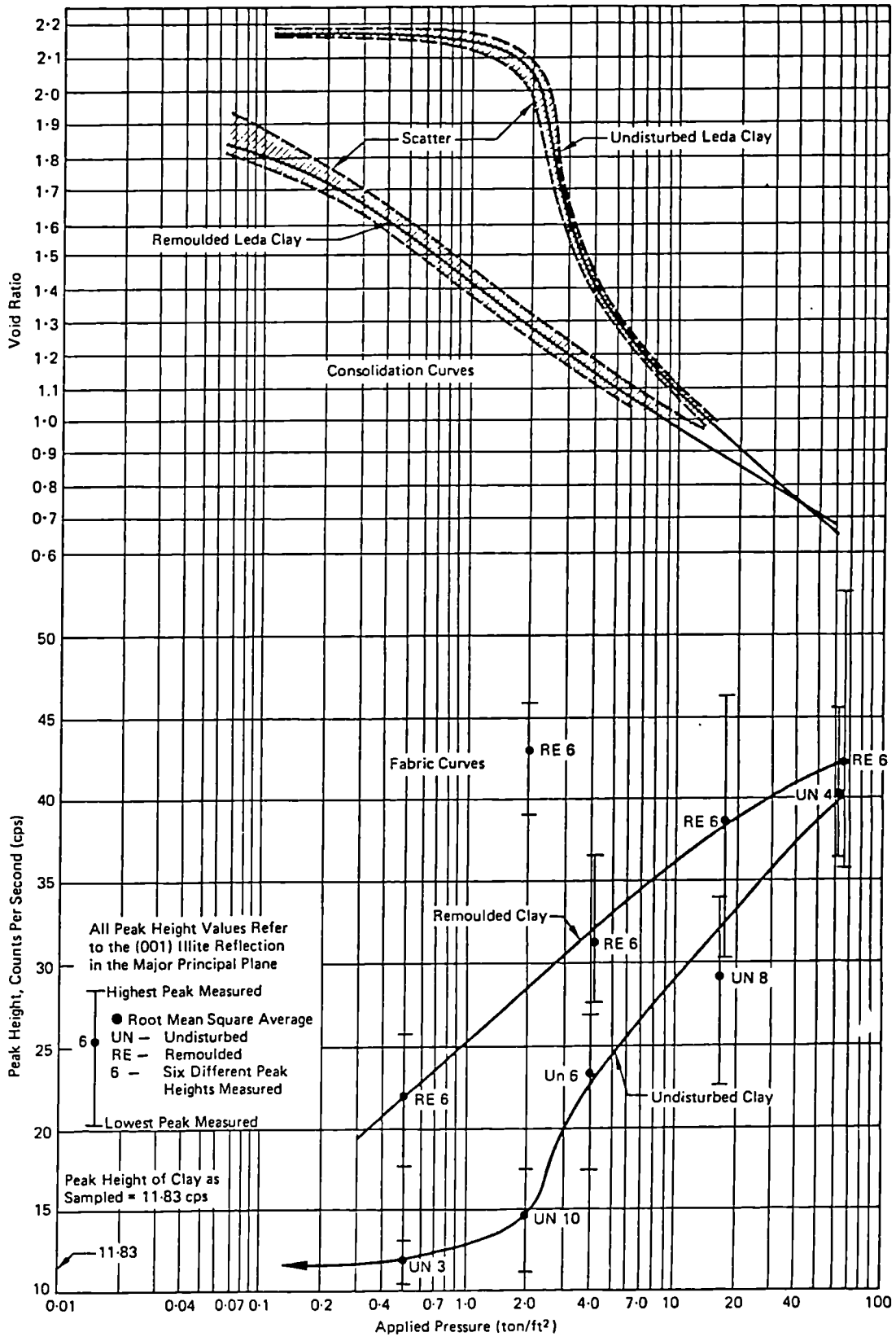

Figure 2.11 Clay particle orientation produced by anisotropic consolidation of undisturbed and remoulded Leda clay (after Quigley and Thompson, 1966).

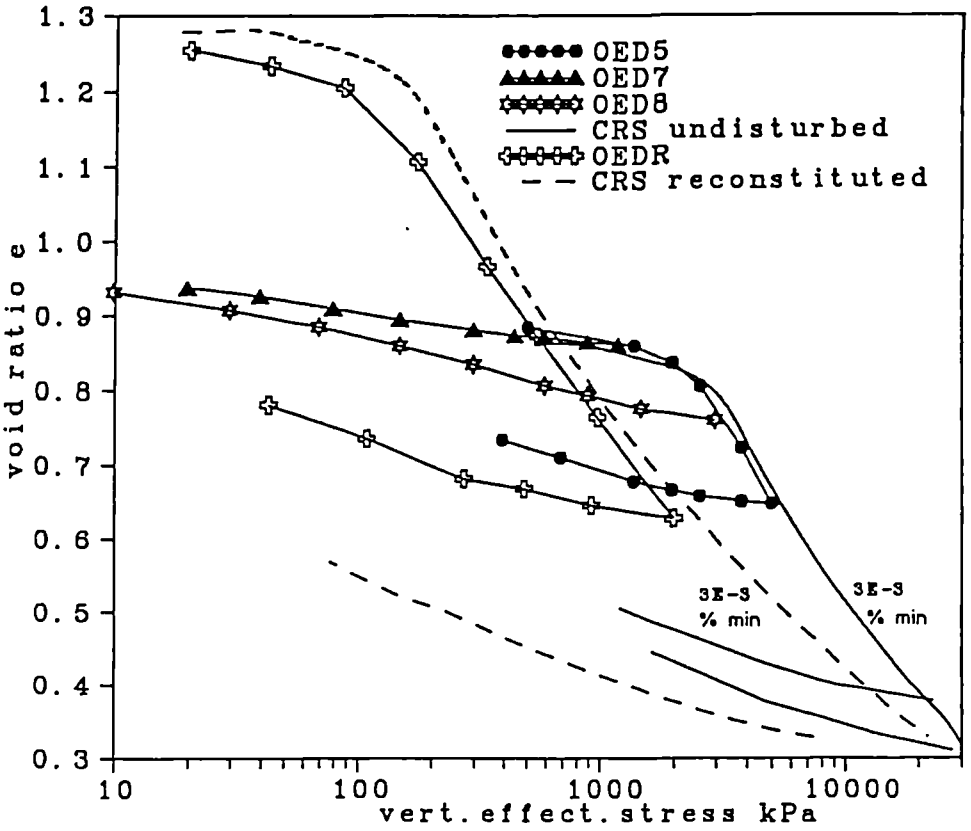

Figure 2.12 Oedometric compression curves for natural and reconstituted Pappadai clay (after Cotecchia, 1996) (OED5, 7 and 8 are natural samples; OEDR is a reconstituted sample)

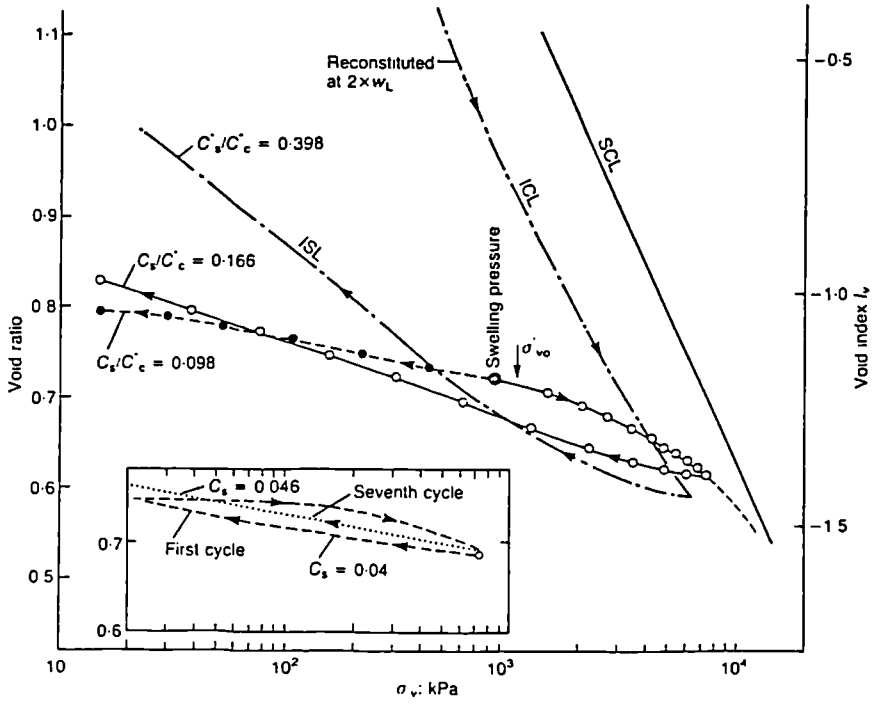

Figure 2.13 Oedometer tests on block samples of Gault clay from the Ely-Ouse tunnel (after Samuels, 1975). (ISL - Intrinsic swelling line)

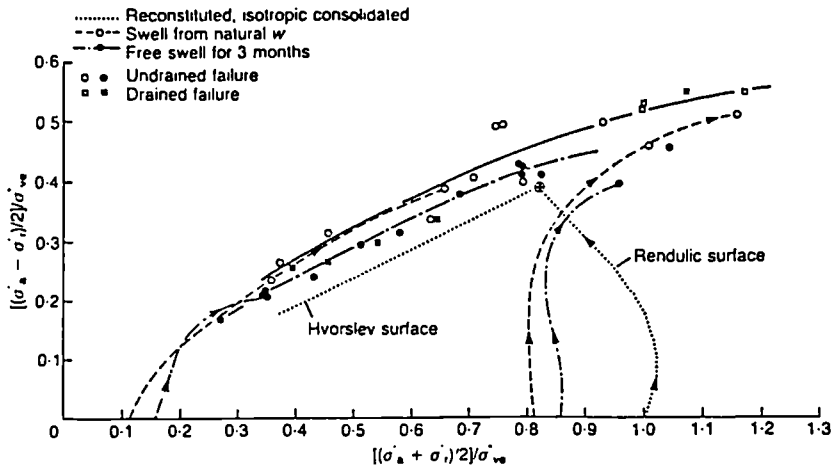

Figure 2.14 Results of triaxial compression tests on Todi clay normalised by the equivalent pressure at failure (after Burland, 1990).

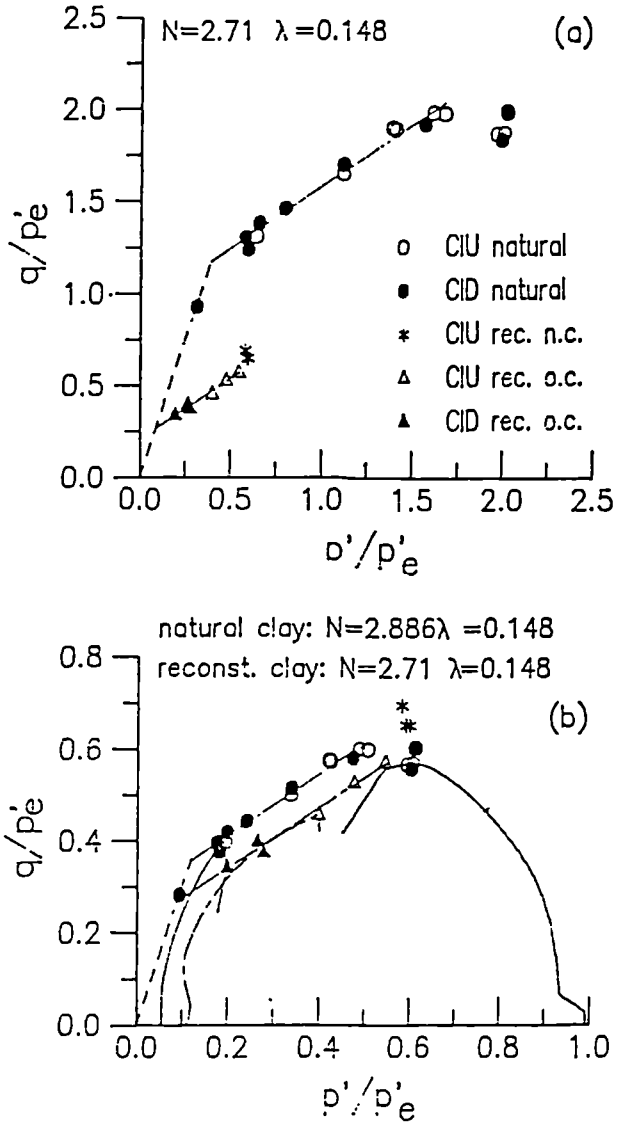

Figure 2.15 Strength envelopes for samples of Vallerica clay normalised by the equivalent consolidation pressure p'_e at failure: a) all samples normalised with respect to the reconstituted normal compression line. b) samples normalised with respect to the appropriate ncl (after Rampello et al. 1993).

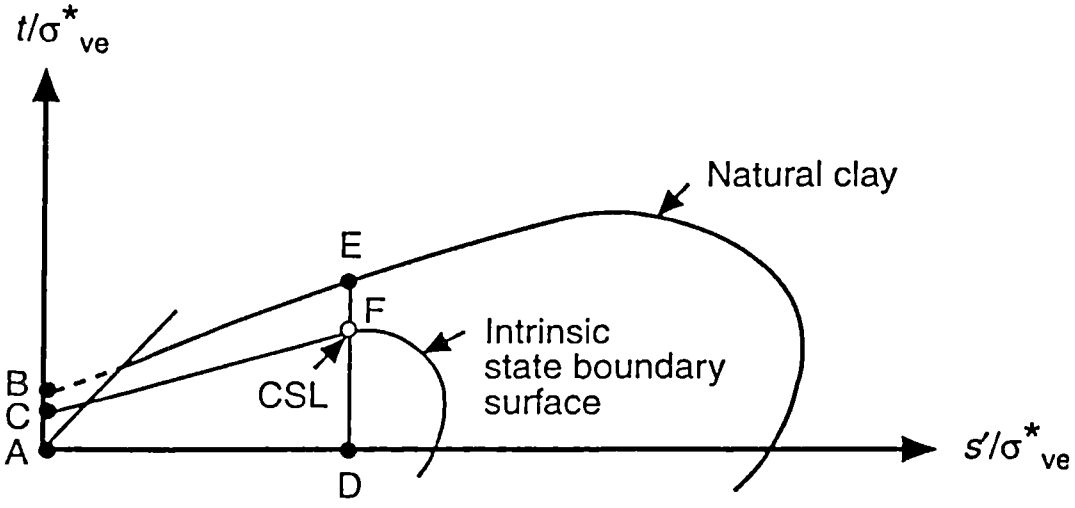

Figure 2.16 Comparison of the natural and intrinsic state boundary surfaces showing increased resistance of the natural clay to compression and swelling (after Burland et al. 1996).

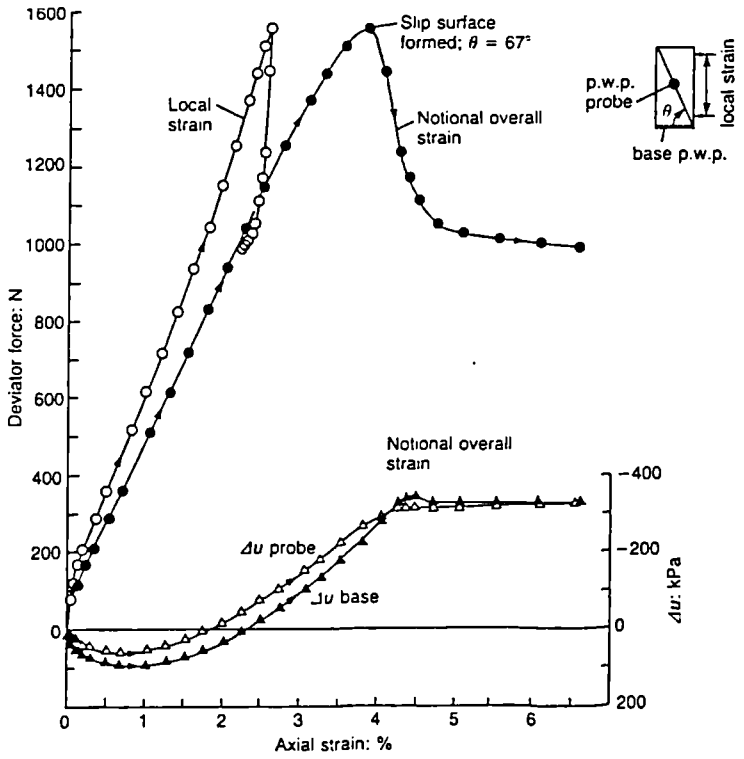

Figure 2.17 An unconsolidated undrained triaxial test on Todi clay showing post-rupture behaviour (after Burland, 1990).

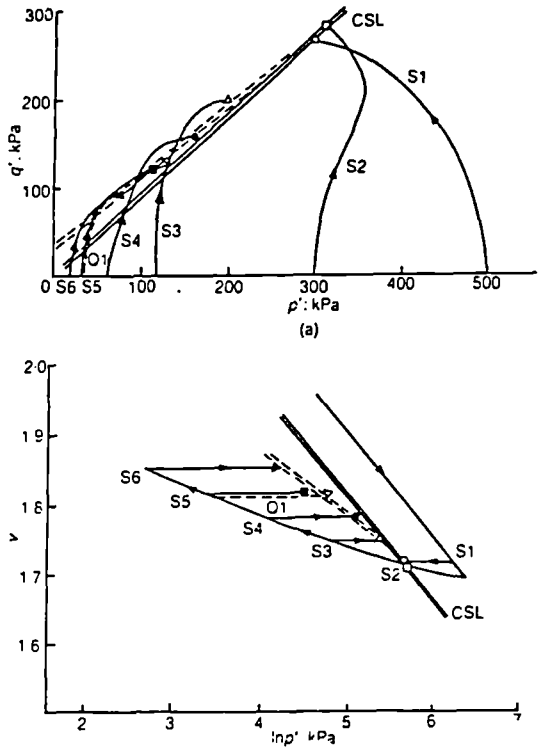

Figure 2.18 Stress and state paths for slow undrained tests on reconstituted samples (after Atkinson and Richardson 1987).

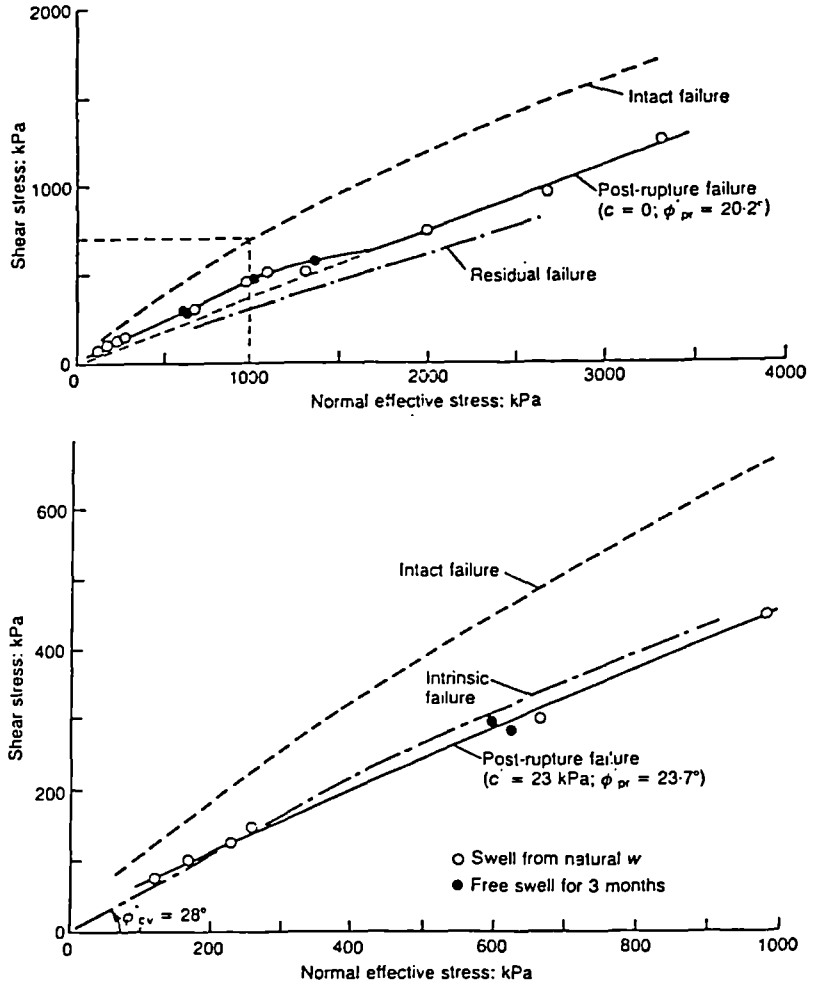

Figure 2.19 The post-rupture failure envelope for a) high pressures and b) low to medium pressures compared with intact, intrinsic and residual failure lines (after Burland, 1990).

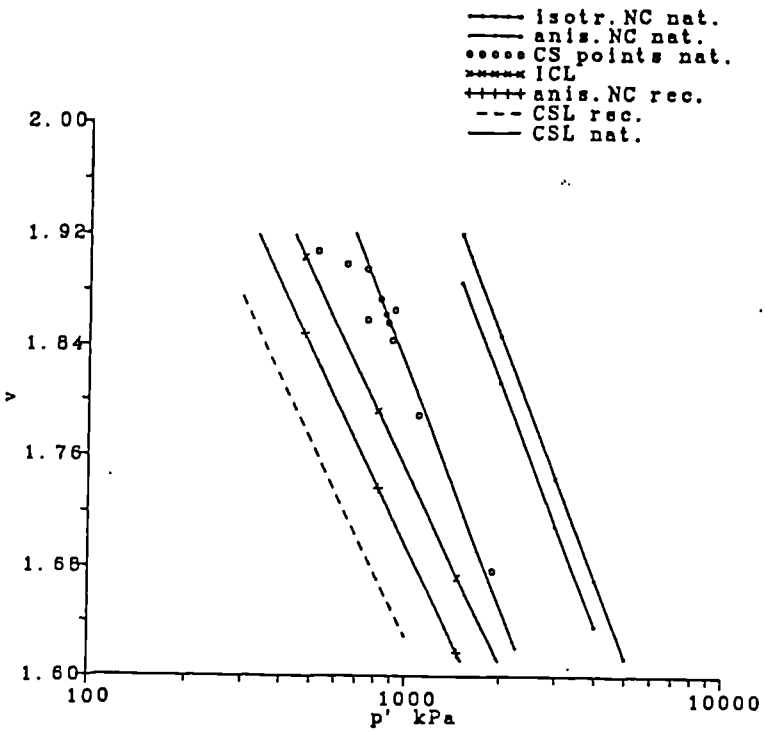

Figure 2.20 Isotropic and K_0 normal compression lines and critical state lines of the natural and reconstituted Pappadai clay (after Cotecchia, 1996).

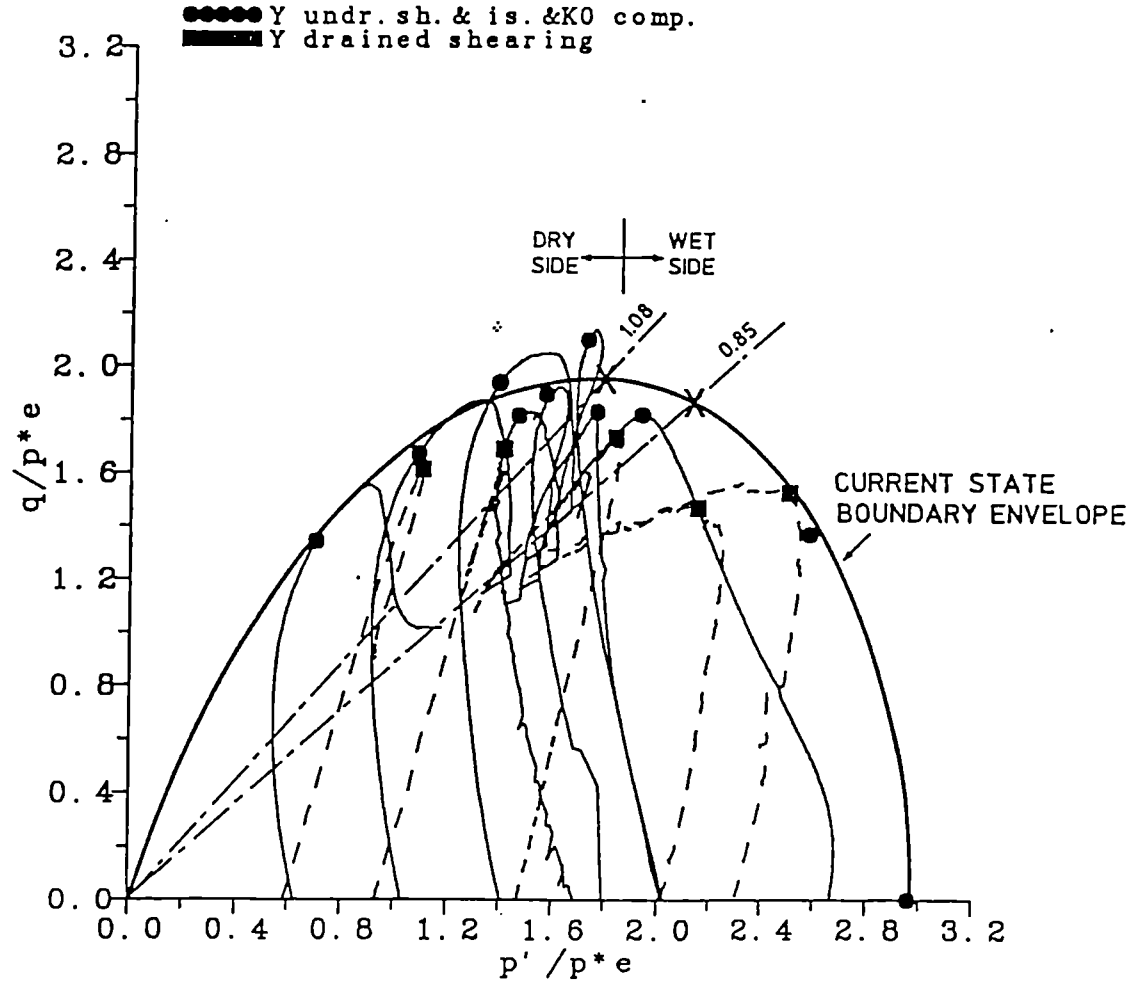

Figure 2.21 Normalised stress paths of the natural Pappadai clay consolidated to states before isotropic yield, showing the dry and wet sides of the natural clay framework of behaviour (after Cotecchia, 1996).

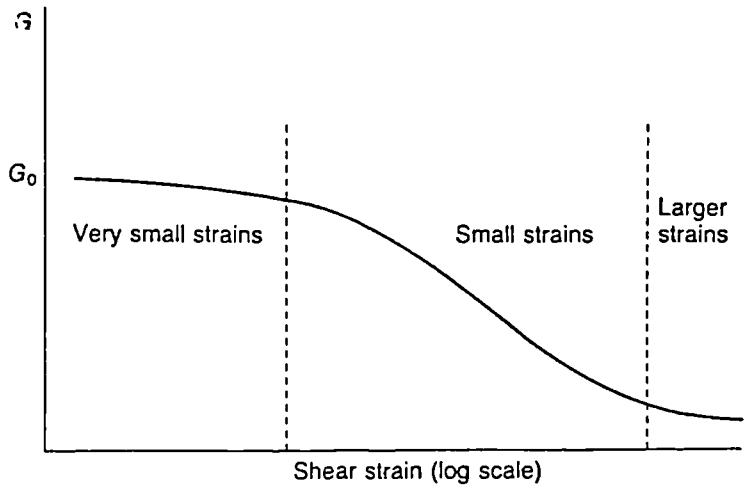

Figure 2.22 Schematic diagram showing the typical variation of shear stiffness with shear strain (after Atkinson and Sallfors, 1992).

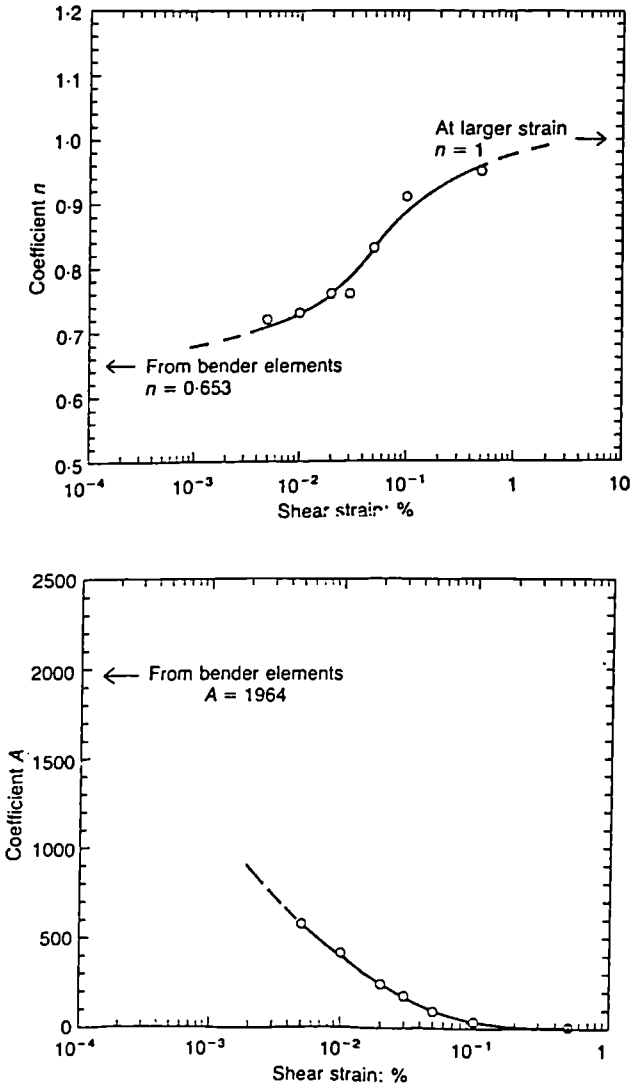

Figure 2.23 Variation of stiffness parameters A and n with strain magnitude (after Viggiani and Atkinson, 1993).

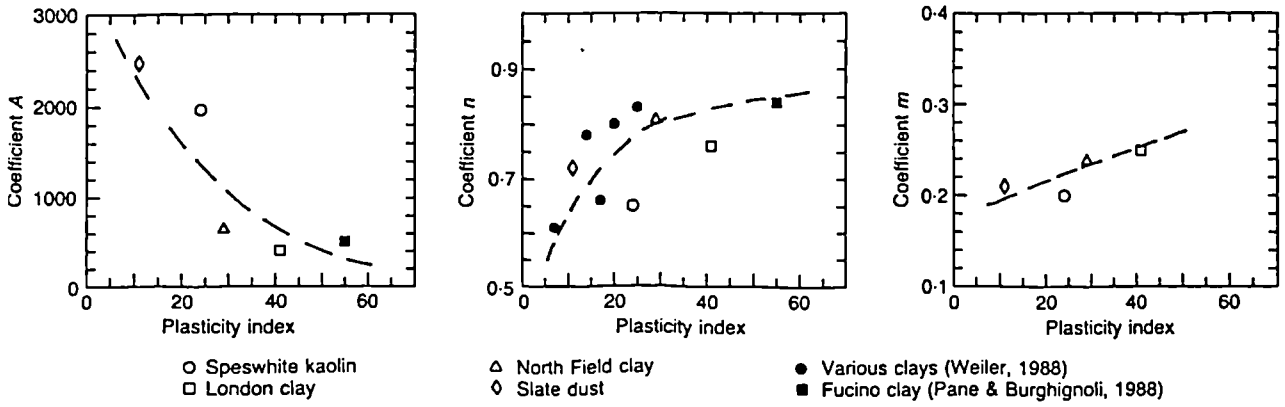

Figure 2.24 Variation of stiffness parameters A, n and m for G_{max} with plasticity index (after Viggiani and Atkinson, 1995).

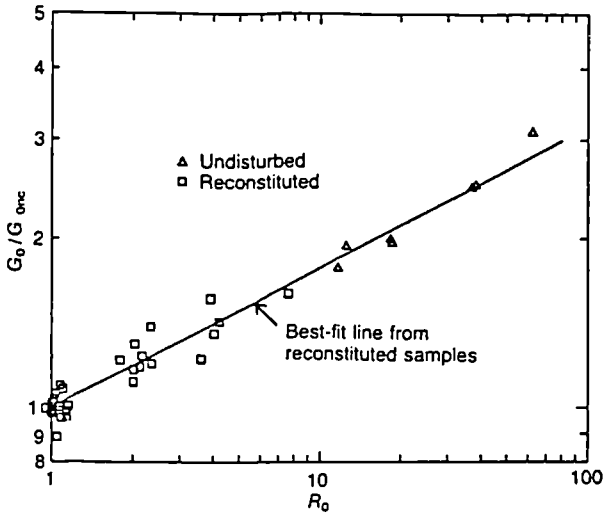

Figure 2.25 Variation of normalised shear modulus with overconsolidation ratio for undisturbed and reconstituted samples of London clay (after Viggiani and Atkinson, 1995)

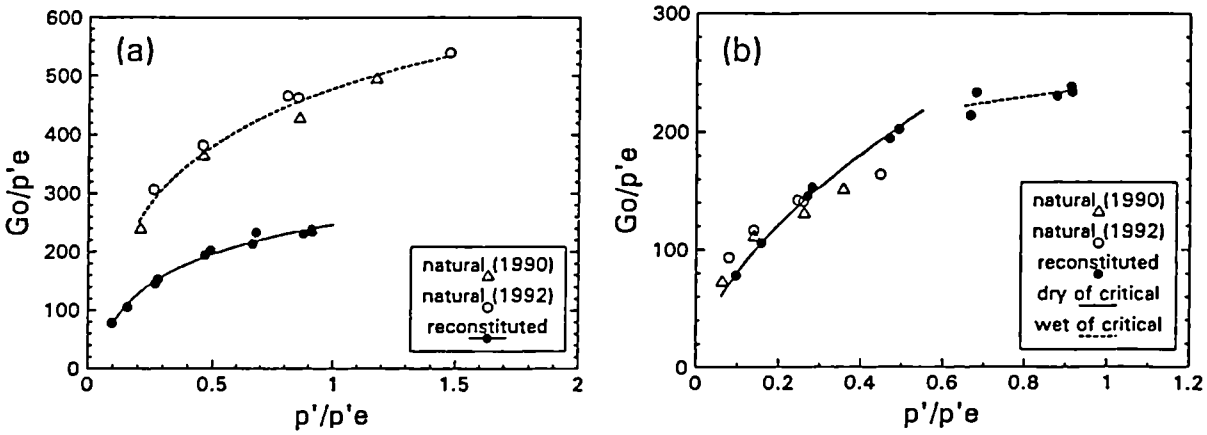

Figure 2.26 The shear modulus (G_0) normalised by the intrinsic (a) and the appropriate (b) equivalent pressure for natural and reconstituted samples of Vallerica clay. (after Rampello and Silvesti, 1993)

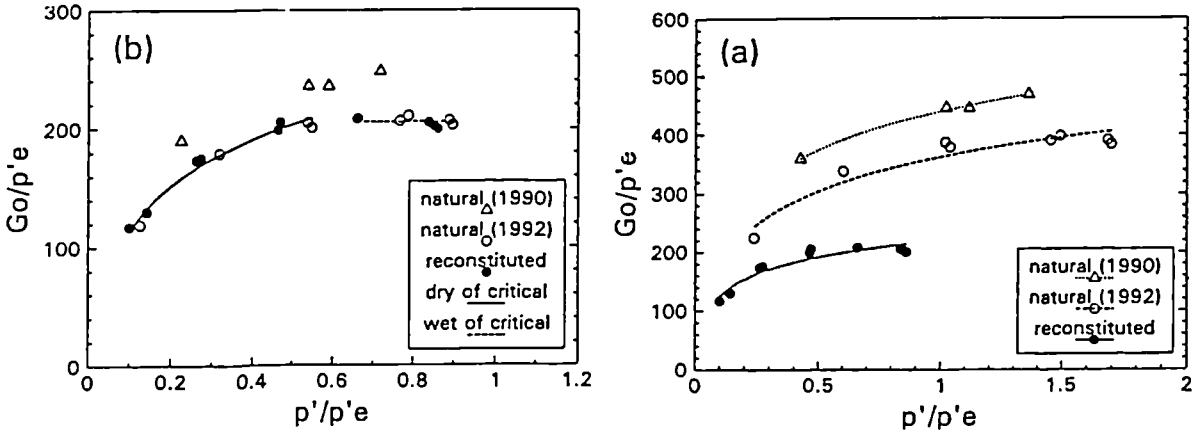

Figure 2.27 The shear modulus (G_0) normalised by the intrinsic (a) and the appropriate (b) equivalent pressure for natural and reconstituted samples of Pietrafitta clay. (after Rampello and Silvesti, 1993)

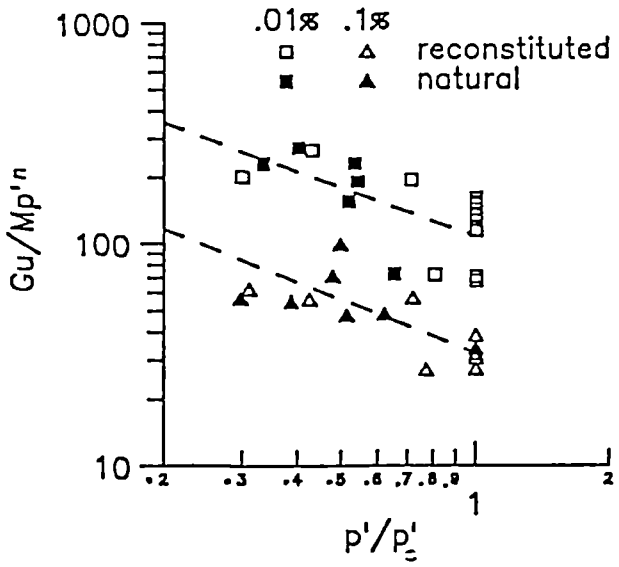

Figure 2.28 Undrained shear modulus of intact and reconstituted Boom clay (after Coop et al. 1995).

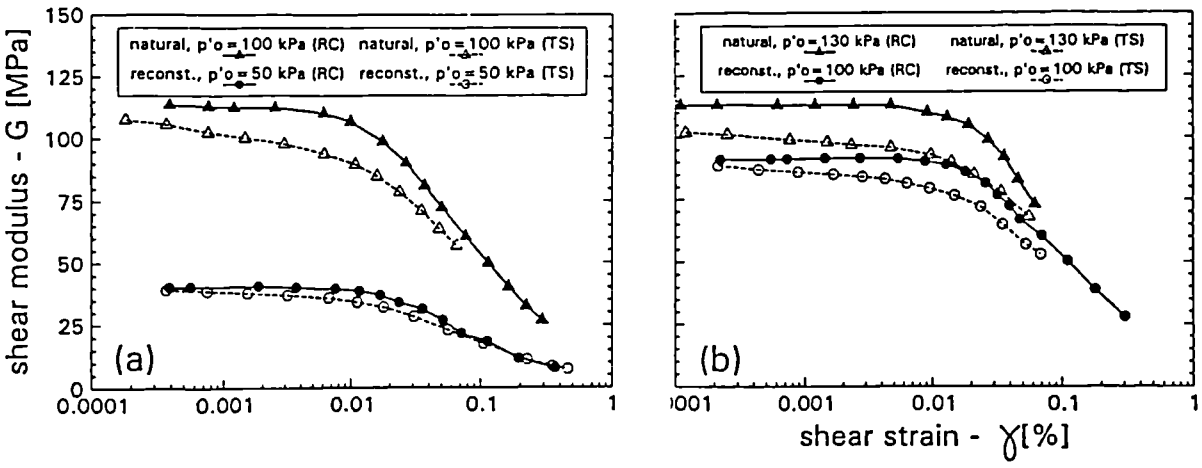

Figure 2.29 Variation of shear modulus with shear strain for (a) Vallerica clay and (b) Pietrafitta clay (after Rampello and Silvestri, 1993).

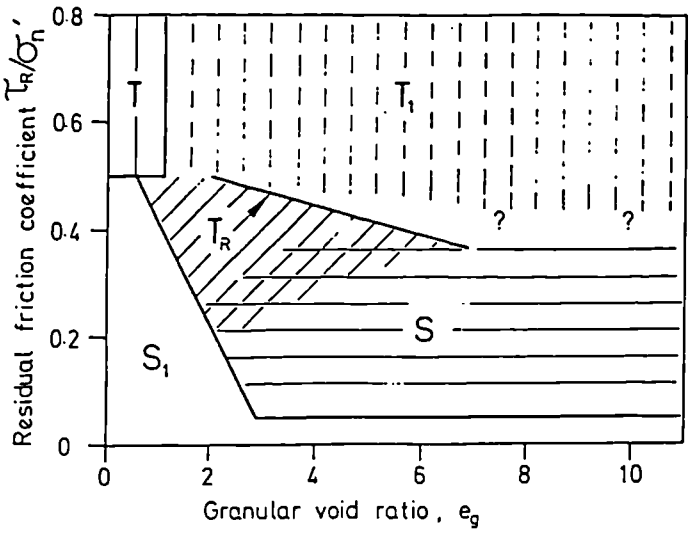

T	Turbulent shear
T_1	Turbulent shear for platy particles if $\phi_\mu > \phi'_{cv}$. Also for soils containing non-platy clay particles if these are excluded from the volume of rotund particles in calculating e_g
S	Sliding shear
S_1	Possible sliding shear when soil is failed against a smooth interface
T_R	Transitional shear. Part turbulent and part sliding. Location of a particular soil within this zone depends on residual friction factors of rotund and platy particles, tested separately, and on soil grading. Platy clay particles mixed with well-graded sand/silt rotund particles fall to left of zone. Gap graded fine clay and sand mixtures fall further right in direction of arrow. Mixtures of platy and rotund particles of comparable size fall to right of zone

Figure 2.30 Residual strength failure mechanisms as a function of particle packing (after Lupini et al. 1981).

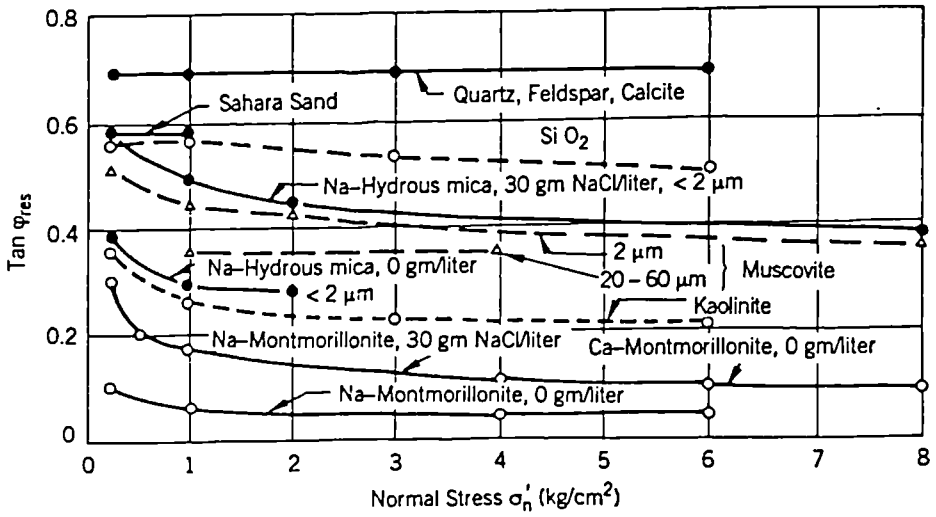

Figure 2.31 Variation in residual friction angle with normal stress for different clay minerals (after Kenney, 1967).

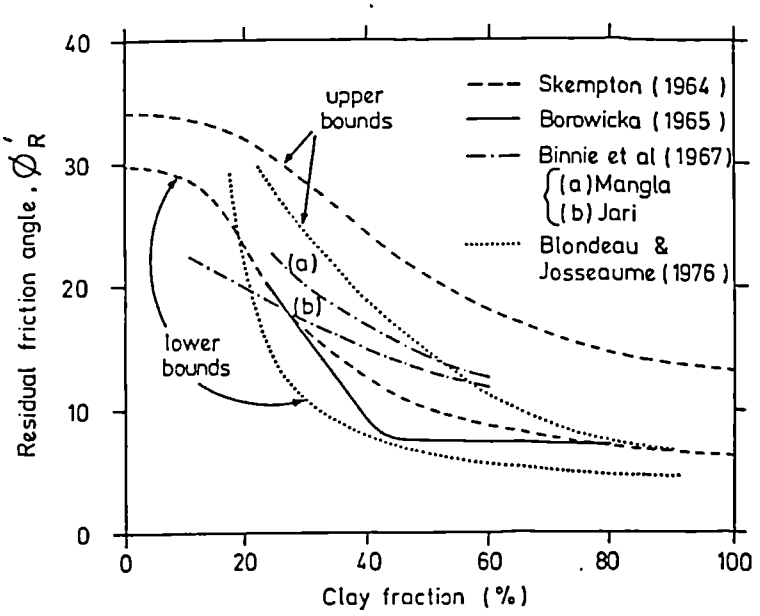

Figure 2.32 Correlations of residual friction angle with clay fraction (after Lupini et al., 1981).

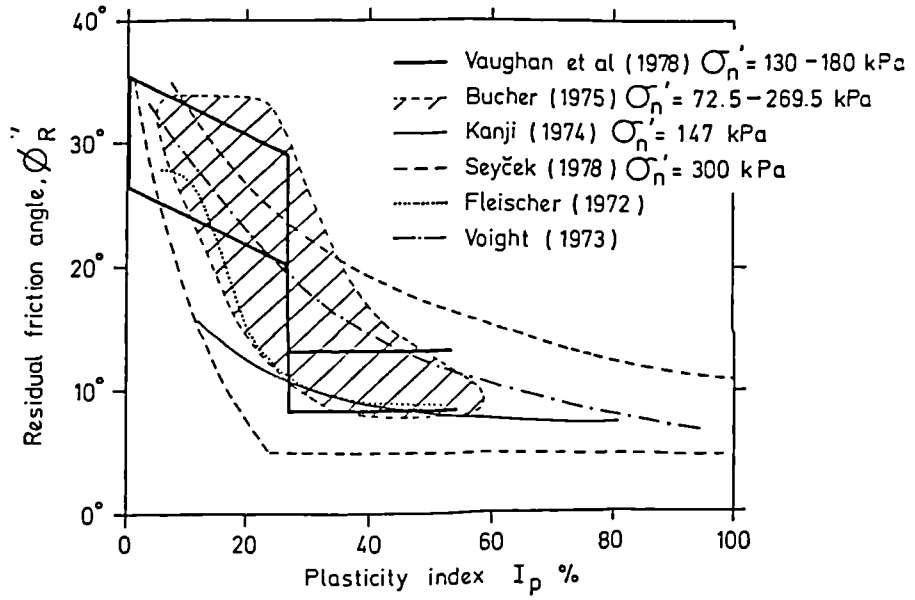

Figure 2.33 Correlations of residual friction angle with plasticity index (after Lupini et al., 1981).

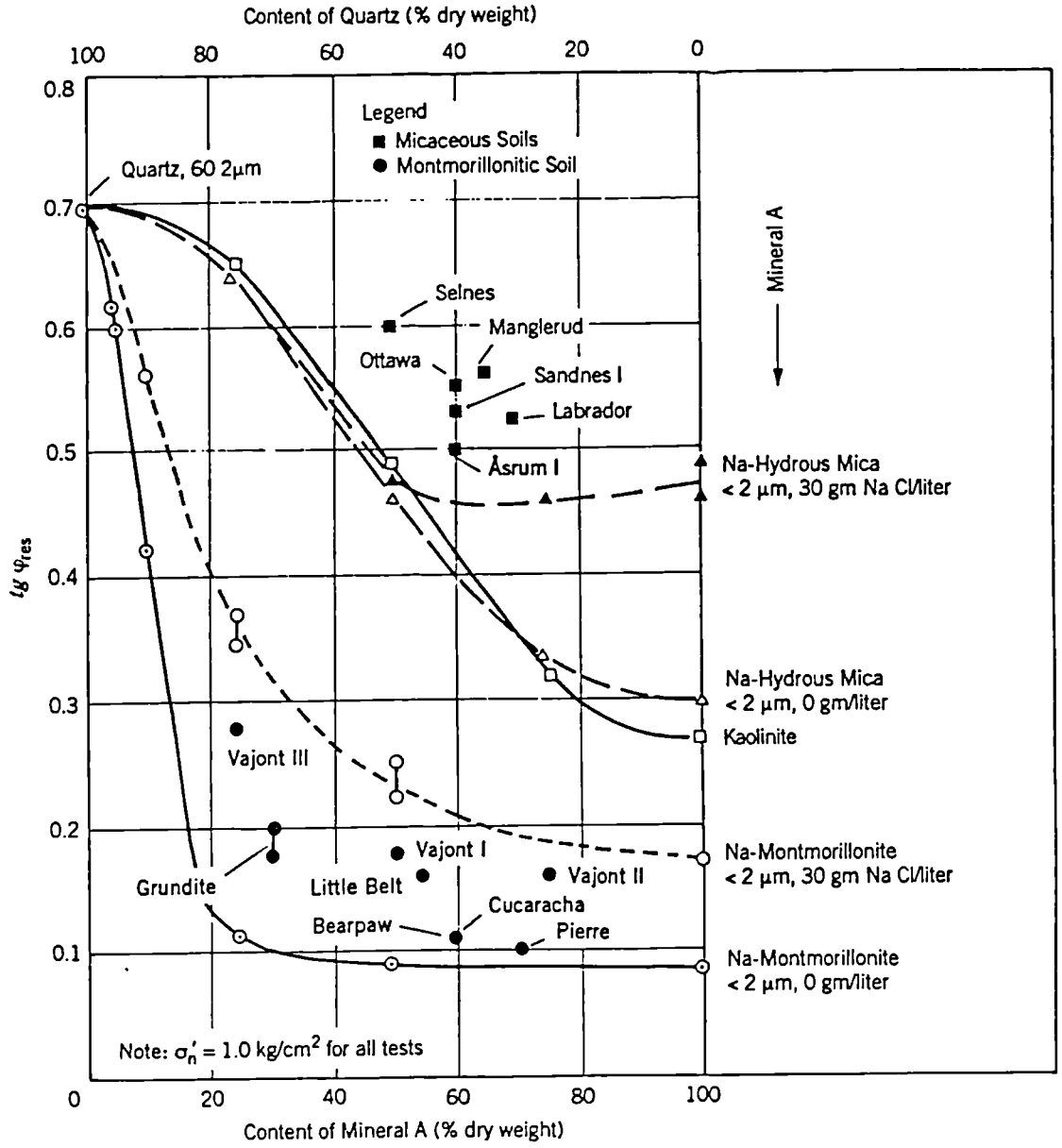

Figure 2.34 Residual friction angles for clay-quartz mixtures (after Kenney, 1967).

UNITS	FORMATION	LOCALITY	PRINCIPAL LITHOFACIES ASSOCIATION	TECTONIC ARRANGEMENT AND STRUCTURES	TYPE OF COMPL.
LIGURIDES	Palombini Shales	Campiano (Berry et al. 1977a)	alternating layers of rock shales and siliceous fine-grained limestones with rare sandstone layers (limestone-shale ratio ~ 1).	zones of ordered layers associated with zones characterised by disarrangement of layers or completely chaotic structures - presence of faults.	B_1 B_2 B_3
	Black Shales	Sinni River Valley (Beomonte and Cavallo, 1977; Cotecchia and Del Prete, 1977)	prevailing rock-shale layers with limestone and sandstone layers.	same as above.	B_1 B_2 B_3
SICILIDES	Variegated Shales (Abruzzo-Molise Unit)	Trigno River Valley (D'Elia 1977)	clay-shales with rare interspersed layers and blocks of limestone and sandstone.	disarranged to chaotic structure formed by a mass of sheared clay-shales with occasional ordered zones.	B_2 B_3
	Variegated Shales (Sannio-Irpinia Unit)	Fiumarella River Valley and Osento River Valley (Evangelista et al. 1977)	clay-shales with rare interspersed layers and blocks of limestone and sandstone.	chaotic structure formed by a mass of sheared clay-shales.	B_3

Figure 2.35 Summary of calcareous-pelitic and pelitic formations (after A.G.I. 1979).

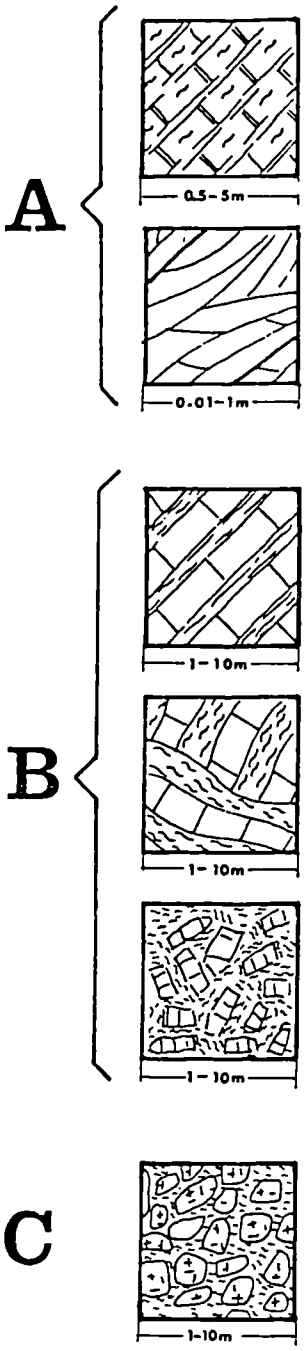

A_1 Layered clay shales and shales (with or without fissility more or less fissurred and/or jointed; geotechnical complexity depending upon mineralogy and stress history (mainly vertical loading).

A_2 Sheared clay shales and shales; geotechnical complexity depending upon mineralogy and stress history (mainly shearing); e.g. Capo di China mudstones (D'Elia et al., 1977).

B_1 Ordered sequences of more or less fissurred and jointed layers of rock and clay or shale; complexity depending on heterogeneity, mineralogy and stress history (mainly vertical loading); e.g. Keuper marls.

B_2 Disarranged layers of rock and from highly fissurred and jointed to sheared clay or clay shale; complexity depending on heterogeneity, mineralogy and stress history (flexural, torsional and shearing loads); e.g. Panagopoula slide (Andronopoulous, 1977).

B_3 As B_2 with a chaotic structure; complexity depending upon heterogeneity, mineralogy and stress history (repeated cycles of flexural, torsional and shearing loads with large displacements); e.g. Irpinia variegated shales (Evangelista et al., 1977).

C Blocks or fragments of more or less weathered rocks in a clayey matrix of various origin; complexity depending upon heterogeneity and mineralogy; residual and colluvial soils.

Figure 2.36 Types of structural complexities (after Esu, 1977).

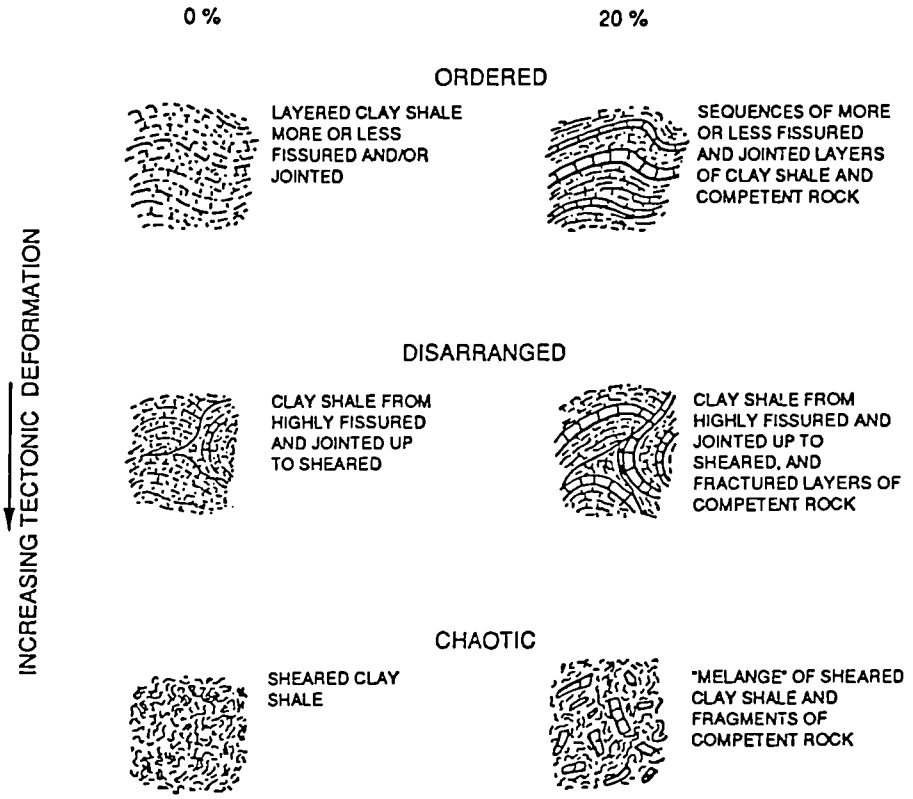

Figure 2.37 Structural features of complex clay soils (after D'Elia, 1991).

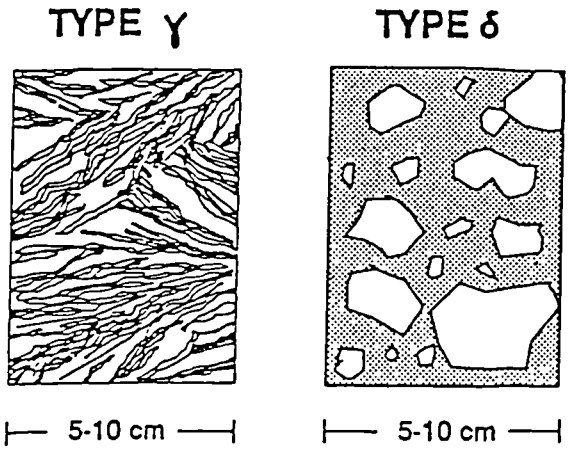

Figure 2.38 Schematic representations of intensely fissured (type γ) and softened (type δ) clay shales (after Guerriero et al., 1995).

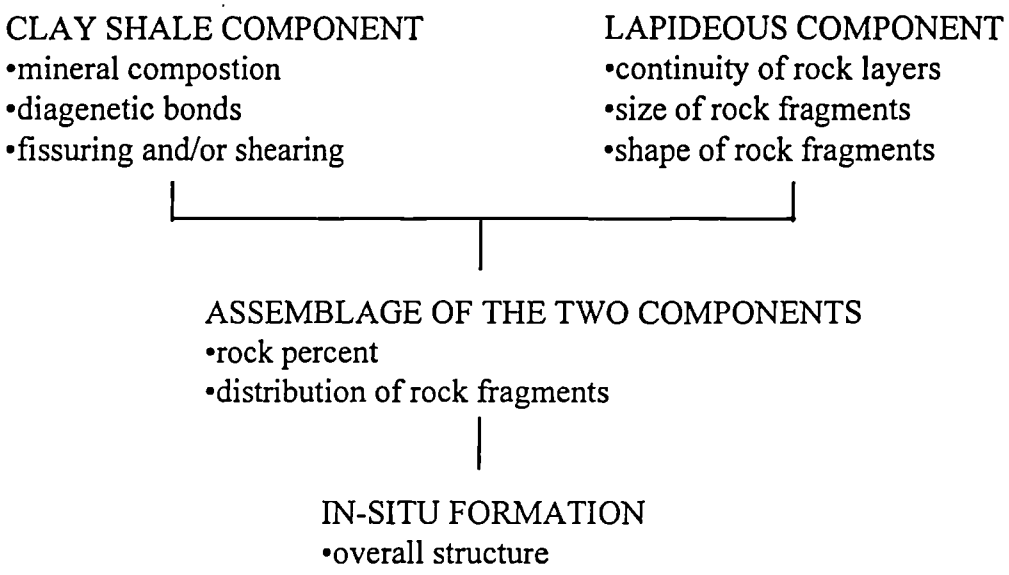

Figure 2.39 Main factors influencing the mechanical behaviour of structurally complex clays (after D'Elia, 1991).

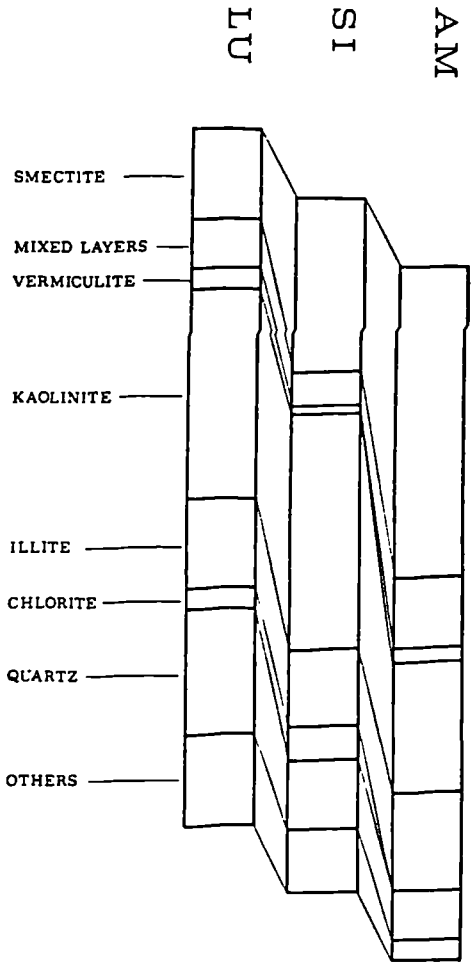

Figure 2.40 Typical mineralogies for structurally complex clays from Abruzzo-Molise (AM), Sanno-Irpinia (SI) and Lucania (LU) (after Belviso et al., 1977).

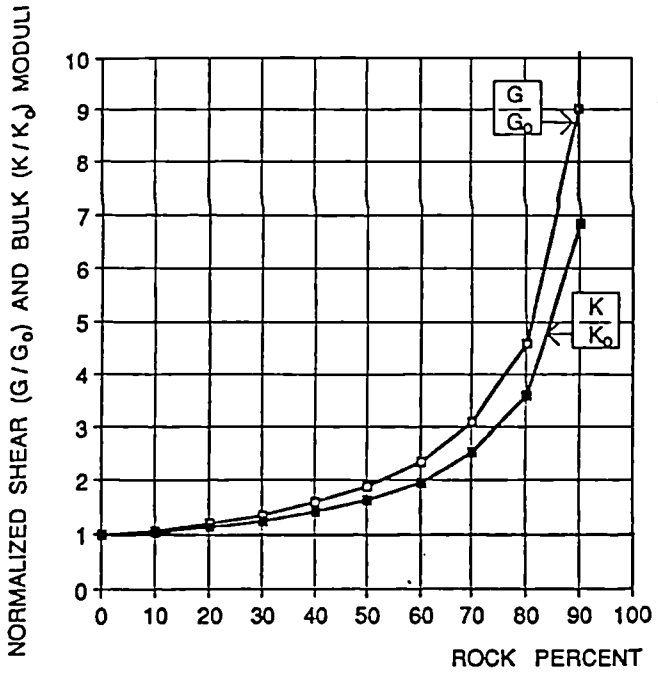

Figure 2.41 A numerical investigation of the influence of rock fraction on the stiffness of scaly clays (after D'Elia, 1991).

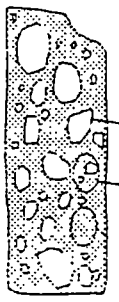

Earthflow body		1		2		3		4	
		w %	I_L%	w %	I_L%	w %	I_L%	w %	I_L%
Overall		30	-0.02	20	-0.29	22	-0.09	23	-0.26
Lithorelict		18	-0.27	13	-0.50	15	-0.31	18	-0.31
General matrix	average	40	0.19	24	-0.10	28	0.11	29	-0.04
	max	77	1.01	36	0.31	47	0.76	33	0.10
True matrix		>77		>36		>47		>33	
Formation		19	-0.25	16	-0.40	16	-0.29	18	-0.31

Figure 2.42 Water content and liquidity index measured in four earthflows in structurally complex clays (after Iaccarino et al., 1995).

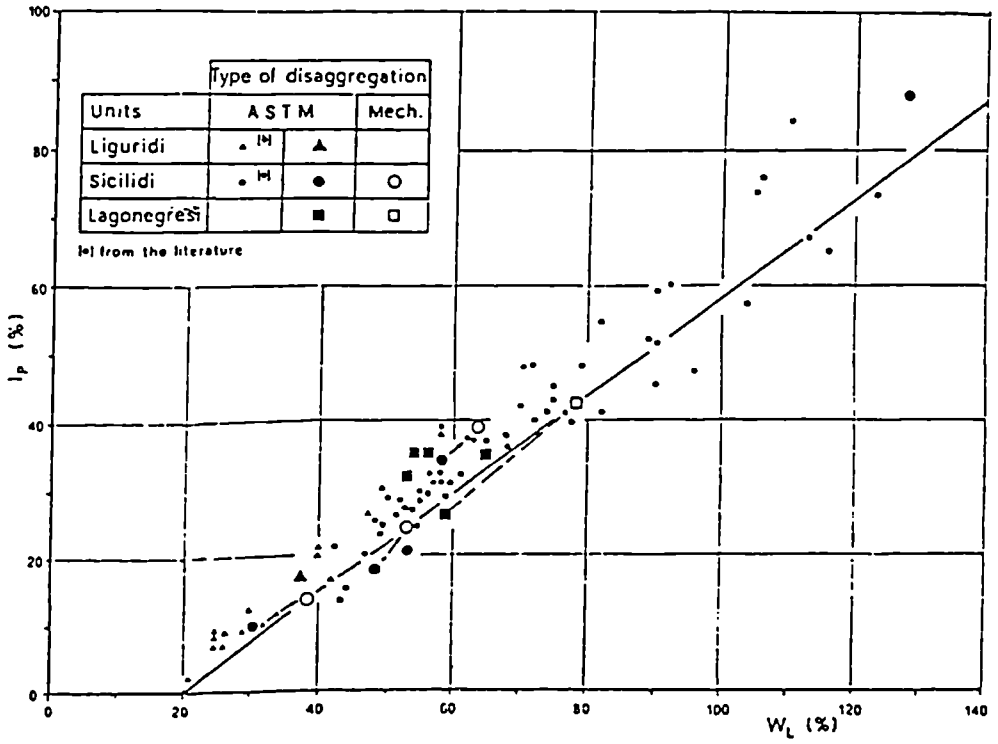

Figure 2.43 Typical plasticity chart for shales of Southern Italy showing effect of preparation method (after Santaloia, 1994 and A.G.I., 1985).

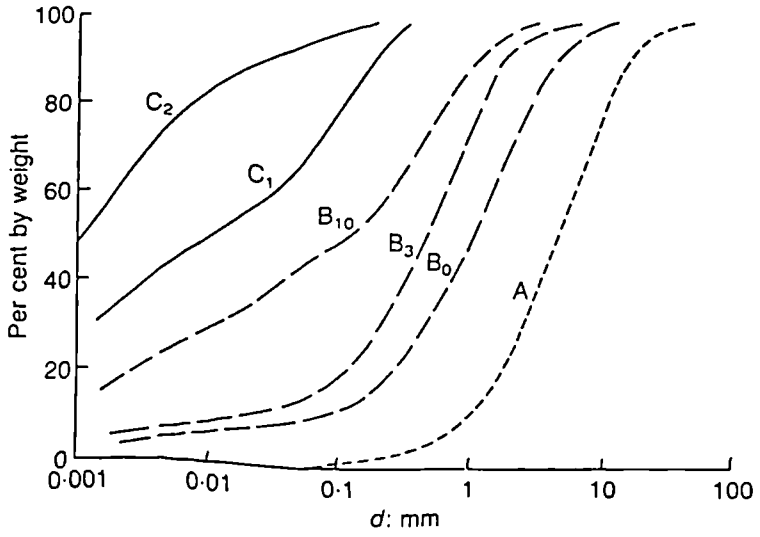

A dry sieving after rough hand separation of the single fragments
B_0 air drying and grain size analysis by sedimentation without shaking
B_3 grain size analysis as B_0 after 3 cycles of wetting and drying at 45°
B_{10} grain size analysis as B_0 after 10 cycles of wetting and drying at 45°
C_1 grain size analysis according to ASTM procedures
C_2 as C_1 but after prolonged working with a spatula to disaggregate the particles completely

Figure 2.44 Influence of treatment method on the particle size distribution of a scaly clay (after Cotecchia et al., 1986).

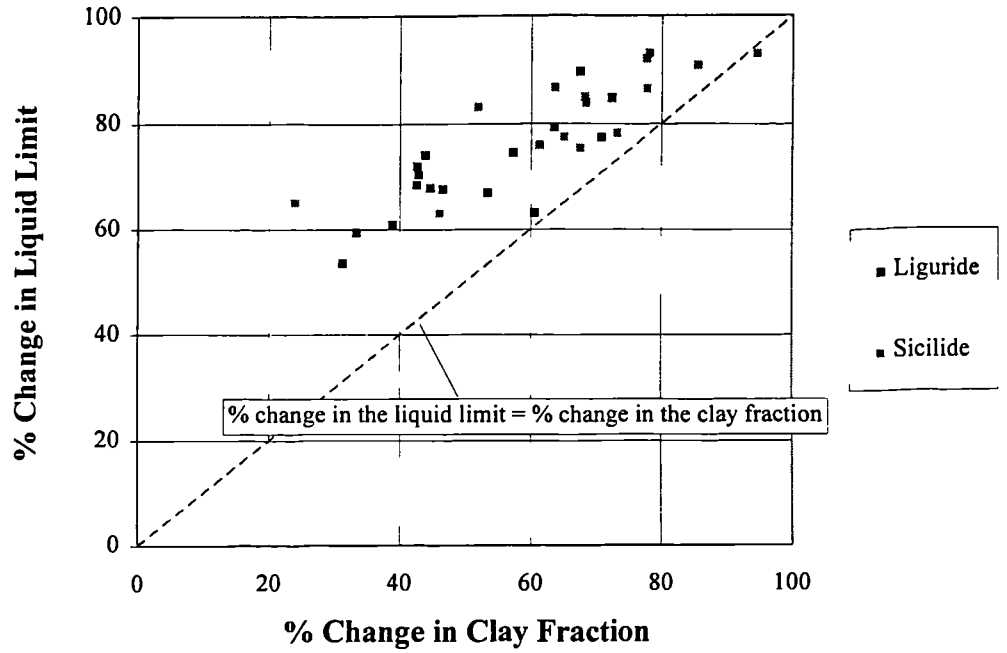

Figure 2.45 Correlation between the percentage increase in liquid limit and the percentage increase in clay fraction.
(Data from Rippa and Picarelli, 1977).

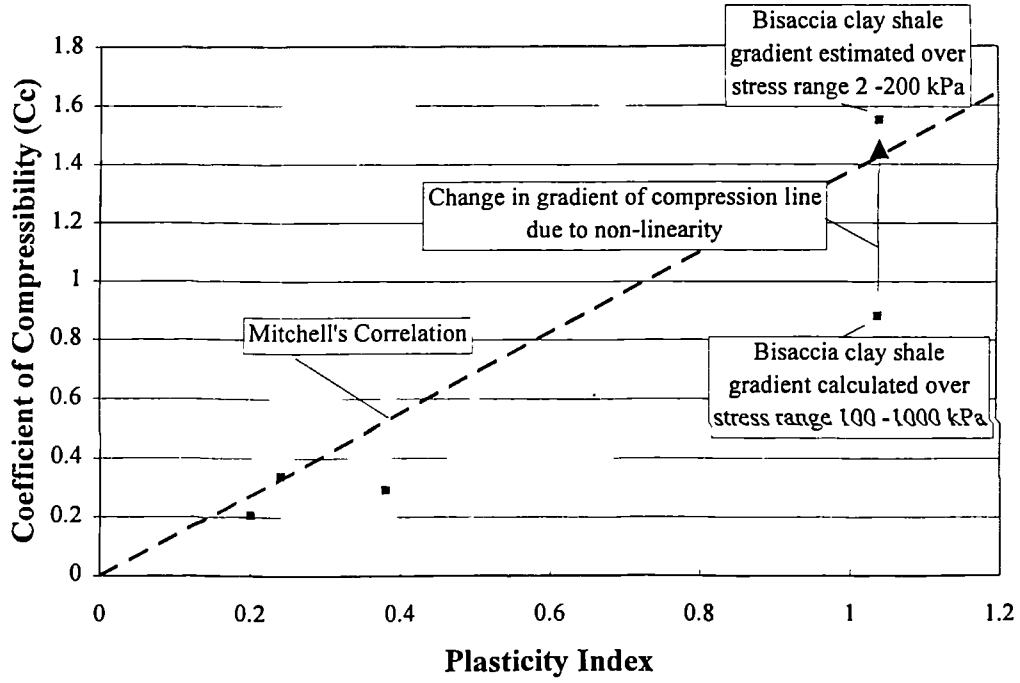

Figure 2.46 Correlation between coefficient of compressibility and plasticity index (after Mitchell, 1976). Data for the structurally complex clays from Guerriero et al. (1995) and Picarelli (1991).

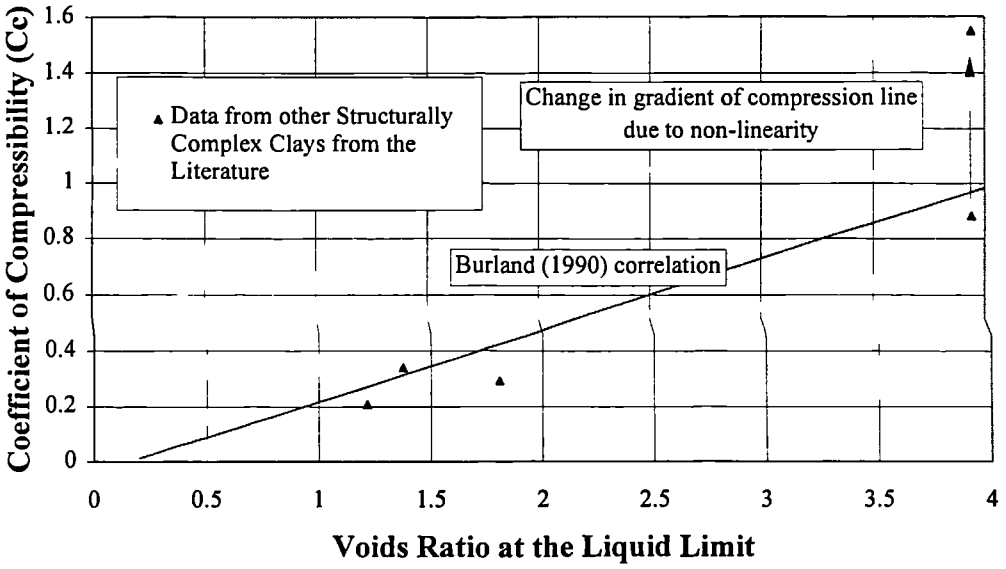

(a)

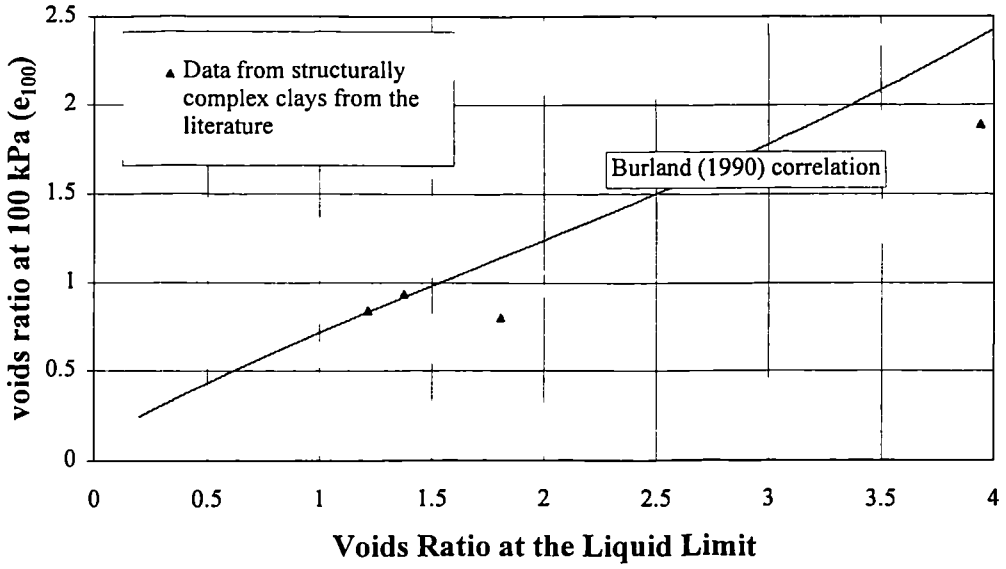

(b)

Figure 2.47 Correlations between (a) coefficient of compressibility and voids ratio at the liquid limit (b) voids ratio at a normal effective stress of 100 kPa on the one-dimensional compression line e^*_{100} and the voids ratio at the liquid limit (after Burland, 1990). Data for the structurally complex clays from Guerriero et al. (1995) and Picarelli (1991).

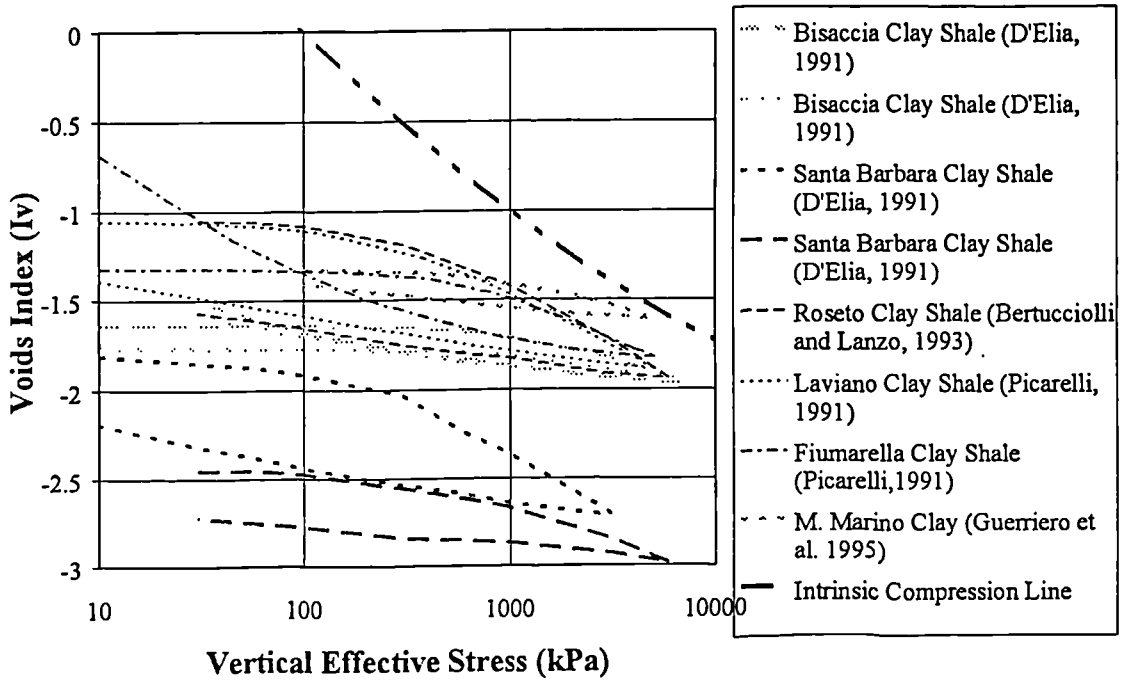

Figure 2.48 Oedometric compressive behaviour of a number of natural samples of structurally complex clays.

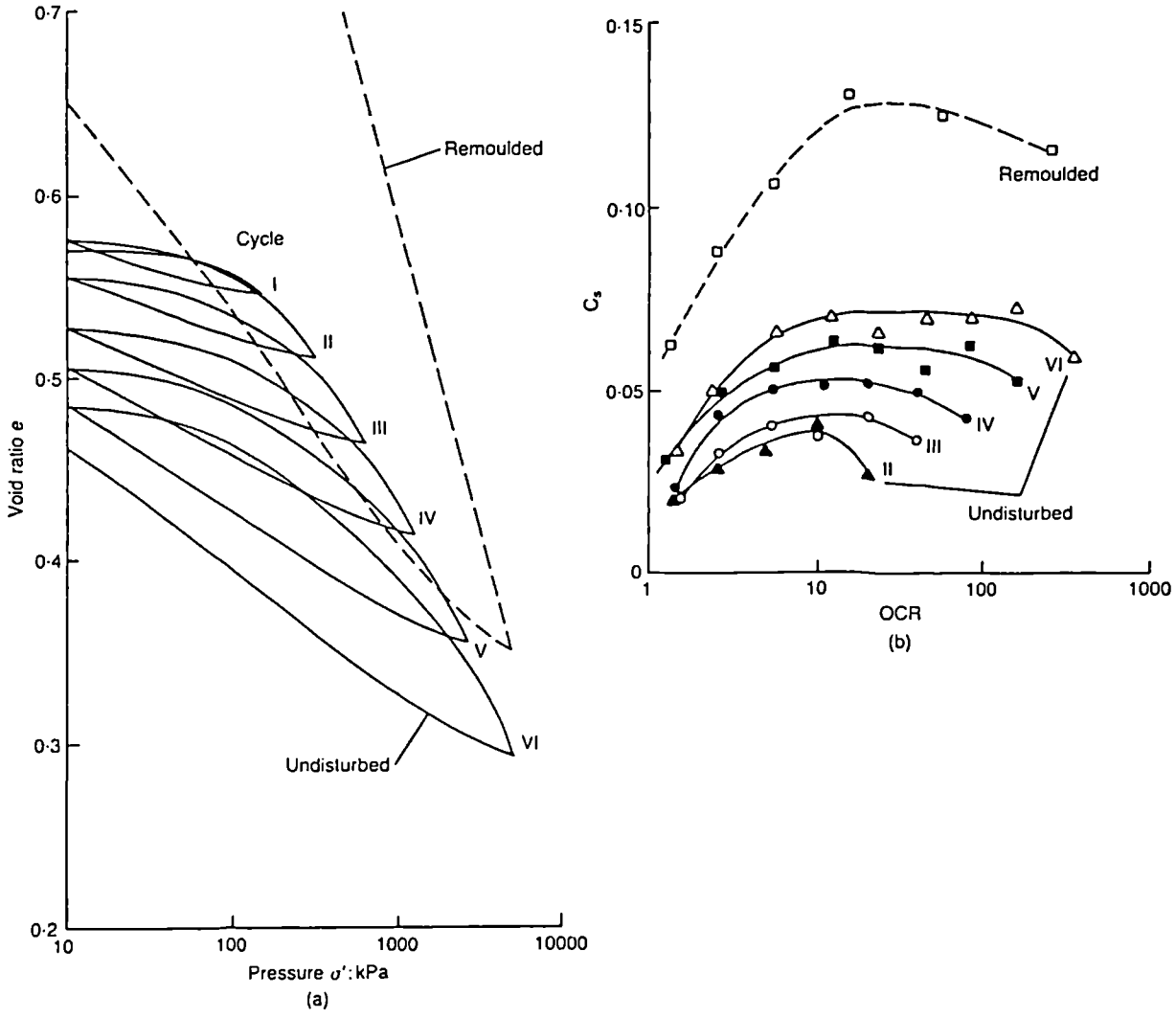

Figure 2.49 Comparison of compression curves of natural and reconstituted (remoulded) samples of Laviano clay shale (after Picarelli, 1991).

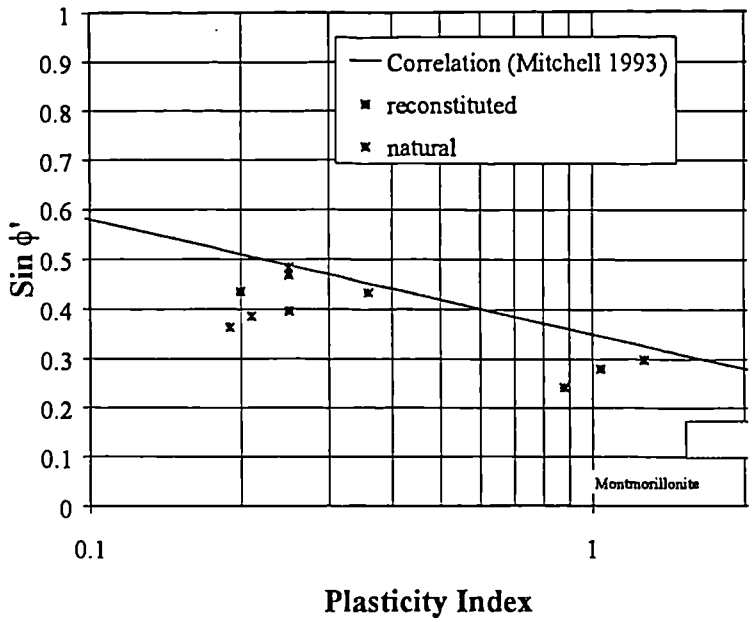

Data for the structurally complex clays

Natural
Bilotta, (1987); Bertuccioli and Lanzo, (1993); D'Elia, (1991); Iaccarino et al., (1996); D'Elia, (1977); Guerriero et al., (1995).

Reconstituted
Iaccarino et al., (1996); Guerriero et al., (1995).

Figure 2.50 Correlation between friction angle and plasticity index for natural and reconstituted structurally complex clays.

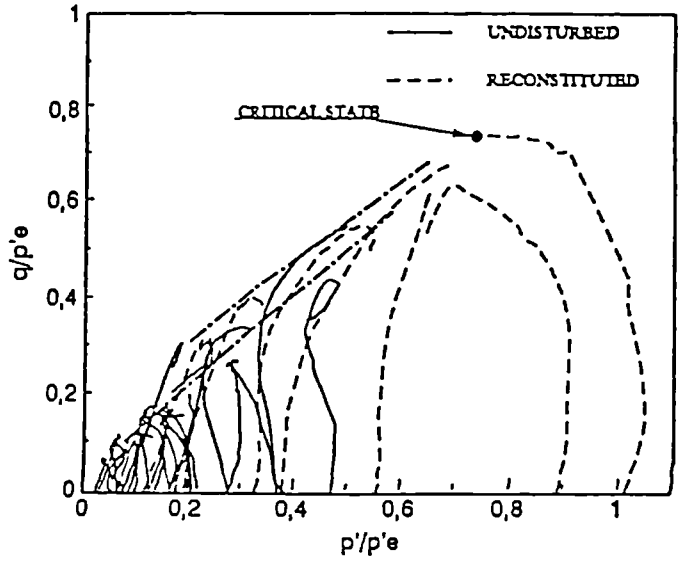

Figure 2.51 Normalised shear strength envelopes of the reconstituted and undisturbed M. Marino clay (after Guerriero et al., 1995).

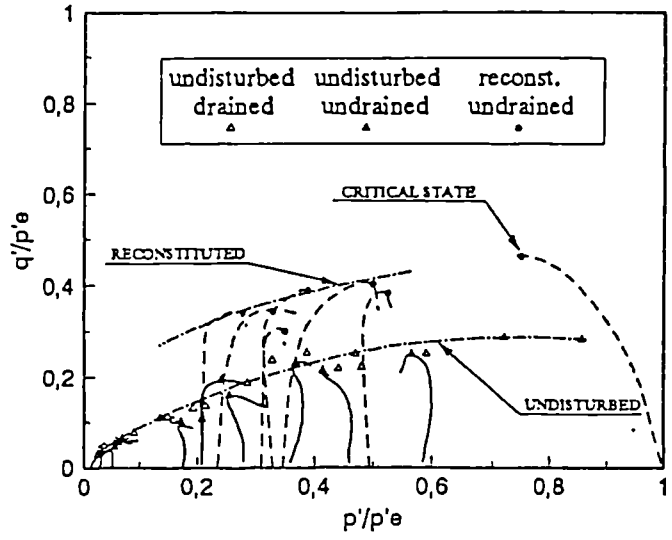

Figure 2.52 Normalised shear strength envelopes of the reconstituted and undisturbed Bisaccia clay (after Guerriero et al., 1995).

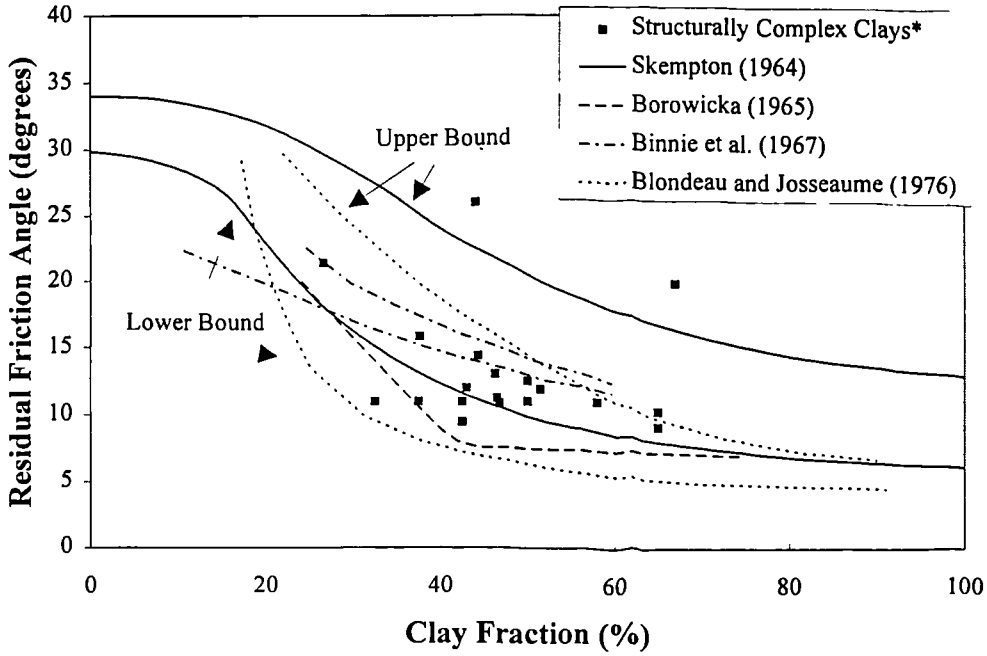

Figure 2.53 Comparison of data for structurally complex clays with correlations between clay fraction and residual friction angle (after Lupini et al. 1981). Data from structurally complex clays from Cotecchia et al. (1986), Del Prete and Trisorio Liuzzi (1992), Cherubini et al. (1990), Cotecchia (1989), Hutchinson and Del Prete (1985) and D'Elia (1977).

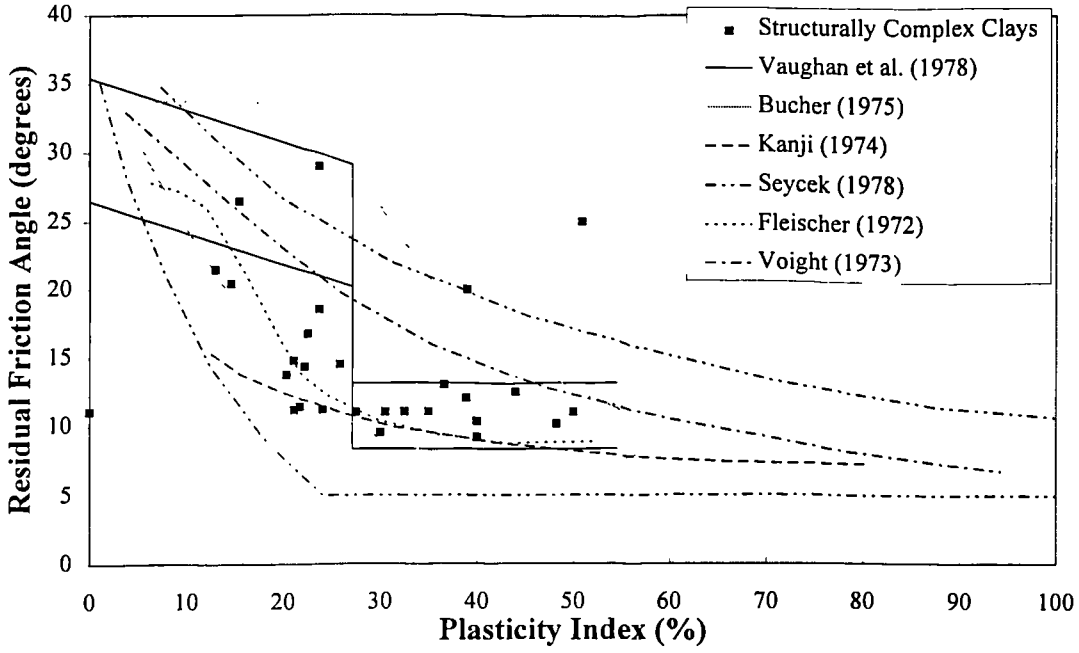

Figure 2.54 Comparison of data for structurally complex clays with correlations between plasticity index and residual friction angle (after Lupini et al. 1981). Data from structurally complex clays from Cotecchia et al. (1986), Del Prete and Trisorio Liuzzi (1992), Cherubini et al. (1990), Cotecchia (1989), Hutchinson and Del Prete (1985) and D'Elia (1977).

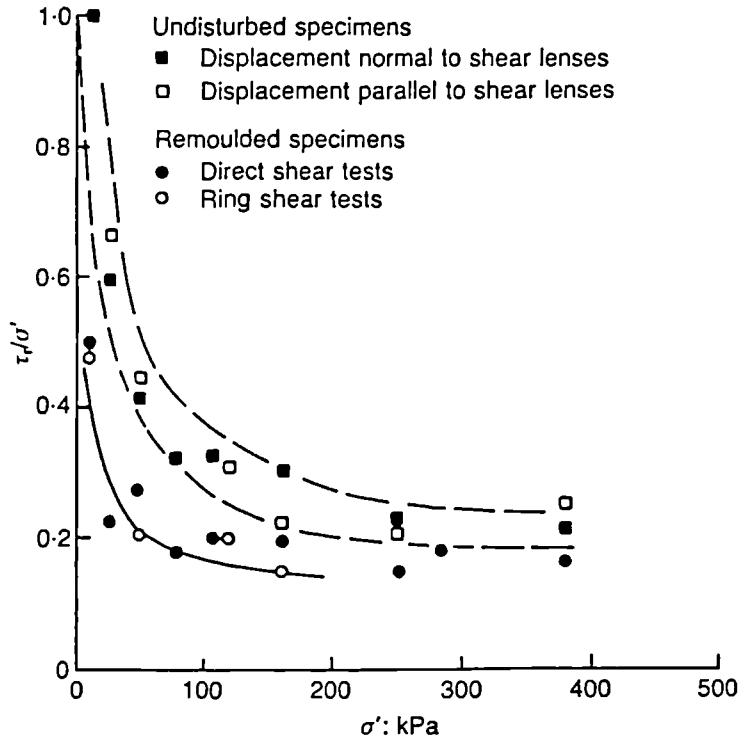

Figure 2.55 Drained residual strength of Laviano clay shale (after Picarelli, 1991).

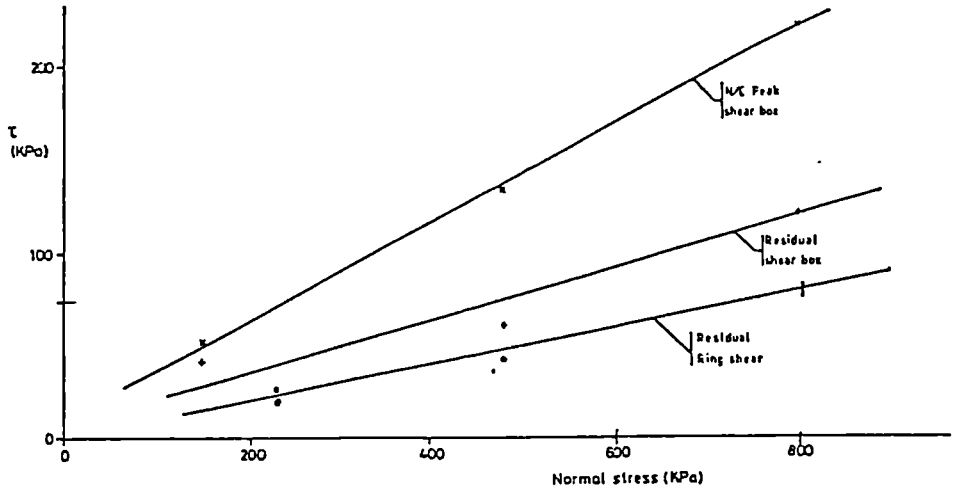

Figure 2.56 Mohr-Coulomb envelopes for remoulded Senerchia soil samples (after Lemos 1986)

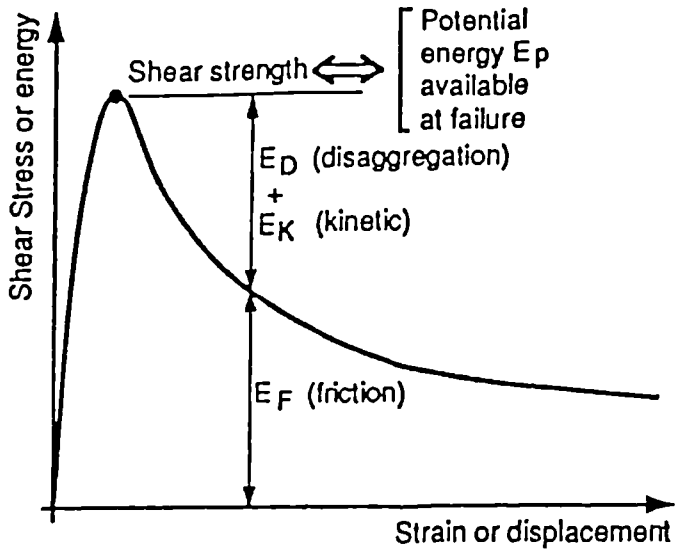

Figure 2.57 Redistribution of the potential energy after failure (after D'Elia et al. 1996).

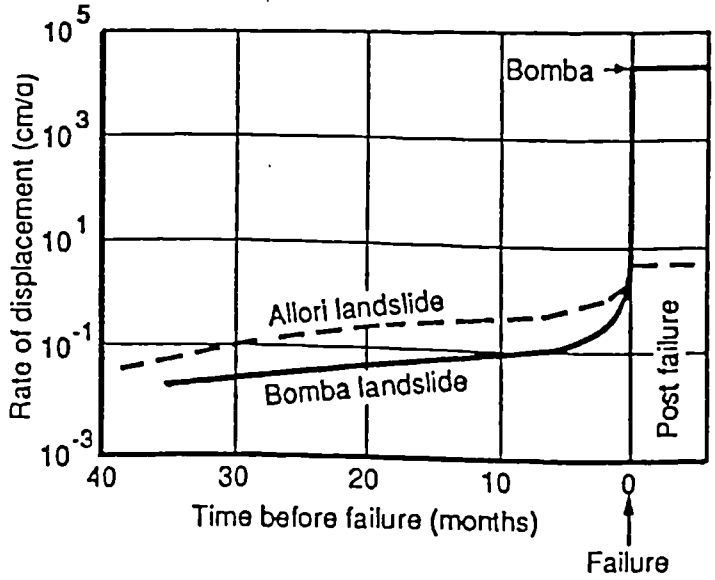

Figure 2.58 Rates of movement in two Italian excavations (after D'Elia et al. 1996).

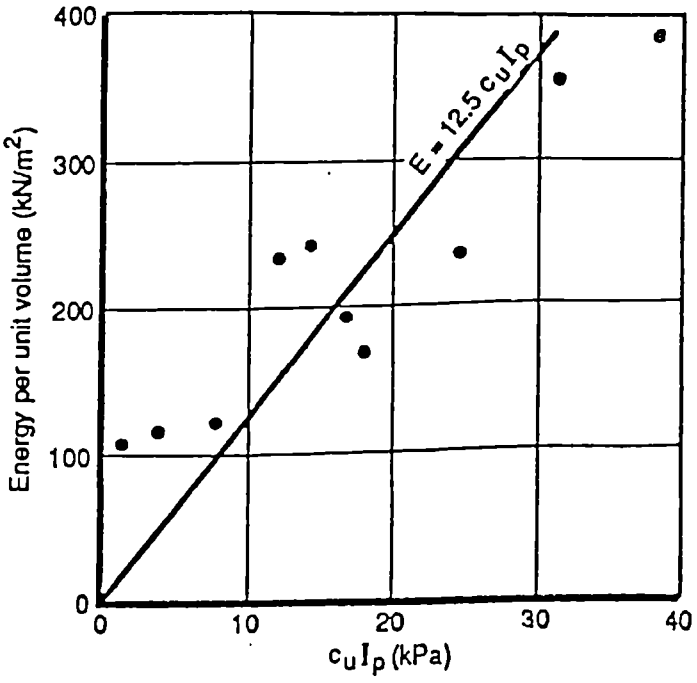

Figure 2.59 Energy per unit volume necessary for reaching a remoulding index equal to 75% in eastern Canada clays (after Tavernas et al. 1983).

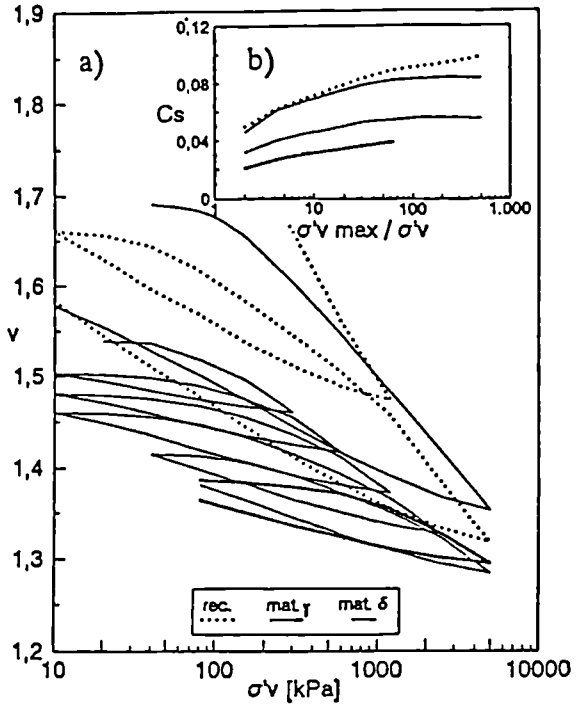

Figure 2.60 Results of oedometer tests on the natural, reconstituted and softened M. Marino clay (after Guerriero et al., 1995)

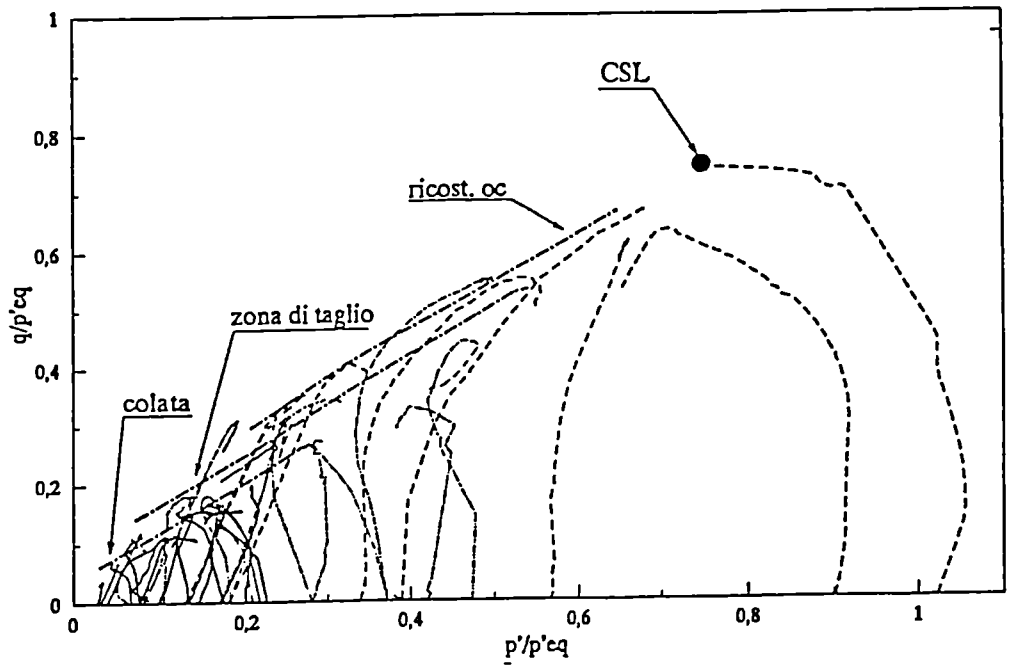

colata - samples from landslide body
zona di taglio - samples from shear surface
ricost. oc - overconsolidated reconstituted samples

Figure 2.61 Normalised shear strength envelopes for natural and reconstituted M. Marino clay (after Guerriero et al., 1995)

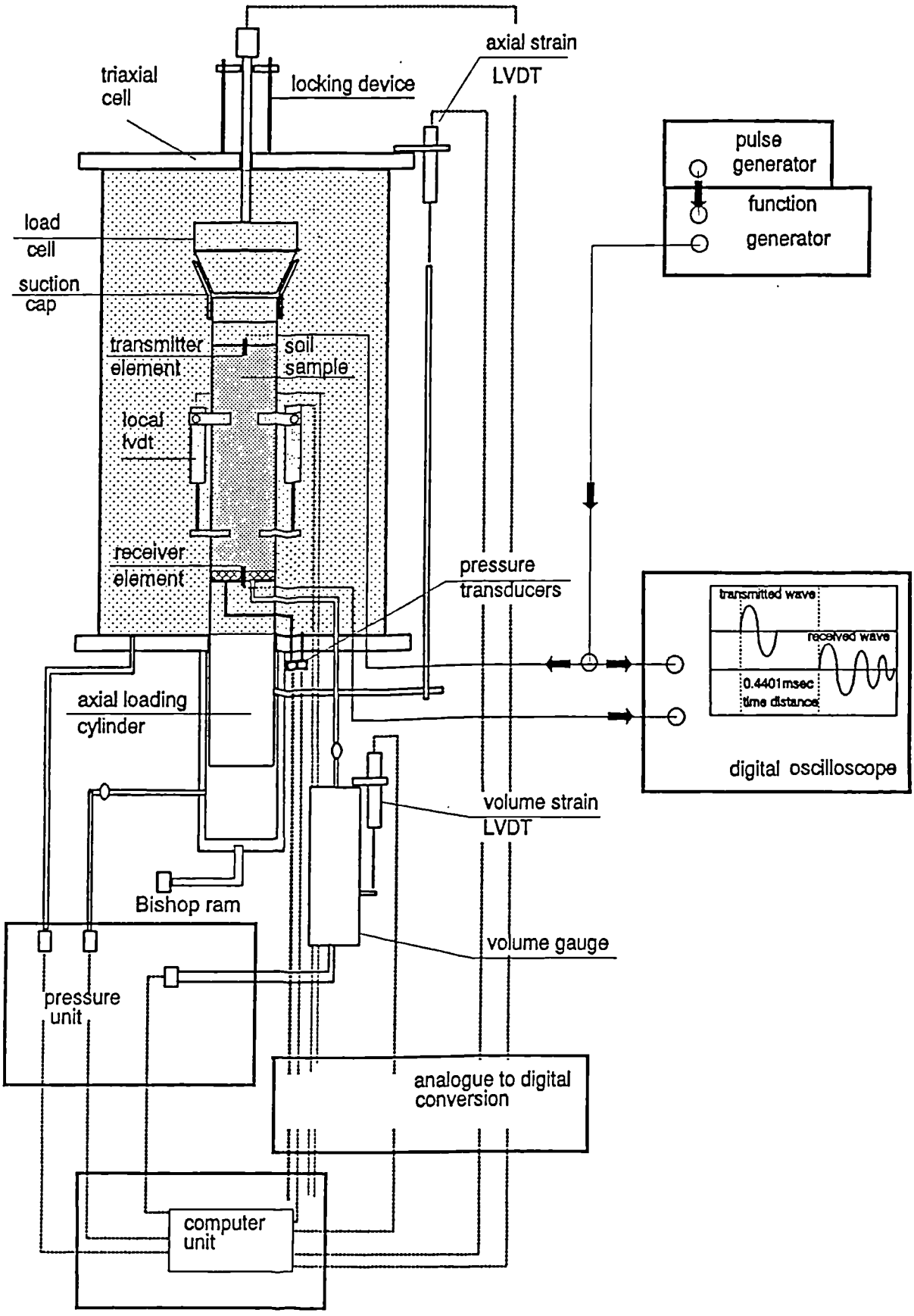

Figure 3.1 Schematic diagram of control system for triaxial apparatus (after Jovicic, 1997)

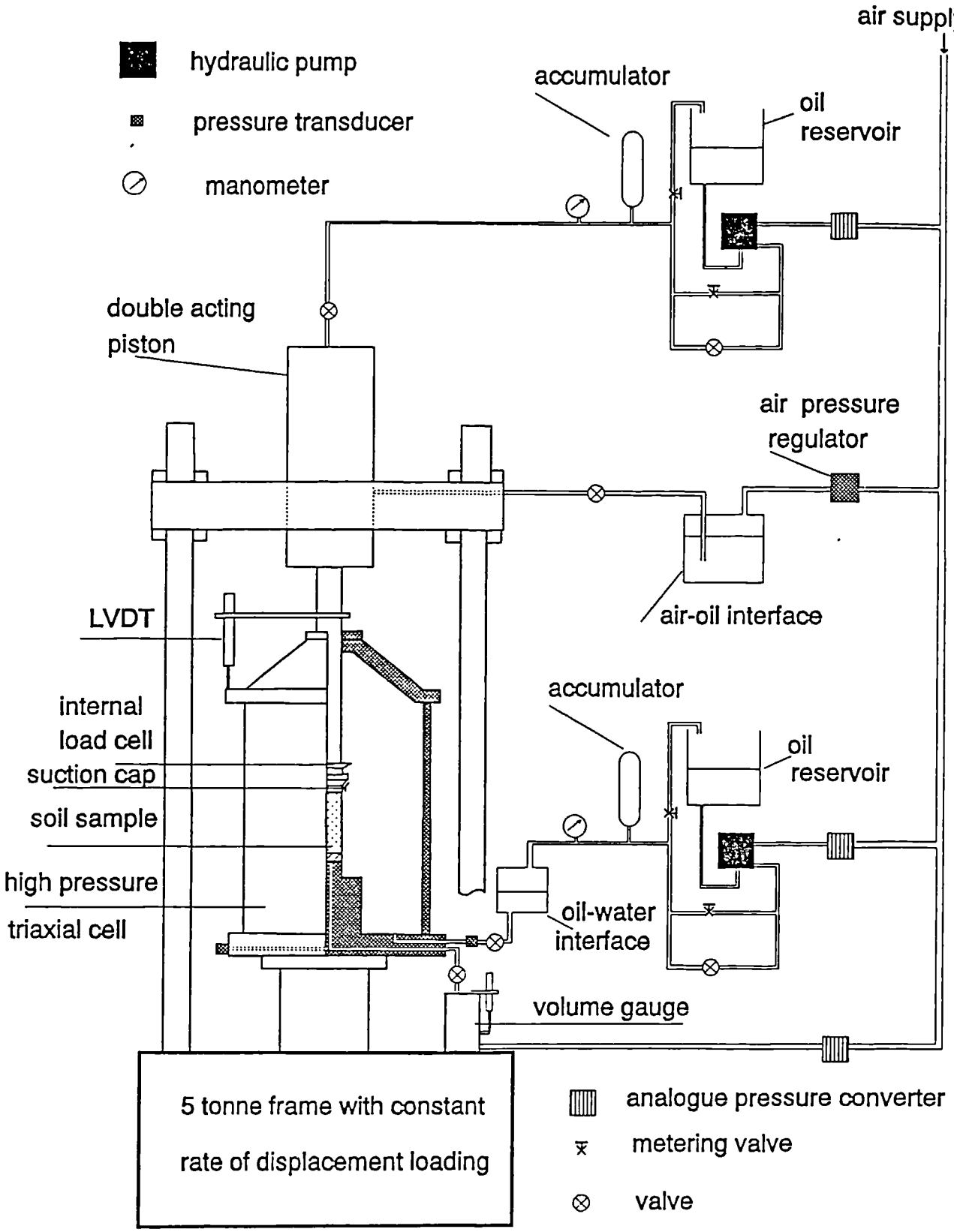

Figure 3.2 Schematic diagram of high pressure triaxial apparatus with a cell pressure capacity of 5 MPa (after Jovicic, 1997)

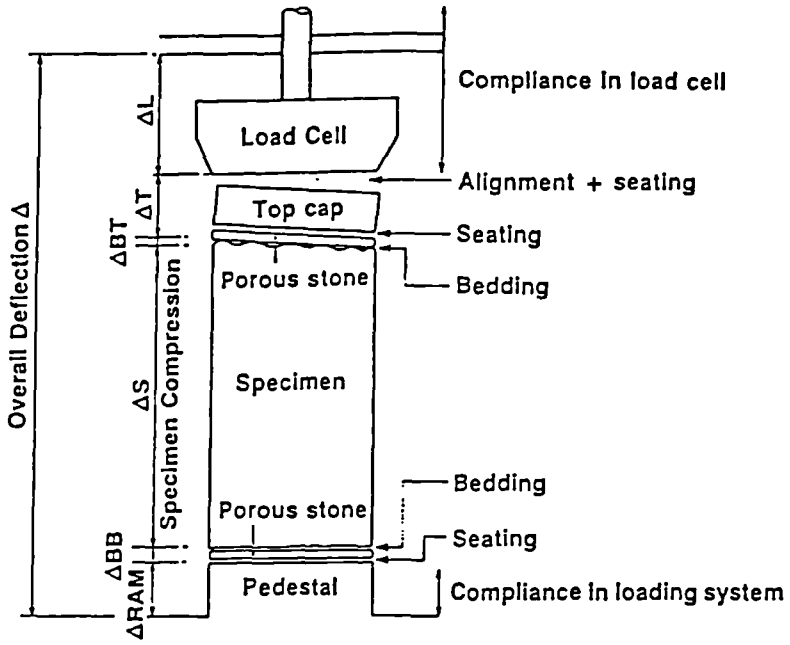

Figure 3.3 Sources of error in external axial deformation measurements (after Baldi et al.1988)

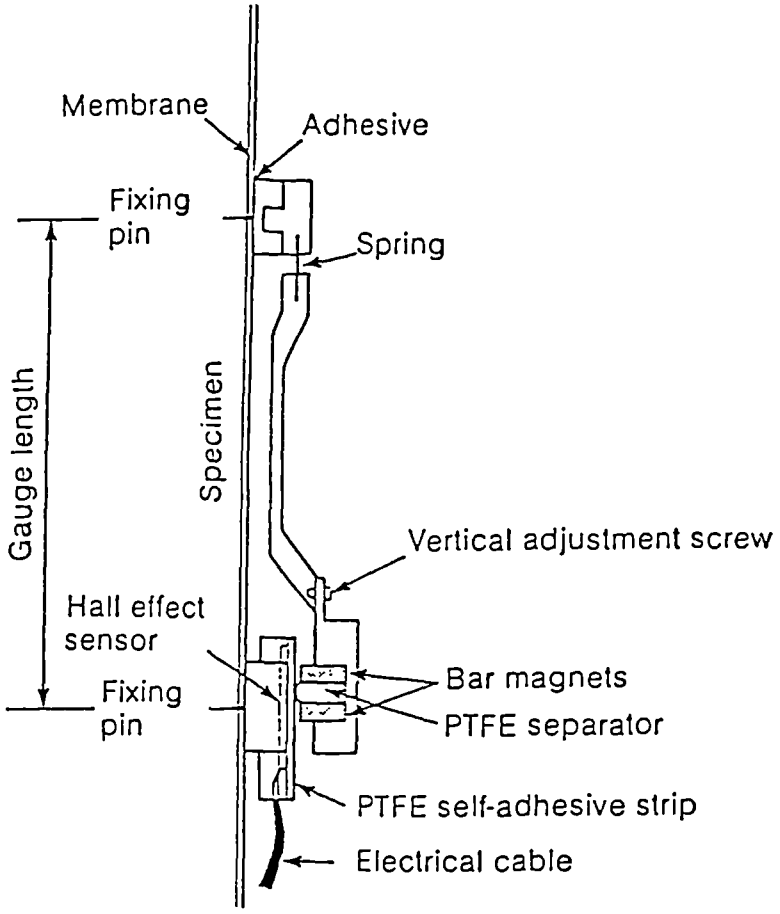

Figure 3.4 Schematic section of Hall-effect gauge (after Clayton and Khatrush, 1986)

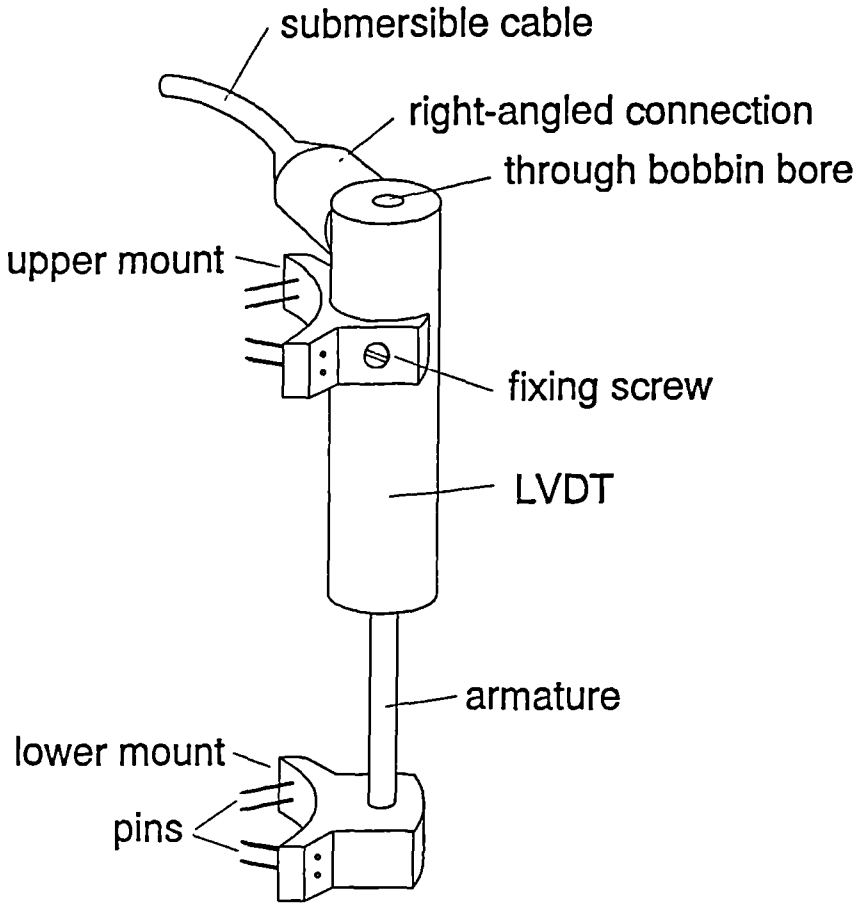

Figure 3.5 Schematic diagram of axial strain measurement using miniature LVDTs (after Cuccovillo and Coop, 1997)

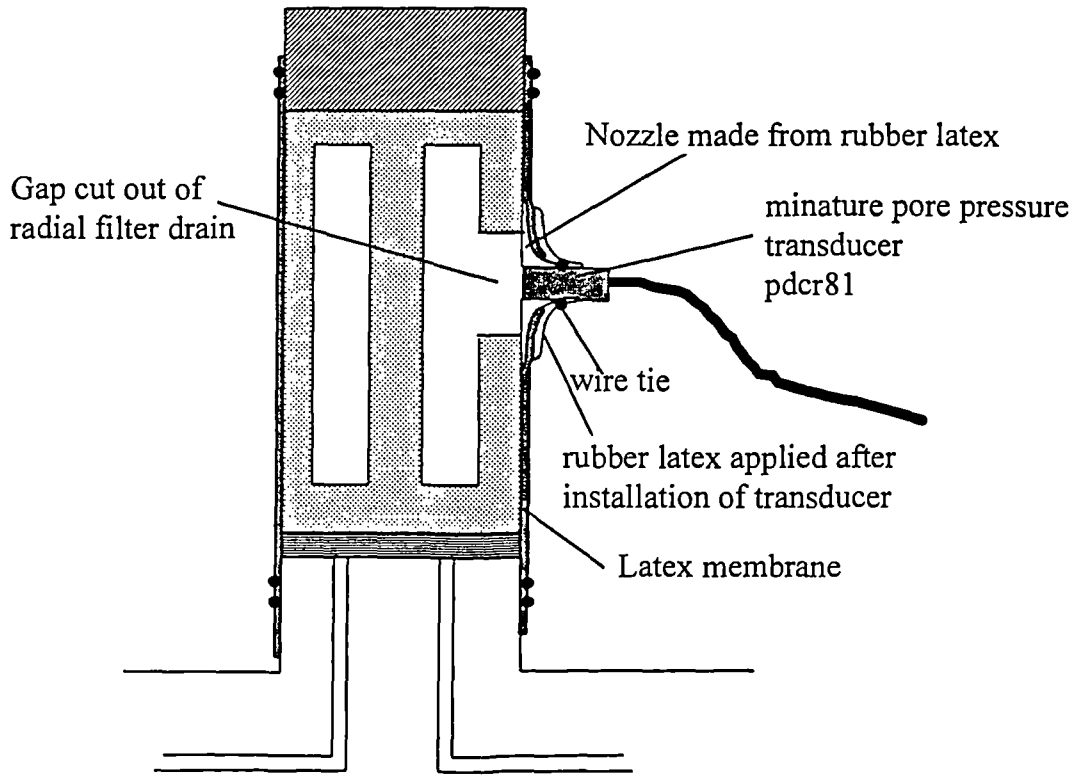

Figure 3.6 Schematic section of mid-height pore pressure transducer

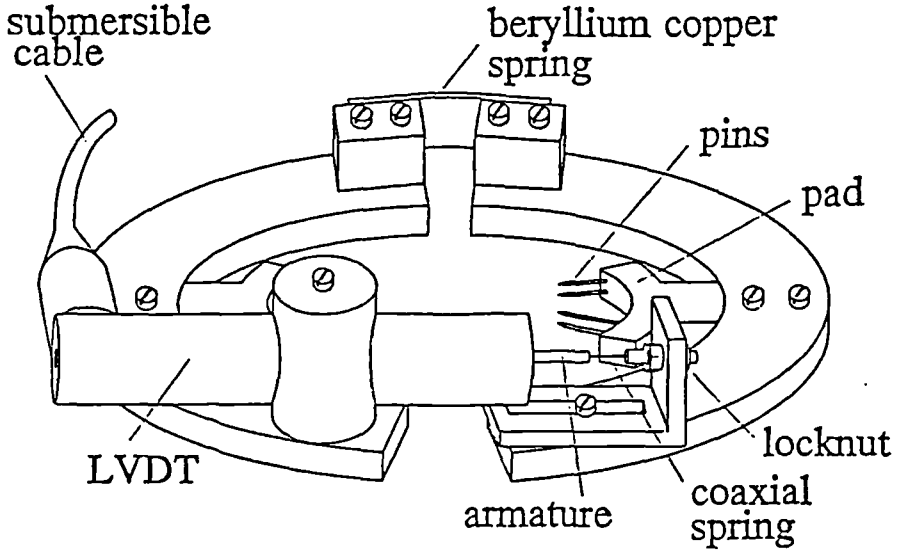

Figure 3.7 Schematic diagram of radial strain belt (after Coop, 1997)

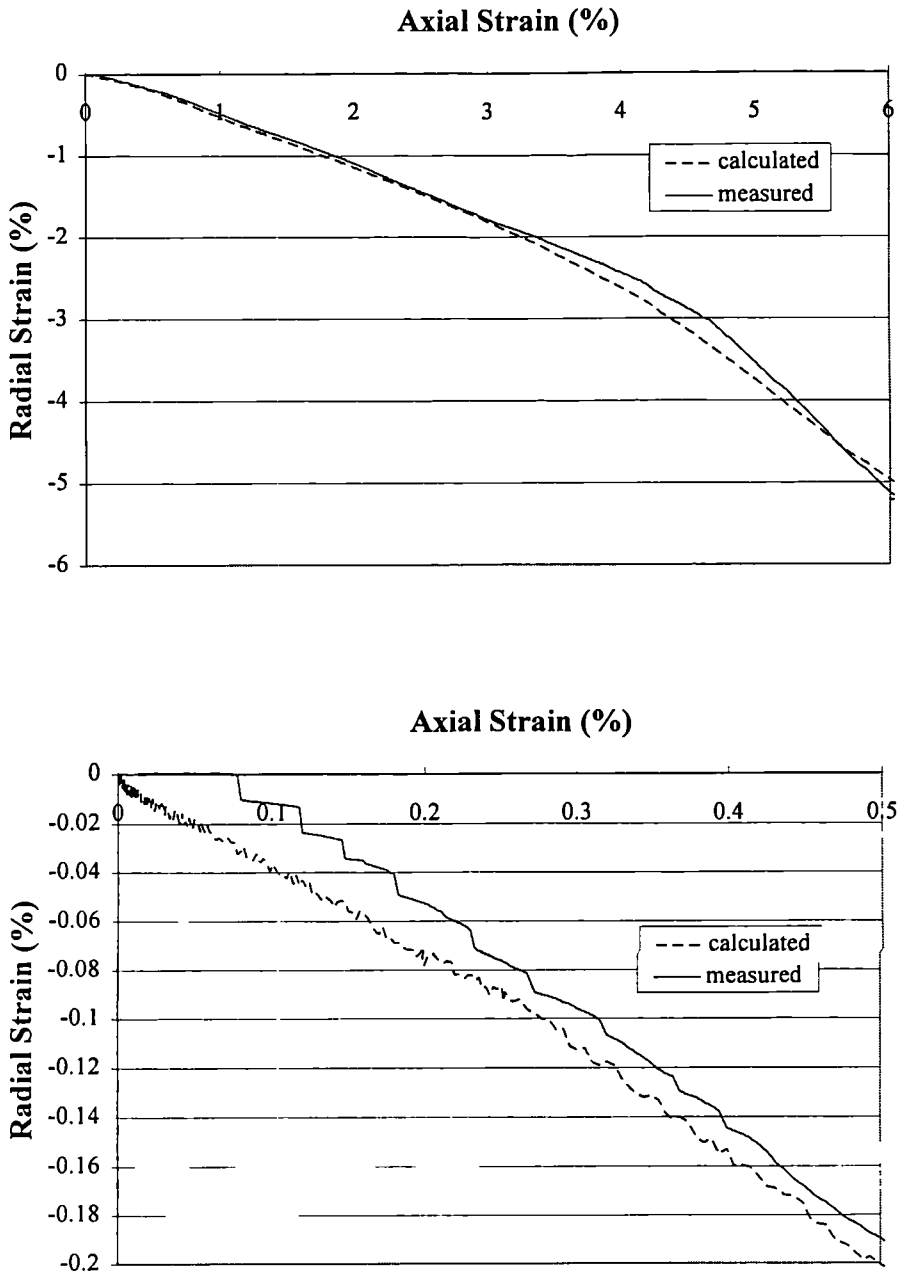

Figure 3.8 Comparison of the radial strains calculated from the axial and volumetric strains and the radial strains measured using the radial strain belt.

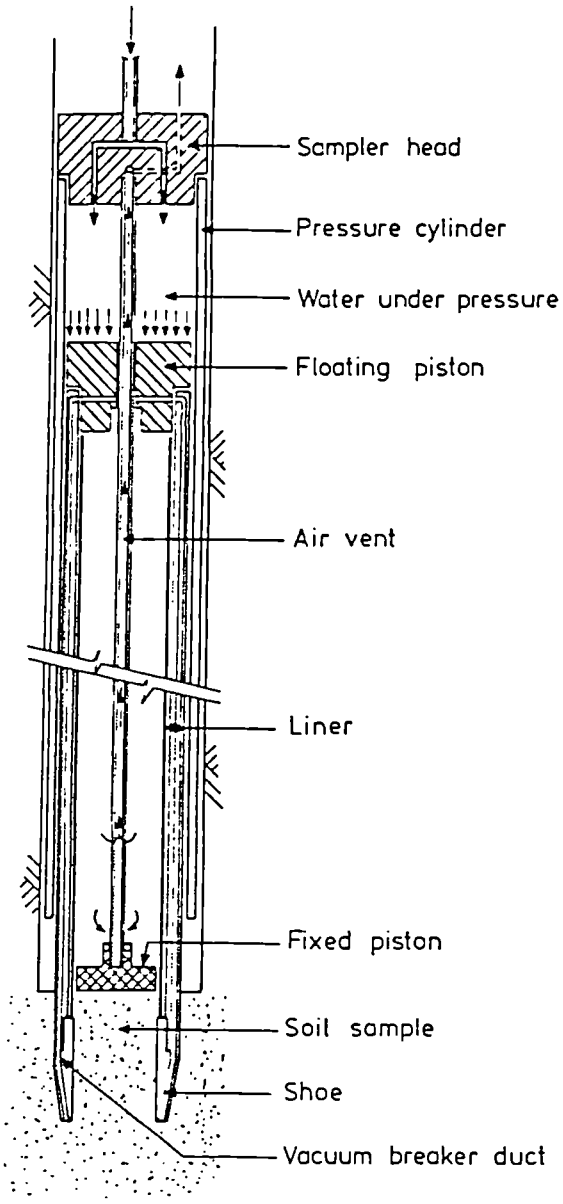

Figure 3.9 Schematic Diagram of Osterberg tube sampler (after Osterberg, 1973 and Clayton et al., 1982)

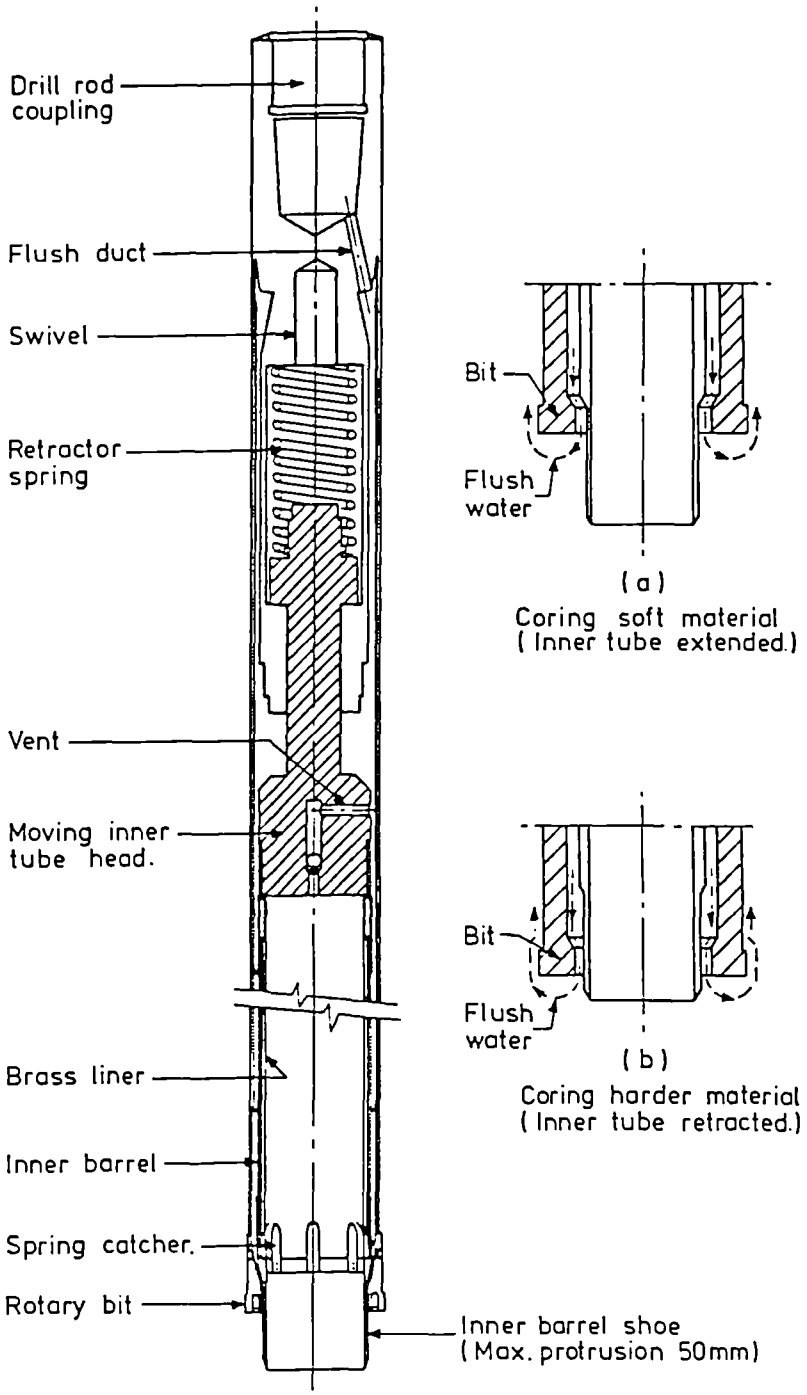

Figure 3.10 Schematic Diagram of Mazier tube sampler (after Clayton et al., 1982)

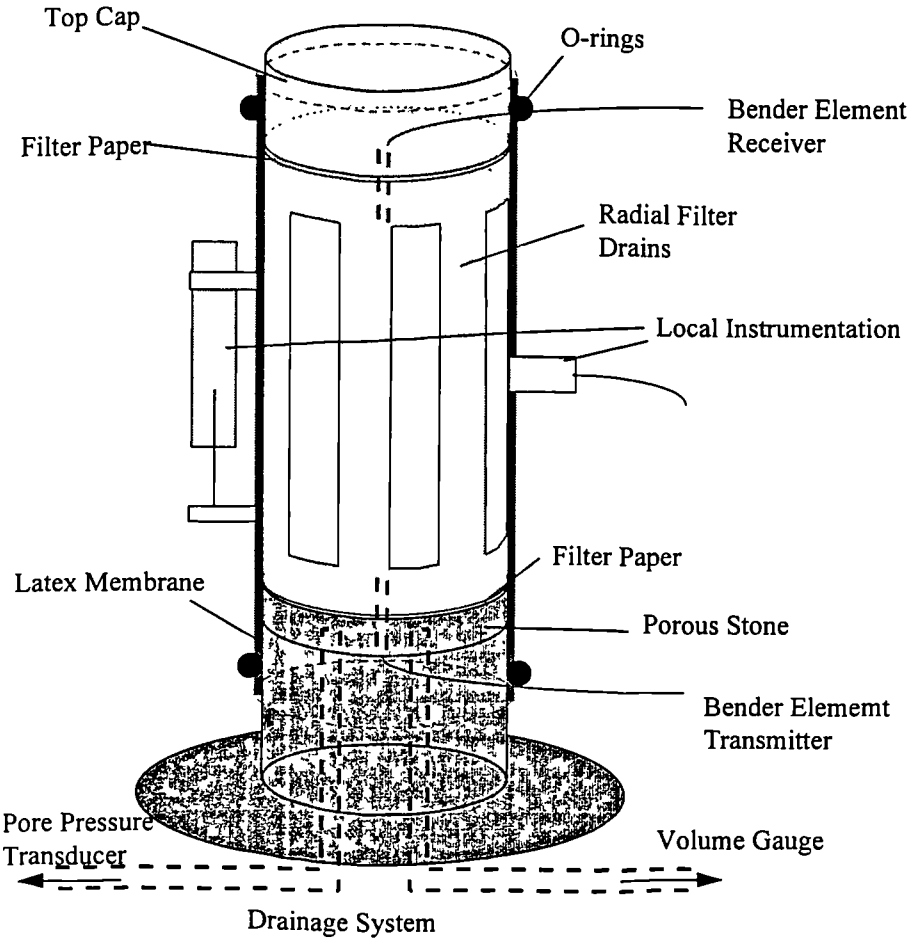

Figure 3.11 Schematic Diagram of Sample Set-up

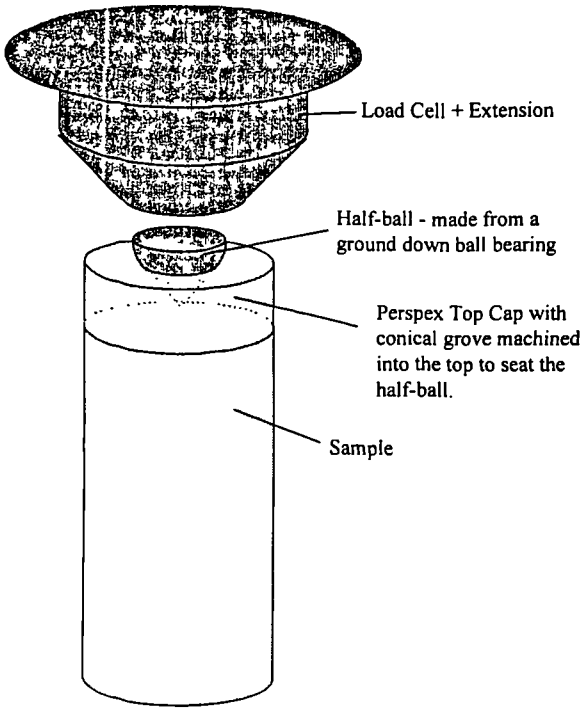

Figure 3.12 Schematic diagram of the halved ball connection.

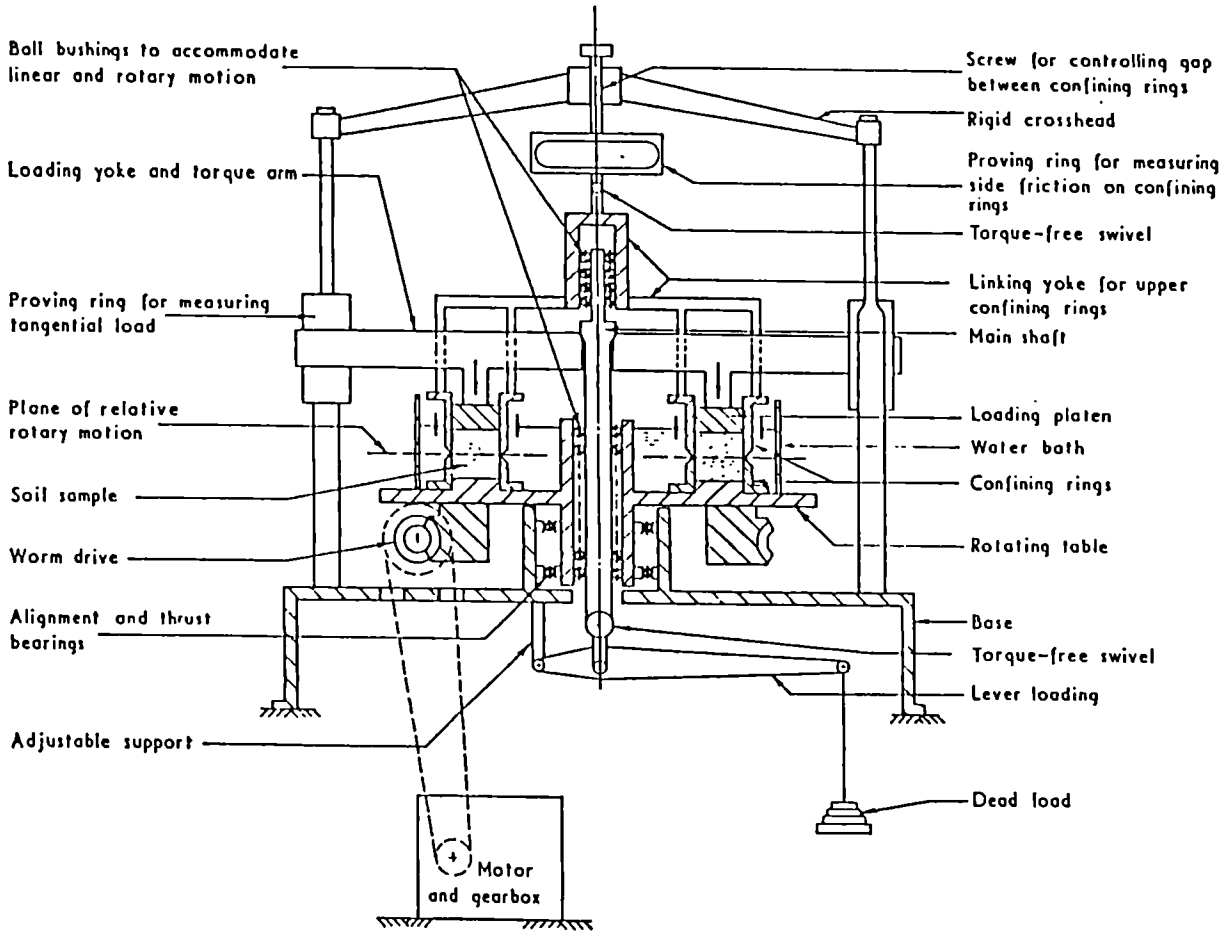

Figure 3.13 Simplified cross-section of the Bishop ring shear apparatus (after Bishop et al., 1971)

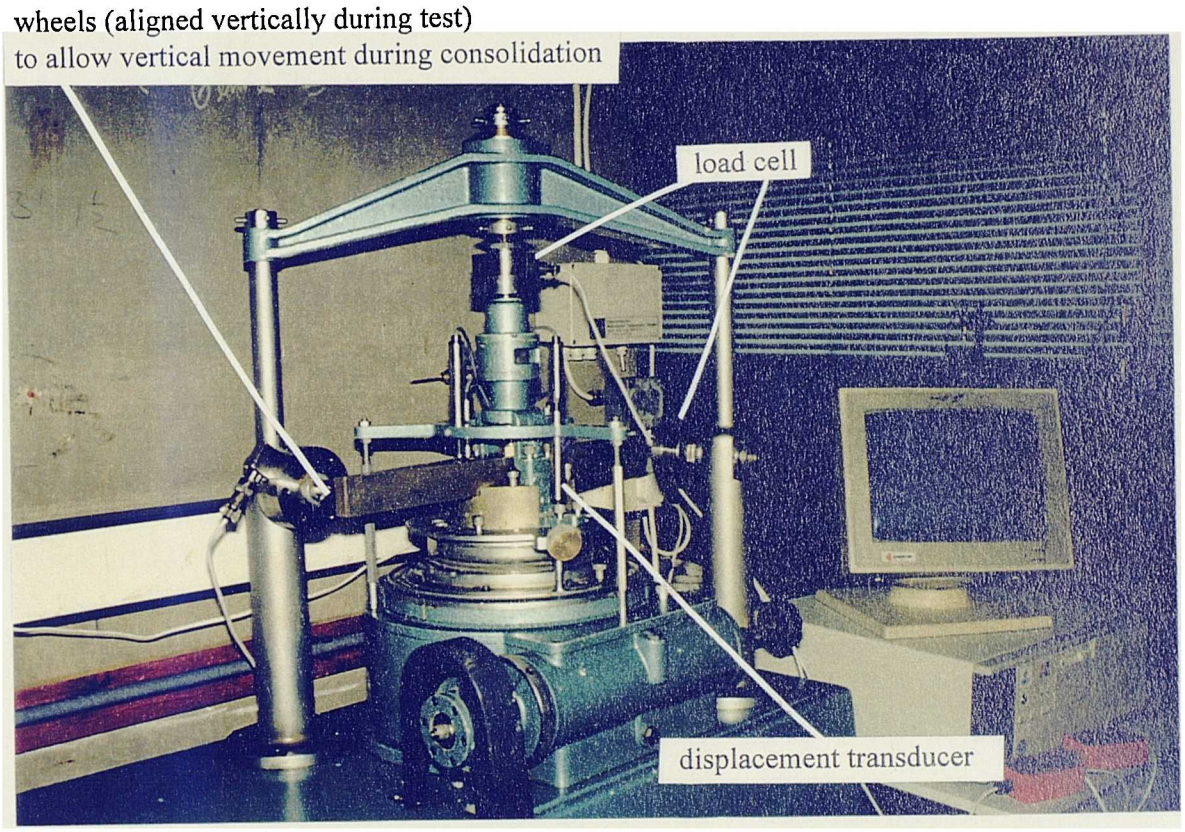

Figure 3.14 Annotated photograph of modified Bishop ring shear apparatus

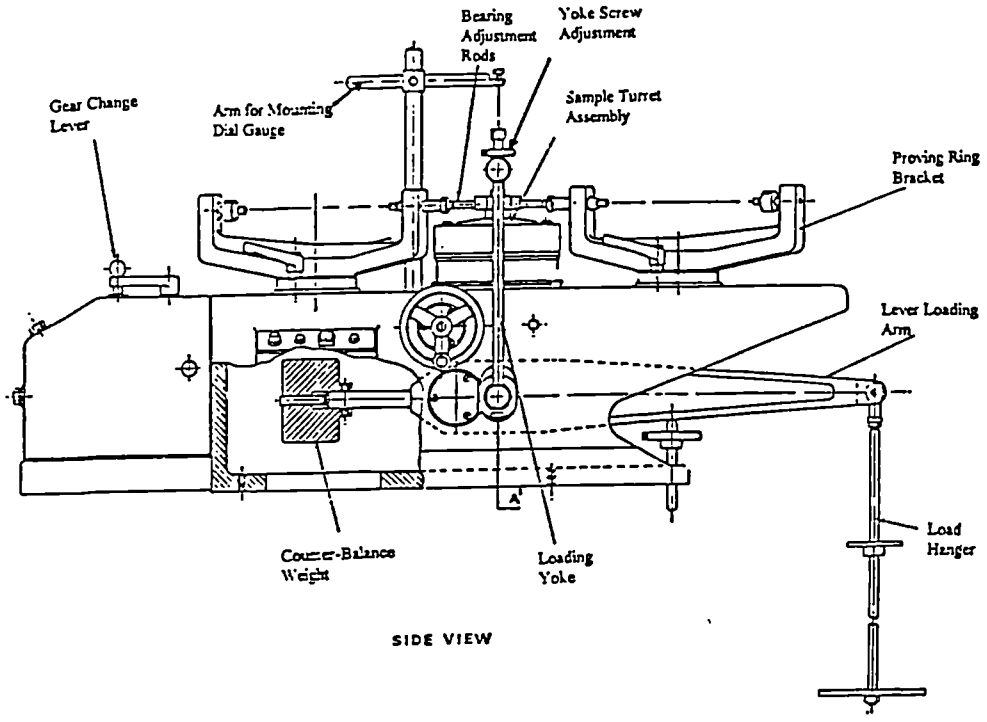

Figure 3.15 Cross-section of Bromhead ring shear apparatus (from manufacturer's handbook).

Figure 4.1 a) Photographs showing examples of the heterogeneity of materials at the landslide site.

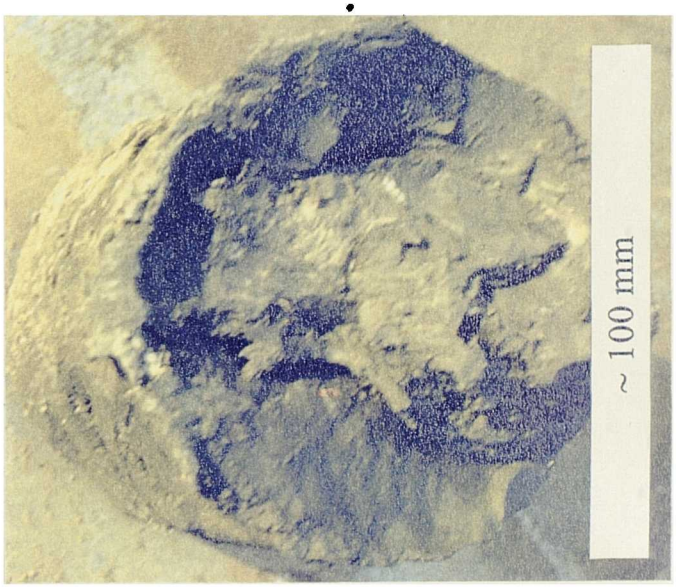

Figure 4.1 b) Photographs showing different argillaceous materials obtained from inside the landslide body.

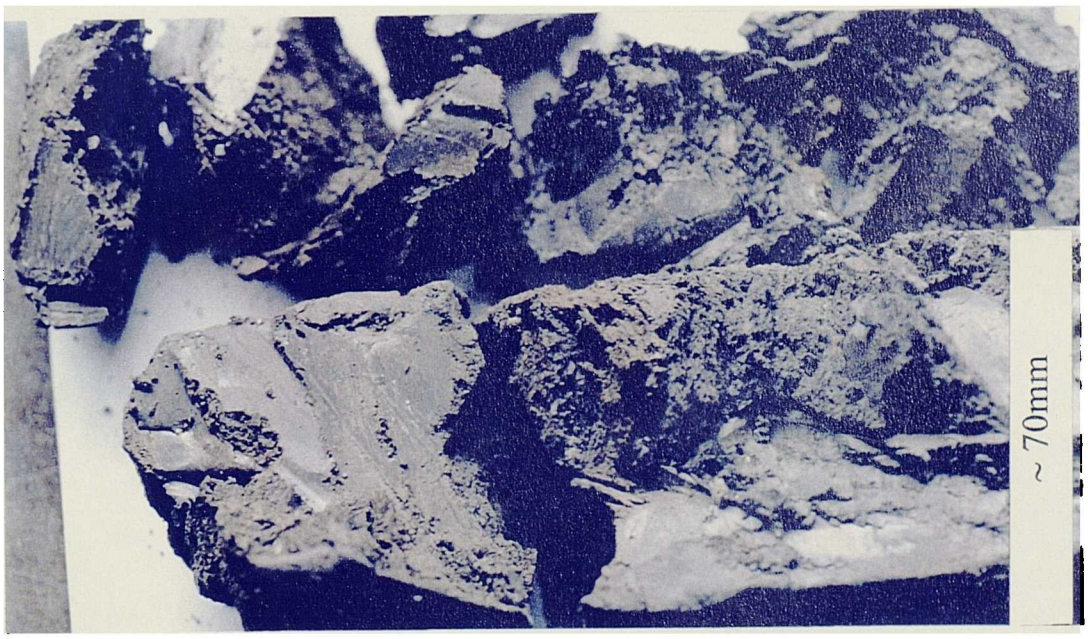

Figure 4.1 c) Photographs showing different argillaceous materials obtained from the underlying formation.

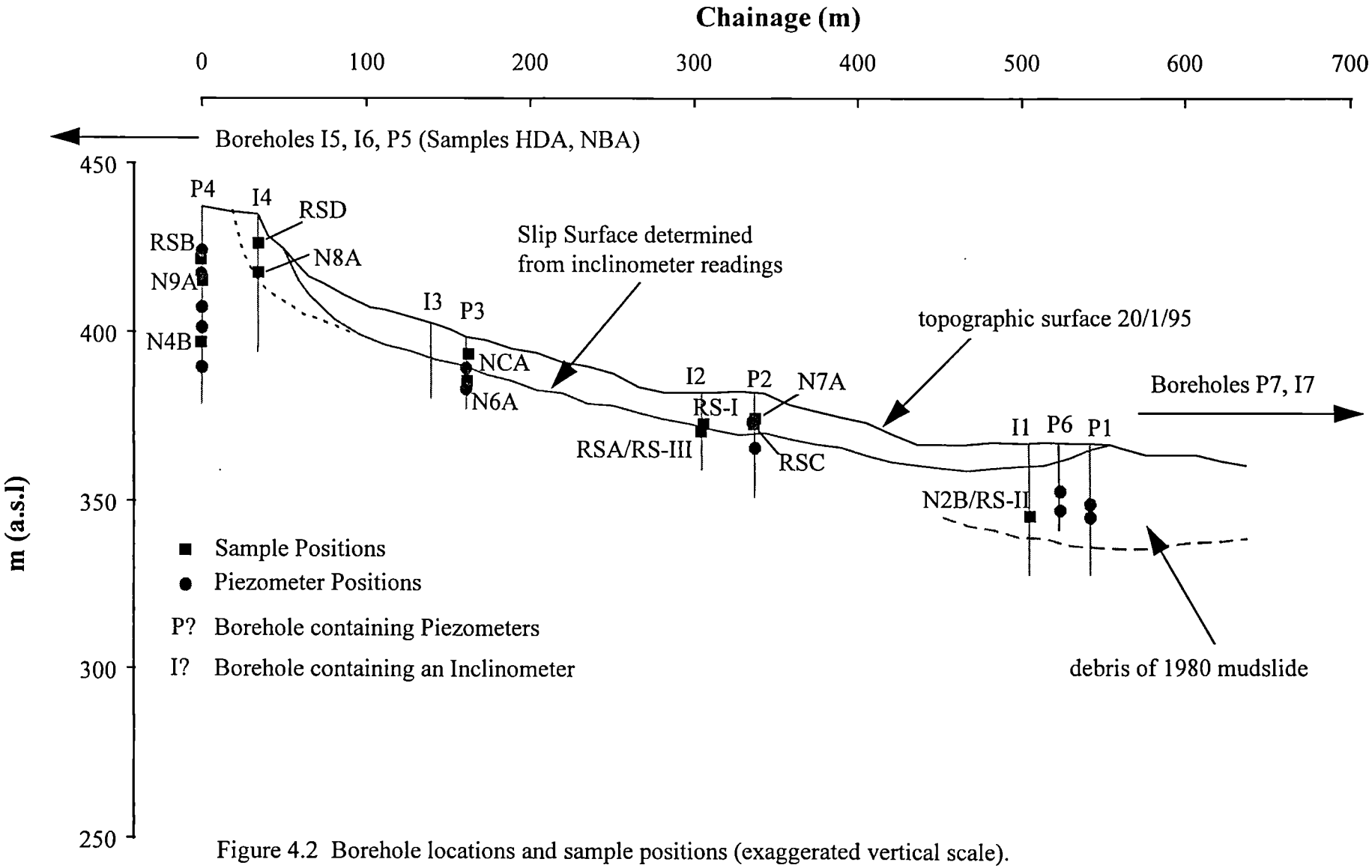

Figure 4.2 Borehole locations and sample positions (exaggerated vertical scale).

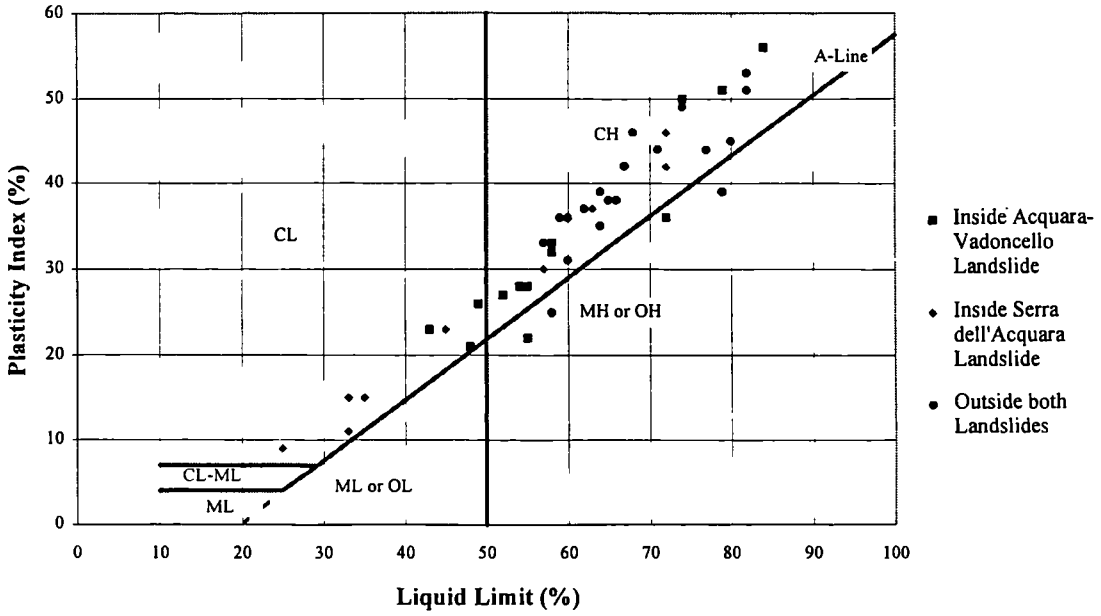

Figure 4.3 Plasticity chart showing the variation of the materials from inside either the current Acquara-Vadoncello landslide, the 1980 Serra dell'Acquara landslides or the underlying formations.

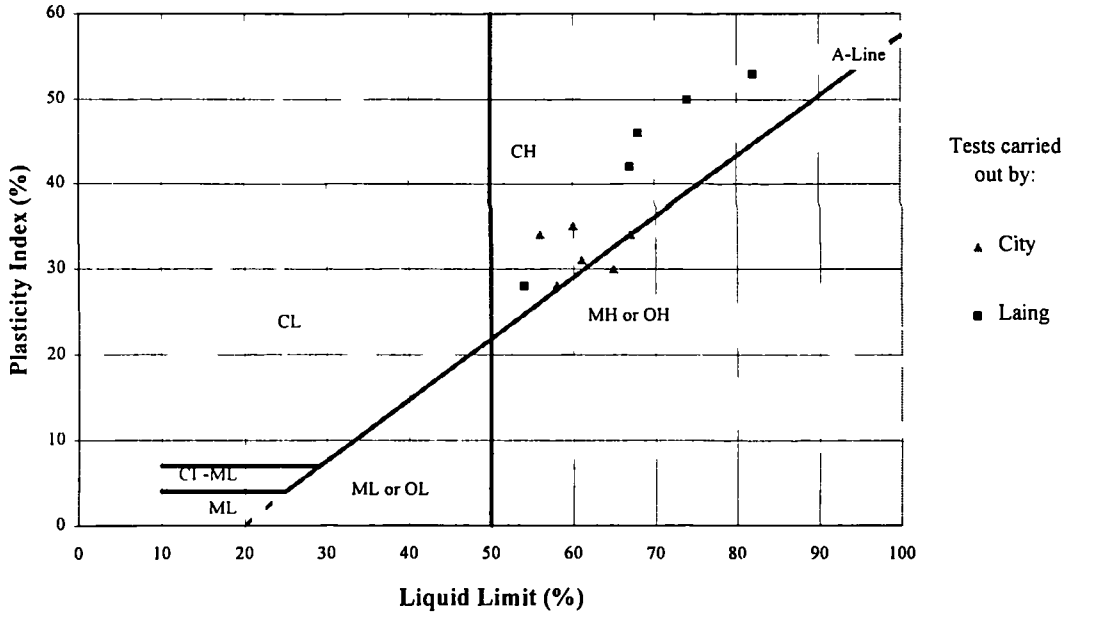

Figure 4.4 Plasticity chart showing the soil plasticities determined by different operators from tests on adjacent samples.

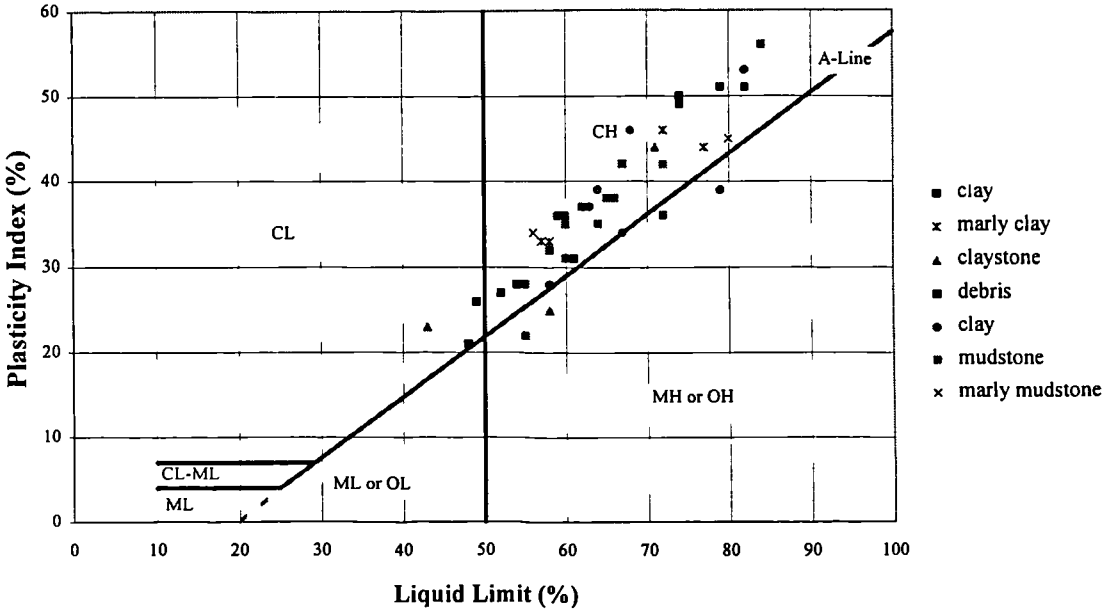

Figure 4.5 Plasticity chart comparing the plasticity indices of materials with different visual descriptions on the borehole logs.

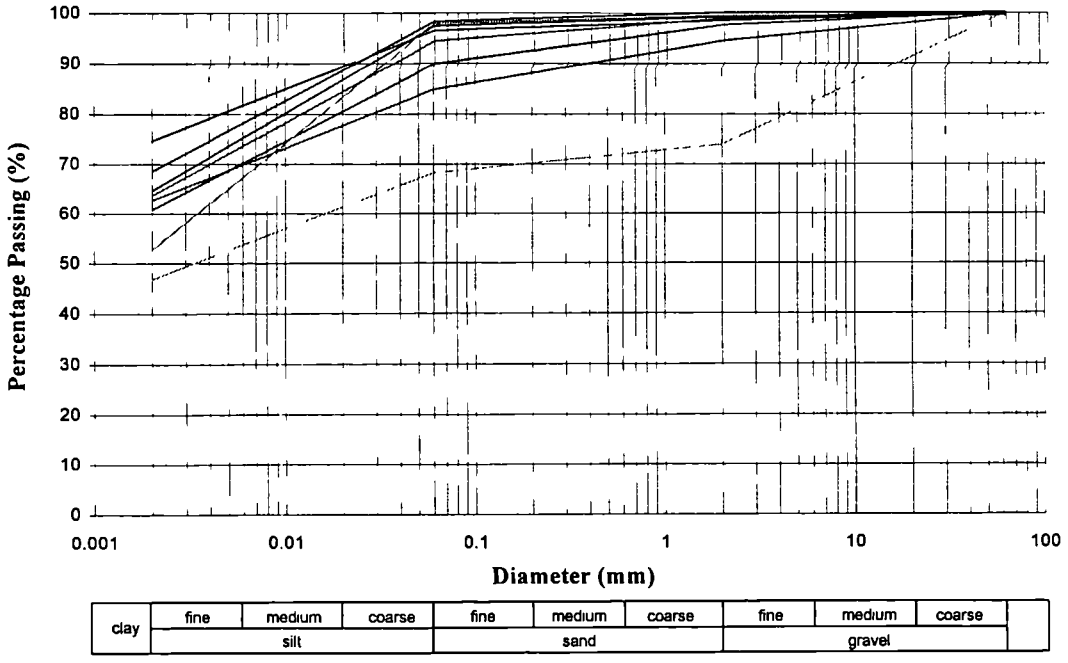

Figure 4.6 Particle Size Distributions

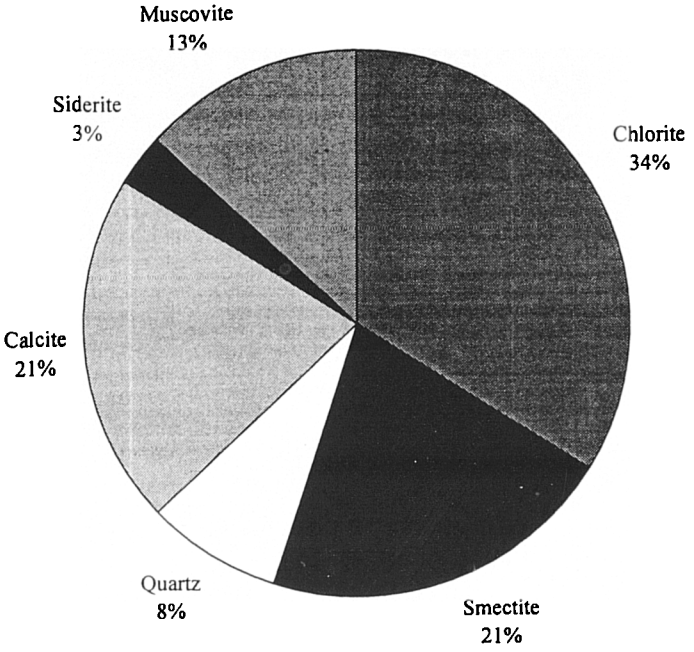

Figure 4.7 Mineralogical Composition determined by X-Ray Diffraction. Sample N8B (Borehole I4: 16.0 -16.4 m bgl)

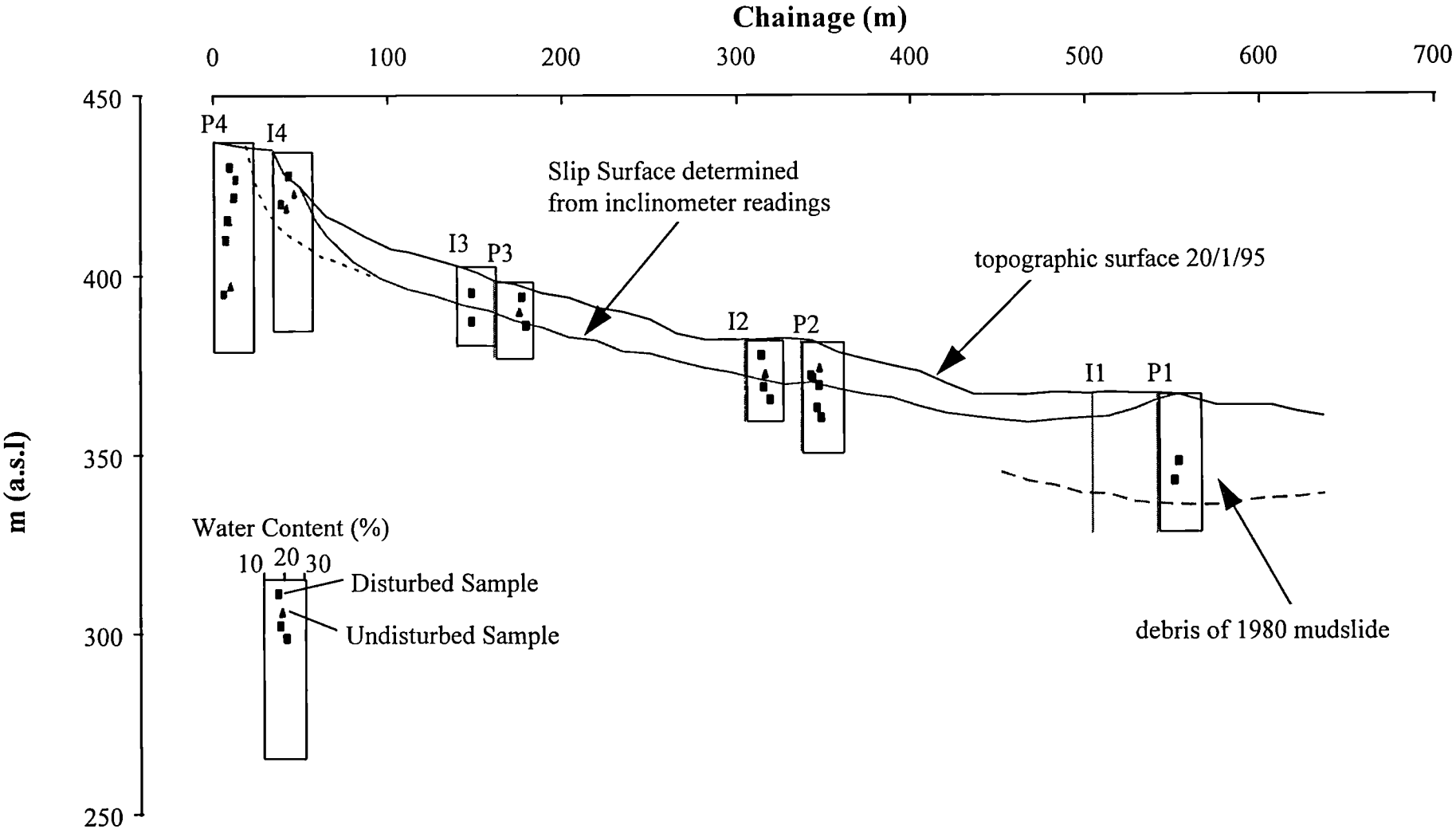

Figure 4.8 The distribution of water contents across the landslide site.

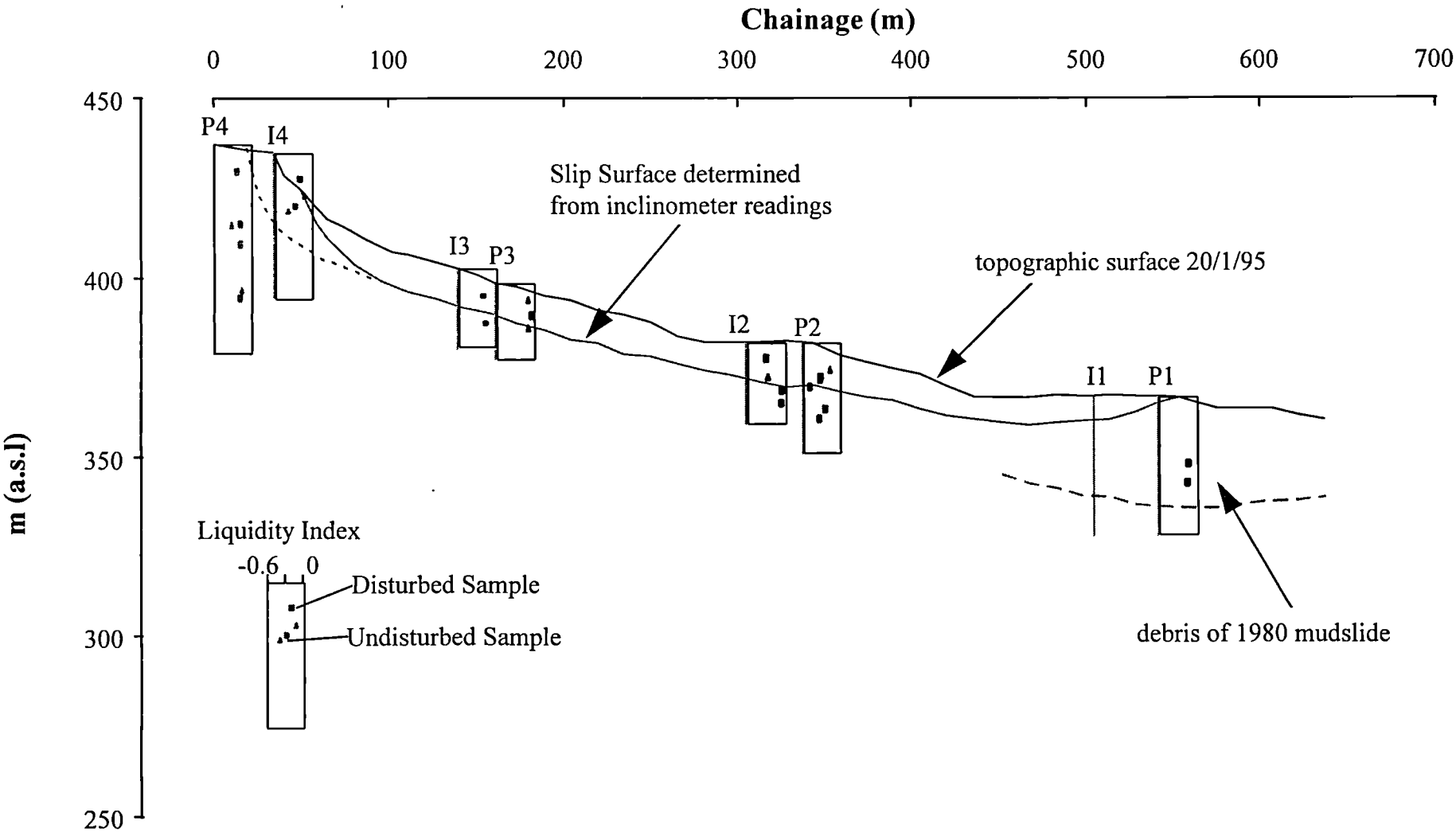

Figure 4.9 The distribution of liquidity indices across the landslide site.

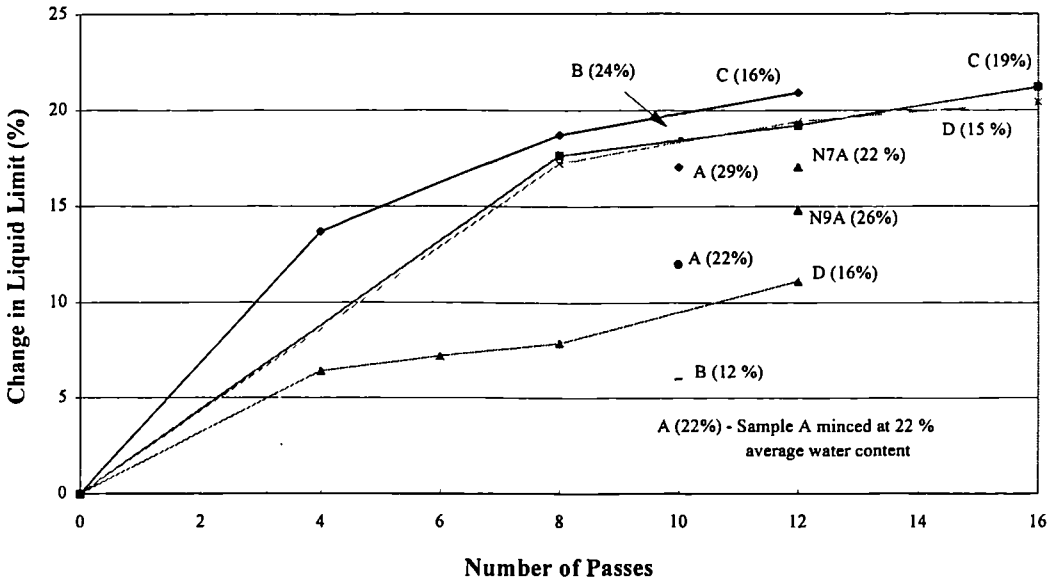

Figure 4.10 Graph showing the increase in liquid limit with the number of times a soil sample was passed through an industrial food mincer.

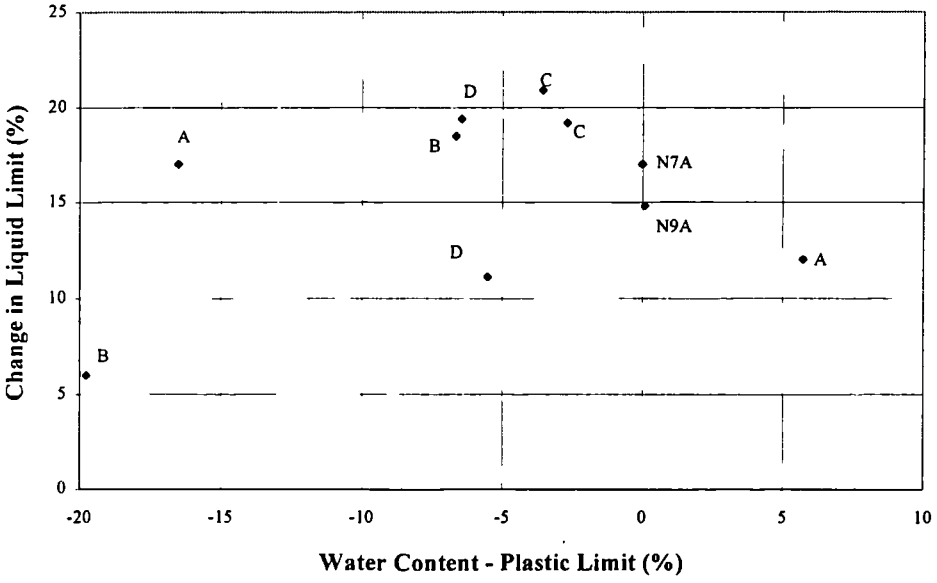

Figure 4.11 Graph showing the relationship between the water content at which the sample is minced and the increase in liquid limit.

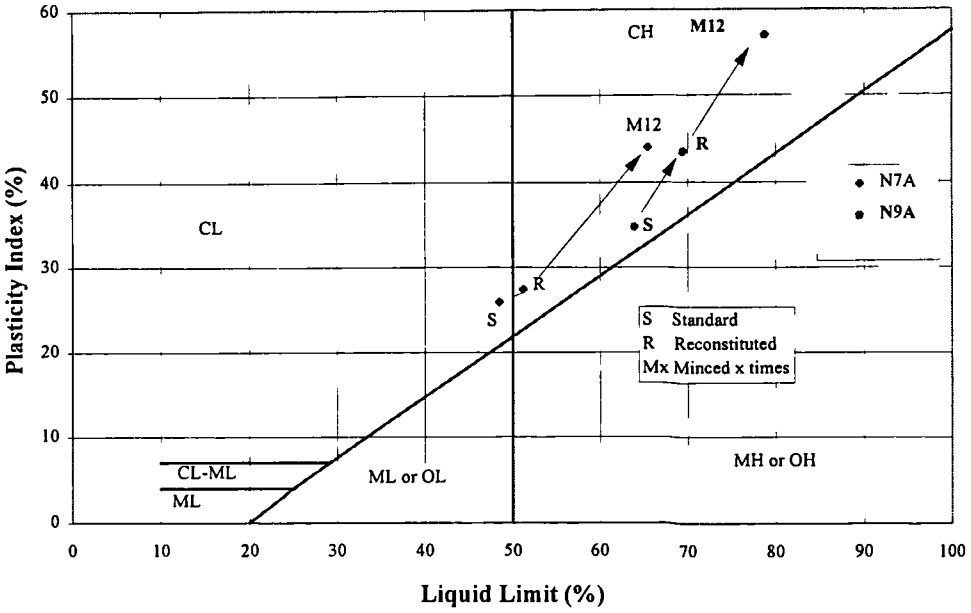

Figure 4.12 Plasticity chart showing the increase in plasticity index with reconstitution and mincing for Samples N7A and N9A

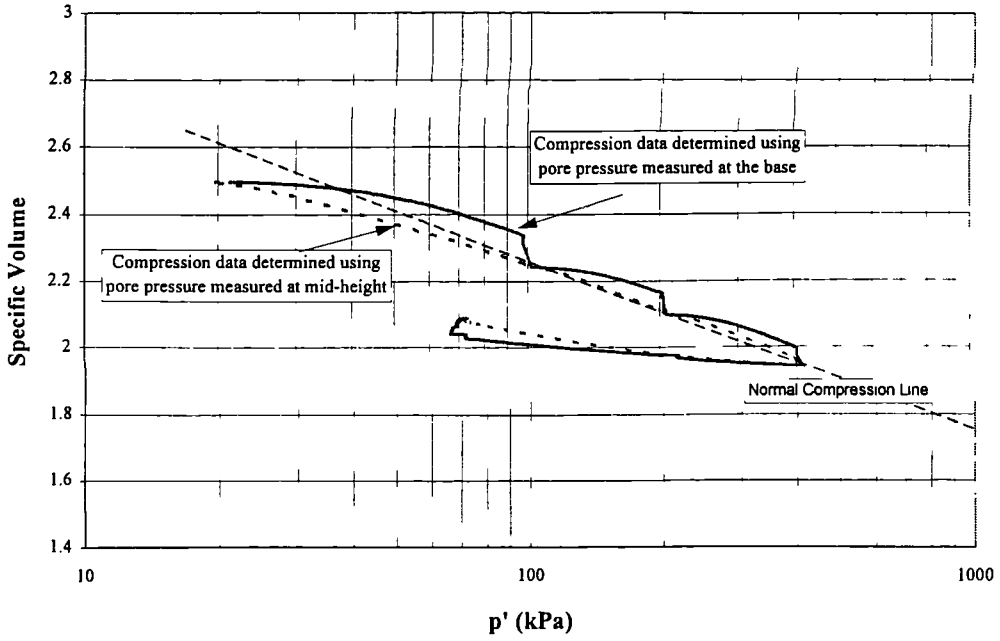

Figure 4.13 Compression data for the reconstituted sample R8A.

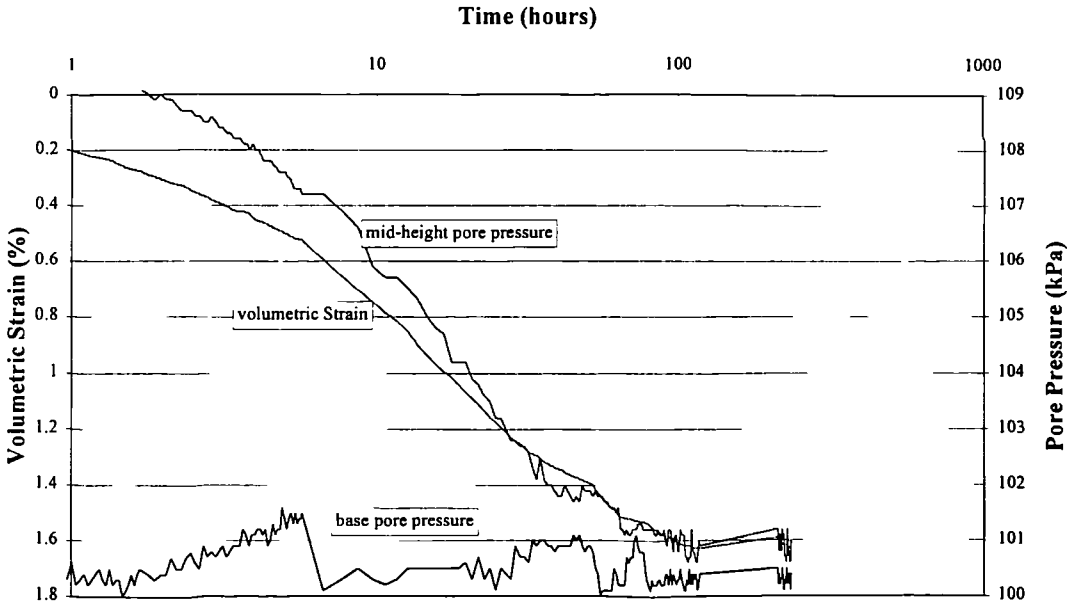

Figure 4.14 Volumetric strains and base and mid-height pore pressures resulting from a one-step consolidation (p' increasing from 10 to 20 kPa) of Sample R8A.

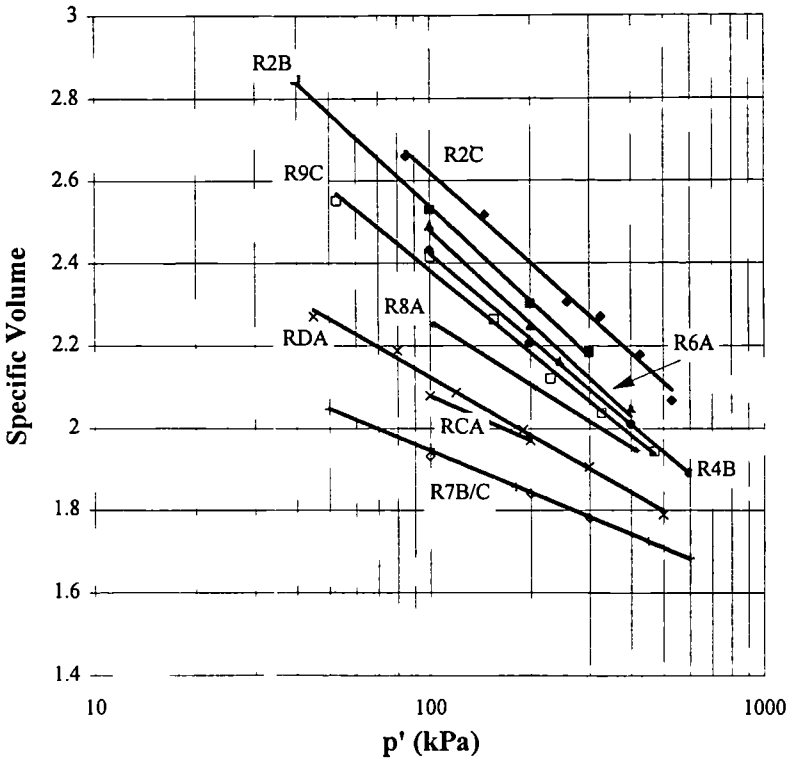

Figure 4.15 The normal compression lines of the reconstituted samples.

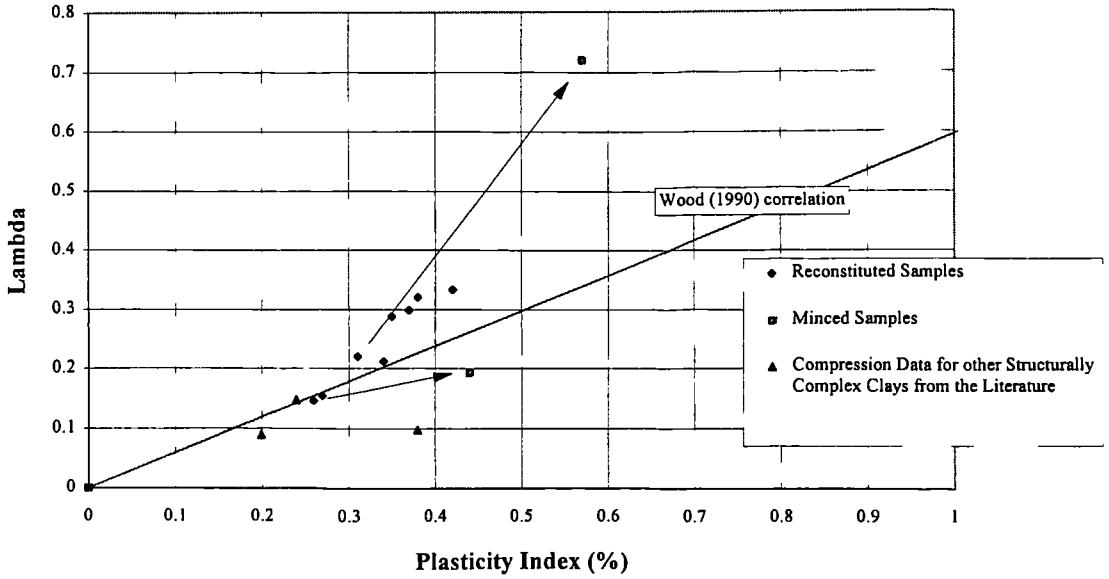

Figure 4.16 Comparison of compressibility with plasticity index. Additional data from Picarelli (1991) and Gueriero et al. (1995).

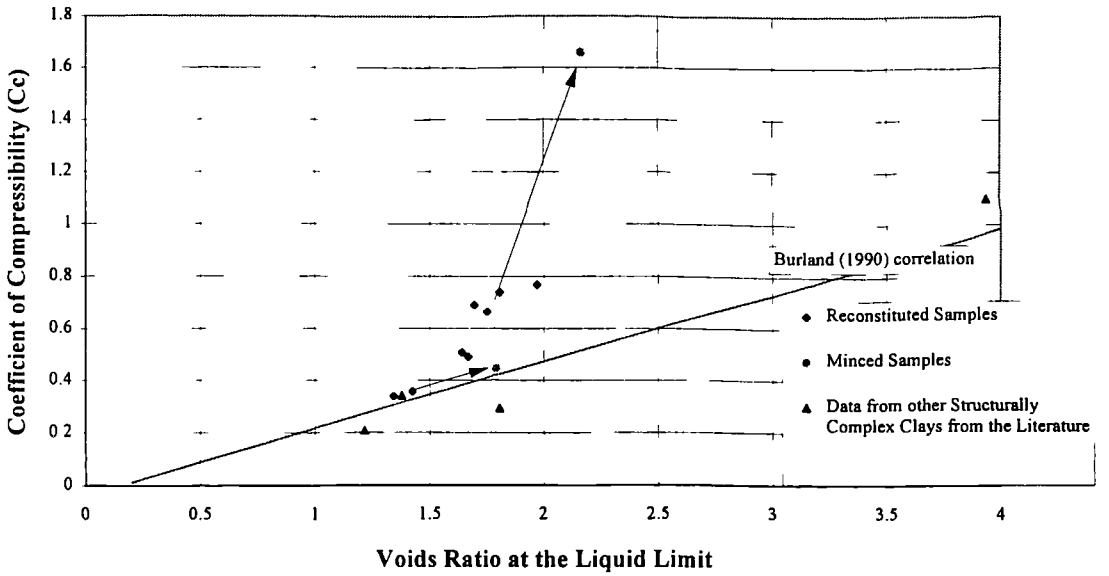

Figure 4.17 Comparison of coefficient of compressibility Cc* with the voids ratio at the liquid limit. Additional data from Picarelli (1991) and Gueriero et al. (1995).

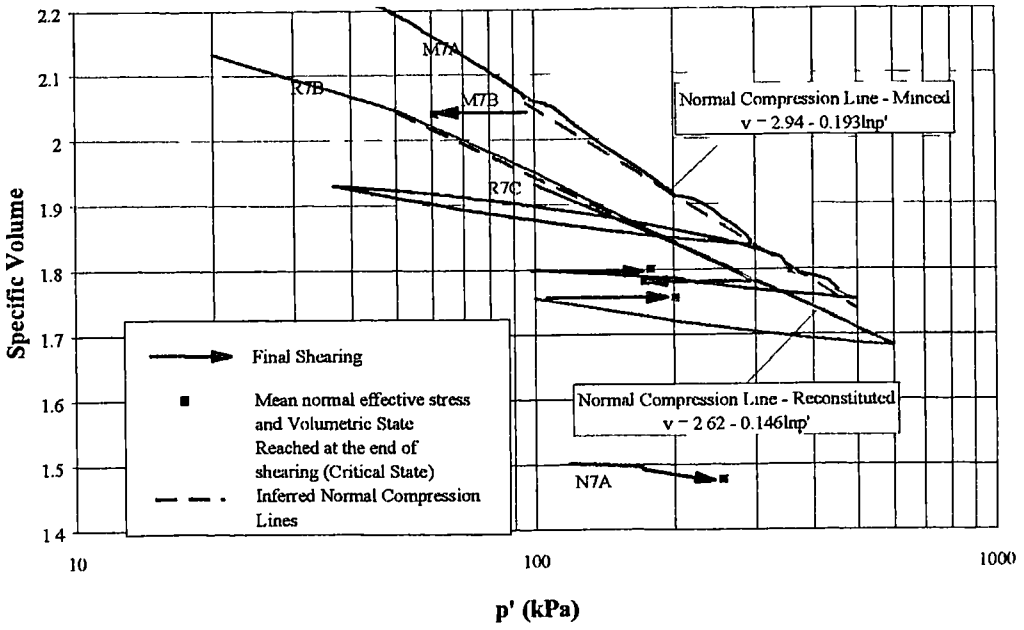

Figure 4.18 Compression data for the reconstituted and minced samples from sample group 7.

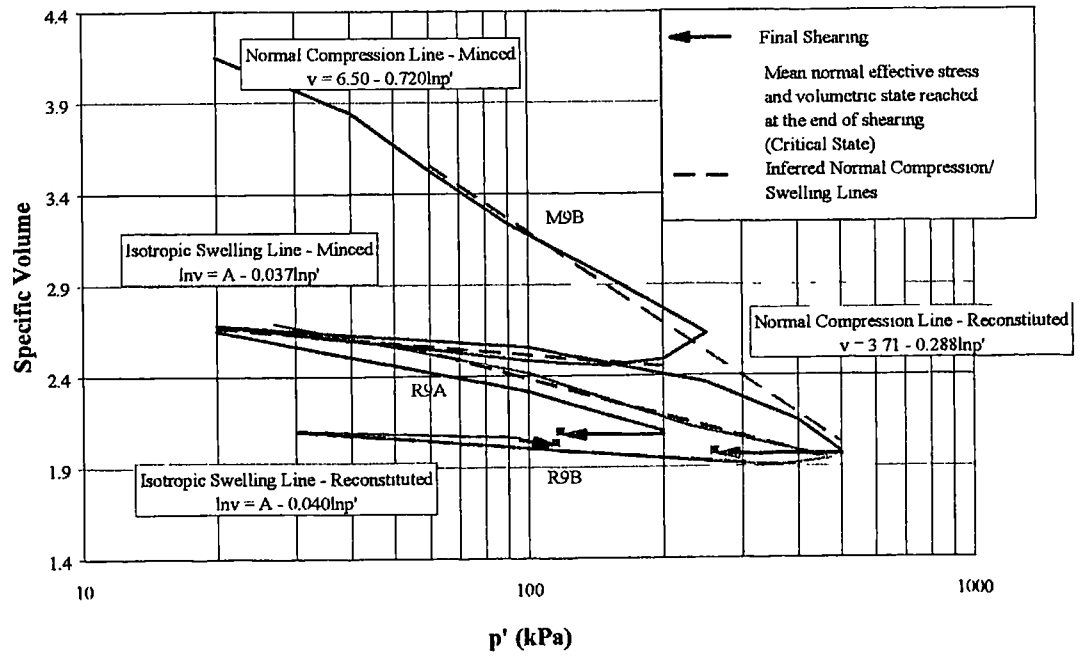

Figure 4.19 Compression data for the reconstituted and minced samples from sample group 9.

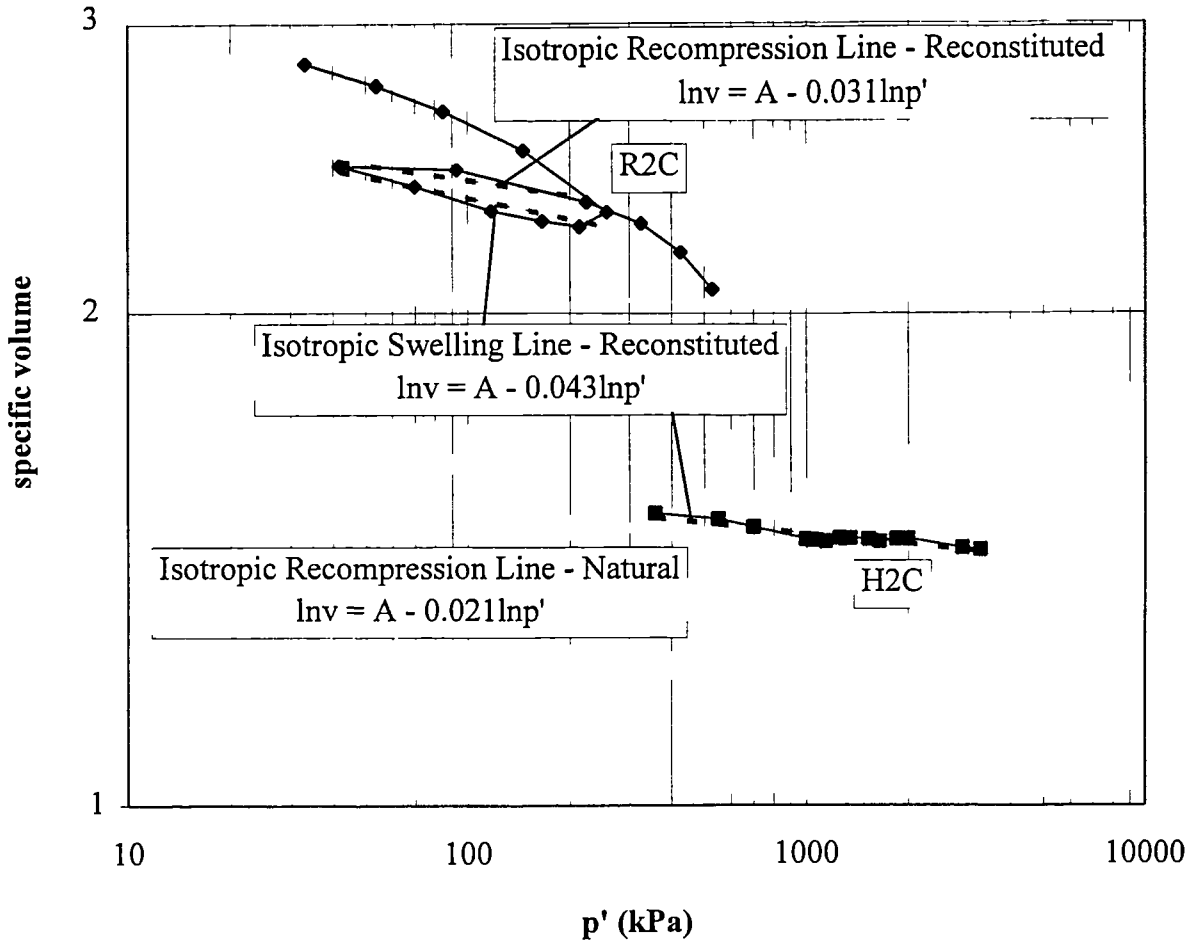

Figure 4.20 Compression data for the natural and reconstituted samples from Sample Group 2

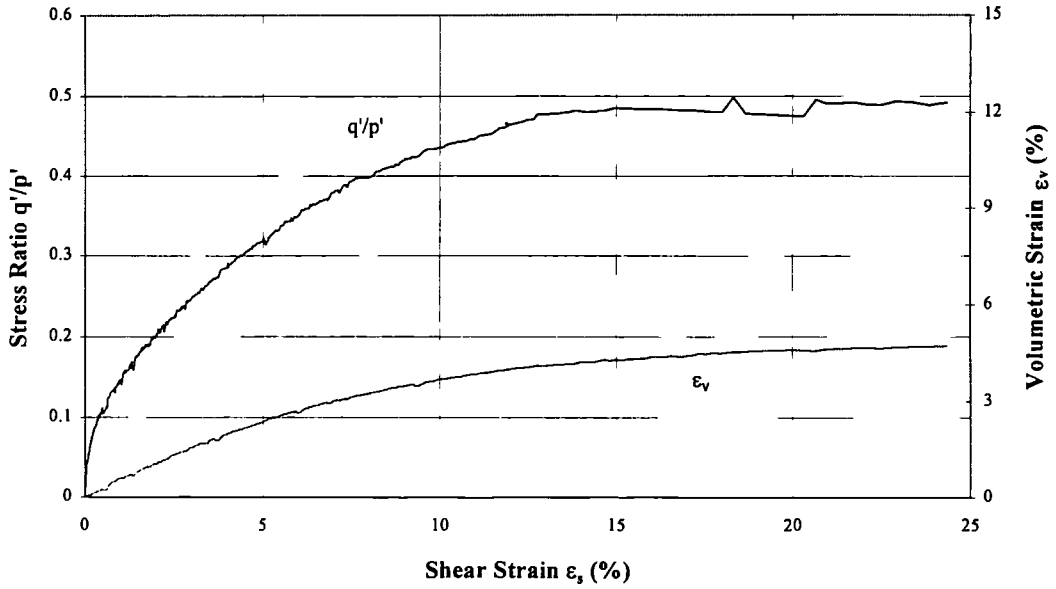

Figure 4.21 Final drained shearing: Sample R2B (p' = 300 kPa)

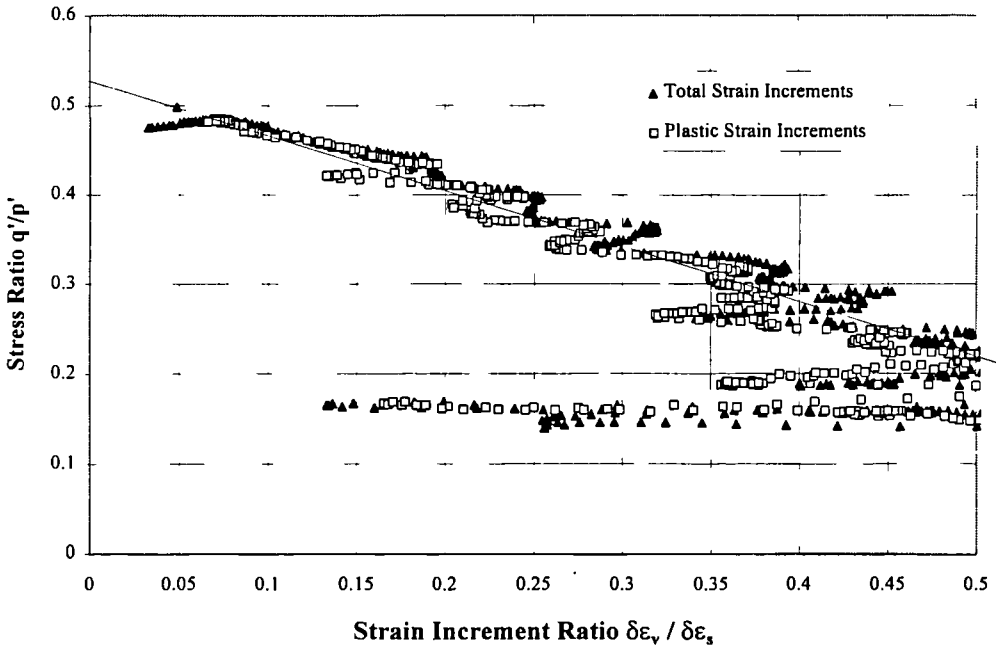

Figure 4.22 Stress-dilatancy data for Sample R2B

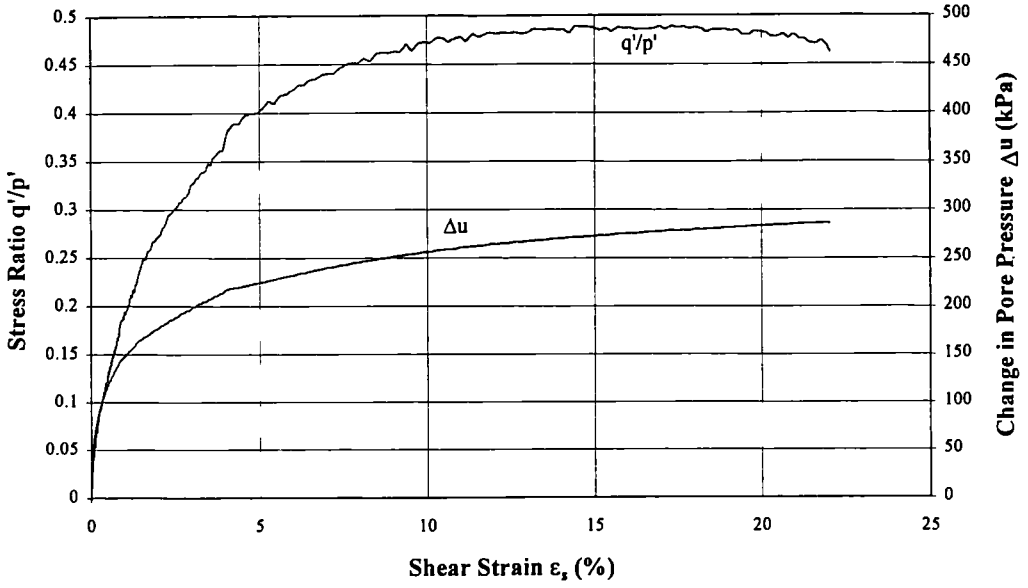

Figure 4.23 Final undrained shearing: Sample R2C (p' = 530 kPa)

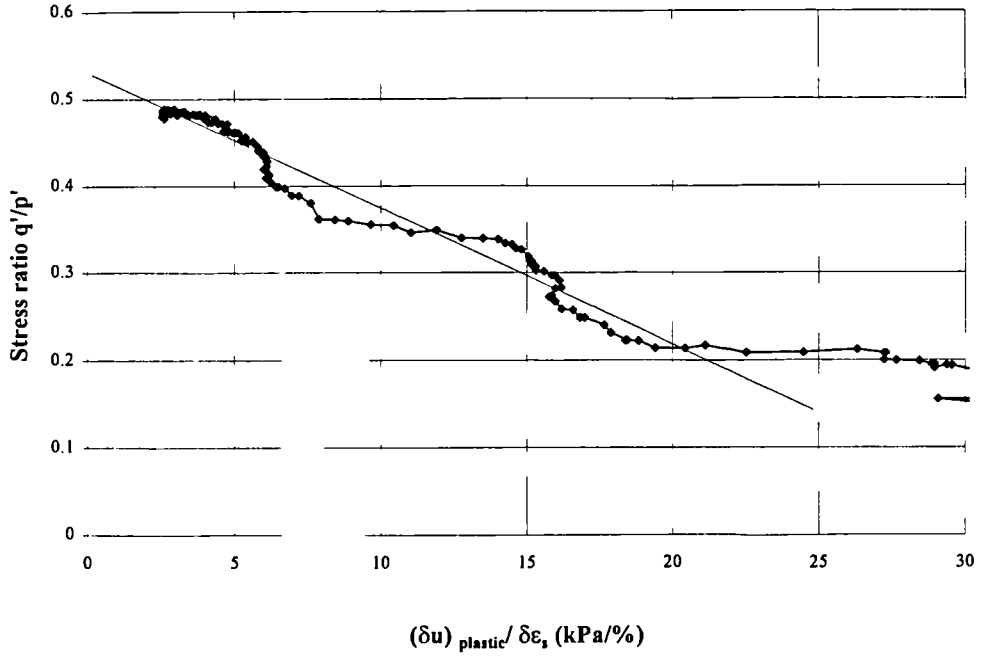

Figure 4.24 Rate of change of the plastic component of the pore pressure (δu_p) and shear strain ($\delta \varepsilon_s$) with the stress ratio (q'/p') for Sample R2C

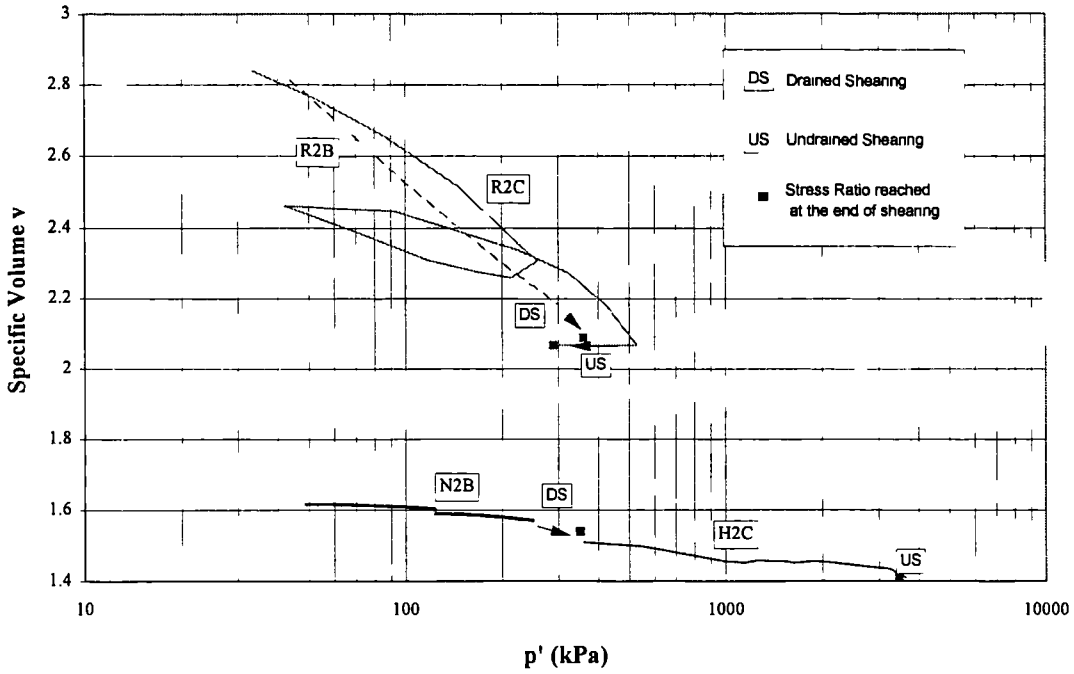

Figure 4.25 Compression and shear behaviour of the reconstituted and natural samples in v-lnp' space from sample group 2.

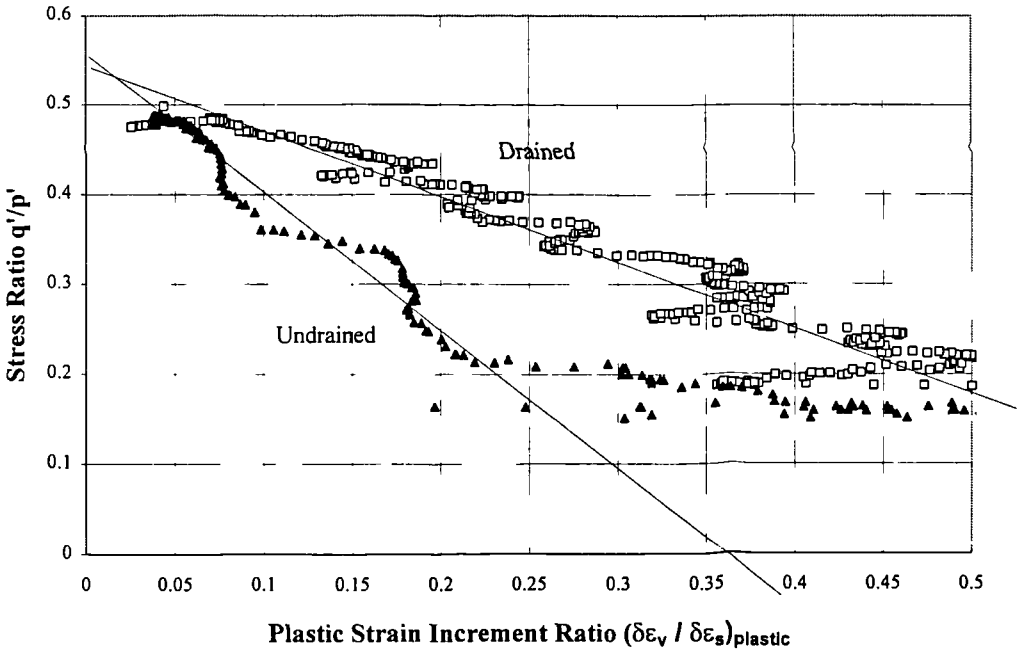

Figure 4.26 Stress-dilatancy relationships for the drained sample R2B and the undrained sample R2C.

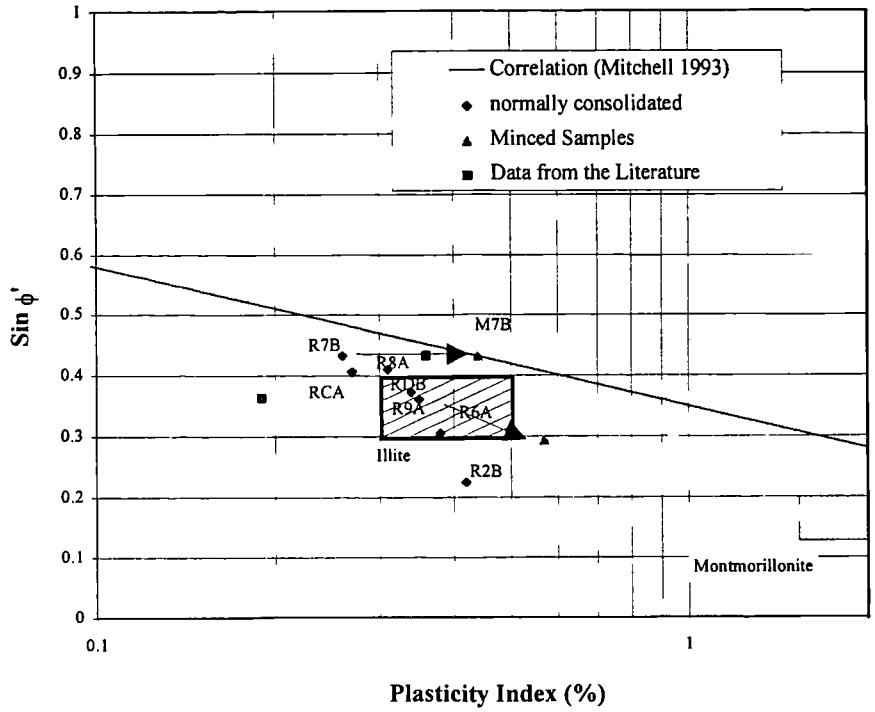

Figure 4.27 Correlation between critical state friction angles and the plasticity indices for the reconstituted samples sheared undrained from a normally consolidated state. Additional data from Guerriero et al. (1995) and Iaccarino et al. (1995).

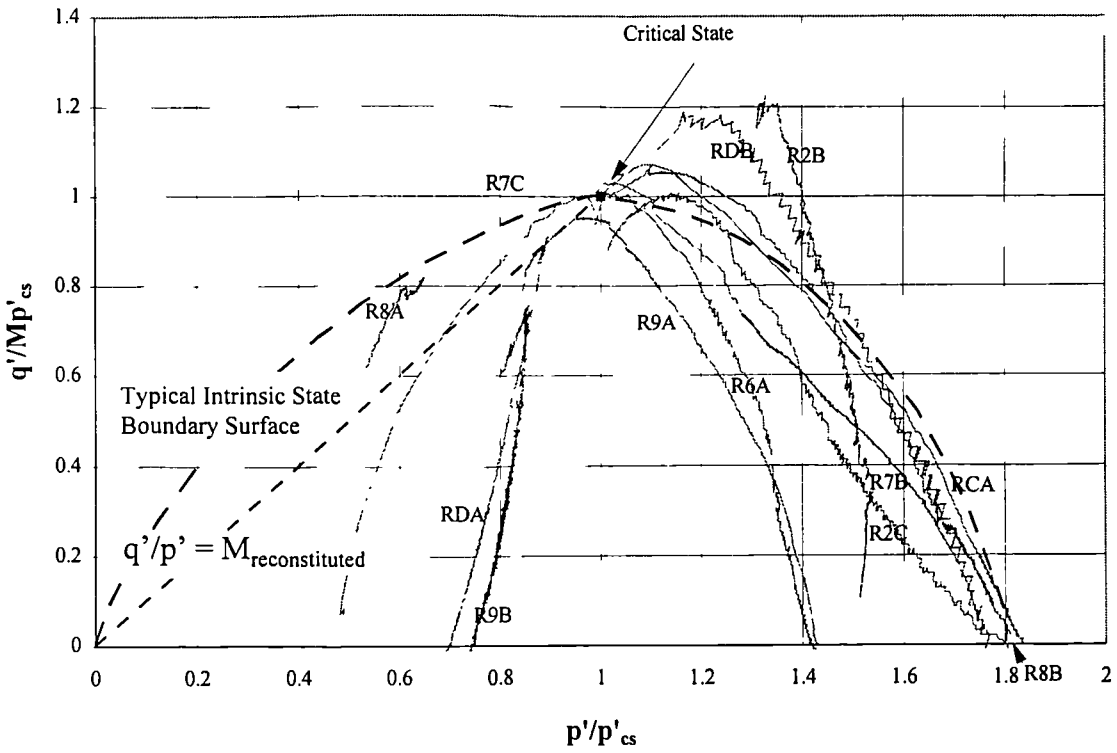

Figure 4.28 Normalised stress paths for the reconstituted samples

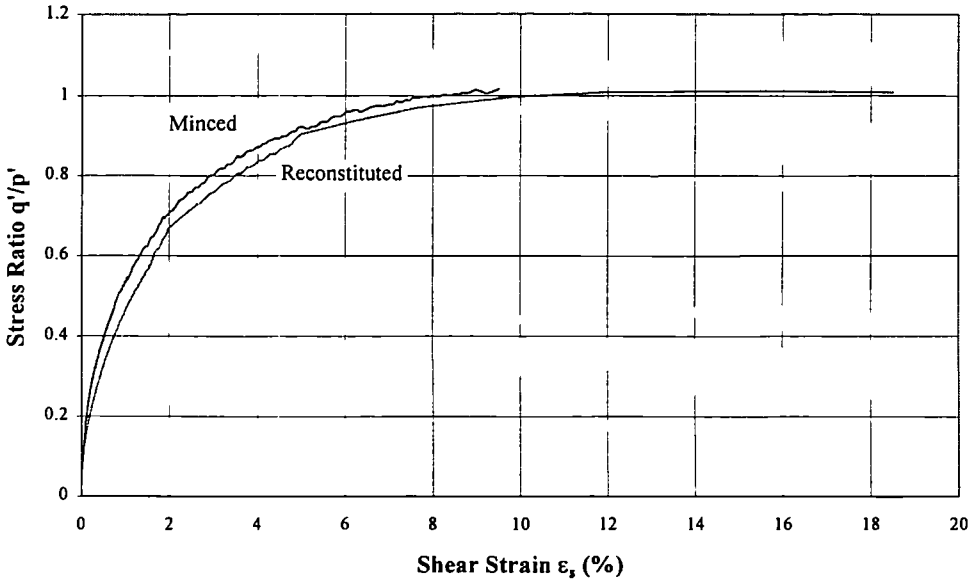

Figure 4.29 Final undrained shearing of reconstituted sample R7C and minced sample M7B.

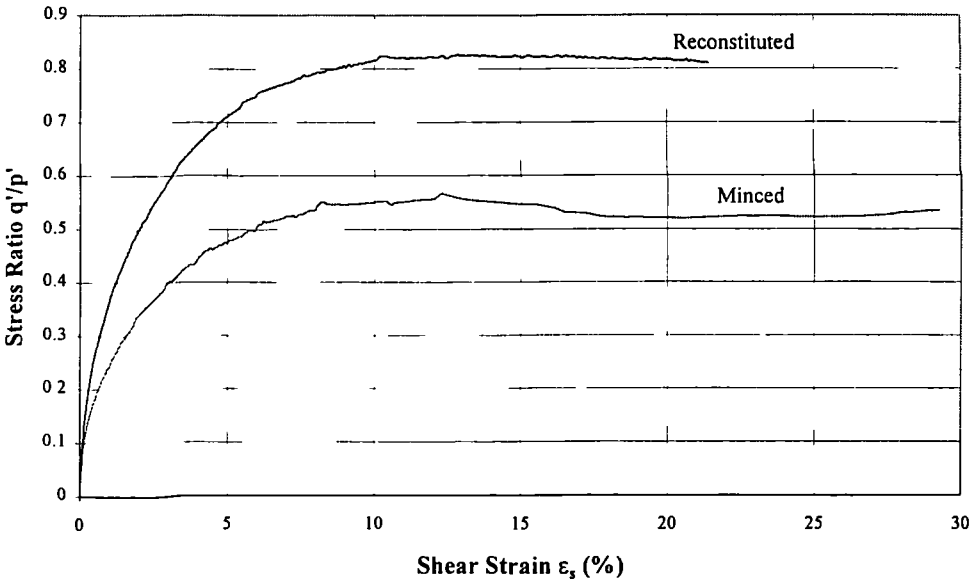

Figure 4.30 Final undrained shearing of reconstituted sample R9A and minced sample M9C.

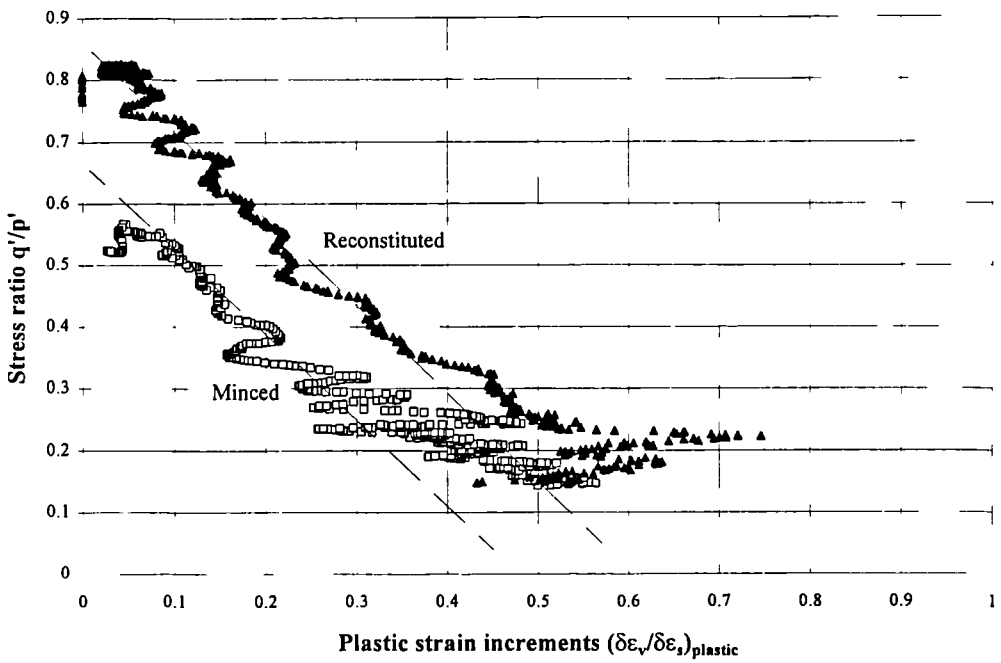

Figure 4.31 Stress-dilatancy relationships for the reconstituted sample R9A and minced sample M9C.

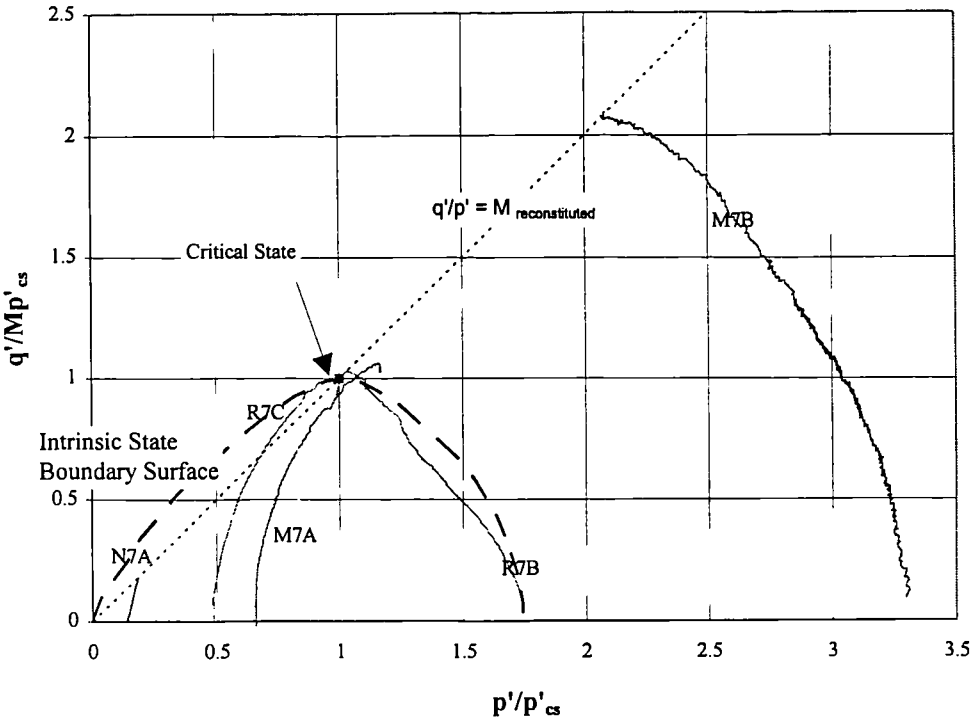

Figure 4.32 Normalised Stress Paths for samples from group 7

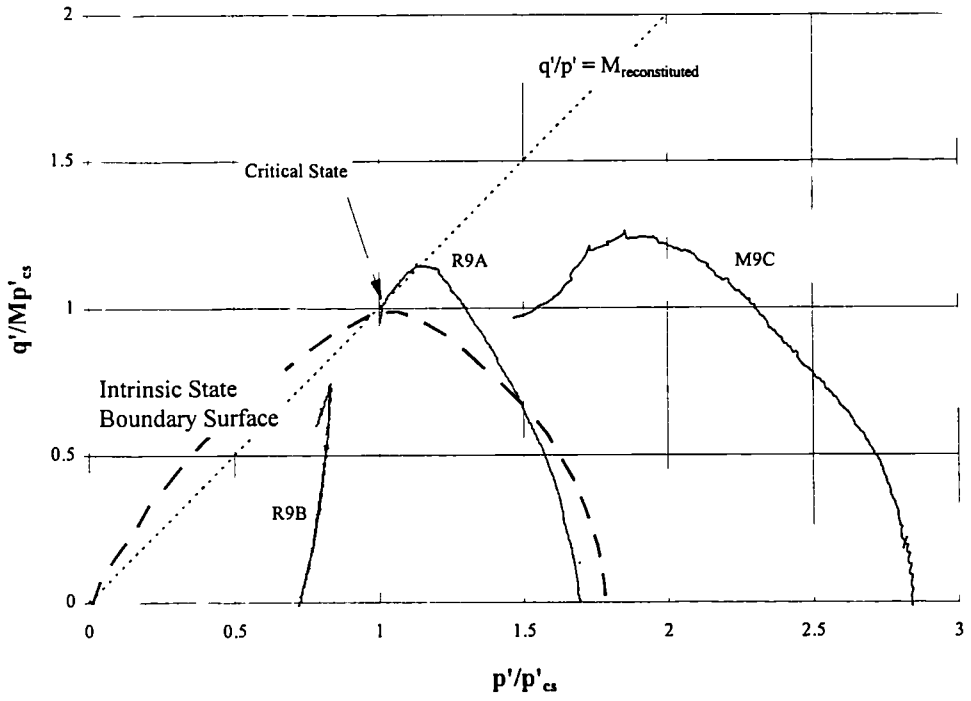

Figure 4.33 Normalised Stress Paths for samples from group 9

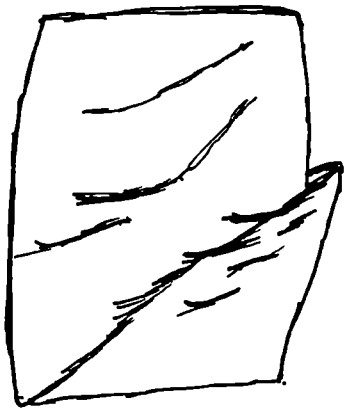

a)

b)

Figure 4.34 Sketches of failed natural samples a) with well-defined slip surface b) with multiple failure surfaces

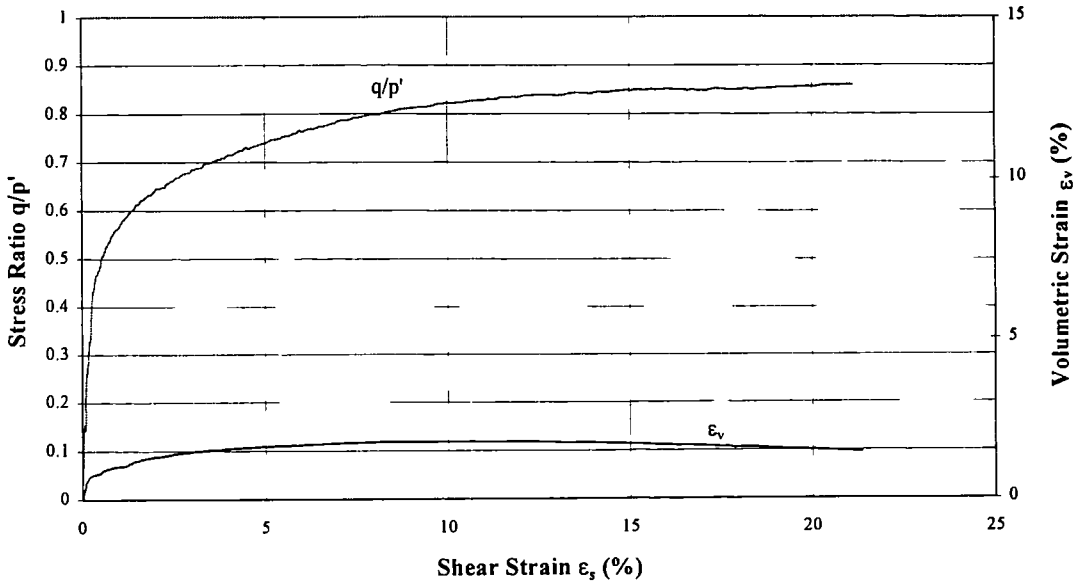

Figure 4.35 Final drained shearing: Sample N2B (initial p' = 250 kPa)

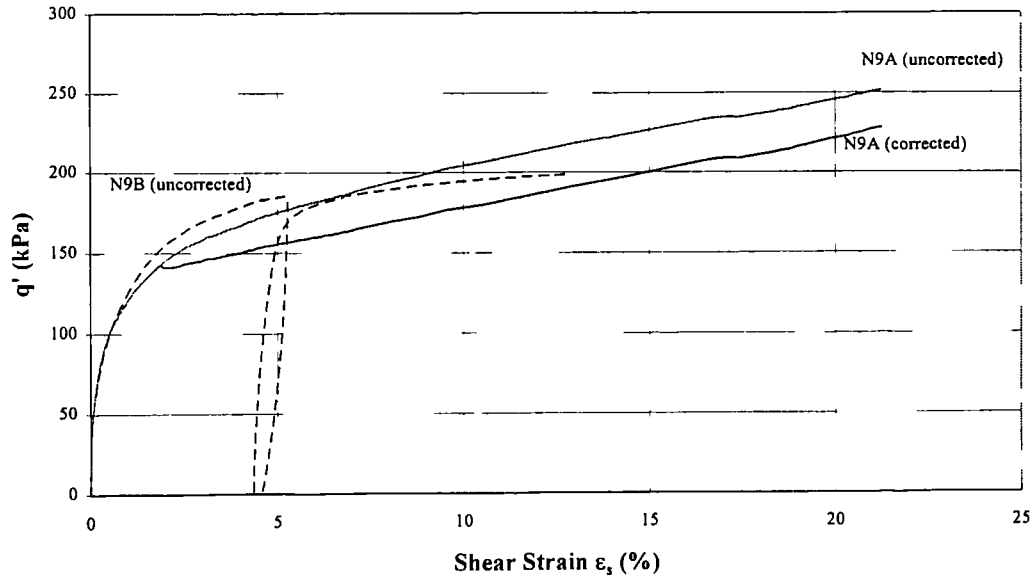

Figure 4.36 Final drained shearing: Samples N9A and N9B (initial p' = 290 kPa) Sample N9A corrected for membrane constraint and change in cross-sectional area as a result of slip plane formation.

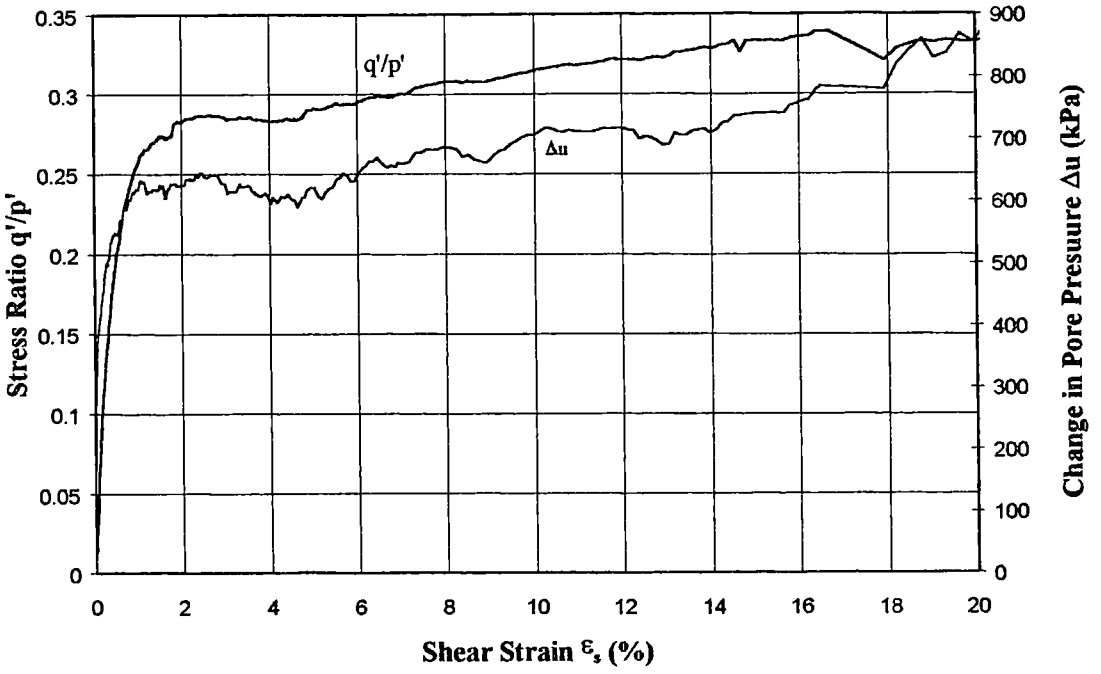

Figure 4.37 Final undrained shearing: sample H2C (initial p' = 3600 kPa)

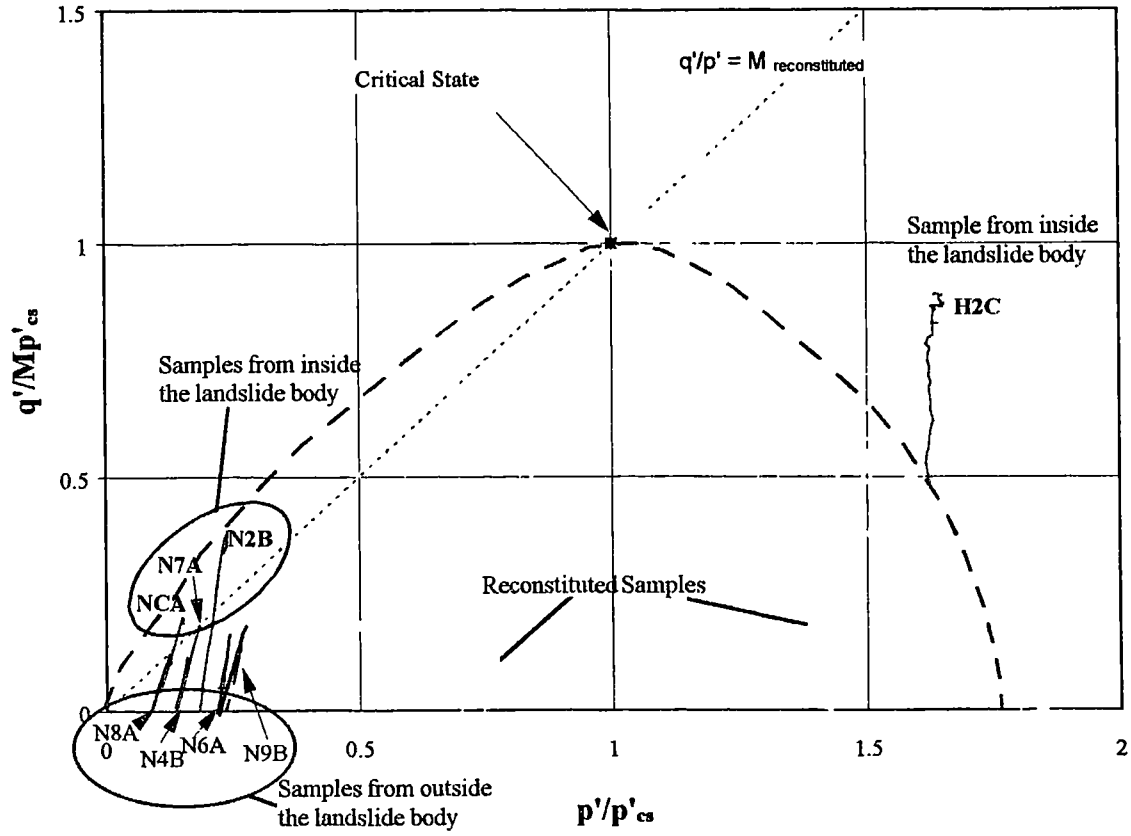

Figure 4.38 Normalised stress paths for the natural and reconstituted samples

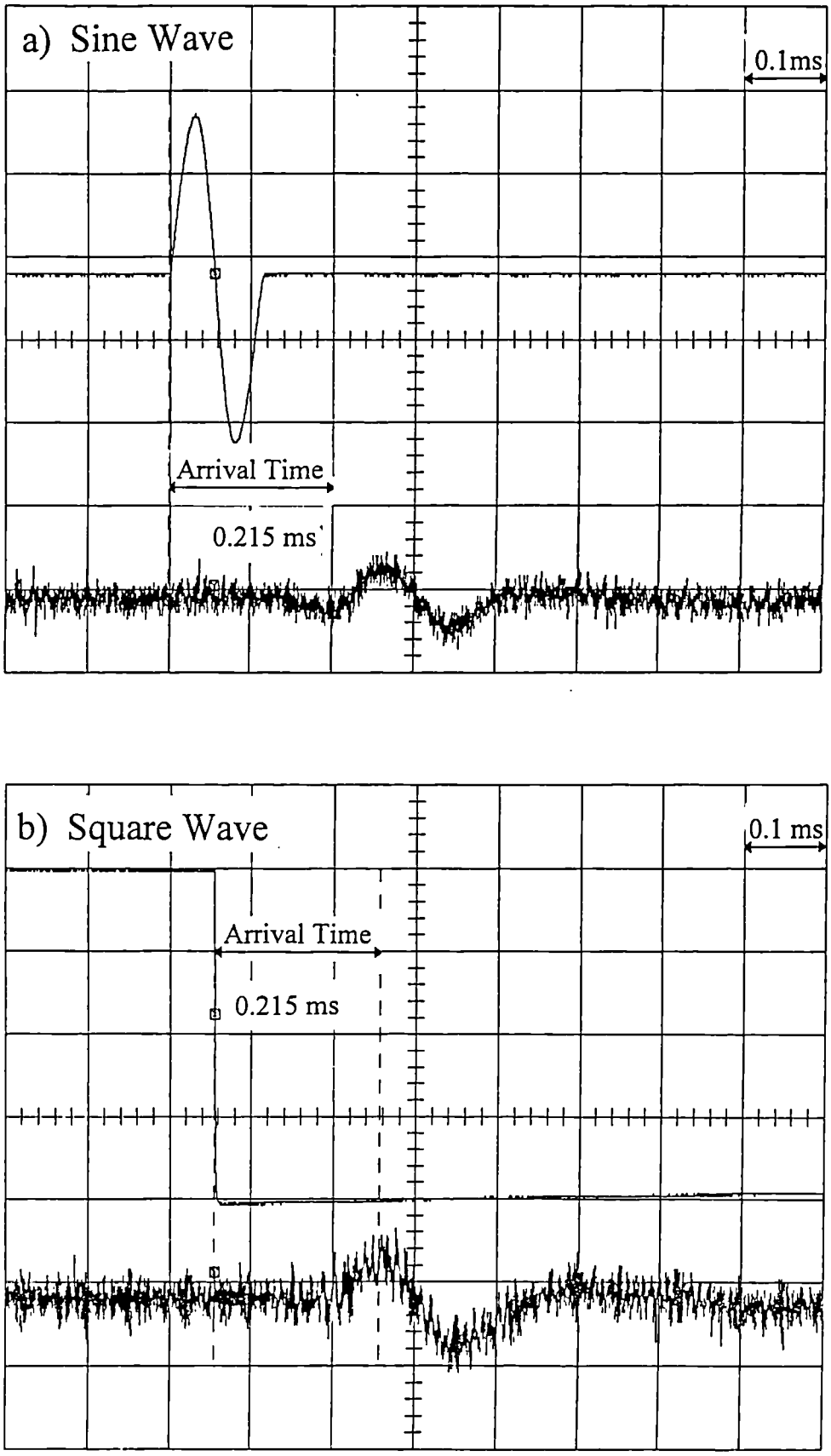

Figure 4.39 Oscilloscope traces showing the shear wave arrival times from the bender element tests

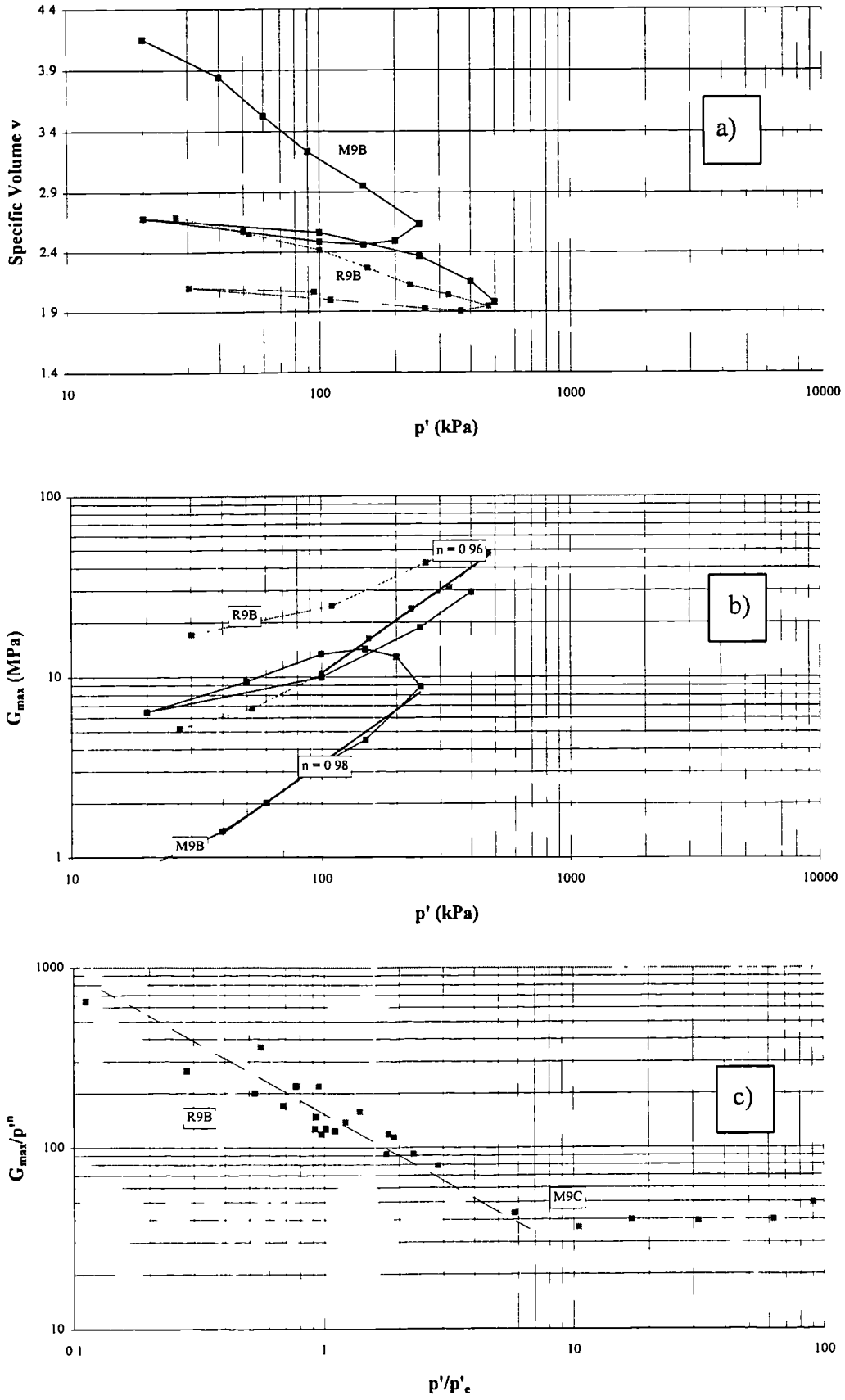

Figure 4.40 Data from bender element tests: for the minced sample (M9C) and reconstituted sample (R9B) from sample Group 9.
a) stress and volumetric state at which readings were taken.
b) G_{max} values measured.
c) normalised stiffness data determined

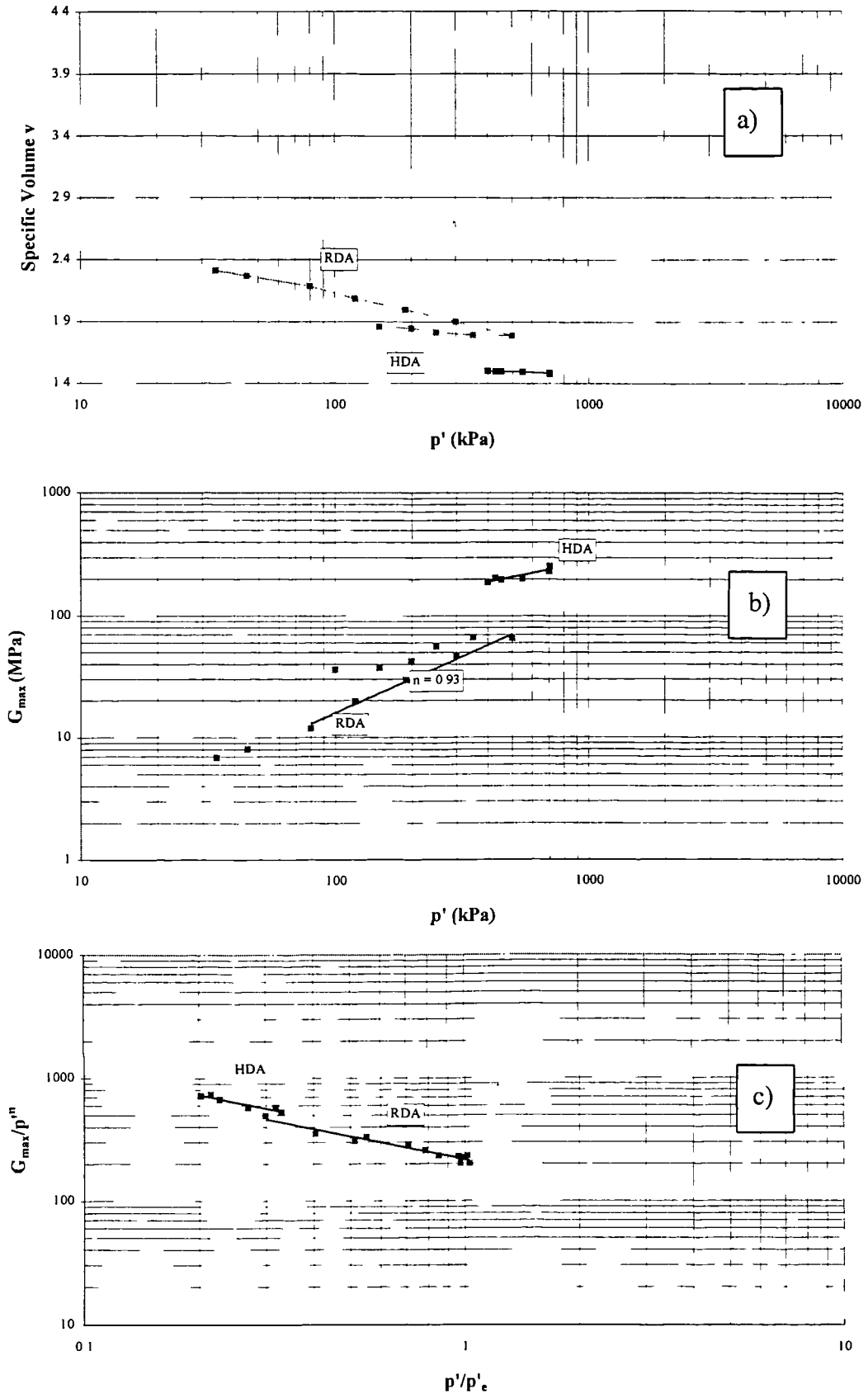

Figure 4.41 Data from bender element tests: for the natural sample (HDA) and reconstituted sample (RDA) from sample Group D.
a) stress and volumetric state at which readings were taken
b) G_{max} values measured
c) normalised stiffness data determined

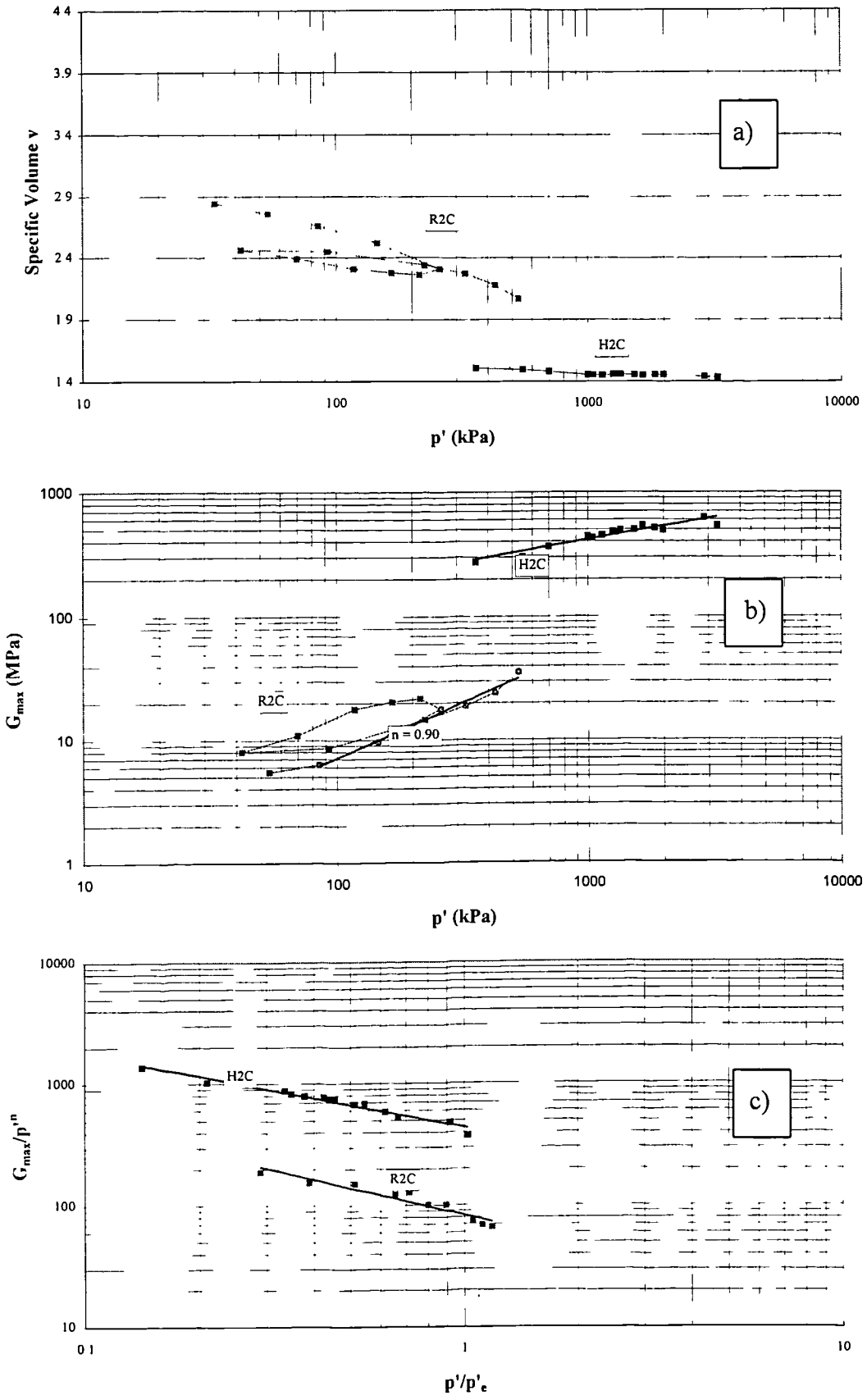

Figure 4.42 Data from bender element tests: for the natural sample (H2C) and reconstituted sample (R2C) from sample Group 2.
a) stress and volumetric state at which readings were taken
b) G_{max} values measured
c) normalised stiffness data determined

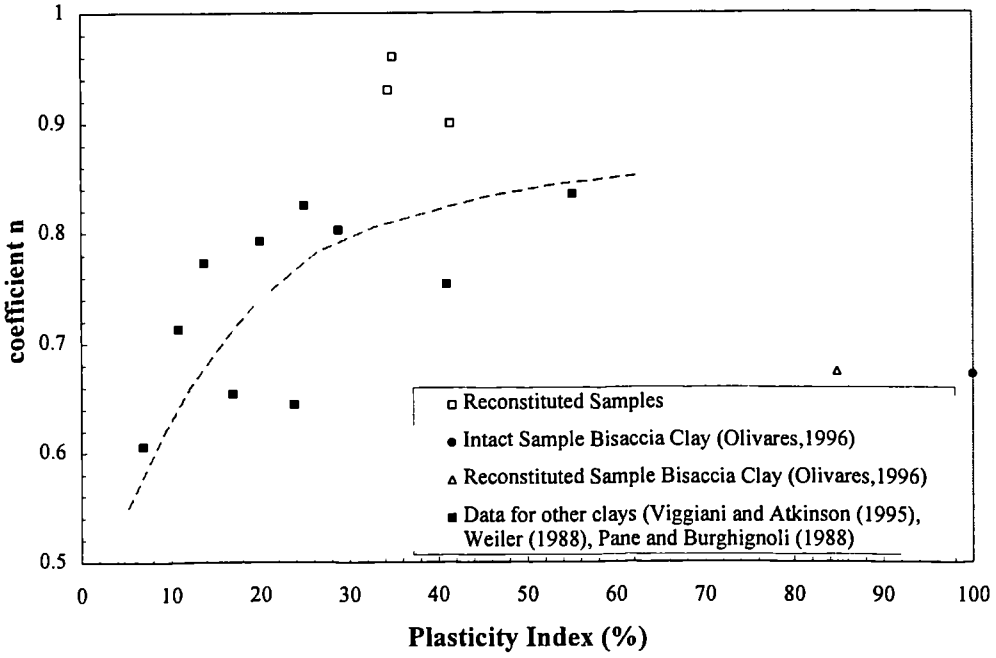

Figure 4.43 Comparison of the exponent n with plasticity index
Modified after Viggiani and Atkinson (1985).

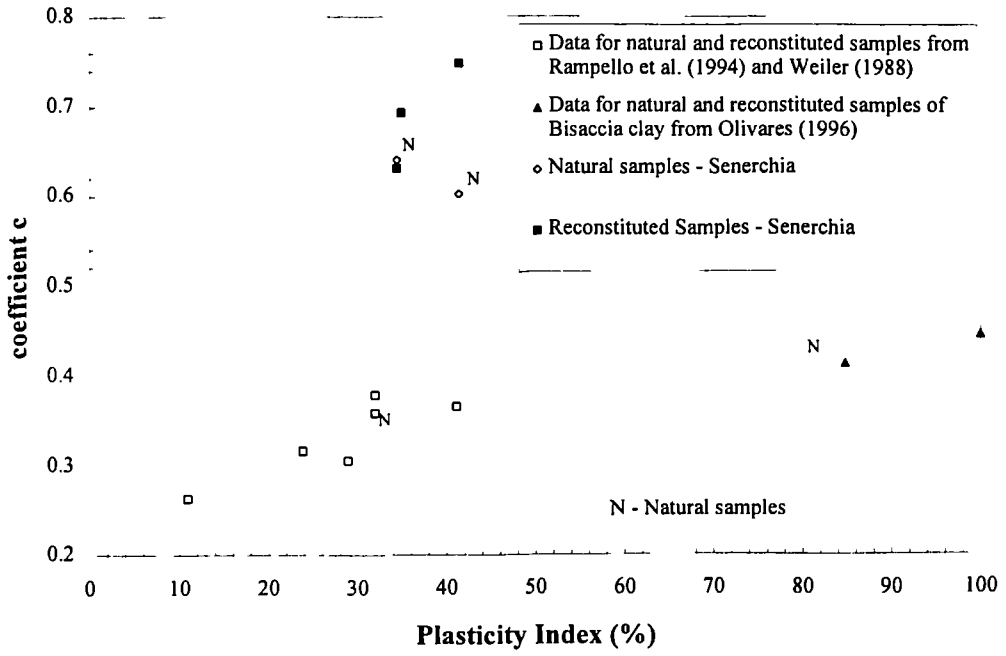

Figure 4.44 Comparison of the exponent c with plasticity index.
Modified after Olivares (1996) and Rampello et al. (1994)

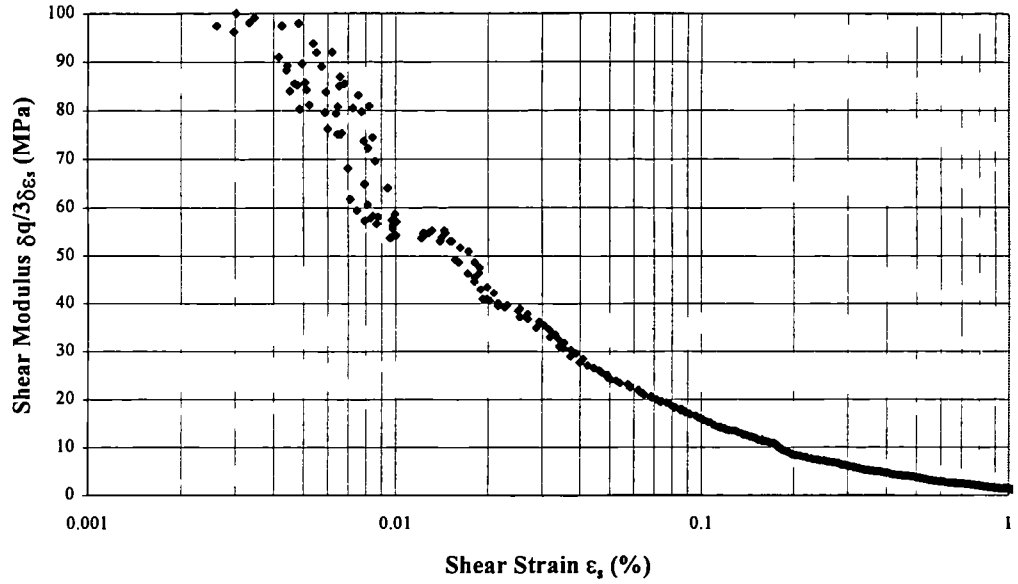

Figure 4.45 Variation of the drained shear stiffness with shear strain for the natural sample (N8A p' initial = 235 kPa)

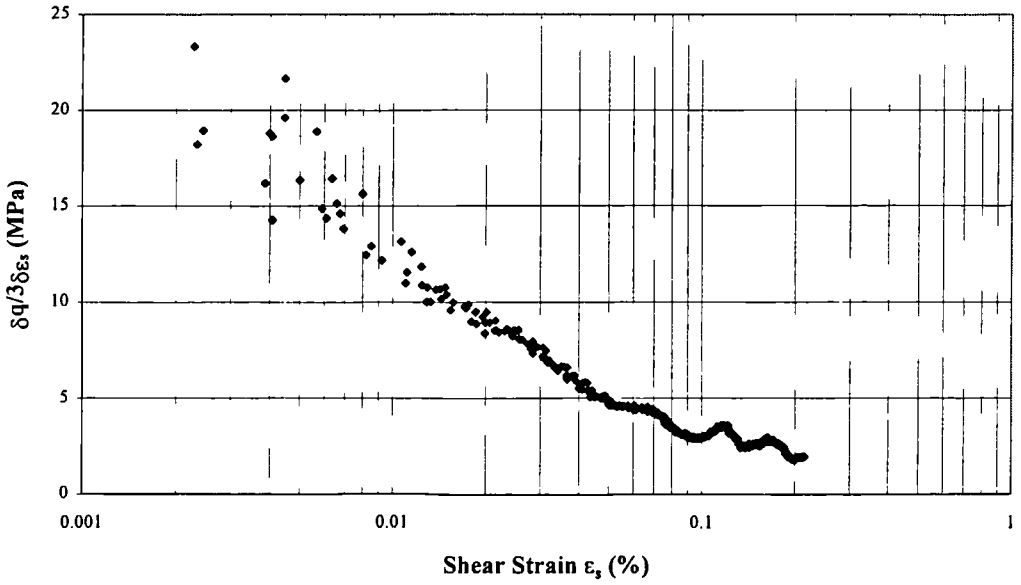

Figure 4.46 Variation of the drained shear stiffness with shear strain for the reconstituted sample (R7B p' initial = 200 kPa)

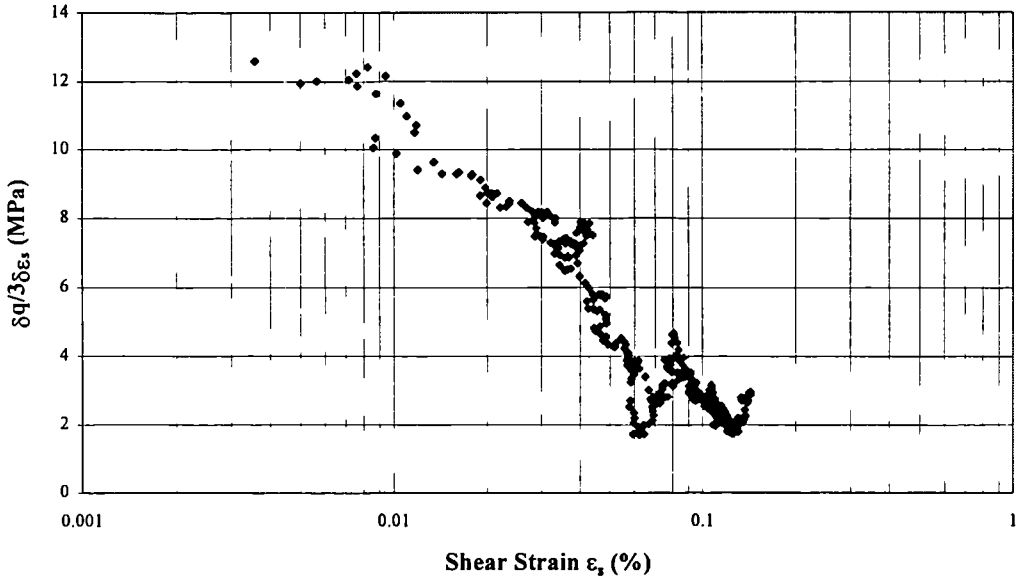

Figure 4.47 Variation of the drained shear stiffness with shear strain for the minced sample (M7B p' initial = 200 kPa)

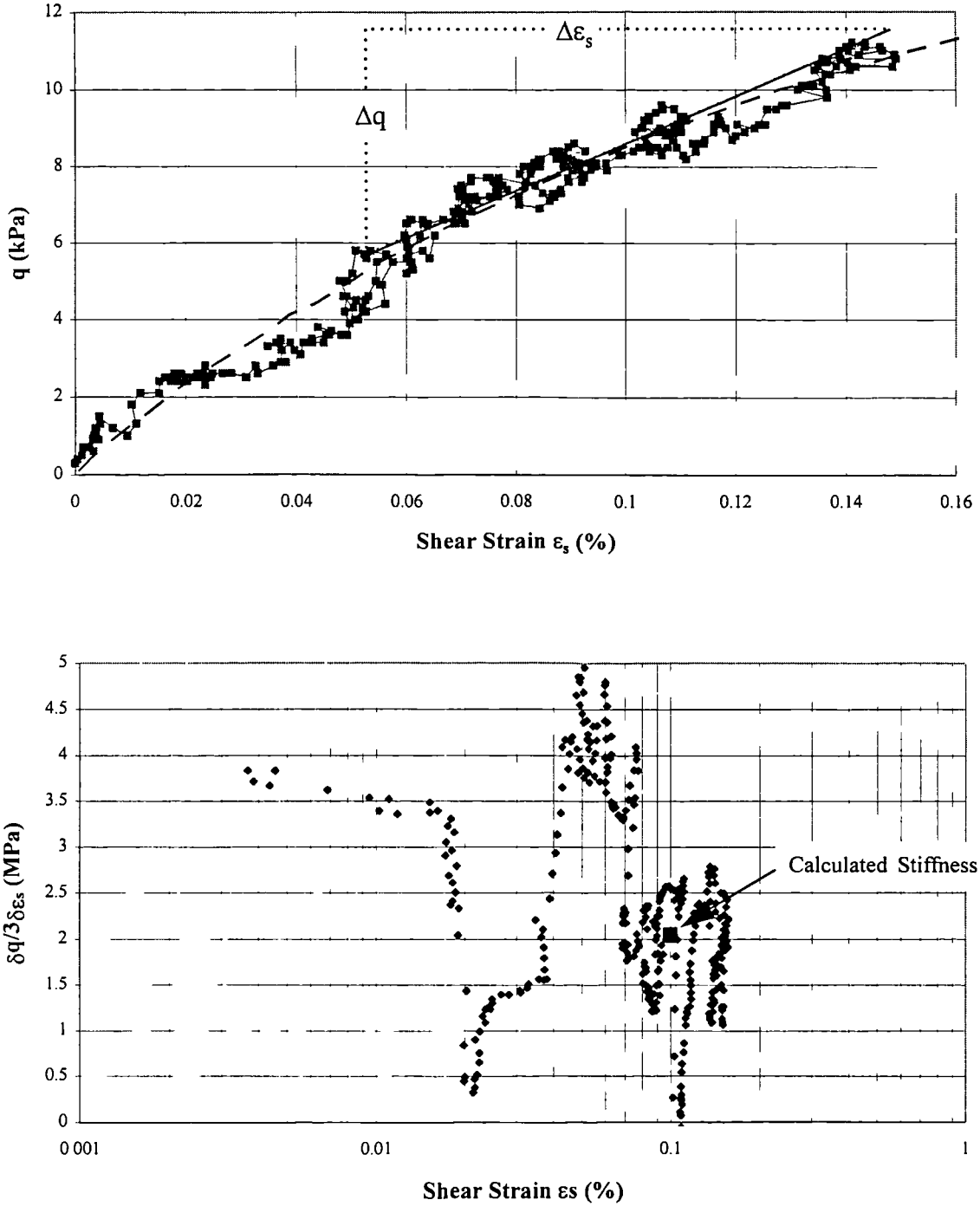

Figure 4.48 Calculation of the shear modulus where the scatter is large

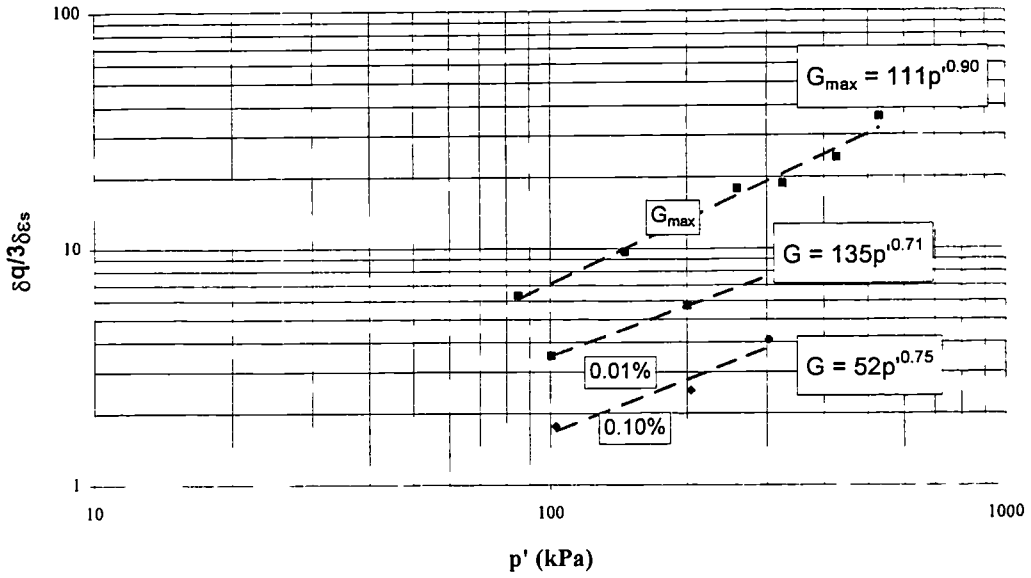

Figure 4.49 Stiffness data for the reconstituted samples from group 2.

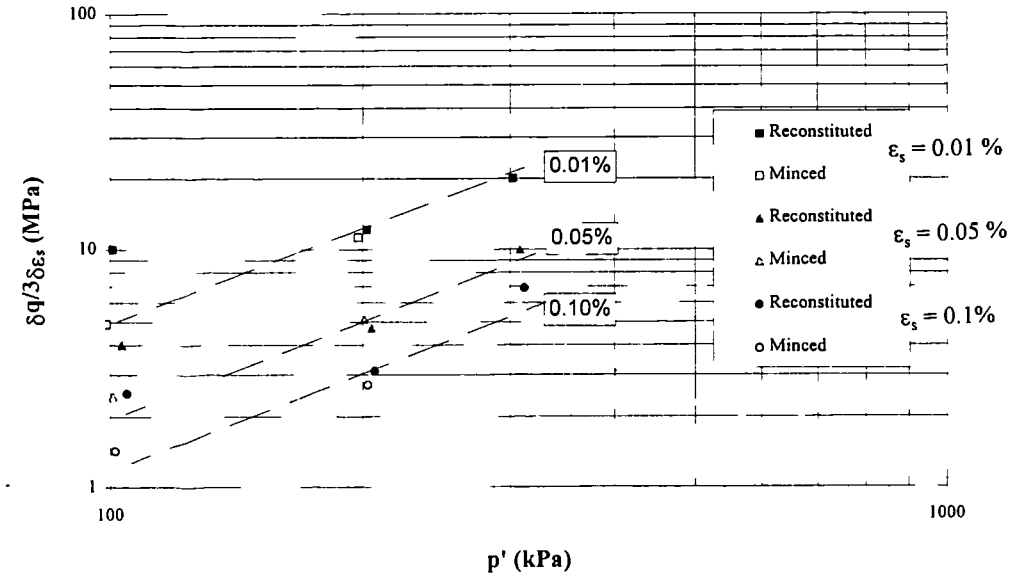

Figure 4.50 Stiffness data for the minced and reconstituted samples from group 7.

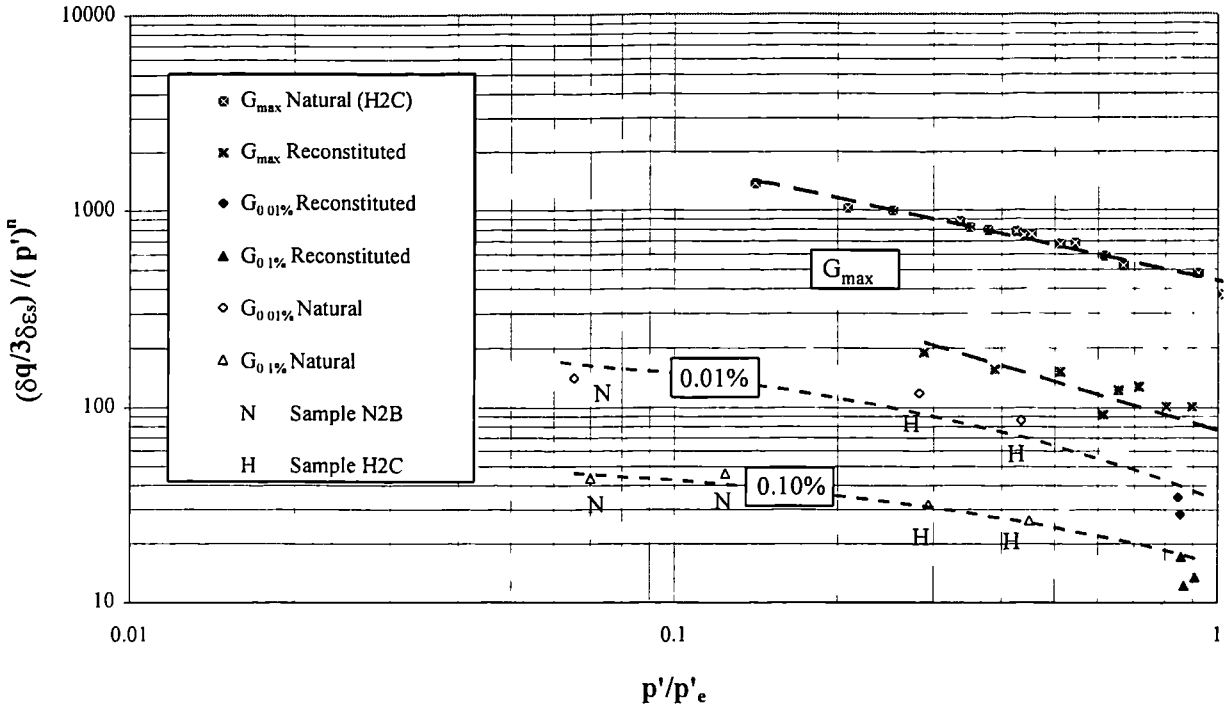

Figure 4.51 Normalised stiffness data for the natural and reconstituted samples from sample group 2.

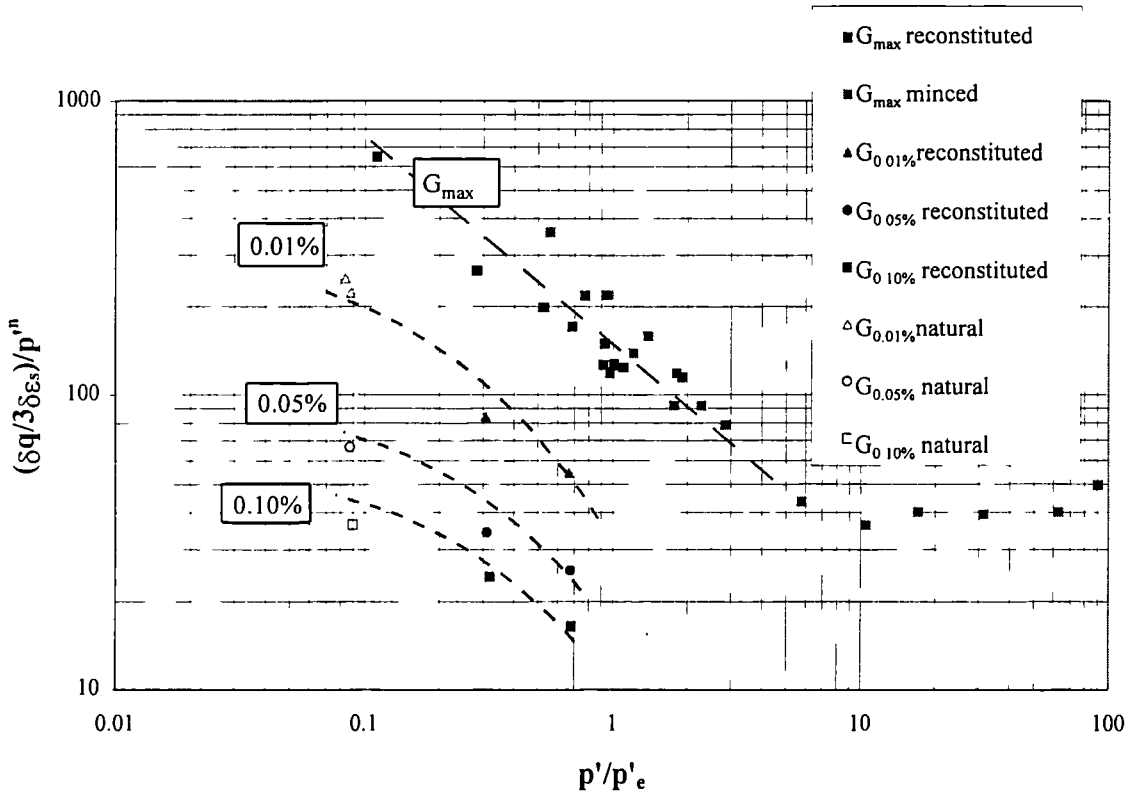

Figure 4.52 Normalised stiffness data for the natural and reconstituted samples from sample group 9.

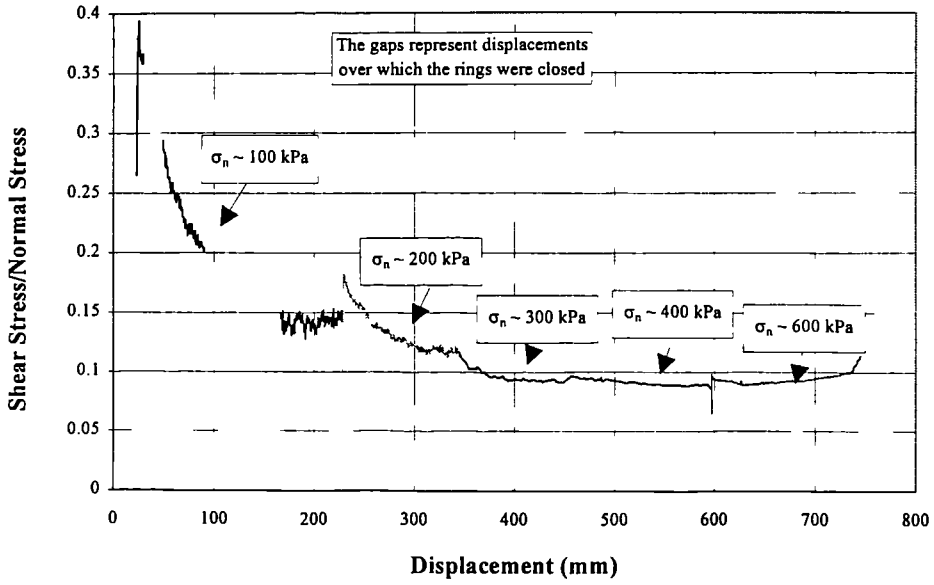

Figure 4.53 a) Residual Strength-Displacement Curve
Reconstituted Sample RS-C (P2 10.2 - 10.5 m bgl)

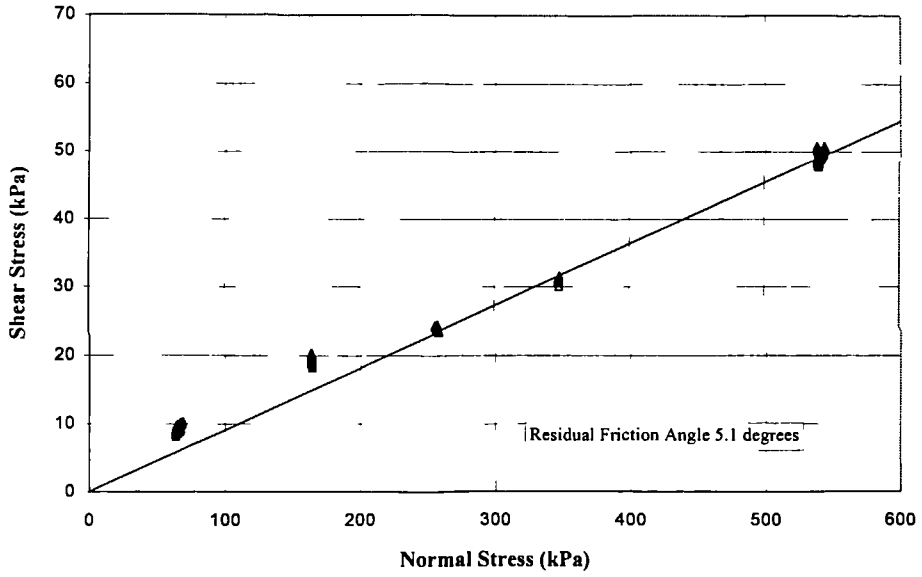

Figure 4.53 b) Residual Strength Failure Envelope
Reconstituted Sample RS-C (P2 10.2 - 10.5 m bgl)

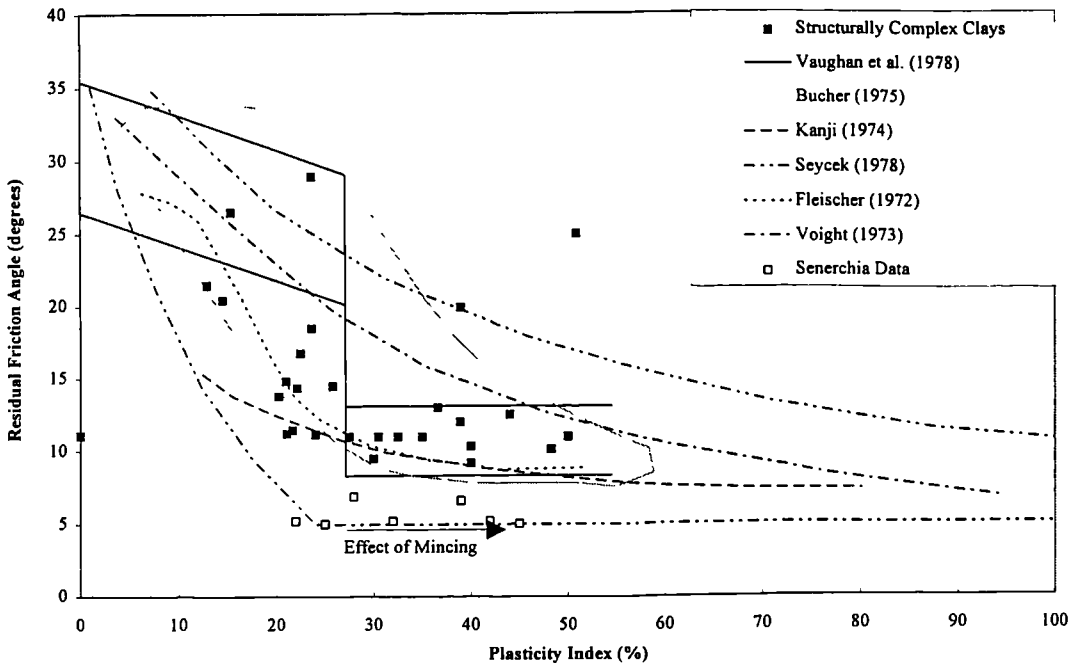

Figure 4.54 Correlations between residual strength friction angle and plasticity index modified from Lupini et al. (1981). Data for the other structurally complex clays from Cotecchia et al. (1986), Del Prete and Trisorio Liuzzi (1992), Cherubini et al. (1990, Cotecchia (1989), Hutchinson and Del Prete (1985), D'Elia (1977).

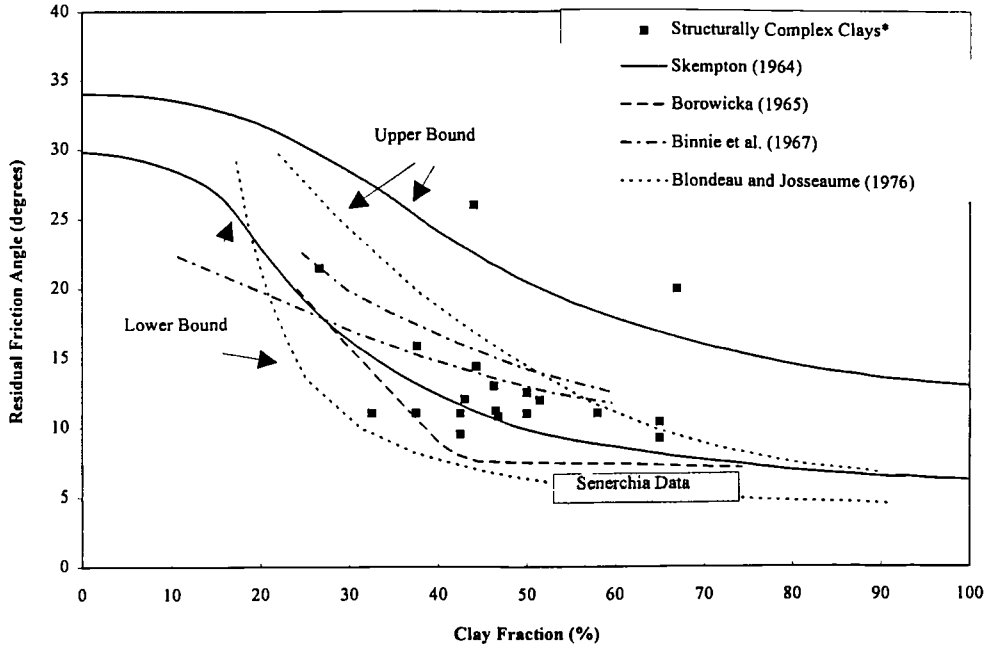

Figure 4.55 Correlations between residual strength friction angle and clay fraction modified from Lupini et al. (1981). Data for the other structurally complex clays from Cotecchia et al. (1986), Del Prete and Trisorio Liuzzi (1992), Cherubini et al. (1990, Cotecchia (1989), Hutchinson and Del Prete (1985), D'Elia (1977)

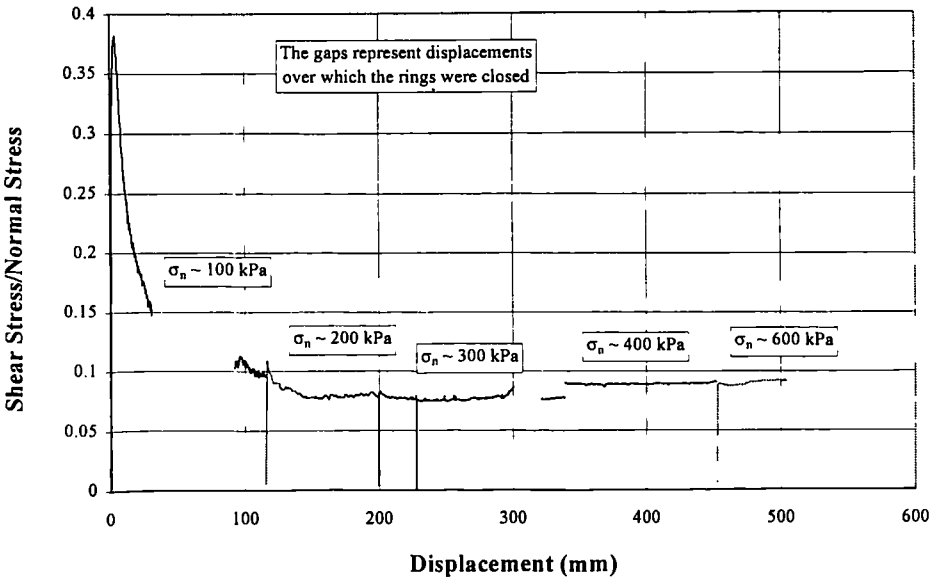

Figure 4.56 a) Residual Strength-Displacement Curve
Reconstituted Sample RS-D (I4 7.5 - 7.8 m bgl)

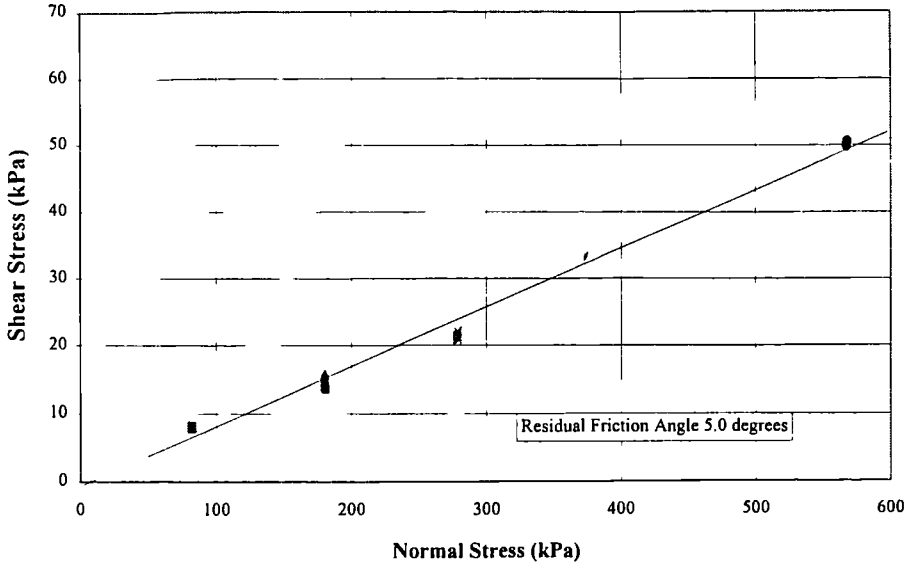

Figure 4.56 b) Residual Strength Failure Envelope
Reconstituted Sample RS-D (I4 7.5 - 7.8 m bgl)

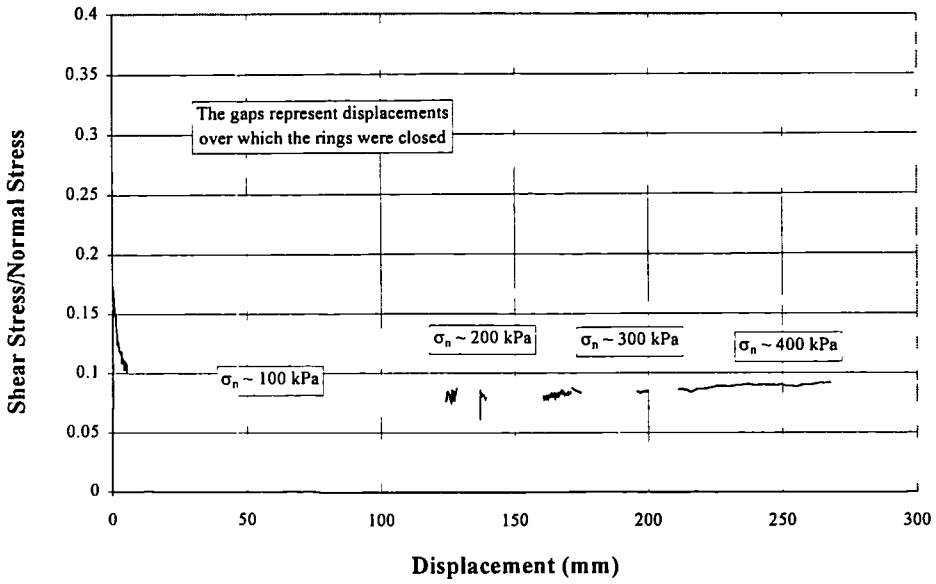

Figure 4.57 a) Residual Strength-Displacement Curve
Minced Sample RS-D(M) (I4 7.5 - 7.8 m bgl)

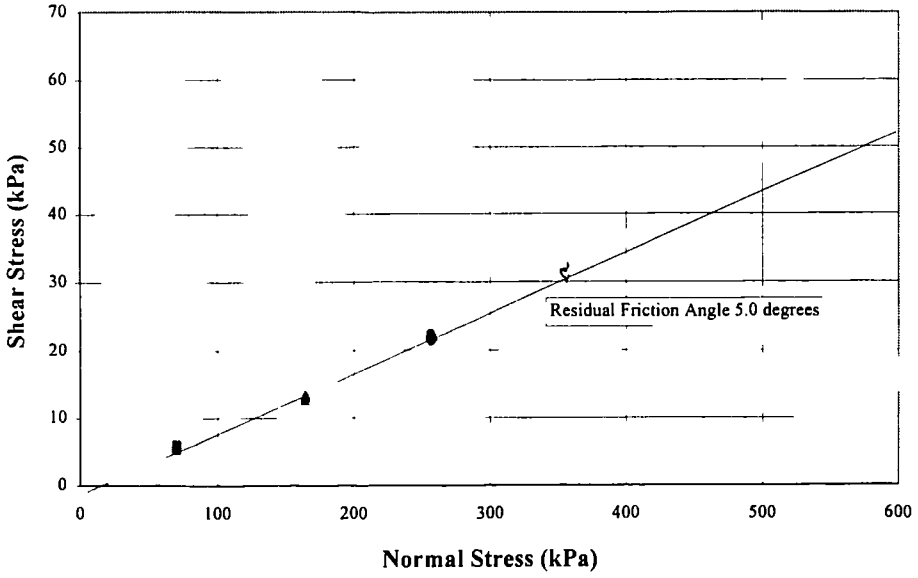

Figure 4.57 b) Residual Strength Failure Envelope
Minced Sample RS-D(M) (I4 7.5 - 7.8 m bgl)

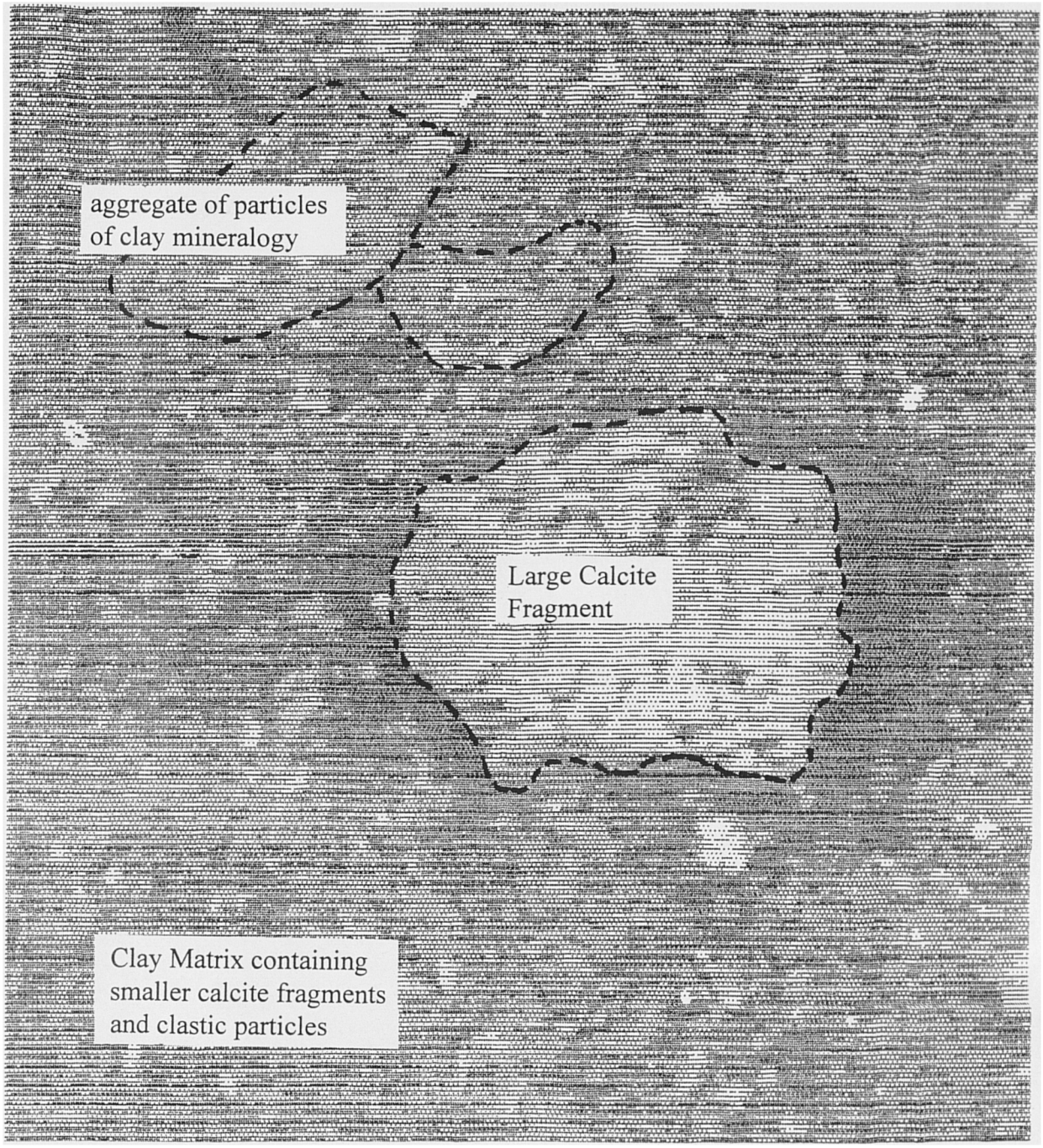

Figure 5.1 Digitised image from the S.E.M. study of the natural material: Horizontal width of magnified sample approximately 100 μm

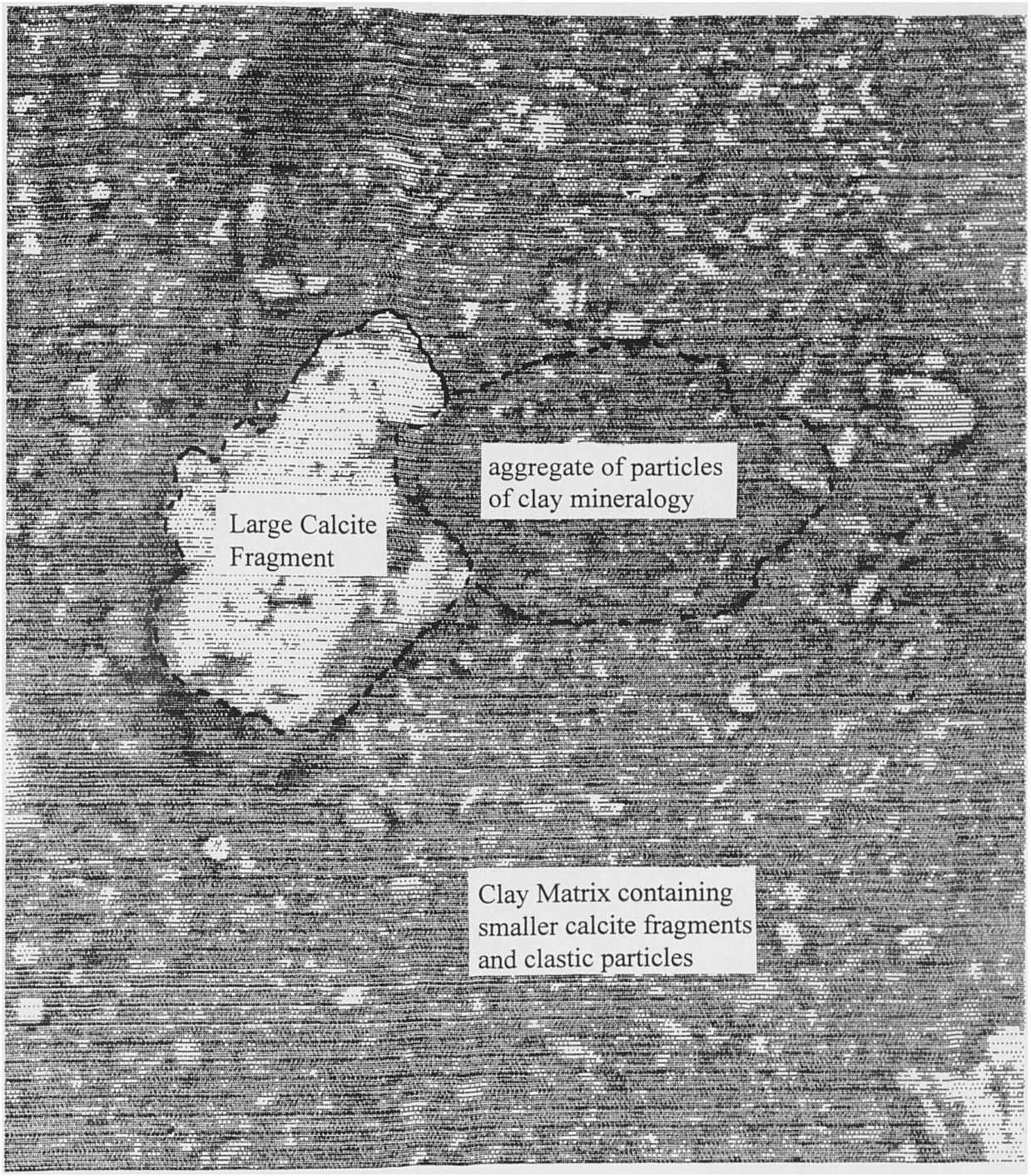

Figure 5.2 Digitised image from the S.E.M. study of the reconstituted material
Horizontal width of magnified sample approximately 100 μm

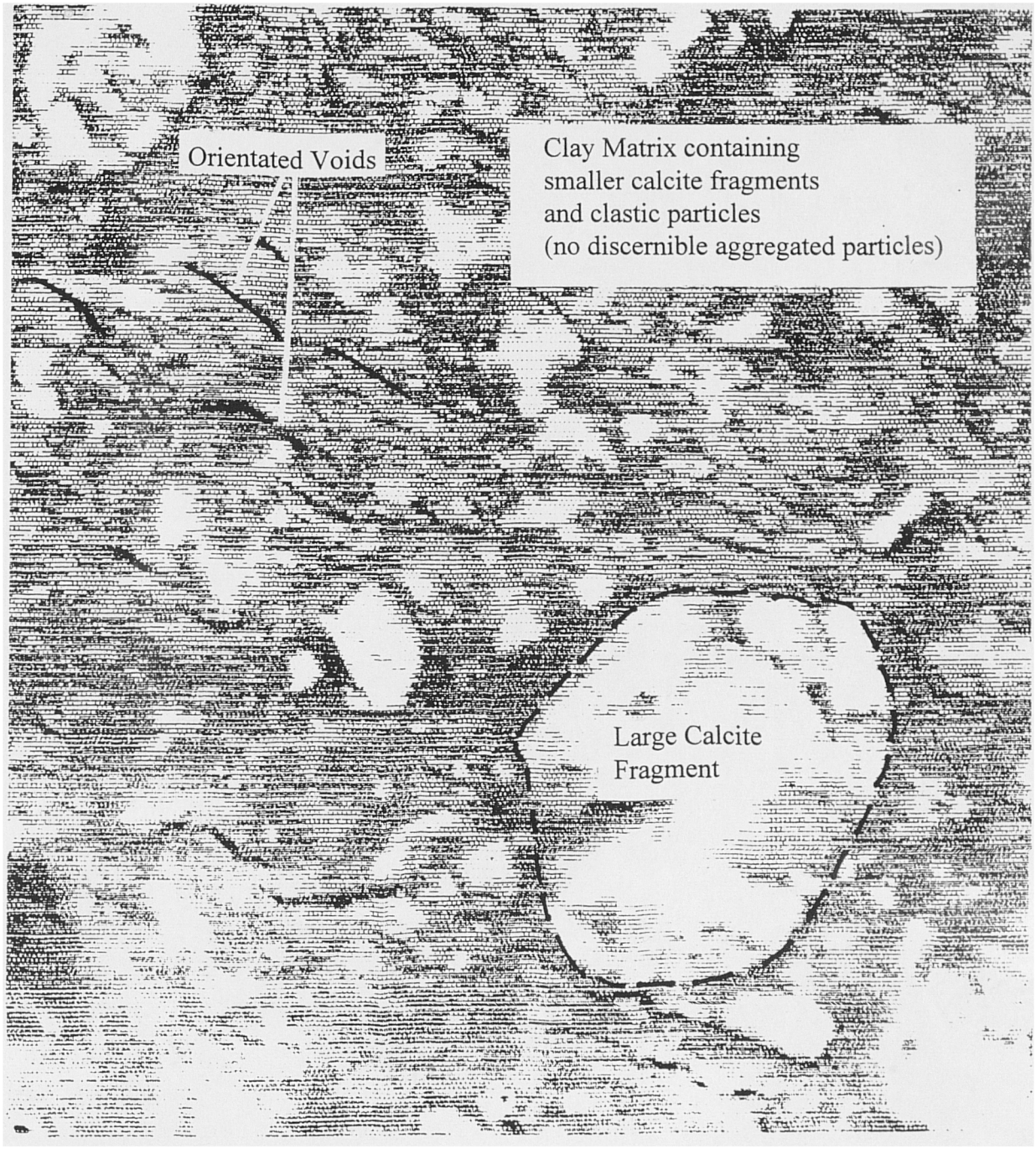

Figure 5.3 Digitised image from the S.E.M. study of the minced material
Horizontal width of magnified sample approximately 100 μm

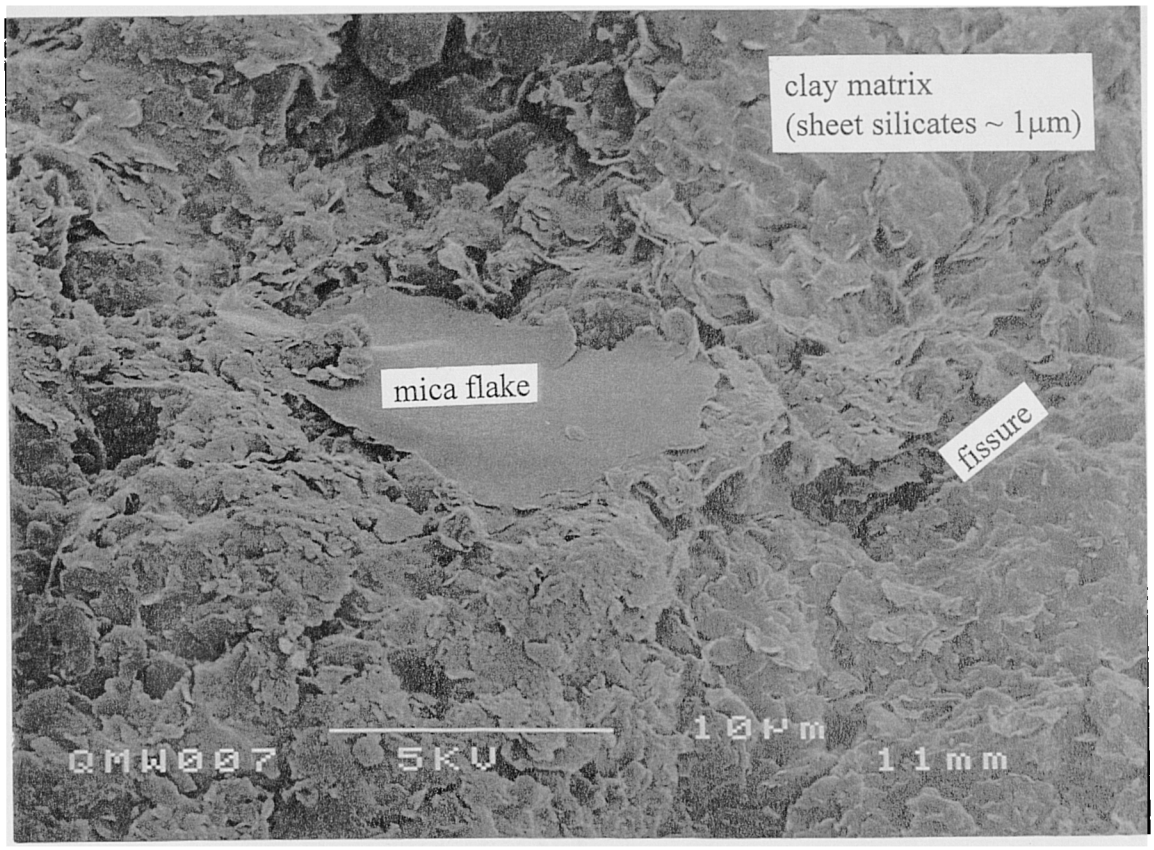

Figure 5.4 Scanning electron microscope photograph of the natural material showing large mica flake in clay matrix.

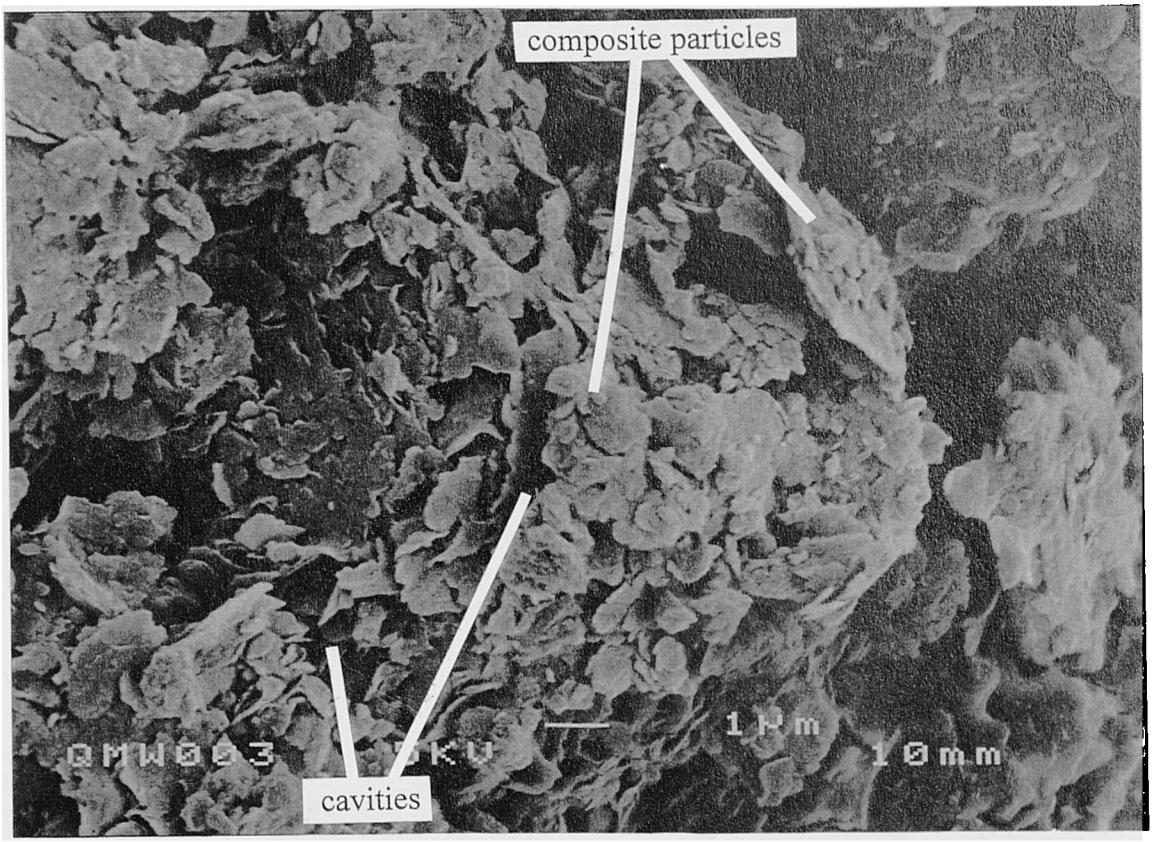

Figure 5.5 Scanning electron microscope photograph of the natural material showing fine grained clay matrix.

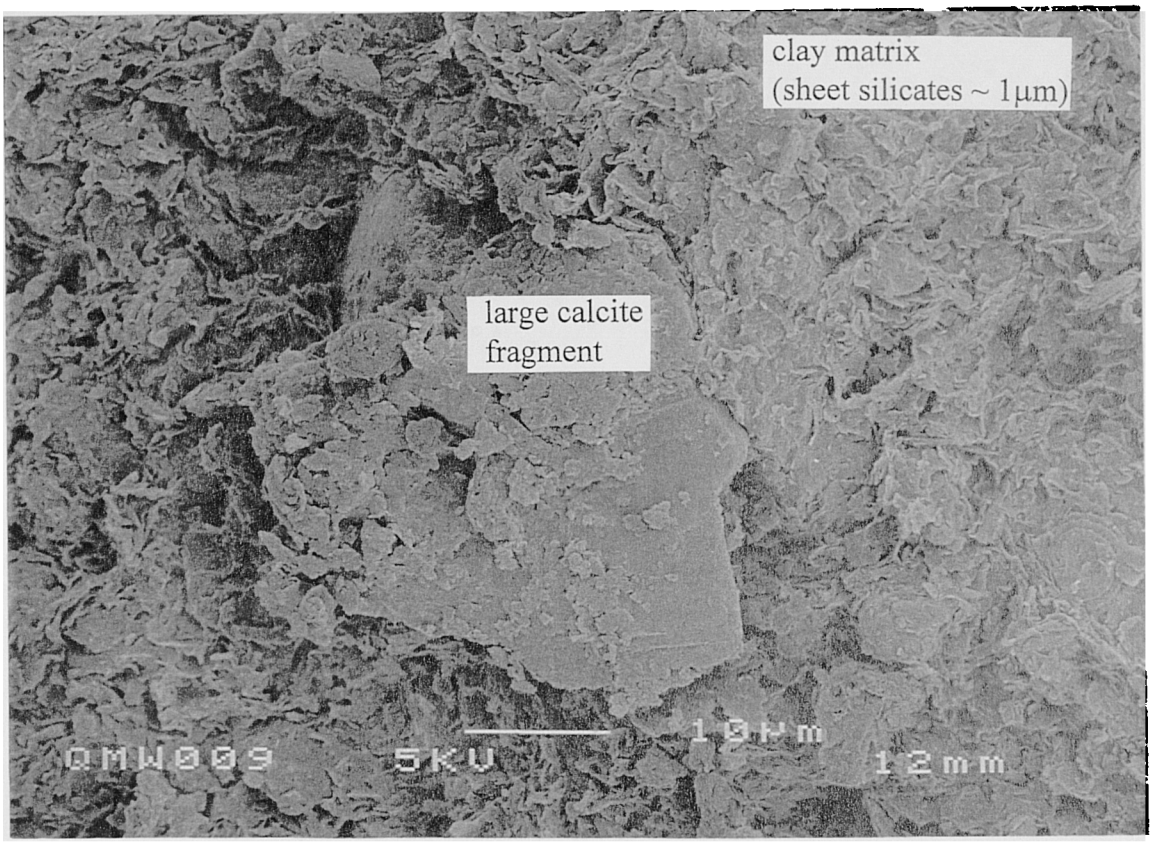

Figure 5.6 Scanning electron microscope photograph of the reconstituted material showing large calcite fragment in clay matrix.

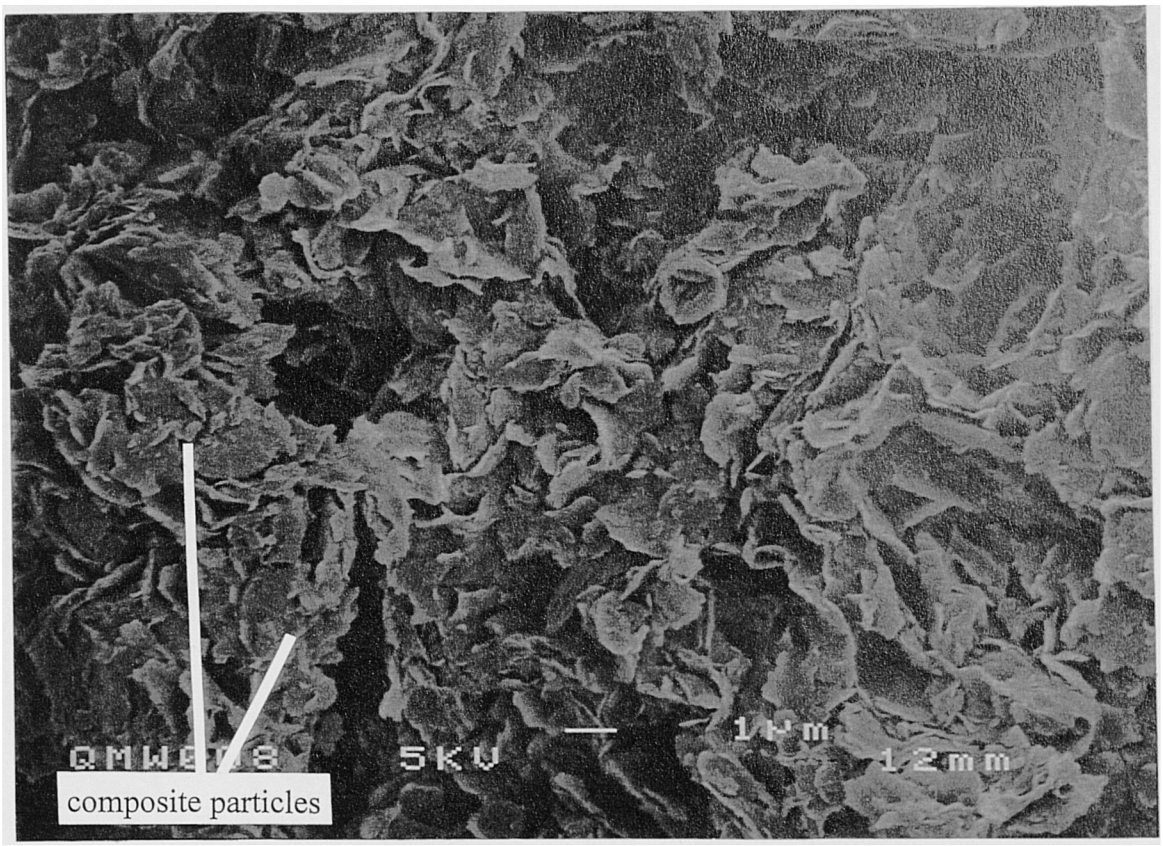

Figure 5.7 Scanning electron microscope photograph of the reconstituted material showing fine grained clay matrix.

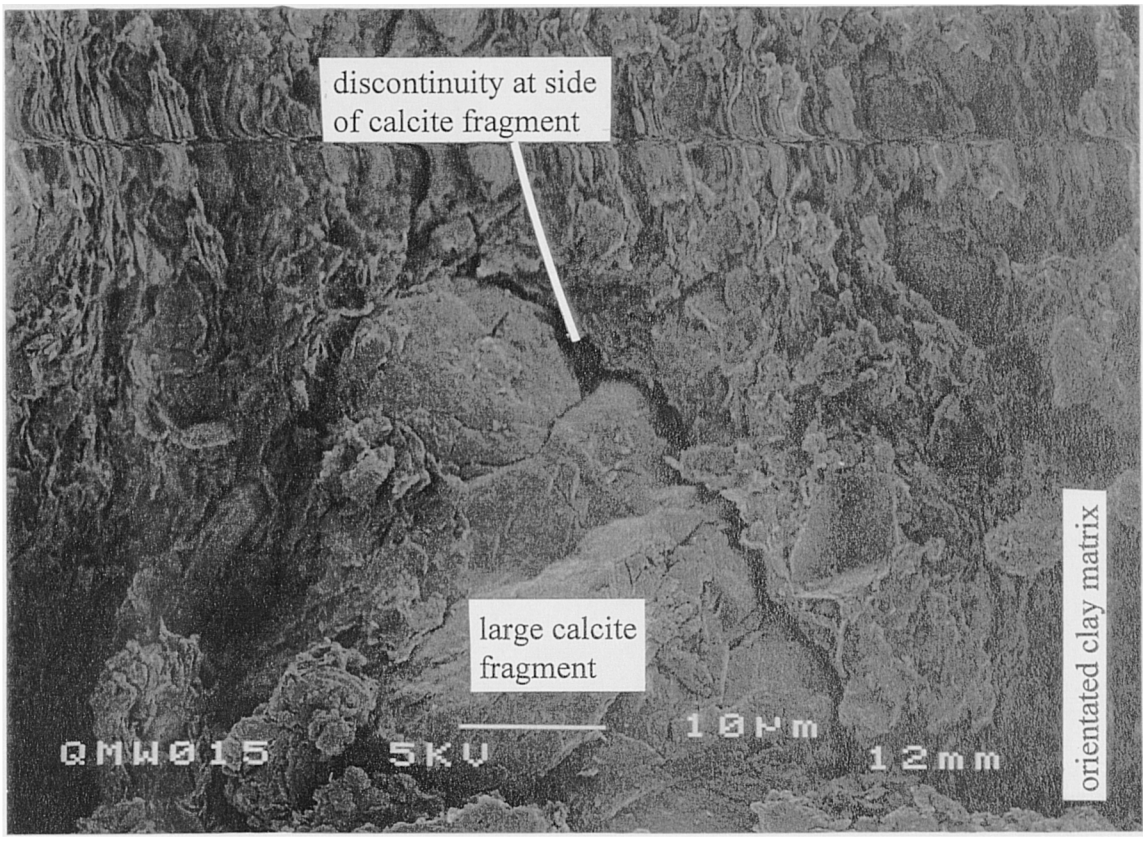

Figure 5.8 Scanning electron microscope photograph of the minced material showing large calcite fragment in clay matrix.

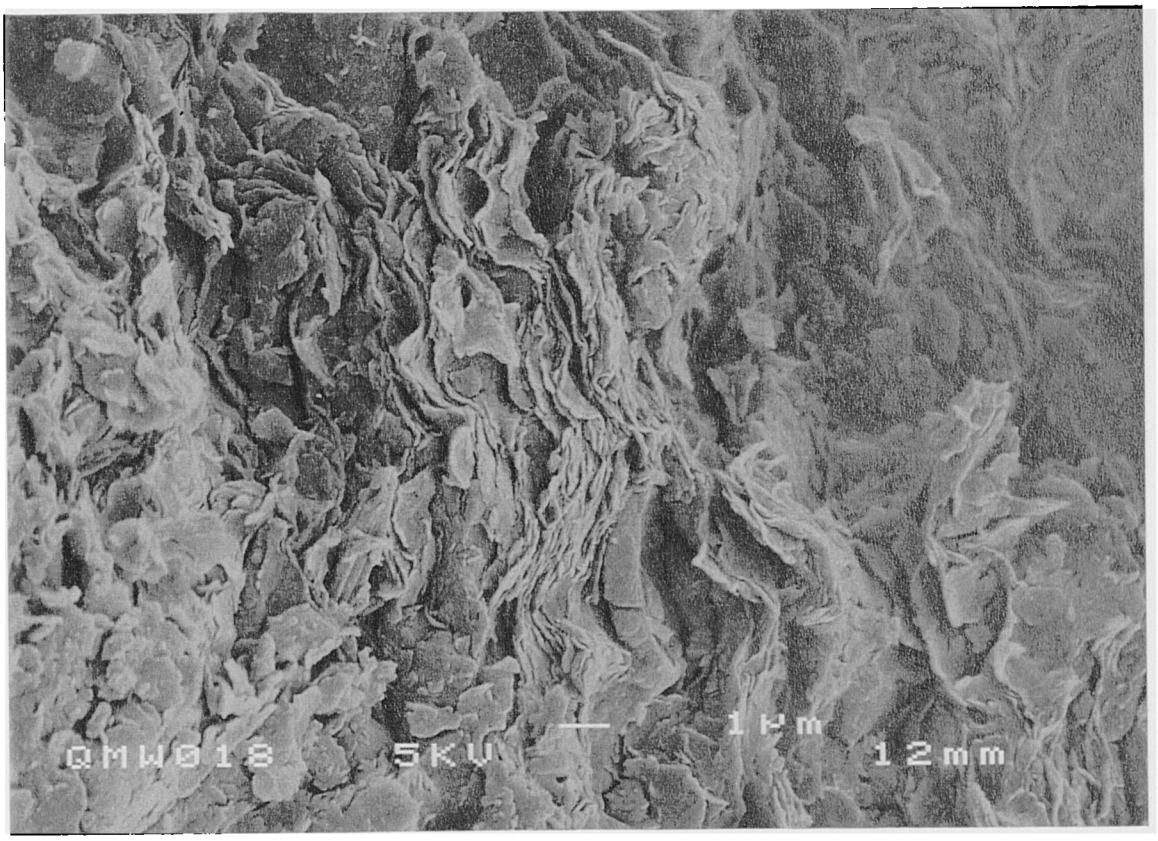

Figure 5.9 Scanning electron microscope photograph of the minced material showing fine grained clay matrix.

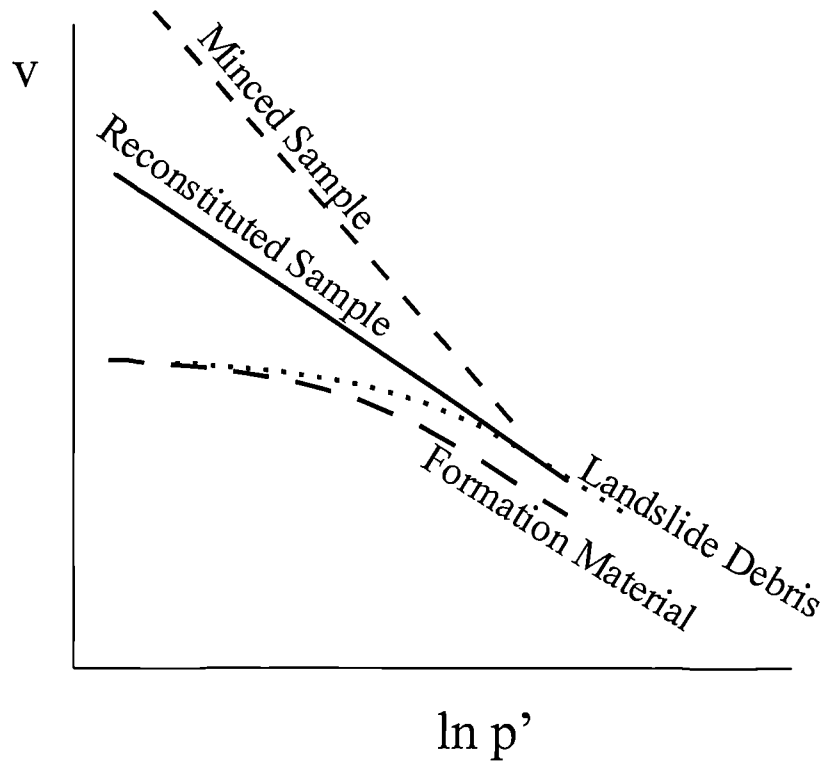

Figure 5.10 Schematic diagram showing the effect of different structures on t he compression behaviour of a structurally complex clay.

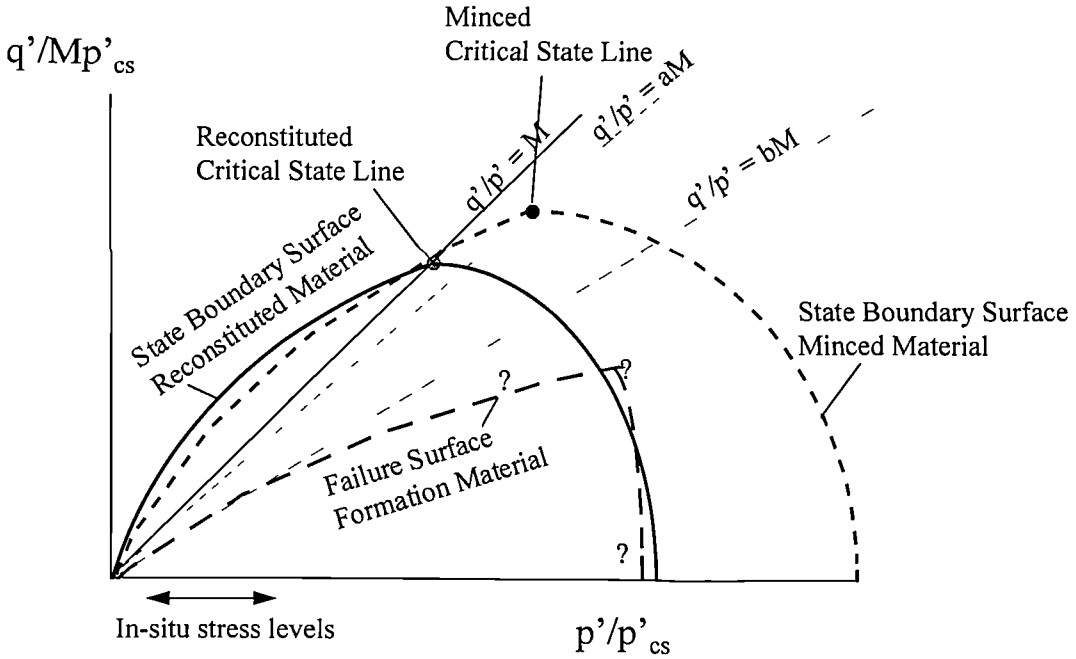

Figure 5.11 Schematic diagram showing the effect of different structure on the normalised shear behaviour of a structurally complex clay.

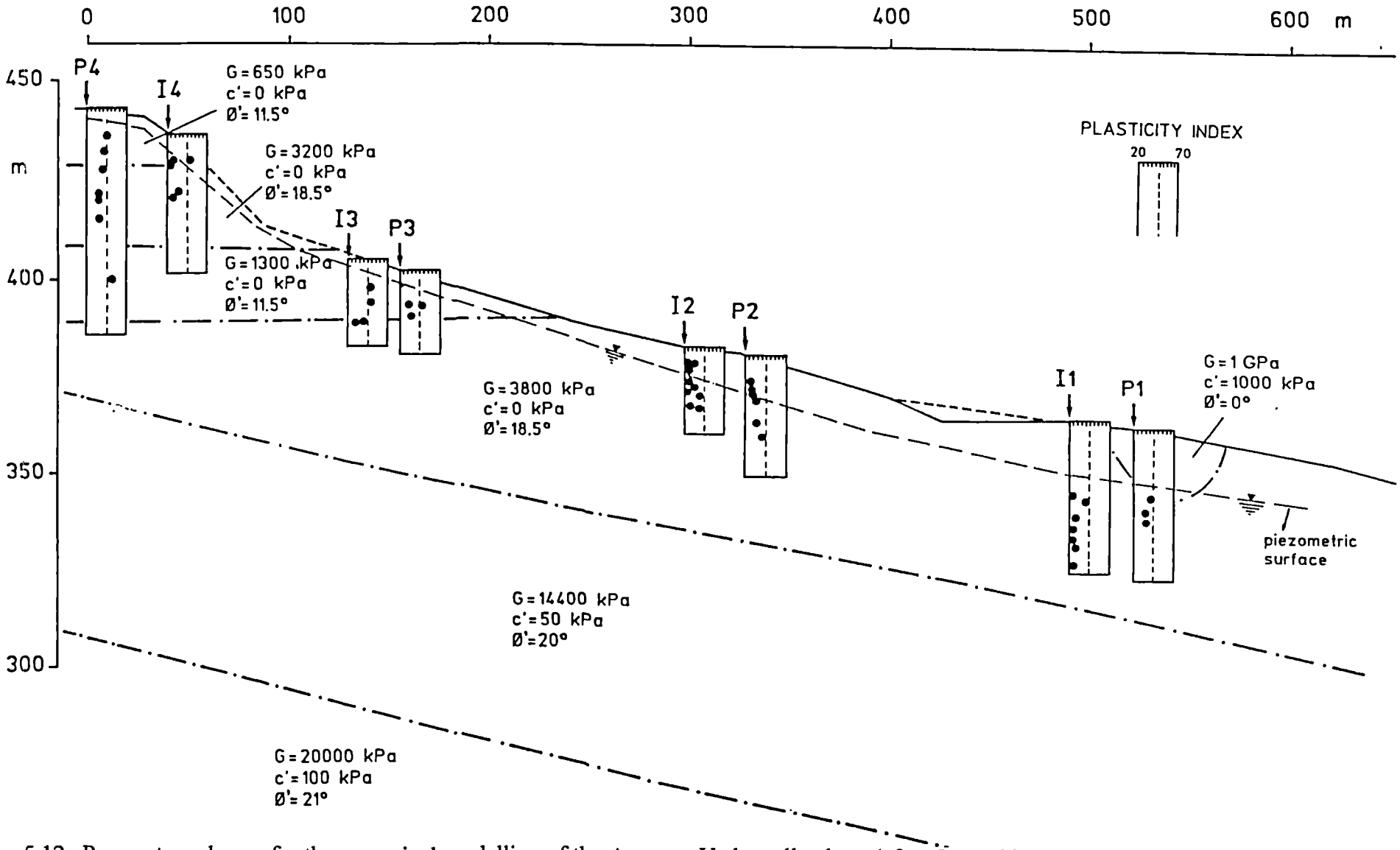

Figure 5.12 Parameters chosen for the numerical modelling of the Acquara-Vadoncello slope (after Cotecchia et al. 1996)

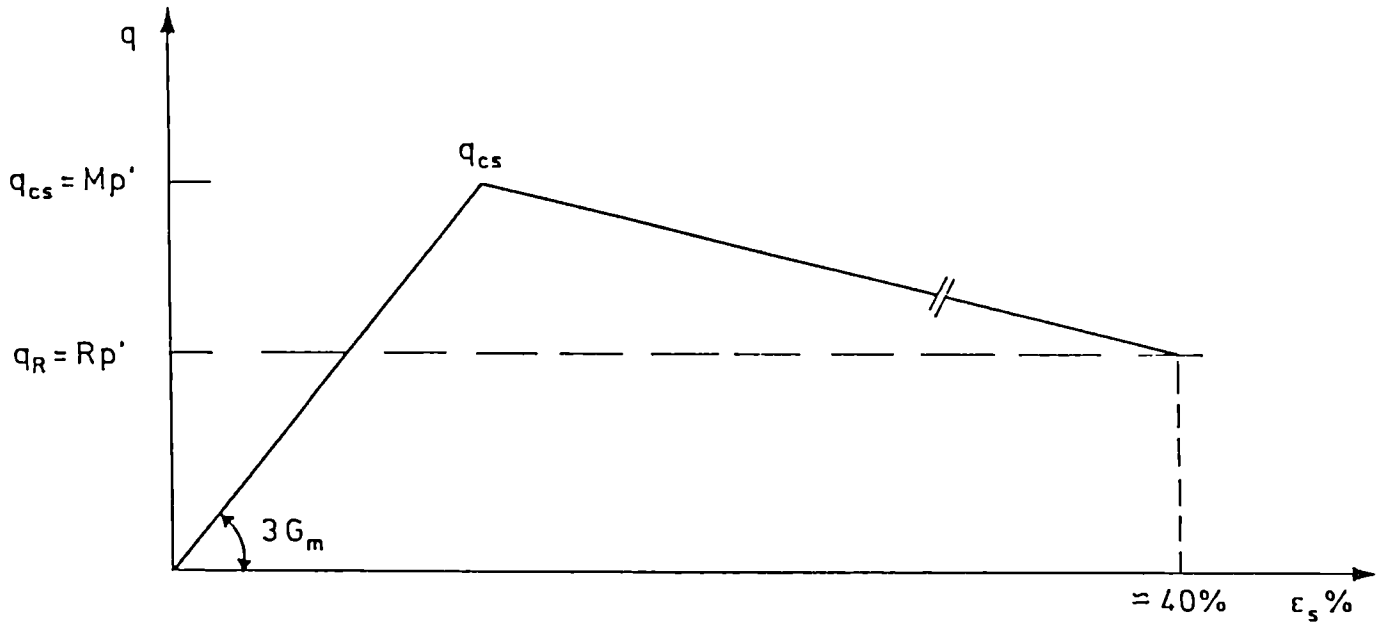

LEGEND:

$$G_m = \frac{75\%\ q_{cs}}{\varepsilon_s (\text{at } q = 75\%\ q_{cs})}, \text{from laboratory test } q\text{-}\varepsilon_s \text{ curve}$$

$$M = \frac{6 \text{ sen } \emptyset'_{cs}}{3 - \text{sen } \emptyset'_{cs}}, \ \emptyset'_{cs} \text{ critical state friction angle}$$

$$R = \frac{6 \text{ sen } \emptyset'_R}{3 - \text{sen } \emptyset'_R}, \ \emptyset'_R \text{ residual friction angle}$$

Figure 5.13 Constitutive model for the numerical analysis (after Cotecchia et al. 1996).

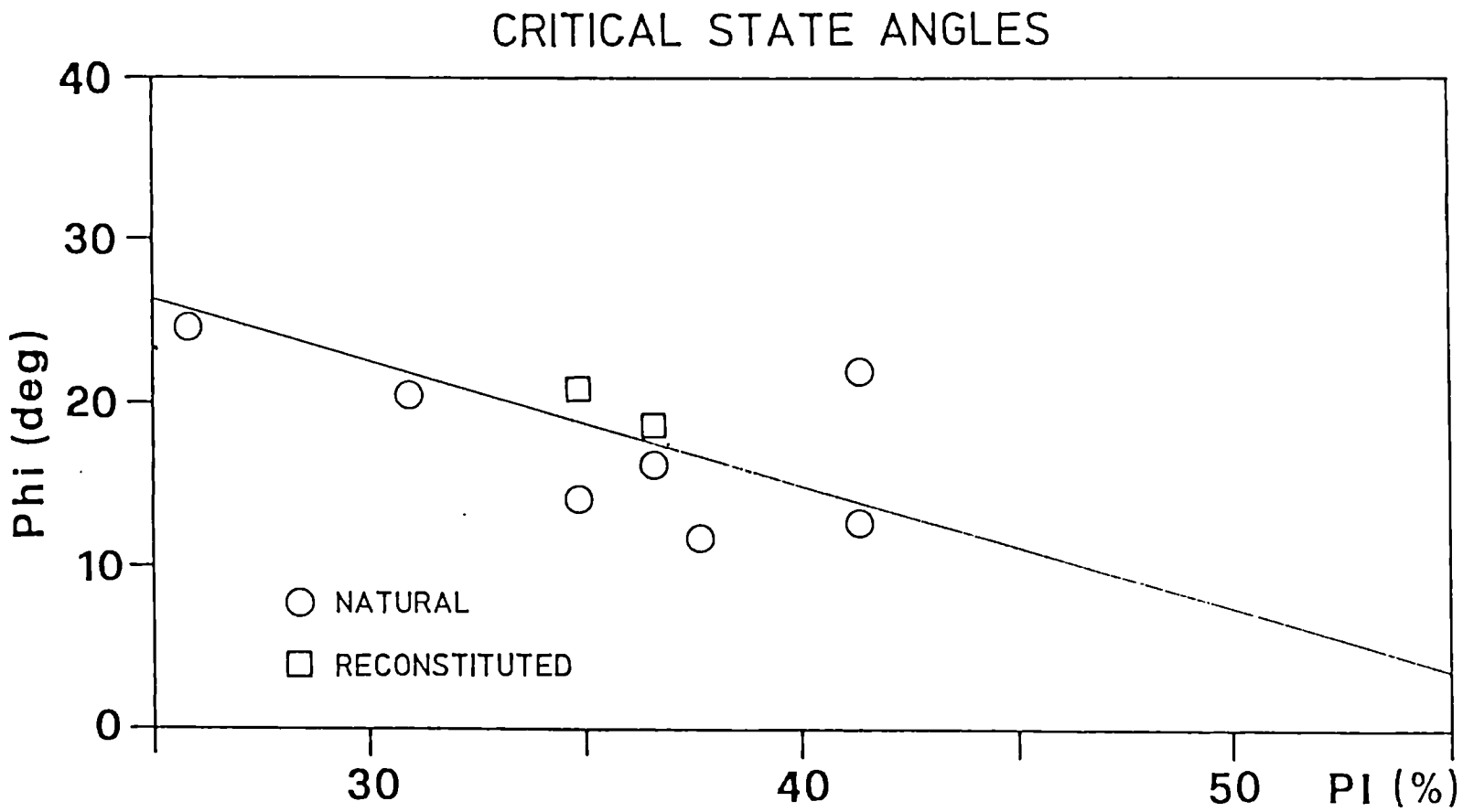

Figure 5.14 Relationship between critical state friction angles and plasticity indices (after Cotecchia et al. 1996)

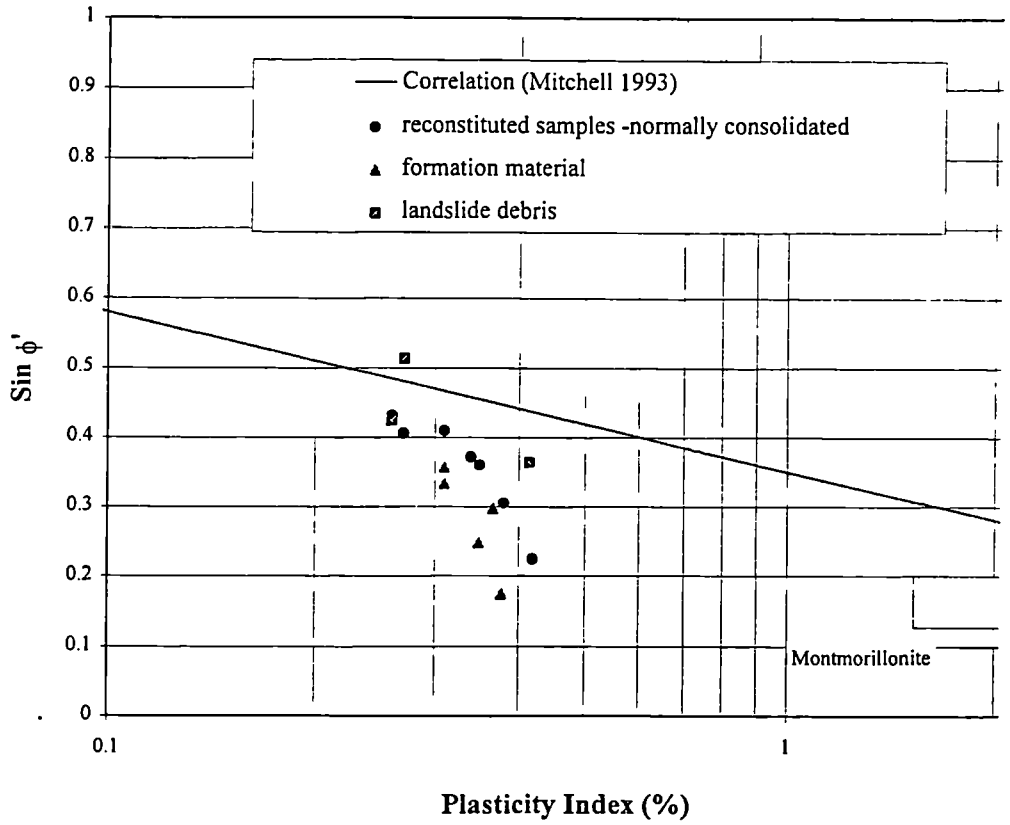

Figure 5.15 Relationship between the sine of the critical state friction angles and plasticity indices.

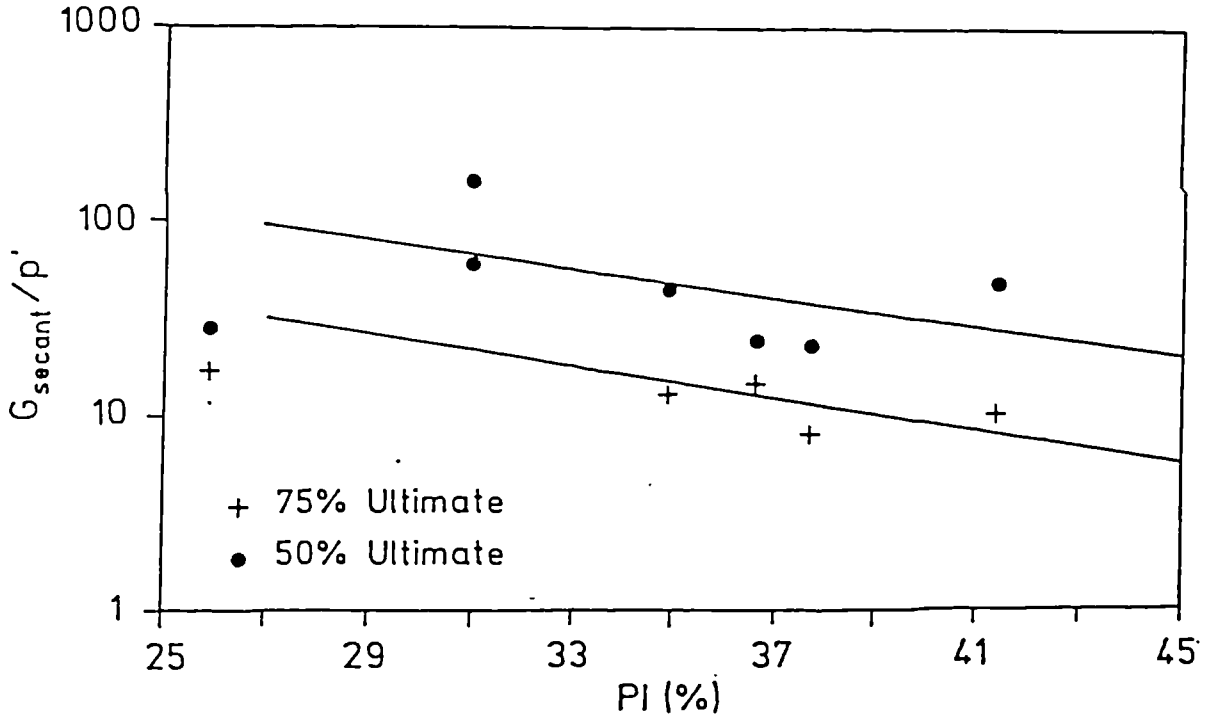

Figure 5.16 Relationship between the normalised shear stiffness (G/p') for the natural samples and the plasticity index (after Cotecchia et al. 1996)

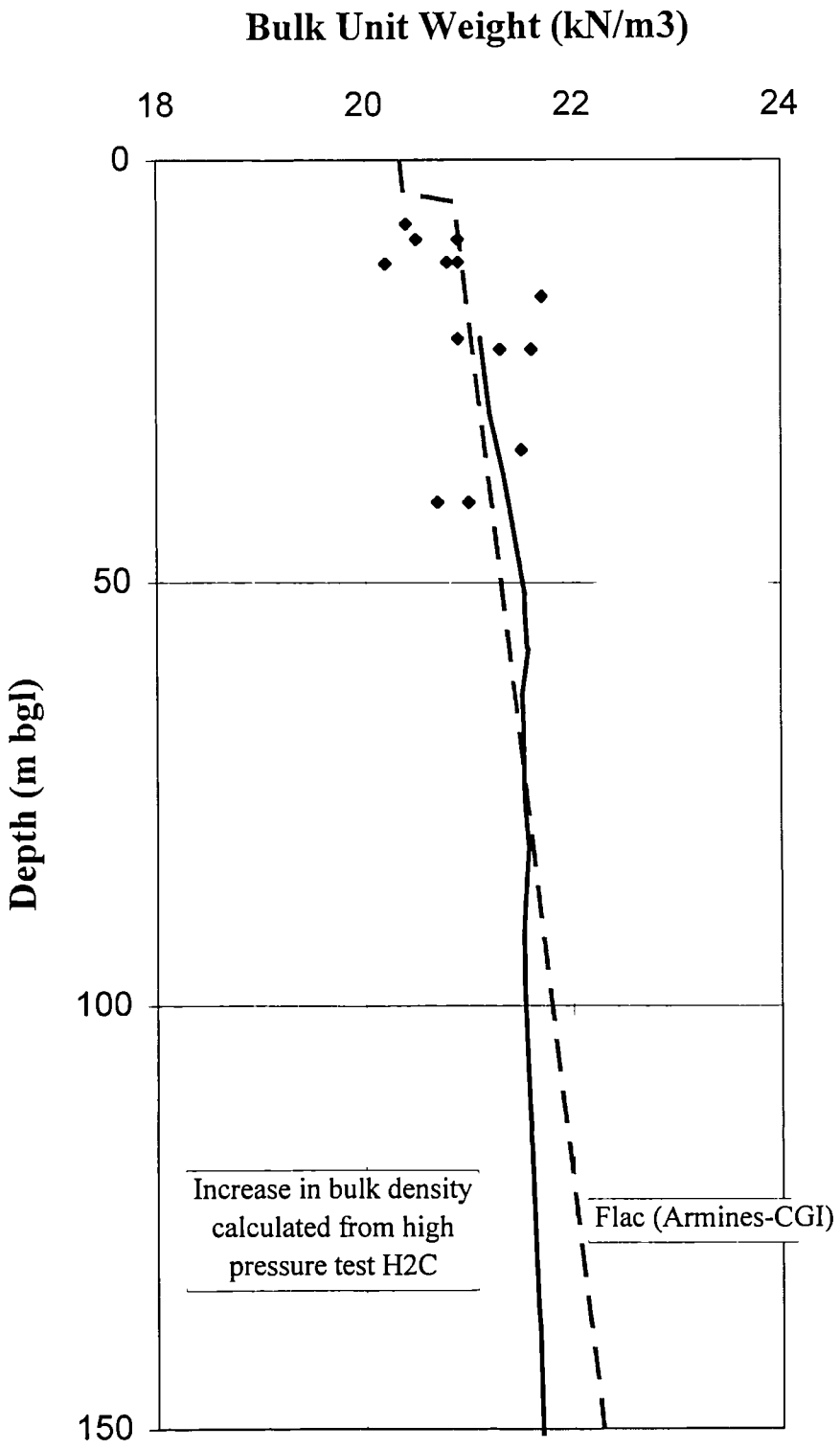

Figure 5.17 Bulk unit weight profile . Data used by Armines-CGI from Cotecchia et al. (1996).

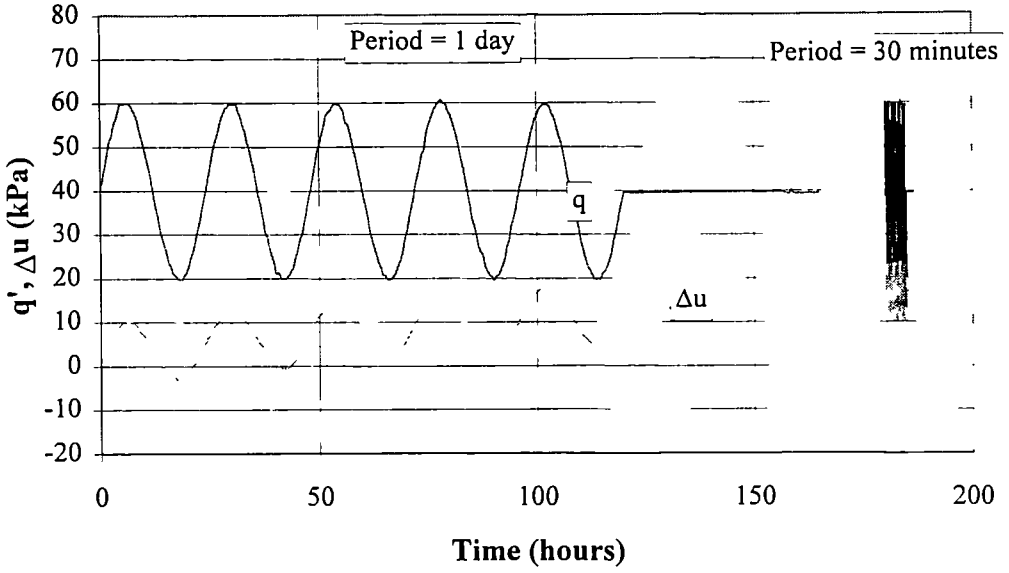

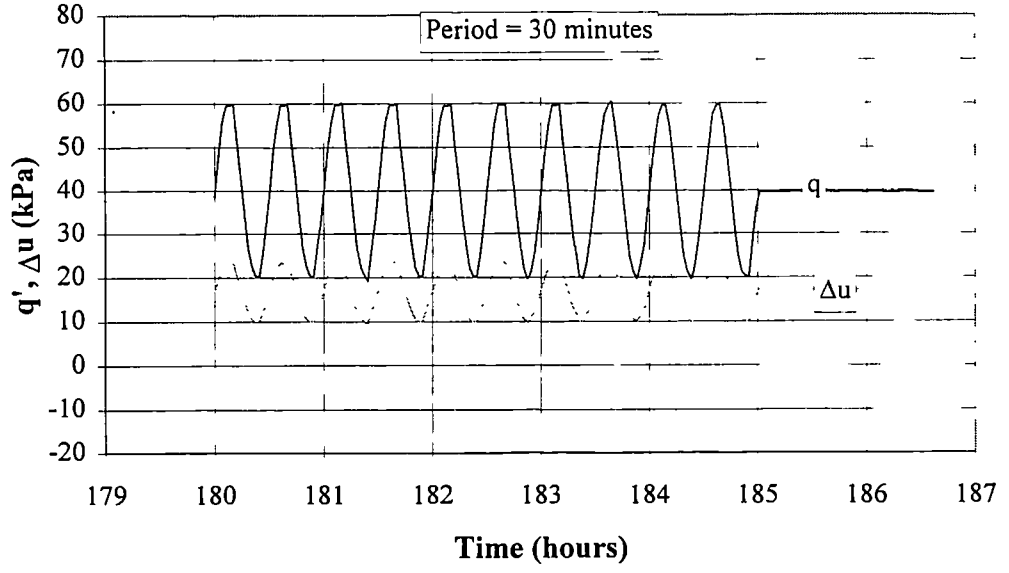

Figure 5.18 Undrained cyclic loading in the triaxial apparatus.